ANALYTICA CHIMICA ACTA

International monthly devoted to all branches of analytical chemistry
Revue mensuelle internationale consacrée à tous les domaines de la chimie analytique
Internationale Monatsschrift für alle Gebiete der analytischen Chemie

ELSEVIER SCIENTIFIC PUBLISHING COMPANY
AMSTERDAM

Anal. Chim. Acta, Vol. 67, No. 1, 1–252, November 1973
Published monthly

Publication Schedule for 1973

Vol. 63, No. 1	January 1973	
Vol. 63, No. 2	February 1973	**(completing Vol. 63)**
Vol. 64, No. 1	March 1973	
Vol. 64, No. 2	April 1973	
Vol. 64, No. 3	May 1973	**(completing Vol. 64)**
Vol. 65, No. 1	June 1973	
Vol. 65, No. 2	July 1973	**(completing Vol. 65)**
Vol. 66, No. 1	August 1973	
Vol. 66, No. 2	September 1973	
Vol. 66, No. 3	October 1973	**(completing Vol. 66)**
Vol. 67, No. 1	November 1973	
Vol. 67, No. 2	December 1973	**(completing Vol. 67)**

Subscription price: Dfl. 410.00 plus Dfl. 30.00 postage. Subscribers in the U.S.A. and Canada receive their copies by airmail. Additional charges for airmail to other countries are available on request. For advertising rates apply to the publishers.

GENERAL INFORMATION

Languages

Papers will be published in English, French or German.

Submission of papers

Papers should be sent to:

PROF. PHILIP W. WEST,
Coates Chemical Laboratories,
College of Chemistry and Physics,
Louisiana State University,
Baton Rouge 3,
La. 70803 (U.S.A.)

or to:

DR. A. M. G. MACDONALD,
Department of Chemistry,
The University,
P.O. Box 363
Birmingham B15 2TT (Great Britain)

Reprints

Fifty reprints will be supplied free of charge. Additional reprints (minimum 100) can be ordered at quoted prices. They must be ordered on order forms which are sent together with the proofs.

PRINTED IN THE NETHERLANDS

THE ACTINIDE ELEMENTS

By **K. W. BAGNALL,** The University of Manchester, U.K.

Topics in Inorganic and General Chemistry, Monograph 15.

1972. 284 pages. Dfl. 80.00 (about US $30.80). ISBN 0-444-41041-4

During the last decade research on the chemistry of protactinium and the transuranium actinide elements has increased the knowledge of the chemistry of the group to an extent sufficient for it to be possible to discuss their behaviour as a group rather than as individial elements. This approach has been adopted in the present monograph, in which the individual chapters deal with the various types of compound formed by the actinide elements. It concludes with a brief introduction to *f* orbitals, and the magnetic properties and spectra of the actinides.

This account of the chemistry of the actinide elements is essentially a broad, up-to-date survey of the subject which should be useful for the chemistry student and for the postgraduate student starting on research in this field. The less well known topics, such as the alkoxides, carboxylates, and chelate compounds, are treated in much greater detail than for instance actinide halides and their complexes, which have been exhaustively reviewed in the literature, but references to such reviews are given to maintain the coverage.

CONTENTS:

Elsevier

P.O. BOX 211

AMSTERDAM, THE NETHERLANDS

1176E

DEVELOPMENTS IN SEDIMENTOLOGY, VOL. 15

The Chemistry of Clay Minerals

By CHARLES E. WEAVER, *School of Geophysical Sciences, Georgia Institute of Technology, Atlanta* and LIN D. POLLARD, *Georgia Institute of Technology, Atlanta.*

1973. 222 pages. Dfl. 65.00 (about US $ 25.00) ISBN 0-444-41043-0

Long overdue, this is the first comprehensive compilation and critical evaluation of data on the chemistry of clay minerals. It includes both oxide data and structural formulae for twenty-five varieties of clay minerals, while for the more common minerals, means, standard deviation, range, limits, histograms and correlation coefficients are presented.
The chemical data is evaluated in terms of the interrelation of composition and structure, including a discussion of the effect of ion size and distribution on the octahedral and tetrahedral sheets as well as how these sheets fit together. The relation of chemical composition to mode of origin is discussed for most of the clay minerals and their low-temperature synthesis is briefly reviewed. Also considered are the nature and significance of hydroxy interlayers and cation exchange.
As a graduate-level research reference the book will be very useful to workers in the field of clay mineralogy and chemistry, but students will also find it invaluable as a supplemental textbook.

CONTENTS:

Elsevier
P.O. Box 211
Amsterdam - The Netherlands

1156 E

MOLECULAR RELAXATION STUDIES

Proceedings of the 8th Colloquium of NMR Spectroscopy, Aachen, April 14-20, 1971

Edited by W. J. ORVILLE-THOMAS, *Department of Chemistry and Applied Chemistry, University of Salford, U.K.*

Special Issue of the Journal Advances in Molecular Relaxation Processes. Volume 3.

1972. 371 pages. Dfl. 100.00 (about US$35.10) ISBN 0-444-4108-0

Contents:

Elsevier

Book Division, P.O. Box 211,
Amsterdam, The Netherlands

1058 E

ANALYTICA CHIMICA ACTA
Vol. 67 (1973)

ANALYTICA CHIMICA ACTA

International monthly devoted to all branches of analytical chemistry
Revue mensuelle internationale consacrée à tous les domaines de la chimie analytique
Internationale Monatsschrift für alle Gebiete der analytischen Chemie

ELSEVIER SCIENTIFIC PUBLISHING COMPANY
AMSTERDAM

PRINTED IN THE NETHERLANDS

Analytica Chimica Acta, 67 (1973) 1–16

MOLECULAR EMISSION CAVITY ANALYSIS—A NEW FLAME ANALYTICAL TECHNIQUE

PART I. DESCRIPTION OF THE TECHNIQUE AND THE DEVELOPMENT OF A METHOD FOR THE DETERMINATION OF SULPHUR

R. BELCHER, S. L. BOGDANSKI and A. TOWNSHEND

Department of Chemistry, The University, P.O. Box 363, Birmingham B15 2TT (England)

(Received 4th June 1973)

A new technique of flame emission analysis has been developed. This technique, which has been named MECA (Molecular Emission Cavity Analysis), employs a small cavity at the end of a rod into which the samples are deposited. The cavity is introduced into the flame in line with the detector, and the resulting emission is recorded[1]. The technique provides a sensitive, reproducible, rapid and extremely versatile method for analysing milligram or microlitre samples. It can be applied to a wide range of elements, metals and non-metals, in an equally wide range of solid, liquid or gaseous samples, some of which cannot be analysed, or can be analysed only with difficulty, by flame spectrophotometric techniques based on conventional nebulization. In this paper, the basic technique is described, and its application to the determination of sulphur in a wide range of compounds, by means of S_2 emission in a dilute hydrogen diffusion flame is discussed. Finally, a brief outline of some other applications and developments is given.

So far MECA has been carried out by measuring molecular emissions in cool flames. Such measurements by conventional flame emission spectrometry have recently become popular for the determination of sulphur, phosphorus and the halogens, whose atomic emission lines lie in the far ultraviolet region. It should not be forgotten, however, that molecular emissions from flames have been studied for more than a century. Of such emissions, one that has received much attention is the band system arising from S_2 molecules. Early workers[2,3] observed the blue emission of sulphur, most usually in the core of a hydrogen-rich flame, which had a distinguishable banded spectrum characteristic of the "metalloids" (*e.g.* S, Se, Te, C, P). Most notable is the work of Salet[4], who examined the S_2 emission spectrum in the hydrogen flame and the geissler tube, as well as the S_2 absorption spectrum. Salet also observed that the blue S_2 emission in a fuel-rich hydrogen flame was enhanced at a cold surface placed in the flame. This phenomenon, now named the "Salet phenomenon", has recently been described by Veillon and Park[5].

In the last few years, many analytical applications of S_2 emission have been reported, both for the analysis of sulphur compounds in discrete samples nebulized into the flame, and for specific monitoring of sulphur compounds eluted from a gas chromatograph[6]. Many of the burner designs[5] include a relatively cool surface, usually in the form of a separator, on which the sulphur emission is most

apparent. A fuel-rich hydrogen flame, cooled by addition of nitrogen or argon, is commonly used[7,8].

The advantages of the use of such cool flames include low background emission, high sensitivity, sufficiently low temperatures to allow a number of molecular emission spectra to be utilized, and a low oxygen content, which allows molecules such as S_2 to exist for appreciable periods. The major limitations are the interferences caused by the presence or formation of compounds that are slow to volatilize and/or decompose[9]. In such instances, the analyte will pass through the flame zone under observation before appreciable emission can be stimulated. The depressive effect of metal ions, observed by all workers with the exception of Veillon and Park[5], may be ascribed to the slow breakdown of the metal salts in the flame, and, possibly, to a reduction in the concentration of radicals necessary for formation and excitation of S_2 molecules, in the presence of metal atoms, *e.g.*:

$$H + H + Na \rightarrow H_2 + Na^*$$

Addition of organic compounds to the flame also reduces the S_2 emission intensity[5]. This quenching effect has been used as the basis of a gas-chromatographic detector for organic compounds[10]; the quenching probably arises from the removal of radicals from the flame by the organic fragments. The S_2 emission intensity from organo-sulphur compounds depends on the nature of the compound; again, the organic fragments released influence the emission intensity.

In the proposed technique, such interference effects can be accommodated because the sample and the associated emission are confined in one small region in the flame, which may be chosen to give the desired sample breakdown whether the compound being analyzed is easy or difficult to decompose.

SAMPLE INTRODUCTION DEVICES FOR FLAME SPECTROMETRY

In addition to the widely used technique of nebulization for introducing samples into the flame, many other devices have been suggested for this purpose. The Massmann[11] or L'vov[12] carbon furnaces, which offer a major advance in atomic absorption spectrometry, are not suited to emission studies. Flameless carbon filament[13] and laser atomization[14], although readily applicable to atomic emission and fluorescence studies, have not been used for the measurement of molecular emissions.

The platinum sample loop developed by Ramsay[15] is suitable for the introduction of microlitre volumes of solutions in flame emission analysis for sodium and potassium. The platinum loop experiment was found to depend critically on the geometry of the loop and the position of the loop in the flame. The less known Brandenberger filament[16], whereby the sample is plated on a platinum spiral which then becomes a heated filament for flameless atomization, has not been applied to flames, although it would be similar to Ramsay's sample loop.

Variations of the "Delves sampling cup"[17,18] design can be found, in which the container is placed into a hot flame so that the analyte boils off into the flame. This "bucket" technique often results in uncontrolled atomization, or more controlled but appreciably slower atomization if a more massive bucket is used.

All these devices are suitable for small volumes of sample, but are solely a means of getting the sample into the flame. None has been applied to molecular emission studies.

Alternatively, small volumes of solution have been nebulized directly into a flame[19,20] (or plasma[21]) by injecting from a syringe at the base of the flame. In these techniques, as with the bucket and loop techniques above, the analyte species are carried along with the flame gases.

MOLECULAR EMISSION CAVITY ANALYSIS

In the MECA technique, the sample is injected into a cavity at the end of a rod held in a sample holder assembly, such as that shown in Fig. 1. By turning the assembly knob, the cavity can be reproducibly positioned into a nitrogen-diluted hydrogen flame in line with a detector. The cavity is introduced into the flame pitched at an angle of 7° downward to optimize contact with the flame gases. The flame serves the binary function of heating the cavity to vaporize the sample and of providing the radicals which maintain the molecular emission.

The flame gas flow and the position of the cavity may be adjusted so that emission is restricted to the cavity. Under such conditions, emission is sustained and enhanced.

Apparatus

The sample holder assembly was constructed to fit into an Evans Electro-selenium EEL 240 atomic absorption spectrophotometer, after removal of the water cooling cage and hollow-cathode lamp assembly. The spectrophotometer was operated in the emission mode, and the nebulizer could be blocked to prevent aspiration of air into the flame. An EEL emission burner head (circ. diam. 2.5 cm) with a maximum slit opening (0.91 mm) was used throughout. A Unicam SP 90 was used for some spectral scans of nebulized compounds.

The flame consisted of hydrogen, introduced via the fuel input system, nitrogen, via the support gas system, and air (when used) via the secondary support gas system[22]. All gases were premixed before entering the burner. The instrument was adapted to function as a wavelength-scanning instrument by coupling an electric motor to the wavelength fine-control drive. Emission intensity was recorded on a Servoscribe recorder (response time, 0.5 s) connected to the 10-mV output of the detector. A Honeywell precision integrator and linear amplifier were connected in parallel to the chart recorder.

The cavity and its properties. In the present study, the cavity was the hexagonal aperture (maximal diagonal 5 mm) at the end of a 3-cm long stainless steel allen screw. The cavity had a volume of 45 μl. By insertion of a chrome–alumel thermocouple into the cavity via a hole drilled in from the side, it was possible to measure the temperature of the portion of the cavity which is not in direct contact with the flame and at which the sample to be tested is deposited, without affecting normal cavity conditions. (The increase in measured temperature is more rapid and the ultimate temperature is higher when the thermocouple is directly exposed to flame gases.)

When the stainless steel screw is introduced into the flame, the cavity

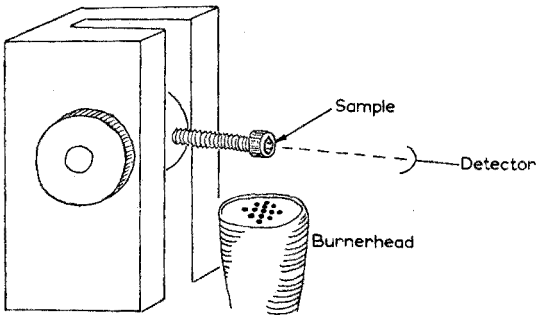

Fig. 1. Sample holder assembly for MECA.

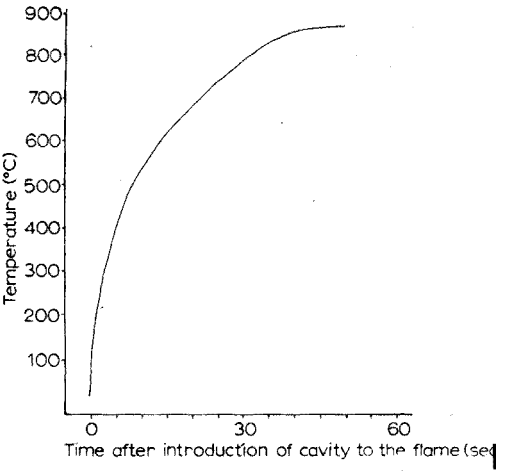

Fig. 2. Rate of heating of stainless steel cavity in a flame.

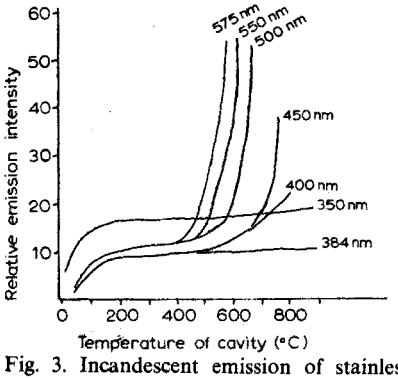

Fig. 3. Incandescent emission of stainless steel cavity at various wavelengths, when heated in a hydrogen–air–nitrogen flame.

gradually becomes hotter, as shown in Fig. 2. The rate of heating and the maximal temperature depend on the amount of oxygen added to the flame. The emission from the cavity itself (thermal incandescence) at various wavelengths and temperatures is shown in Fig. 3. The information in Figs. 2 and 3 allows the heating time required to produce measurable emission at a particular wavelength to be calculated.

The rate of heating of the cavity can also be changed without change of flame conditions. An asbestos layer around the screw head reduces the rate of heating by the hot outer edge of the flame. The use of a cavity of higher thermal conductivity (*e.g.* aluminium) has a similar effect, in that the heat is conducted away more effectively. The heating rate of the cavity has a direct bearing on the decomposition and vaporization rate of the sample, and it is important that this can be adjusted to suit particular samples.

Emission of sulphur compounds

Emission from S_2 molecules has the well-known band spectrum shown in Fig. 4. In the present study, the intensity of the peak at 384 nm was measured.

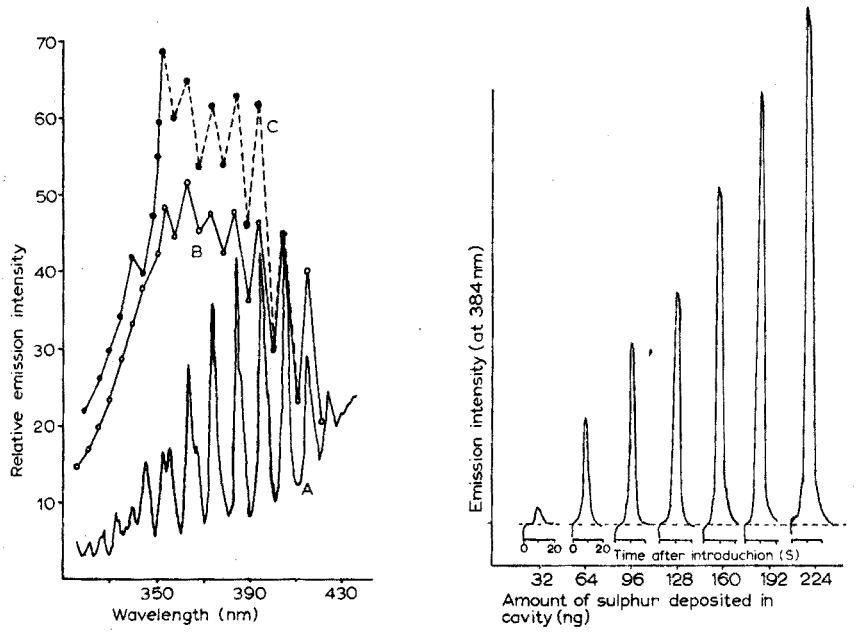

Fig. 4. S_2 emission spectra obtained from thiourea: A, by aspiration into a hydrogen diffusion flame; B, by MECA, in the absence of air; C, by MECA with a high air flow rate ($\frac{1}{3}$ scale).

Fig. 5. S_2 emission from increasing amounts of iron(II) sulphate.

At this wavelength, incandescent radiation from the cavity (Fig. 3) is not observed at the temperatures studied.

S_2 emissions at 384 nm for various volumes (1–10 μl) of 0.01 *M* iron(II) sulphate solution injected into the cavity, are shown in Fig. 5. The recorded emission reaches a peak intensity and then returns to the base line response. The time that elapses between introducing the cavity into the flame and the appearance of maximal intensity (t_m) was found to be characteristic of the sulphur compound; it is related to its vaporization/decomposition temperature, and thus the rate of heating. The peak intensity and, more particularly, the time integral of the emission, are related to the quantity of sulphur placed in the cavity. Both parameters depend on cavity and flame conditions, and are discussed in more detail below.

Effect of gas composition

The blue S_2 emission obtained by aspirating a sulphur compound into a nitrogen-diluted hydrogen diffusion flame can clearly be seen only in the central core of the flame, *i.e.* the portion that is oxygen-free. Introduction of air into this flame extinguishes the blue emission (Fig. 6), as a result of increased temperature and the destruction of S_2 molecules to form sulphur–oxygen compounds.

The effect of air on S_2 emission in the cavity is rather different (Fig. 6). Although initially an increasing oxygen content of the flame decreases the S_2 emission to the same degree as for an aspirated sample, further increase in oxygen content restores and enhances the emission. This effect occurs with all sulphur

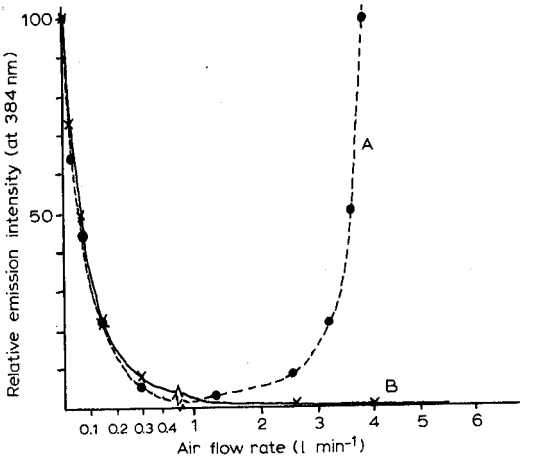

Fig. 6. Variation in S_2 emission intensity with amount of air introduced into the flame: A, MECA; B, a conventional nebulization procedure.

compounds tested, inorganic and organic (*e.g.* thiourea, diphenylsulphide, thioanisole, tetrahydrothiophene), and is directly proportional to the volatility of the sulphur compound. The spectrum for a sample of thiourea in the presence of much air (Fig. 4) confirms that the emission observed still arises from S_2 molecules.

The effect of hydrogen flow rate, at constant nitrogen flow rate and at various air flow rates, on S_2-emission intensity from iron(II) sulphate is shown in Fig. 7. For these conditions, the optimal hydrogen:air ratio is such that the H_2:O_2 mole ratio is 8:1. This ratio depends somewhat on the volatility of the analyte. For a more volatile species (thiourea), the corresponding ratio was 6.6:1. The effect of nitrogen flow rate at constant hydrogen:air ratios is shown in Fig. 8.

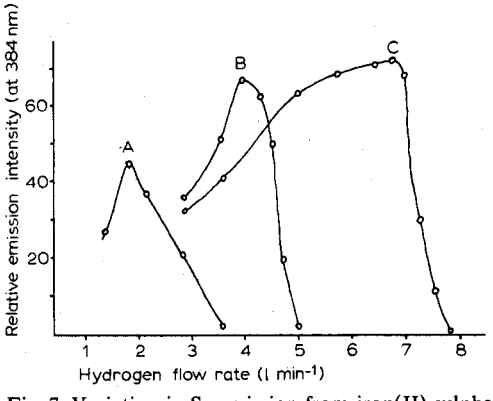

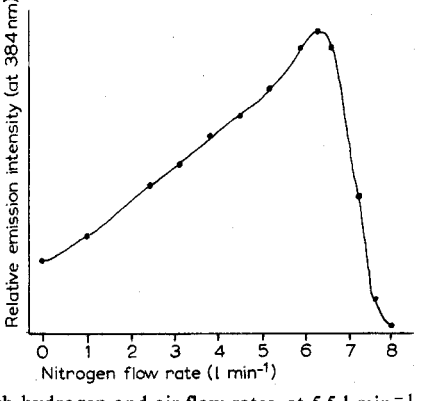

Fig. 7. Variation in S_2 emission from iron(II) sulphate with hydrogen and air flow rates, at 5.5 l min^{-1} nitrogen flow rate. Air flows: A, 1.5; B, 2.7; C, 4.5 l min^{-1}.

Fig. 8. Variation in S_2 emission from iron(II) sulphate with nitrogen flow rate, at 2.65 l min^{-1} air and 4.2 l min^{-1} hydrogen flow rates.

These results indicate that there is an optimal gas composition for the determination of sulphur, which varies somewhat with the particular sulphur compound.

The relationship between S_2 emission and flame gas composition in a gas chromatographic detector has been discussed by Sugujama *et al.*[23]. The relationship is exceedingly complicated, as also appears to be true for MECA.

Position of the cavity in the flame

Pitch of the cavity. The pitch of the screw and hence the cavity was found not to be extremely critical when varied between 5° and 20° below the horizontal. A pitch of less than 5°, *i.e.* almost horizontal, severely reduced the sulphur emission, presumably because of the limited mixing of the sample with the flame gases in the cavity. Larger angles appeared to extend the highest permitted air flow rates (see Fig. 7), but also tended to decrease the precision of the emission measurements. For all the studies presented in this paper, the cavity rod was set at an angle of 7° below horizontal.

Distance of cavity above burner. Figure 9 shows the effect of the distance between the burner head and the cavity on the S_2-peak emission intensity. The integrated emission response as well as peak height are plotted in Fig. 9, together with the time (t_m) to maximal emission from introduction to the flame. The integrated response decreases almost linearly with the distance of the cavity above the burner instead of the exponential decrease one would expect if it were related only to the hydrogen atom concentration in the flame. The sudden decrease in emission intensity which occurs close to the burner corresponds to an increase in t_m, and thus a decrease in cavity heating rate, as the cavity passes through the reaction zone of the flame: t_m is affected higher in the flame than the emission intensity because the lower portion of the screw head enters the cooler zone beneath the reaction zone while the cavity orifice is still in the reaction zone.

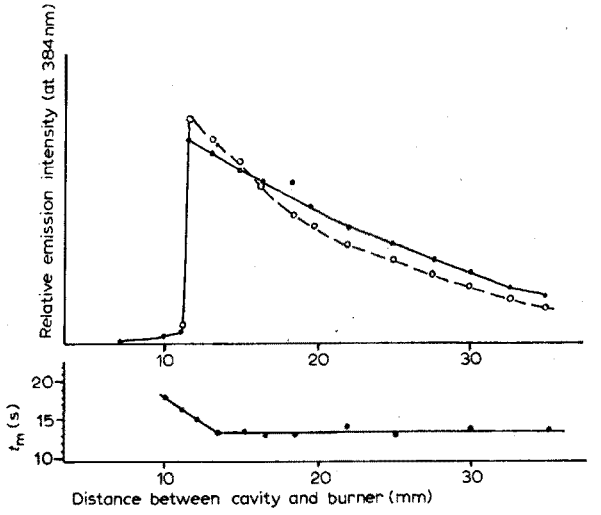

Fig. 9. Variation in S_2 emission and time to maximal emission (t_m) with height of cavity above burner top, for 5 μl of 0.01 *M* $FeSO_4$ solution (cavity orifice vertically above central axis of burner). (○), Peak height; (●), integrated emission peak.

Distance of cavity from edge of flame. Figure 10 shows the effect on emission intensity of the horizontal position of the cavity in the flame. As the cavity moves further into the flame the emission occurs more quickly, *i.e.* a sharper, higher peak is obtained.

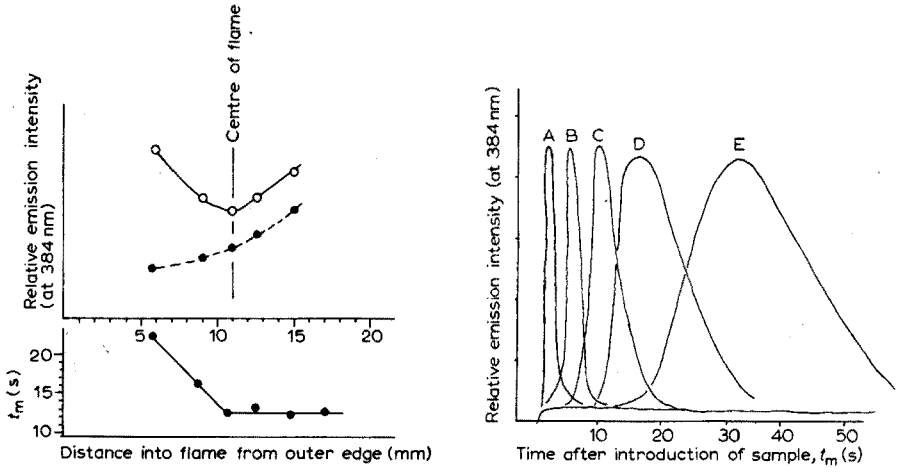

Fig. 10. Variation in S_2 emission and time to maximal emission (t_m) with horizontal displacement of cavity orifice, 2.5 cm above burner top. (●), Peak height; (○), integrated emission peak.

Fig. 11. S_2 emission for: A, thiourea; B, H_2SO_4; C, $FeSO_4$; D, $MnSO_4$; E, Na_2SO_4 (intensities not to scale), to illustrate the effect of sample volatility on rate of emission.

Effect of various sulphur compounds

Inorganic compounds. Aqueous solutions (5 μl) of various sulphur-containing compounds were injected into the cavity. The cavity was placed in the sample holder, and introduced into the flame, and the emission intensity at 384 nm was recorded. Figure 11 shows the emission responses obtained from H_2SO_4, $FeSO_4$, $MnSO_4$ and Na_2SO_4, as well as from thiourea. Since the intensity of emission decreases for less volatile compounds, the concentrations of these compounds were increased to keep the response obtained on the same scale. The time taken for a given sulphur compound to reach its maximal emission intensity is characteristic of that compound, and is related to the thermal breakdown and volatilization which occurs in the presence of the flame gases. The maximal intensity or, more exactly, the time integral of the intensity (areas under the peaks in Fig. 5) represents the total amount of the given sulphur compound placed in the cavity and can be used for quantitative analysis (see below).

Many interferences occurring in cool-flame emission analysis can be attributed to the formation of compounds which are not decomposed at very low temperatures, as discussed above. This effect is no longer a disadvantage with MECA, and can be used to confer selectivity based on the differences in thermal stability of compounds exposed to the flame.

By using the cavity temperature–time curve (Fig. 2), the time taken to reach maximal intensity after sample introduction (t_m) can be related to the temperature

TABLE I

TEMPERATURE OF MAXIMAL EMISSION

Compound	*Approximate temperature (°)*	*Reported decomposition* temperature (°)*
Thiourea	< 200	180 (decomp)
H_2SO_4	350	330 (b.p.)
$CuSO_4$	580	598–910 (decomp)
$FeSO_4$	550	> 720 (decomp)
$CoSO_4 \cdot 7H_2O$	530	820 (decomp)
$MnSO_4 \cdot 4\ H_2O$	640	> 940
Na_2SO_4	820	> 880

of the cavity at maximal emission. Table I gives this temperature for the compounds tested. The absolute values of temperature measured must be regarded as approximate.

The broadening effect seen in Fig. 11 for peaks obtained after increasing times t_m arises from the asymptote-like temperature curve in Fig. 2; the temperature range over which emission occurs is approximately the same for all the compounds studied in Fig. 11. The half-widths of the peaks all correspond to a 100° temperature change.

Peak measurement, and especially the sharpness of peaks obtained at the higher temperatures, can be improved by connecting the thermocouple output, via an amplifier, to the X-axis of an X–Y recorder, with emission intensity recorded on the Y-axis. This results in a direct plot of emission intensity *vs.* cavity temperature, and the peaks obtained are almost equally sharp and symmetrical for all analytes. Such a refinement appears to improve the resolution of different compounds.

The temperatures at which the metal sulphates give maximal emission are generally lower than the reported decomposition temperatures, and emission begins at even lower temperatures. This is almost certainly due to exposure to the highly reducing flame gases, which bring about decomposition at lower temperatures than by normal thermal processes. A detailed study of such effects may give some insight into the decomposition and volatilization processes that occur in the cavity to produce excited S_2 molecules.

Organic compounds. Organic compounds containing sulphur are usually more volatile than inorganic compounds. With a hydrogen–nitrogen–air flame, the cavity heats up rapidly, yielding a very rapid response for more volatile compounds, limited by the response time of the chart recorder. As a result, the precision of measurement of these more volatile compounds is rather poor ($\sigma = 8$–10%) when done with flames of relatively high air content, when a chart recorder is used. The precision can be improved by reducing the rate of heating of the cavity, thereby avoiding the almost explosive volatilization of the compound. This can be achieved by changing to a hydrogen–nitrogen diffusion flame and insulating the screw head with asbestos from the hot edge of the flame. The systems with and without air are compared in Fig. 12. This modification reduces the sensitivity although it does

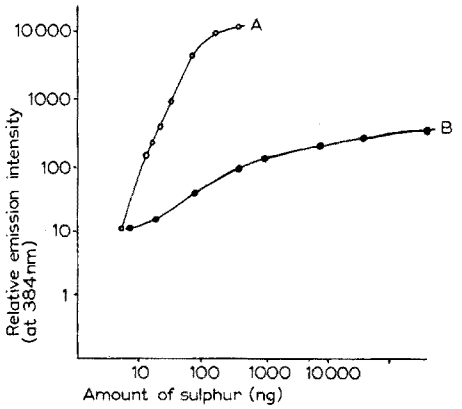

Fig. 12. Calibration plots for thiourea: A, with air added to the flame; B, without added air.

not appear to affect the limit of detection. Under the modified conditions, less volatile sulphur compounds (such as $MnSO_4$, $FeSO_4$ and Na_2SO_4) do not emit unless air is added to the flame.

At such reduced temperatures, the emission–time response from organic compounds becomes increasingly complex with increasing amounts of sample. Figure 13a shows how the single emission peak obtained from 16 and 32 ng of thiourea builds into multiple peaks with larger amounts of thiourea. Very large amounts of thiourea give the profile shown in Fig. 13b.

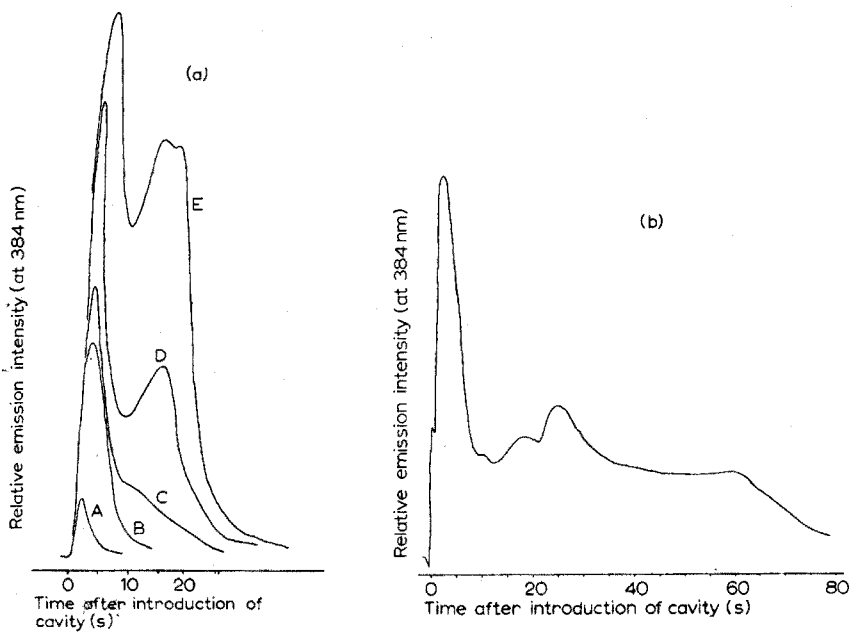

Fig. 13. (a) Effect of thiourea on the S_2 emission–time profile in a hydrogen–nitrogen diffusion flame. A, 16 ng; B, 32 ng; C, 160 ng; D, 400 ng; E, 800 ng of sulphur. (b) S_2 emission–time profile of 32 μg of thiourea in an asbestos-insulated screw in an air–hydrogen–nitrogen flame.

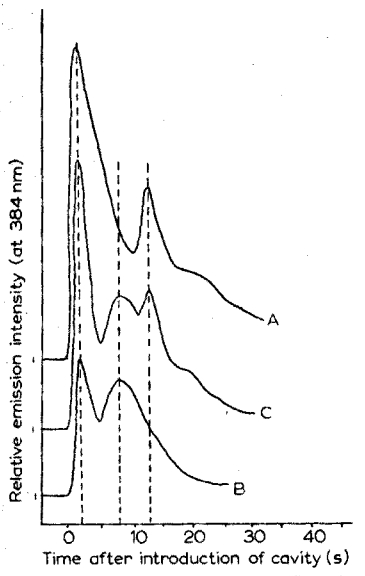

Fig. 14. S_2 emission–time profiles for: A, thiourea (200 ng); B, dimethylsulphoxide (200 ng); C, 1:1 (w/w) mixture of thiourea and dimethylsulphoxide (200 ng), in a hydrogen–nitrogen diffusion flame.

Similar effects were observed with other organic compounds. The emission–time profile appears to be characteristic of the particular sulphur compound. Thiourea and dimethylsulphoxide each have a characteristic profile (Fig. 14). The emission profile of a mixture of the two compounds is additive (Fig. 14), and thus offers the possibility of determining some mixtures of organic sulphur compounds. The emission profile is considered to be related to the volatilization and thermal and reductive breakdown of the sample in the steel cavity, as well as to possible suppressive effects arising from the various organic fragments that are produced during the decomposition.

Effect of solvent

Water in the cavity will remove hydrogen atoms from the flame by participating in the equilibrium:

$$H + H_2O \rightleftharpoons H_2 + OH$$

The emission intensity will therefore be reduced, unless water is removed before S_2 emission begins. For many inorganic compounds, removal of water is readily achieved by evaporation, without affecting the sample. Organic solvents would also be expected to remove hydrogen atoms from a fuel-rich flame, an effect which has been commented upon above. Figure 15 illustrates the effect of 50% (v/v) propanol–hexane as solvent for diphenylsulphide. Injection of 5 μl of the solution into the insulated cavity, and immediate introduction into the hydrogen–nitrogen flame, gives a delayed single peak. If solvent is allowed to evaporate in a nitrogen stream before insertion of the cavity into the flame, a new peak, appearing rapidly, emerges, which increases in intensity as the time allowed for solvent

evaporation is increased. The solvent, therefore, suppresses the first peak of diphenylsulphide emission, but is without significant effect on the second peak. In addition to its effect on emission intensity, solvent evaporation occurring during emission measurement decreases the precision of the measurement ($\sigma > 8\%$).

Procedure for the determination of sulphur in compounds

For the calibration curves obtained, reagent-grade iron(II) sulphate, sodium sulphate and thiourea were dissolved in distilled water and diluted to make 0.1 *M* solutions, which were then diluted to appropriate concentrations. To prepare the sulphur dioxide solution, sulphur dioxide was bubbled through distilled water which was then sealed with a septum. The concentration of sulphur dioxide was determined alkalimetrically after addition of hydrogen peroxide; the 1.47 *M* solution obtained in this way was diluted to appropriate concentrations by injecting known volumes into a series of septum-capped bottles containing distilled water.

The general procedure for the analysis consisted of taking 5-μl amounts of the given sample and injecting into a cavity at room temperature. The 5-μl volume of solution was sufficient to cover the back wall of the cavity and thereby deposit the analyte most reproducibly. The volume of liquid added with sodium sulphate and iron(II) sulphate was not critical, since the water was volatilized during the analysis before the analyte, and was not very critical with thiourea. On the other hand, a 2-μl volume was optimal for the sulphur dioxide sample which varied in the emission obtained for a given amount of sulphur with the volume of water present. In the sulphur dioxide determination the analyte vaporizes with the aqueous solvent.

Several depositions and evaporations could be used to concentrate the sample into the cavity (except in the case of sulphur dioxide).

The samples injected into the cavity in the above manner were then introduced into the flame as previously described, the emission at 384 nm being recorded and integrated.

Calibration graphs for various samples

Calibration graphs for various compounds are shown in Fig. 16. The integrated emission intensity decreases as the time for emission increases with different compounds, *i.e.* at higher cavity temperatures. This is attributed to the stronger molecular associations which may bind the sulphur, and to a possible enhancement of the S_2 emission at lower cavity temperatures as a result of the Salet phenomenon. The limit of detection for sulphur remains in the low nanogram region despite the large differences in emission intensity, except in compounds such as sodium sulphate.

When the hydrogen–nitrogen–air flame was used, the standard deviation throughout the calibrations of the various sulphur compounds remained at about 5%, except for thiourea, for which the standard deviation was about 10%. This poorer precision can be attributed to the speed at which the thiourea volatilizes, which is almost too fast for the recorder's 0.5-s response time.

Sulphuric acid gives only the $FeSO_4$ emission (occurring about 11 s after sample introduction and caused by reaction of the acid with the steel) when the amount of sulphur is less than 270 ng (5 μl of $3.33 \cdot 10^{-3}$ *M* solution). Greater

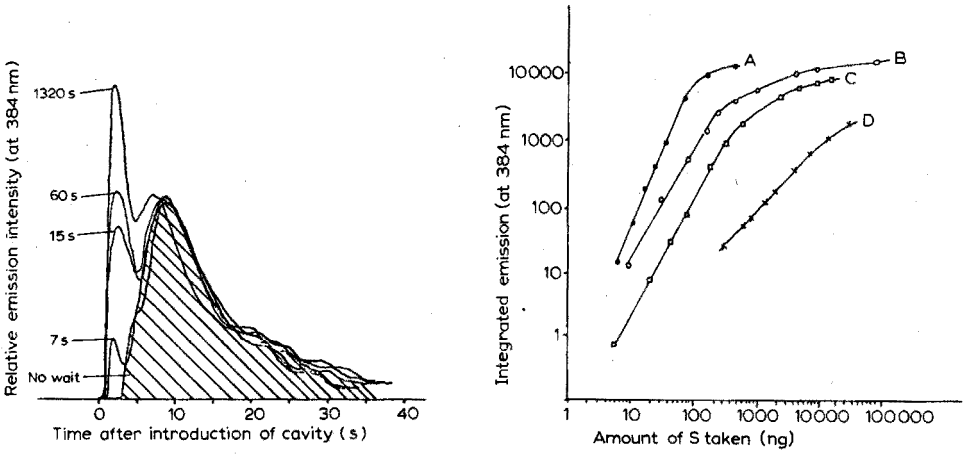

Fig. 15. Effect of solvent evaporation on S_2 emission–time profile of 13 μg of diphenylsulphide in 1:1 (v/v) hexane–propanol, for a hydrogen–nitrogen–air flame (see text).

Fig. 16. Calibration plots for: A, thiourea; B, SO_2 in water; C, $FeSO_4$; D, Na_2SO_4, with a hydrogen–nitrogen–air flame.

amounts of sulphuric acid also give another peak (4.5 s after introduction) from the acid itself.

OTHER MODIFICATIONS OF MECA

Hollow sample holder

Figure 17 is a diagram of a cavity into which samples can be introduced from the rear whilst the cavity orifice remains in an optimal position in the flame. Gases may be introduced directly into the cavity with this device. Additionally, the incorporation of a heated gas chromatography port, as shown in the Figure, allows solutions to be injected and vaporized in the port, and carried to the cavity by an inert gas stream. Solids can be pyrolyzed in a similar device, and the evolved gases carried to the cavity for analysis.

Continuous gas streams can be analysed by means of the hollow sample holder, including effluents from gas chromatography columns.

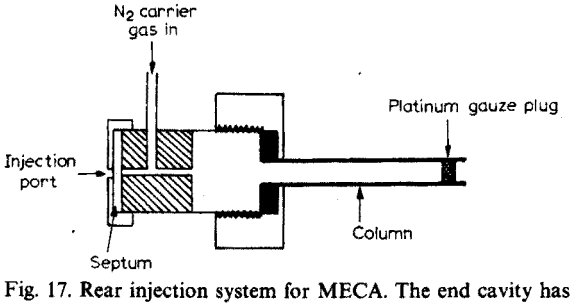

Fig. 17. Rear injection system for MECA. The end cavity has a diameter of *ca.* 4 mm.

Oxygen injection into cavity

A small flow of oxygen can be directed into the cavity via a small hole drilled in the side. This tends to concentrate an oxygen-rich portion of the flame inside the cavity, and makes the hydrogen flow rate less critical. In the presence of oxygen, the sulphur emission is destroyed because S_2 molecules are oxidized, but a number of emissions (*e.g.* boron and arsenic) are markedly enhanced. This technique also enables high temperatures to be reached within the cavity without the cavity and its immediate surroundings becoming incandescent.

Determination of other elements

The MECA technique can be applied essentially to all compounds that are sufficiently volatile and give an emission. Elements that give well-known emissions in cool flames, such as boron and phosphorus, can be determined very sensitively, as can chloride, bromide and iodide, based on indium halide emission. Metals that give volatile halides (*e.g.* Co, Sn, Pb, Cu) can also be determined, as well as elements that cannot be determined by emission measurements with nebulization for sample introduction (Se, Te, Si, As, Sb, etc.). Metal chelates, such as lead pyrrolidinedithiocarbamate and the nickel, palladium and copper chelates of amino-substituted β-diketones, on introduction to the cavity give emission bands characteristic of the metal and of the ligand, and very sensitive determination of the metal becomes possible. Organic halides[24] and other organic compounds also give intense characteristic emissions, that have analytical implications. These, and other applications, will be reported in detail in later papers.

CONCLUSIONS

MECA is a simple, versatile and very effective technique for carrying out cool-flame emission analysis. The sensitivity, although already reasonably high, is expected to be greatly enhanced when an instrument purpose-built for MECA has been constructed. The technique also offers the advantage for cool-flame emission analysis of allowing the analysis of microlitre volumes of solution.

The cavity enhances molecular emission intensity by:

(1) retaining the emitting species, thereby allowing the focussed emission to be measured by a relatively slow responding detector–recorder system;

(2) acting as a relatively cold body (Salet phenomenon);

(3) possibly acting as a third body in the ensuing molecular formation and/or excitation;

(4) localizing and concentrating the analyte into the most sensitive region in the flame;

(5) allowing introduction of the analyte without possible interfering effects of a solvent.

The MECA technique offers increased selectivity by differentiating between compounds via their thermal stability in a reducing medium, the flame, and MECA will enable the thermal properties of various compounds in the flame to be studied.

S. L. Bogdanski thanks the U.K.A.E.A., Aldermaston, for the provision of a research studentship.

SUMMARY

Analysis by molecular emission in cool flames is reviewed. A new analytical technique, utilizing such emissions, is described; the sample is deposited within a cavity at the end of a rod, and emission is stimulated within the cavity when placed in a hydrogen flame. The advantages of the technique are given, and the effects of many experimental parameters on the S_2 emission from sulphur compounds are studied in detail. Methods for the determination of ng amounts of inorganic and organic sulphur compounds in μl samples are described. Other applications are briefly outlined.

RÉSUMÉ

Les analyses par émission moléculaire en flammes froides sont passées en revue. Une nouvelle méthode est décrite: on dépose l'échantillon à analyser dans une cavité à l'extrémité d'une baguette. L'émission est stimulée à l'intérieur de la cavité, dans une flamme d'hydrogène. Les avantages de cette technique sont donnés. On examine en détail l'influence de nombreux paramètres expérimentaux sur l'émission S_2 de composés sulfurés. Des méthodes sont décrites pour le dosage de composés sulfurés inorganiques et organiques, en quantité de l'ordre du ng par μl. D'autres applications sont brièvement décrites.

ZUSAMMENFASSUNG

Es wird ein Überblick über die Analyse durch Molekülemission in kühlen Flammen gegeben. Ein neues analytisches Verfahren unter Verwendung solcher Emissionen wird beschrieben. Die Probe wird in einen Hohlraum am Ende eines Stabes gebracht, und die Emission wird innerhalb des Hohlraumes angeregt, wenn dieser in eine Wasserstoff-Flamme eingeführt wird. Die Vorteile des Verfahrens werden angegeben, und der Einfluss vieler experimenteller Parameter auf die S_2-Emission von Schwefelverbindungen wird im einzelnen untersucht. Methoden für die Bestimmung von ng-Mengen anorganischer und organischer Schwefelverbindungen in μl-Proben werden beschrieben. Andere Anwendungen werden kurz angeführt.

REFERENCES

1 R. Belcher, Lecture presented at *Euroanalysis I Conference, Heidelberg, Germany*, R. Belcher, *Z. Anal. Chem.*, 263 (1973) 257; R. Belcher, S. Bogdanski, Z. Kassir and A. Townshend, *Provisional Patent*, August, 1972, (no. 39443/72).
2 E. Muldar, *J. Prakt. Chem.*, 91 (1864) 111.
3 W. N. Hartley, *Phil. Trans. R. Soc., Ser. A*, 185 (1894) 161.
4 G. Salet, *C. R.*, 68 (1869) 404; 73 (1871) 559; 74 (1872) 865.
5 C. Veillon and J. Y. Park, *Anal. Chim. Acta*, 60 (1972) 293.
6 S. S. Brody and J. E. Chaney, *J. Gas Chromatogr.*, 4 (1966) 293.
7 R. M. Dagnall, K. C. Thompson and T. S. West, *Analyst*, 92 (1967) 506.
8 A. Syty and J. A. Dean, *Appl. Opt.*, 7 (1968) 1331.
9 R. Smith, C. M. Stafford and J. D. Winefordner, *Anal. Chim. Acta*, 42 (1968) 523.
10 W. L. Crider and R. W. Slater, *Anal. Chem.*, 41 (1969) 531.

11 H. Massmann, *Proc. Colloq. Spectrosc. Int., XIII*, Adam Hilger, London, (1967) 284.
12 B. V. L'vov, *Spectrochim. Acta*, 24B (1969) 53.
13 T. S. West and X. K. Williams, *Anal. Chim. Acta*, 45 (1969) 27.
14 E. S. Beatrice, I. Harding-Barlow and D. Glick, *Appl. Spectrosc.*, 3 (1969) 23.
15 J. A. Ramsay, *J. Exptl. Biol.*, 27 (1950) 407.
16 H. Brandenberger, *Chimia*, 22 (1968) 449.
17 D. Clark, R. M. Dagnall and T. S. West, *Anal. Chim. Acta*, 58 (1972) 339.
18 F. J. Fernandez and H. L. Kahn, *At. Absorption Newslett.*, 7 (1968) 35.
19 J. R. Sarbeck, P. A. St. John and J. D. Winefordner, *Mikrochim. Acta*, (1972) 55.
20 K. M. Aldous, R. M. Dagnall and T. S. West, *Analyst*, 95 (1970) 417.
21 S. Greenfield and P. B. Smith, *Anal. Chim. Acta*, 59 (1972) 341.
22 R. Belcher, S. Bogdanski and A. Townshend, *Talanta*, 19 (1972) 1049.
23 T. Sugujama, V. Suzuki and T. Takeuchi, *J. Chromatogr.*, 77 (1973) 309.
24 W. L. Crider, *Anal. Chem.*, 41 (1969) 534.

Analytica Chimica Acta, 67 (1973) 17–28

THE ACCURATE DETERMINATION OF MAJOR COMPONENTS IN Ga_xSe_y BY MEANS OF INSTRUMENTAL NEUTRON ACTIVATION

E. BRUNINX

Philips Research Laboratories, Eindhoven (The Netherlands)

(Received 4th April 1973)

In a recent survey[1] of neutron activation analysis it was stated that the accuracy of analysis by this technique lies around 2%. This statement is slightly ambiguous, but it seems quite astonishing that after nearly 20 years of activation analysis, no well supported arguments or facts are given to indicate why uncertainties smaller than 2% cannot be obtained.

This paper describes an examination of neutron activation for the accurate determination of the major components in a binary compound. To be useful the analytical method must satisfy the following criteria.

(*a*) The overall uncertainty* arising from all sources of systematic errors and imprecision, should be of the order of 0.1% of the final concentration for both components separately (10% by weight < concentration < 90% by weight).

(*b*) Standards should be made up from combinations of the pure elements. It is unreasonable to expect certified standards to be available for every possible binary chemical compound. The composition of these standards must be known with an overall uncertainty of better than 0.1%.

(*c*) *A priori* assumptions about the relation between measured signal and concentration must be strictly minimized.

In a previous paper[4], it was shown that Ga_xSe_y could be analysed for gallium by neutron activation with an overall uncertainty of 0.1%. The selenium content could not be determined owing to the inefficiency of the detection system.

In this paper the detection system has been considerably improved so that analyses for selenium are equally feasible. In addition, the comparative analytical method (wavelength-dispersive X-ray fluorescence) has been improved in various respects, so that the titrimetric method used in the earlier work as a second comparative method could be omitted.

In the following paragraphs, the method of analysis, the counting technique and the data analysis are discussed. Experimental details and mathematical formulae are described at the end.

METHOD OF ANALYSIS

For the determination of a major component of a binary compound by neutron activation, the following conditions must be met.

* The adopted terminology is described in detail by Ku[2] and Eisenhart[3].

(*a*) The concentration of impurities that can be activated by neutrons must be such that

$$\frac{\text{activity of impurities}}{\text{activity of major component}} \leqslant 1:10^4$$

This requirement is especially important for short-lived activities: long-lived activities might perhaps be incorporated in the background, provided that they can be estimated with a sufficiently small overall uncertainty. This condition is reasonable, because a stoichiometric analysis usually means the availability of compounds with a very low concentration of impurities.

(*b*) The cross-sections of the two major elements and the half-lives of the nuclides formed after neutron irradiation must be such that after a short or long irradiation only the short-lived or the long-lived component, respectively, is measured (after the long irradiation, the short-lived nuclide must obviously be allowed to decay away before the long-lived nuclide is measured*).

(*c*) The compound to be analysed must be soluble in a readily controllable medium (*e.g.* acid). The preparation of standards is then greatly simplified. The use of solutions has also the advantage that effects caused by different γ-ray absorption in samples and standards are greatly reduced. Moreover, the weighing technique has a small overall uncertainty.

(*d*) The approximate composition of the compound must be known, so that the standards can be restricted to a narrow concentration range.

Conditions (*a*) and (*b*) imply that only one nuclide at a time is counted, so that simple integral counting techniques can be used.

In view of conditions (*c*) and (*d*) it is easy to "surround" the sample by a number of standards chosen in such a way that the amount of gallium (or selenium) is within 20% of the expected concentration in the Ga_xSe_y. In the example shown in Fig. 1, standards 1 and 2 are rather close together and about 20% below the expected concentration in the sample; standard 3 is near the expected selenium concentration in Ga_xSe_y and standard 4 is about 20% above the third standard[5].

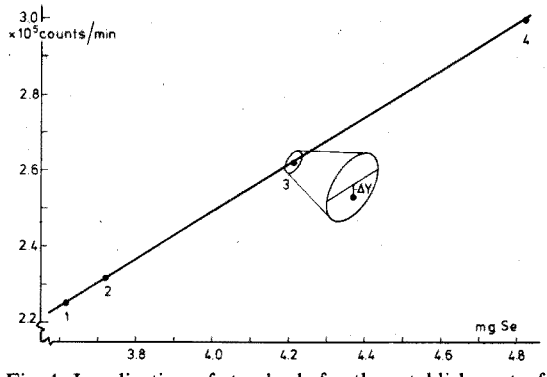

Fig. 1. Localization of standards for the establishment of the calibration line in a neutron activation experiment. Δy = difference between calculated line and measured point.

* Analysis of two-component decay curves is possible but requires a somewhat different approach.

These experiments were designed to achieve minimal overall uncertainty, hence the analyses were done on samples taken from a single stock solution of Ga_xSe_y. In this way, possible interferences from sample inhomogeneity and sampling were largely eliminated.

The principle of instrumental major component analysis by means of neutron activation can be written as follows:

$$A = KN \tag{1}$$

where A is the measured radioactivity, K the proportionality factor, and N the number of nuclei present in sample (standard). $K = \sigma\phi$, where σ is the cross-section, and ϕ the neutron flux.

Some comments regarding eqn. (1) are necessary. Since N depends on the isotopic composition[6], differences in the isotopic abundance of standards and elements will obviously influence the inaccuracy of the results. It has been shown that the usual stationary irradiation technique gives too large a spread in the value of K[7]. During all irradiations (long or short), samples and standards were therefore rotated by means of a pneumatic device (Fig. 2); 4 standards and 2 samples (unknowns) can be irradiated simultaneously. The simple relation (1) may not be applicable under all circumstances, especially when N and σ become large. For the gallium (or selenium) concentrations employed in the irradiations, the fractional reduction, f, of the neutron flux inside the sample is 0.99985 for gallium and 0.99955 for selenium. These reductions are negligible, so that a calibration curve can be constructed with standards containing only gallium or selenium.

In wavelength-dispersive X-ray fluorescence analysis, the proportionality factor is a complicated function of the elements present, their absorption coefficients, etc. Accordingly, all standards must contain gallium and selenium in such quan-

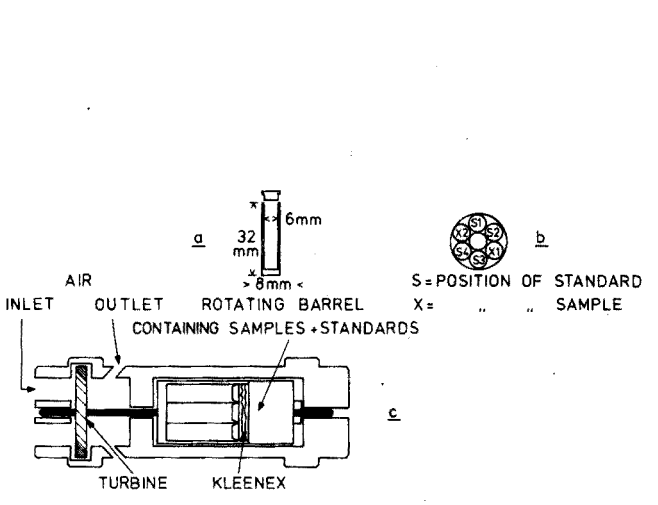

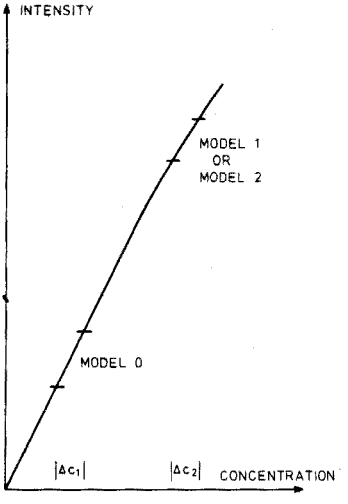

Fig. 2. (a) Dimensions of polythene sample tube. (b) Distribution of standards and samples in irradiation can. (c) Schematic drawing of rotating sample holder.

Fig. 3. Dependence of X-ray intensity upon concentration and choice of model.

tities that:

$$([Ga]+[Se])_{standard} = [Ga_xSe_y]_{sample}$$

Moreover, an expression analogous to eqn. (1) is not always applicable to X-ray fluorescence. As an example, Fig. 3 shows schematically the intensity of gallium KX-rays as a function of the amount of gallium present. In a narrow concentration region such as $\Delta C1$, the intensity–concentration relation may be expressed by

$$\text{Model 0:} \quad A = K_1 C \tag{2}$$

and in the region $\Delta C2$ by

$$\text{Model 1:} \quad A = K_1' C + K_0' \tag{3}$$

If the imprecision of the measured intensities is sufficiently small, it might even be more appropriate to fit the data in region $\Delta C2$ with

$$\text{Model 2:} \quad A = K_2'' C^2 + K_1'' C + K_0'' \tag{4}$$

The choice of the most appropriate model is discussed under Data analysis.

In X-ray fluorescence standards and samples must receive the same quantity of exciting X-rays, and rotation as for neutron activation is, of course, impossible. Reliance must therefore be placed on the stability of the X-ray apparatus.

The most important sources of uncertainty in the application of eqn. (1) to the neutron activation of major components are therefore: possible fluctations in the value of K during irradiation (this contribution is evaluated later); and weighing of standards and samples. On the basis of the smallest amounts weighed (200 mg of solution in a 700-mg polythene vial) the standard deviation was found to be $0.4 \cdot 10^{-3}\%$. The maximum possible systematic error in the weights found with the Mettler M5 balance is about 20 μg[8,9].

COUNTING TECHNIQUE FOR NEUTRON-ACTIVATED SAMPLES AND STANDARDS

The overall uncertainty, ΔA, in a counting experiment can be described by

$$\Delta A = (\sigma_p^2 + \sigma_i^2)^{\frac{1}{2}} \pm \text{systematic errors} \tag{5}$$

where σ_p^2 is the variance arising from counting statistics, and σ_i^2 is the variance arising from instrumental instabilities.

An important source of systematic errors was found in the dependence of the count rate on small differences in the height of the solutions filling the small polythene vials. Three detectors—2 well-type crystals and a scintillation chamber—were compared. The scintillation chamber is a counter developed during this project. It is insensitive to source displacements and similar in geometric shape to the ionization chamber, but with a much higher detection efficiency[10].

The comparison was made as follows. A small glass vial was filled to a height of 22 mm (about 2 ml) and the activity ($A22$) was measured in all three detectors. Water was added to raise the solution level to 32 mm and the activity ($A32$) of the samples was measured again in all three detectors. Figure 4 shows the position of the sources in both types of counters. Table I shows the $A32/A22$ ratios; D is the percentage change in activity for a deviation of 1 mm in the

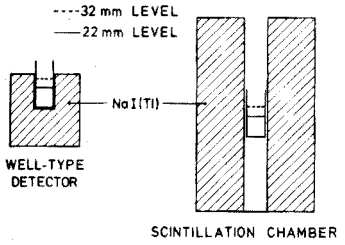

Fig. 4. Well-type detector and scintillation chamber.

TABLE I

RESPONSE OF WELL-TYPE DETECTORS AND SCINTILLATION CHAMBER FOR SMALL DISPLACEMENTS OF SAMPLE

Detector	*Dimensions (mm)*	$\frac{A32}{A22}$	*D (%/mm)*
NaI(Tl) Well-type detector	44∅ × 50.8 Well: 16.7∅ × 39	0.945	0.550 ± 0.045^a
	76.2∅ × 76.2 Well: 22∅ × 38	0.947	0.530 ± 0.007^a
NaI(Tl) Scintill. chamber	133 × 205∅ Shaft: 25∅ × 205	0.9997	0.003 ± 0.013

[a] *D* varies with the filling height of the solution in the vial.

solution level. The imprecision in the *D* values is based upon counting statistics only (1σ).

These differences of *D* (in %/mm) may appear fairly small, but it must be remembered that filling a vial to an identical height within 0.1 mm (in order to reduce the change in activity to less than 0.1%) is almost impossible. Besides the advantage of being insensitive to source displacements, the scintillation chamber has the additional advantage of much higher efficiency than the usual well-type detectors.

Apart from errors arising from the type of detector, the method of counting has also its errors (systematic or random). γ-Ray spectrometry is effective for the determination of many nuclides, but it has the drawback that the determination of the photopeak area is often exposed to a fairly large uncertainty[11]. Since only one nuclide—either gallium or selenium—was counted at one time, and since the purity of the material was such that no interfering nuclides were present, γ-ray spectrometry was superfluous in this work. All neutron-activated samples were therefore counted by integral counting techniques. Every sample was counted 5 times and the number of counts collected in each counting interval was about 10^6; details are given under Experimental.

The stability of the whole counting chain was such that over a period of 1 day, a standard deviation (single determination) of 0.03% was observed for a

series of measurements (*ca.* 10^7 counts collected in each measurement). For longer periods (2 weeks) the standard deviation was somewhat higher: (0.09%).

DATA ANALYSIS

Before it can be decided which model should be chosen to relate measured net activities to weighed standards, three assumptions are necessary:

(*a*) the measured activities are distributed normally, which is reasonable in view of the large number of counts collected;

(*b*) the measured activities all have the same standard deviation, which is not entirely true, but is permissible since the activities of the four standards do not differ very much (see above);

(*c*) the weights of the standards have an error which is negligible compared to the error of the activities.

The technique to decide whether to choose Model 0 (eqn. 2), Model 1 (eqn. 3), or Model 2 (eqn. 4) to relate the activities—from either neutron activation or X-ray fluorescence—to the weights of the standards is discussed briefly under Experimental and in greater detail by Mandel[12]. Table II summarizes the results.

TABLE II

TYPE OF EQUATION CHOSEN TO RELATE MEASURED ACTIVITIES AND CONCENTRATION OF STANDARDS

	Ga	*Se*	*Number of points on calib. line*
Neutron activation			
Irrad. 1	Mod. 0	Mod. 0	4
Irrad. 2	Mod. 0	Mod. 0	4
Irrad. 3	Mod. 0	Mod. 0	4
Wavelength-dispersive X-ray fluorescence			
Mo tube, SA[a]	Mod. 1	Mod. 0	4
Mo tube, HS[a]	Mod. 2	Mod. 2	4, but counted
W tube, HS	Mod. 2	Mod. 2	3 times each

[a] See Experimental, Irradiation sources.

Six neutron irradiations (three each for gallium and selenium) were done, each of them with 4 standards and 2 samples, spread out over a period of several months. Analysis with X-ray fluorescence has no restrictions regarding the number of samples, so that the measurements with one type of instrument can easily be done in one day. It was found that in all six neutron irradiations the simple eqn. (2) (Model 0) could be applied.

The models chosen for the X-ray fluorescence results with SA were 1 and 0 for gallium and selenium, respectively, while model 2 was chosen for all HS results. This can be explained as follows: for SA only 4 standards (counted once) were used to make the calibration line. With HS, 4 standards (counted 3 times) were available, making a total of 12 points. Near the end of this work, however, it was

found that the SA instrument had not been allowed sufficient time after the high voltage and current settings had been altered; this longer stabilization period was observed for HS. The lower imprecision and the larger number of data points would therefore be expected to yield a quadratic curve as the optimal relation between measured activities and weights of the standards. The use of higher-order polynomials for the calibration line does not yield a significant improvement.

Since the data are best represented by eqn. (2) for neutron activation, the differences, Δy, between the fitted line and the experimental values can be calculated (see Fig. 1). These differences can be attributed to the following sources of uncertainty: fluctuations of $\sigma\phi$ ($\Delta\sigma\phi$), weighing error (ΔW), and counting error (ΔA). Thus

$$(\Delta y)^2 = (\Delta\sigma\phi)^2 + (\Delta W)^2 + (\Delta A)^2 \qquad (6)$$

Since Δy, ΔW and ΔA are known, the contribution of $\Delta\sigma\phi$ can be estimated crudely. This can be illustrated by means of the counting and calibration data of ^{75}Se in all 3 irradiations.

$\Delta A = 0.06\%$ (based on 3×4 standards)
$\Delta W = 0.410^{-3}\%$ (see: Method of analysis)
$\Delta y = 0.11\%$ (this represents the average of all deviations (12 in total) from the calibration line).

Substitution in eqn. (6) yields:

$$(\Delta\sigma\phi)^2 = 0.11^2 - 0.06^2 - (0.410^{-3})^2 \cong 0.09^2$$

This value of 0.09 is a rough indication of the fact that the major source of uncertainty is found in the irradiation stage.

The basic features of the neutron activation method for the accurate analysis of major components can be summarized as follows:

1. samples and standards are in the form of solutions; all preparations are made on a weighing (not pipetting) basis;
2. absence of impurities;
3. simultaneous irradiation of standards and samples in a rotating irradiation facility;
4. integral counting techniques by means of the scintillation chamber.

So far the uncertainties in the various steps of neutron activation have been described and estimated separately. In the next section the overall uncertainty of the whole procedure will be estimated from a number of analyses.

FINAL RESULTS OF ANALYSES

The results for both analytical techniques, neutron activation and wavelength-dispersive X-ray fluorescence, are summarised in Table III.

On the basis of the F test[13], no evidence was found that the variances in the neutron activation and X-ray fluorescence method differ for gallium. Pooling all gallium data for the four techniques and applying the Bartlett test likewise failed to yield any differences in the variances[13].

The F test again indicates no difference for the selenium variances in the two methods although the SA results are closer to the critical value; the Bartlett

TABLE III

SUMMARY OF ALL ANALYTICAL RESULTS

(Concentrations in weight %)

	Neutron activation		*X-ray fluorescence*					
	Ga	*Se*	*SA, Mo tube*		*HS, Mo tube*		*HS, W tube*	
			Ga	*Se*	*Ga*	*Se*	*Ga*	*Se*
Mean, C	41.76	58.19	41.78	58.46	41.76	58.19	41.80	58.36
Stand. dev., s	0.04	0.06	0.04	0.14	0.08	0.06	0.07	0.05
Relat. stand. dev. (%)	0.10	0.10	0.09	0.24	0.18	0.10	0.17	0.09
95% confidence level ($ts/\sqrt{n}$)	0.05	0.06	0.05	0.18	0.05	0.04	0.05	0.03
No. of meas. (n)	6	6	5	5	12	12	12	12

test indicates a difference which can be traced back to the SA results.

Another important point is whether or not there are significant differences between the mean values for one element by the two techniques. No difference[14] could be detected for the gallium results, whereas the results from SA and HS (W tube) were different for selenium. Although it was found that SA was not sufficiently stabilized (see Data analysis), it is not clear how this could influence the mean value. The higher results from HS can be explained by the interference of the W $L\gamma_1$ line which lies close to the Se $K\alpha_{1,2}$ line, so that an inaccurate background correction may be reflected in a higher selenium percentage.

These two simple tests make it possible to eliminate the results from the SA instrument (probably insufficiently stabilized) and the results from the HS instrument with the W tube (inaccurate background correction).

CONCLUSIONS

For the various intermediate steps of the instrumental neutron activation analysis of a binary compound, the different sources of error are summarized in Table IV. Of all the systematic errors mentioned, few have been studied in sufficient detail in order to give a numerical value; all the others must be considered as an indication of possible sources of trouble.

The analysis time is a function of the half-life of the nuclide measured; *e.g.*, for gallium, a complete analysis of 2 samples and 4 standards can be done in 2 days while for selenium 2 weeks are required (decay of induced gallium activity). The X-ray fluorescence method is certainly much faster since both elements can be done in about 1 day. In both methods, small quantities of material can be analysed.

A drawback of neutron activation is the necessary rotation during irradiation. Since these rotating sample holders are made of plastic, their useful life is limited especially in neutron fluxes of 10^{12} n cm^{-2} s^{-1}.

TABLE IV

SUMMARY OF SOURCES OF RANDOM ERROR AND SYSTEMATIC ERROR

Source	*Imprecision*[a] *(%)*	*Systematic errors*
Weighing	10^{-3}	Evaporation during filling: negligible[9]
		Electrostatic charging; magnitude unknown; probably small when equilibration is observed
		Deviations from the nominal weight: < 20 μg absolute[9]
Irradiation	0.1	Sharp fluctuations in neutron flux during irradiation in the reactor
		Variations in isotopic abundances
Counting	0.03	Variation of dead time
		Half-life effects; probably very small

[a] Expressed as $s \times 100/\bar{x}_n$, where $s=[d^2/(n-1)]^{\frac{1}{2}}$, d being the difference of the measurement and the mean, and n the number of measurements.

Mutatis mutandis, the described techniques can be employed for measuring variations in stable isotope abundances. The very stable scintillation chamber together with its insensitivity to source displacements is then a big asset.

EXPERIMENTAL

Standard and sample solutions

Gallium metal (Alusuisse) and selenium metal (M.C.P. El. Ltd.) were the starting materials for the standard solutions. The principal impurities were oxygen and carbon (20 p.p.m. each). No metallic impurities were present. Ga_xSe_y was also free of any metallic impurity. Both metals were dissolved (separately) in 7 *M* nitric acid in weighed volumetric flasks. Gallium dissolved slowly: about one week was required. After dissolution the acidity was reduced to 2 *M* nitric acid. Ga_xSe_y was treated in the same way. The amounts of Ga, Se and Ga_xSe_y were chosen so that the final concentration was 10 mg g^{-1} of solution. Especially for the X-ray fluorescence method, it was desirable that all the final concentrations should be as nearly identical as possible. All weighings were made after thermal equilibrium had been reached at a temperature of $(22 \pm 1)°$. Corrections for buoyancy had to be applied. All weighings for neutron activation were done on a Mettler M5 balance and all the others on a Mettler B5 balance.

Sample and standard holders

Standards and samples for neutron activation were prepared by weighing the desired amount of solution into small (6-mm i.d., 32-mm high) polythene cylinders (Model TS 730, Emergo Plastics, Landsmeer, The Netherlands). All cylinders were tested for possible leaks before use. After the desired amounts of Ga (or Se) or Ga_xSe_y solution were weighed, all the volumes were made up so that the tubes were filled to the same height.

After filling the covers were sealed to the tubes by means of a heat sealer ("Sealine" sealer, Century, Chicago). This step requires careful control since small leaks can sometimes develop.

Holders for the X-ray fluorescence method were the standard solution holders (Philips PW 1527/30) with a 12.5-μm Mylar window; 5 ml of solution were used both for standards and for samples. During irradiation the holders were covered with a watchglass.

Irradiation sources

Neutron activation. Irradiations were done in the BR-1 reactor (Mol, Belgium). Gallium irradiations lasted about 3–4 min and selenium irradiations 2 h. The approximate thermal flux was $3 \cdot 10^{11}$ n cm^{-2} s^{-1}.

X-ray fluorescence. Two instruments were employed. One was a Philips PW 1220, Mo tube 40 kV, 20 mA, LiF 200 crystal, scintillation detector with a narrow collimator and automatic pulse-height discrimination (referred to as SA). The second instrument was a Philips PW 1540, with the same instrument settings and using a Mo or W tube but without automatic pulse-height discrimination (referred to as HS).

The instrument was housed in an air-conditioned room ($t = 22 \pm 1°$). The high-voltage generator was connected to the ordinary 220 V mains, while all electronic measuring units were fed by a stabilized motor generator set.

The formula[15] used to estimate the fractional reduction of the neutron flux inside the sample was:

$$f = \frac{r\left[1 - \frac{n\sigma r}{2}\left(0.9228 + \ln\frac{1}{n\sigma r}\right)\right] + 1\left[1 - \frac{4}{3}n\sigma r\right]}{r + l}$$

where r = inner radius of polythene cylinder,
l = height of solution in the polythene vial,
n = atom density (atoms cm^{-3}),
σ = average thermal neutron cross-section (cm^2).

Counting

Neutron-activated samples. Samples for gallium analysis were counted after a 3–4 h waiting period (decay of short-lived Ga and Se activities). Selenium was counted after a 2 weeks' waiting period (decay of ^{72}Ga). All gallium samples were counted with the scintillation chamber described previously[10]. The liquid scintillator filling of this version does not permit the measurement of ^{75}Se radiations; ^{75}Se was therefore measured on a NaI(T1) detector of similar shape and dimensions. Counting times varied between 40s(Ga) and 400s(Se). The measurements were done in the following sequence: S1–S2–X1–S3–S4–X2, S denoting the standards and X the samples.

The counting data were corrected for background, dead-time and counting time by means of a computer program. This program calculates the activity at a given time by means of a least-squares analysis and a fixed half-life[16] of 14.0 h for ^{72}Ga and 119.9 d for ^{75}Se. Deadtimes were measured by means of the method of proportional sources[17]. High-voltage supply, Philips PW 4221; amplifiers, Ortec 486 followed by an Ortec 442 pulse stretcher; scaler-timer, Ortec 431.

Wavelength-dispersive X-ray fluorescence. The counting sequence for the HS instrument (see above) was as follows.

	Thick Cu standard	40 s
Se data: Standard:	BG-1 (background)	40 s
	Se-line	3×40 s
	BG-2	40 s
Ga data: Standard:	BG 3	40 s
	Ga-line	3×40 s
	BG 4	40 s
Se in sample:	BG 1	40 s
	Se-line	3×40 s
	BG 2	40 s
Ga in sample:	BG 3	40 s
	Ga-line	3×40 s
	BG 4	40 s
	Thick Cu standard	40 s

All counting was done in the integral mode. The counting cycle in the case of the SA (Mo tube) was simplified: the copper standard was omitted and the element line was counted for 40 min only. The data were only corrected for background.

The purpose of the copper standard was simply to verify the stability of the instrument.

Choice of model of calibration line

The K coefficients in eqns. (2), (3) and (4) were calculated by means of least squares. Then Model 2–Model 1 and Model 1–Model 0 were compared. In other words, we tested whether K_0'' or K_0' was zero, using the quantity F at the 95% level as a criterion.

The assistance of M. van Meijl during the earlier phases of the work, the discussions with M. Prins on aspects of statistical methodology, and the preparation of the Ga_xSe_y sample by M. van Dommelen, are gratefully acknowledged.

SUMMARY

The various phases of the major component analysis of Ga_xSe_y by means of instrumental neutron activation were examined. The overall uncertainty for each element was of the order of 0.1% of the final concentration, and no indication of systematic error was found between neutron activation analysis and the comparative method, *i.e.* wavelength-dispersive X-ray fluorescence analysis. The pronounced reduction in the overall uncertainty was made possible by an improved version of a NaI(Tl) detector (scintillation chamber) and by rotation of the samples during irradiation.

RÉSUMÉ

On examine les diverses phases de l'analyse de Ga_xSe_y par activation

neutronique. L'incertitude pour chaque élément est de l'ordre de 0.1% de la concentration finale. Aucune indication d'erreur systématique n'a été trouvée entre l'analyse par activation neutronique et la méthode de comparaison, analyse de fluorescence aux rayons-X. On diminue au maximum l'incertitude en utilisant un nouveau modèle de détecteur NaI(T1) (chambre de scintillation) et par rotation des échantillons au cours de l'irradiation.

ZUSAMMENFASSUNG

Die verschiedenen Schritte bei der Analyse der Hauptbestandteile von Ga_xSe_y mittels instrumenteller Neutronenaktivierung wurden untersucht. Die Gesamt-Unsicherheit für jedes Element war grössenordnungsmässig 0.1% der Endkonzentration; Anzeichen für einen systematischen Fehler wurden zwischen Neutronenaktivierungsanalyse und der Vergleichsmethode, d.h. wellenlängendispersiver Röntgen-Fluoreszenz-Analyse, nicht festgestellt. Die vorhergesagte Verringerung der Gesamt-Unsicherheit wurde durch eine verbesserte Ausführung eines NaJ(T1)-Detektors (Szintillationskammer) und durch Drehung der Proben während der Bestrahlung verwirklicht.

REFERENCES

1 V. Guinn, in Weissberger and Rossiter, *Physical Methods of Chemistry*, Vol. I, Part IIID, Wiley–Interscience, New York, 1972, Ch. VII, p. 491.
2 H. H. Ku. *Meas. Data*, 2, No. 4 (1968) 72.
3 C. Eisenhart, *Science*, 160 (1968) 1201.
4 E. Bruninx, *Meetings on Activation Analysis, Saclay, Oct. 1–6, 1972.*
5 A. Hubaux and G. Vos, *Anal. Chem.*, 42 (1970) 849.
6 P. Kruger, *Principles of Activation Analysis*, Wiley–Interscience, New York, 1971, Ch. 2.
7 E. Bruninx, *Anal. Chim. Acta*, 60 (1972) 207.
8 Y. le Gallic, *Rapport CEA-R-4169*, 1971.
9 W. van der Eyk and R. Vaninbroukx, *Nucl. Instrum. Methods*, 102 (1972) 581.
10 E. Bruninx, *Nucl. Instrum. Methods*, 106 (1973) 613.
11 P. Baedeker, *Anal. Chem.*, 43 (1971) 405.
12 J. Mandel, *The Statistical Analysis of Experimental Data*, Wiley–Interscience, New York, 1967, Ch. 8.
13 K. Brownlee, *Industrial Experimentation*, H.M.S.O., London, 1953.
14 H. H. Ku (Editor), *Precision Measurement and Calibration*, NBS Spec. Publ. 300, Vol. 1, 1969, p. 318.
15 J. Gilat and Y. Gurfinkel, *Nucleon.*, 21, No. 8 (1963) 143.
16 C. Lederer, J. Hollander and I. Perlman, *Table of Isotopes*, J. Wiley, New York, 6th Ed., 1967.
17 G. Rudstam, *Nucleon.*, 19, No. 12 (1961) 62.

Analytica Chimica Acta, 67 (1973) 29–36

DETERMINATION OF INDIUM IN ROCKS BY SUBSTOICHIOMETRIC RADIOISOTOPE DILUTION ANALYSIS

L. PAUL GREENLAND and E. Y. CAMPBELL
U.S. Geological Survey, Washington, D.C. 20244 (U.S.A.)
(Received 15th, February 1973)

Studies of the geochemistry of indium require a rapid technique applicable to the 0.01 p.p.m. concentration range. Conventional spectrophotometric, atomic-absorption, and spectrographic methods are not adequately sensitive. Neutron activation[1–3] has the requisite sensitivity, but the necessary radiochemical separations preclude efficient analysis of large numbers of samples.

Substoichiometric isotope dilution methods for the determination of nanogram amounts of a number of elements[4,5], including indium[6], have been described. The methods are based on the reaction of a metal with less than a stoichiometric amount of a complexing reagent, separation of the excess of metal, and a determination of the specific activity of the complexed metal. The reaction conditions can be calculated from known stability constants (*e.g.* ref. 7). Separations preceding the determination need not be quantitative as long as the metal is in excess of the complexing reagent. The present paper describes a substoichiometric isotope dilution procedure suitable for routine analysis of the low concentrations of indium in silicate rocks.

EXPERIMENTAL

Reagents

Standard indium solution. Dissolve 0.100 g of metallic indium in 10 ml of concentrated nitric acid. Dilute to 1 l in a volumetric flask with 0.18 *M* sulfuric acid to give a concentration of 100 μg In ml^{-1}. Make further dilutions as necessary with 0.18 *M* sulfuric acid.

EDTA solution. Prepare an 0.01 *M* solution by dissolving 0.372 g of disodium ethylenediaminetetraacetate dihydrate in 100 ml of water. Prepare a dilute stock solution each week by dilution of this solution to $4 \cdot 10^{-5}$ *M* with water. Prepare the reagent solution just before use by further dilution to $4 \cdot 10^{-7}$ *M*.

Tracer solution. Dilute commercially available ^{114}In solution with 0.18 *M* sulfuric acid so that 0.05 ml yields about 3000 counts per min. From our supplier a 0.05-ml aliquot contained about 15 ng In; adjustment may be necessary for tracers from other suppliers.

Reagent purification. Sulphuric acid was J. T. Baker Co. ultra-pure grade. All other reagents were "reagent grade" and were used without further purification. Distilled water was passed through an ion-exchange column and redistilled from a Vycor still before use.

Counting apparatus

A 3 × 3 in NaI (Tl) detector coupled to a single-channel analyzer was used for counting ^{114}In. The analyzer window was set to include only the 0.19-MeV ^{114}In γ-ray.

Procedure

Transfer a 0.5-g sample containing 10–140 ng In g^{-1} to a Teflon beaker and add 10 ml of 40% hydrofluoric acid and 5 ml of concentrated nitric acid. Prepare four standards in the range 5–70 ng of indium with the same acid additions. Add 0.05 ml of ^{114}In tracer to each beaker and also to 10 ml of 0.0054 *M* sulfuric acid in a counting vial as a counting standard. Dissolve the samples and expel acids by overnight evaporation on a steam bath. Dissolve the residue with 30 ml of 0.8 *M* nitric acid, transfer to a separatory funnel, add 5 ml of 8.8 *M* hydrobromic acid, and extract with 15 ml of methyl isobutyl ketone. Discard the aqueous phase. Wash the organic phase twice with 5-ml portions of 0.88 *M* hydrobromic acid, and then with 10 ml of 12% (w/v) potassium bromide solution; discard the aqueous washes. Add 10 ml of chloroform to the funnel and strip indium with 10 ml of 0.06 *M* acetic acid. Add 5 ml of aqueous 1.2% (w/v) cupferron solution to the aqueous phase and extract with 10 ml of xylene. Discard the aqueous phase and wash the organic phase with 5 ml of 0.06 *M* acetic acid. Add 10 ml of chloroform to the funnel and strip indium with 10 ml of 0.18 *M* sulfuric acid. Add 0.5 ml of ammonia liquor to the aqueous phase and extract with 10 ml of (5+95) acetylacetone–xylene solution. Discard the aqueous phase, wash the organic phase with 5 ml of water, and strip indium with 10 ml of 0.0054 *M* sulfuric acid. Drain the aqueous phase into a 30-ml polypropylene screw-top bottle, add 0.25 ml of EDTA reagent solution, and heat in an oven for 1 h at 120°. Transfer the contents to a separatory funnel, add 0.25 ml of aqueous 5% (w/v) ammonium acetate solution, and extract the excess of indium with 15 ml of the acetylacetone–xylene solution. Drain the aqueous phase to a counting vial, and count samples and standard for 5 min.

Prepare a calibration curve by plotting the mass of indium in tne standard solution against A/a, where A is the counting rate of the counting standard and a is the counting rate of the processed standards. Derive the original concentration of indium in the samples from this curve. Note that the calibration curve should be a straight line with an intercept equal to the mass of indium in the tracer and reagent blank (almost entirely from the tracer) and a slope equal to the mass of indium corresponding stoichiometrically to the amount of EDTA used.

DISCUSSION

The principles of substoichiometric radioisotope dilution analysis have been discussed in detail by Ružička and Stary[4], while Briscoe and Dodson[8] have developed the theory for chelate separation of the excess of element after reaction with substoichiometric amounts of EDTA. Recently[9]. a derivation has been given for the equation

$$m = \left(\frac{A}{a}\right) m_c - m_b \qquad (1)$$

relating the mass of indium in the sample (m) to the counting rates of the counting standard (A) and final sample solution (a), the mass of indium stoichiometrically complexed by the reagent (m_c) and the mass of indium in the added tracer and reagent blank (m_b). This formulation, in contrast to that of Ružička and Stary[4], permits a ready comparison of the empirical standard curve with theory.

Selection of optimal conditions

Ružička and Stary[6] described a substoichiometric EDTA reaction for the determination of as little as 0.05 ng of indium, with ion exchange to separate the excess of metal. They apparently obtained an instantaneous reaction between indium and EDTA at room temperature and a pH of 2–3. However, in preliminary experiments with 15 ng of indium to verify the reaction, it proved impossible to complex more than a small fraction of the stoichiometric amount of indium (11 ng) with EDTA at room temperature in reaction times up to 1 h. Heating the reaction mixture for 1 h on the steam bath usually forced the reaction to completion, but in some samples the reaction was still incomplete. Heating to 120° (in closed polypropylene bottles) was required to ensure complete reaction on a routine basis.

It is possible that Ružička and Stary did not obtain a complete reaction between indium and EDTA and thus the discrepancy is only apparent. The calculation procedure used by them does not contain explicitly the mass of the element in the complex, and the requisite data for its calculation are not given. For the substoichiometric procedure to work, it is only necessary that a constant mass of the element be complexed and it does not necessarily follow that all of the substoichiometric reagent must be utilized. Standard curves were obtained with only occasional erratic results by heating the solution for 30 min on a steam bath, although the reaction was far from complete and the calibration curves did not have the expected slope and intercept. Such a procedure can be adequate under carefully controlled conditions but is not satisfactory for routine analysis of large numbers of samples of variable and unknown composition. With the method described in this paper, calibration curves were reproducible with slopes and intercepts in agreement with theory. The use of standards was actually necessary only to determine the reagent blank which, in this case, was less than 2, and usually less than 1, ng (excluding tracer).

The analytical sensitivity is limited in principle by the specific activity of the radioactive indium added, the stability of the indium–EDTA complex, and the kinetics of the complexing reaction. The amount of ^{114}In tracer solution used here contained about 15 ng of indium to obtain an adequate counting rate and thus set a lower detection limit of about 5 ng of indium. This limit could be reduced by using carrier-free ^{113}In or ^{115}In although the short half-life of these isotopes would be inconvenient.

The limit of 5 ng of indium is about two orders of magnitude greater than that imposed by the stability of the indium–EDTA complex. The conditional stability constant is

$$K_y = \frac{[\mathrm{In\ Y}]\alpha}{[\mathrm{In}]\,[\mathrm{Y'}]} \qquad (2)$$

where α is the coefficient relating the total equilibrium concentration of EDTA in all its forms, [Y′], to [Y]. With the requirement that 99% of the total EDTA, C_{HY}, be used in the complex $[Y'] = 10^{-2}\ C_{HY}$, and for 50% substoichiometry ([In] = [In Y]), eqn. (3) is obtained:

$$C_{HY} = \frac{100\alpha}{K_Y} \tag{3}$$

Flaschka and Barnard[10] give log $K = 25$ and, at pH 2.2, log $\alpha = 13$. The detection limit imposed by the stability of the complex is therefore 10^{-10} M EDTA which corresponds to about 0.2 ng of indium for the proposed method. The sensitivity limit of 0.05 ng of indium reported by Ružička and Stary[6] had an experimental error of 45% while their experiments with 0.2 ng of indium showed an error of only 6.5% which is in reasonable agreement with the predicted limit.

From these considerations, it appears that the sensitivity of the procedure could be extended by more than an order of magnitude. On the other hand, the slowness of the reaction with 15 ng of indium found here and the concentration dependence of reaction rates suggest that such an extension might be difficult. The limit of 5 ng of indium in the sample is adequate for most rocks and minerals.

After the EDTA reaction, the pH and chelate concentration must be adjusted so that all of the excess metal is removed while none of the complexed metal is decomposed to free metal and EDTA. Briscoe and Dodson[8] have developed the theory necessary for the calculation of the requisite conditions, and their analysis will be followed here. Conditions for the extraction of indium can be obtained from eqn. (4):

$$K_A = \frac{[\mathrm{In\,A_3}][\mathrm{H}]^3}{[\mathrm{In}][\mathrm{HA}]^3} \tag{4}$$

where A refers to the anion of the chelating reagent. Combining eqns. (2) and (4) gives:

$$\frac{K_A}{K_Y} = \frac{[\mathrm{In\,A_3}]\,[\mathrm{H}]^3\,[\mathrm{Y'}]}{[\mathrm{In\,Y}]\,[\mathrm{HA}]^3\,\alpha} \tag{5}$$

from which conditions precluding the decomposition of the indium–EDTA complex may be calculated.

The conditions assumed in applying these equations are as follows: (*a*) all of the chelate is present in the organic phase (justified in the case of acetylacetone from its dissociation and partition coefficients); (*b*) 99% of the free indium is extracted, $[\mathrm{In\ A_3}] = 10^2\ [\mathrm{In}]$; (*c*) 99% of the EDTA is consumed, $[Y'] = 10^{-2}\ C_{HY}$; and (*d*) 90% stoichiometry for the lowest indium concentration, $[\mathrm{In\ Y}] = 10\ [\mathrm{In\ A_3}]$. With the procedure recommended here, the concentration of EDTA is 10^{-8} M, the pH of the EDTA reaction is 2.2, and the pH at which the excess indium is extracted is 4.8. Stary[7] cites a value of log $K_A = -7.2$ for acetylacetone in benzene and the same value was assumed here with xylene as diluent. Under these conditions, eqn. (4) yields 0.018 M as the minimal concentration of acetylacetone which can be used, while eqn. (5) yields 0.93 M as the maximum.

The equations given above neglected hydrolysis and acetate complexing of indium. Therefore, an acetylacetone concentration (0.5 M) near the permissible upper

limit was chosen, and it was experimentally confirmed than 95% of the free indium could be extracted under these conditions without any observable decomposition of the EDTA complex. Further, standard curves based on these conditions had the theoretical slope and intercept.

It would be preferable to avoid hydrolysis problems by extracting the excess of indium at the same pH as the indium–EDTA reaction. Unfortunately, there is a threshold pH, independent of chelate stability constant or concentration, below which excess of indium cannot be extracted without decomposition of the EDTA complex. Equating the minimal and maximal chelate concentrations from eqns. (4) and (5) gives:

$$\frac{[\mathrm{In\,A_3}]}{[\mathrm{In}]} = \frac{[\mathrm{In\,A_3}]\,[\mathrm{Y'}]\,K_\mathrm{Y}}{[\mathrm{In\,Y}]\,\alpha} \tag{6}$$

With the ratios of indium species and other conditions specified above, this yields $\log \alpha = 12$, and from the pH dependency of α given by Flaschka and Barnard[10], a threshold pH of 2.5 can be inferred. For the routine analysis of large numbers of samples, it is judicious to work well above this limit where all of the solution variables become critical.

Selectivity of the method

The selectivity of the substoichiometric EDTA reaction with indium is sufficiently great that few elements interfere at normal rock abundance levels. Combination of the EDTA stability constants of indium and any element X gives:

$$\frac{K_\mathrm{X}}{K_\mathrm{In}} = \frac{[\mathrm{XY}]\,[\mathrm{In}]}{[\mathrm{X}]\,[\mathrm{In\,Y}]} \tag{7}$$

If no more than 1% of the EDTA is to be lost from the EDTA complex of indium, and subscript T is used to indicate the sum of free and complexed metal, one can write:

$$\frac{K_\mathrm{X}}{K_\mathrm{In}} = \frac{[\mathrm{In}]_\mathrm{T} - [\mathrm{In\,Y}]}{100[\mathrm{X}]_\mathrm{T} - [\mathrm{In\,Y}]} \approx \frac{[\mathrm{In}]_\mathrm{T} - [\mathrm{In\,Y}]}{100[\mathrm{X}]_\mathrm{T}} \tag{8}$$

For the limiting value of 90% substoichiometry, the concentration at which the element X interferes can be calculated from eqn. (9)

$$[\mathrm{X}]_\mathrm{T} = 10^{22}\,\frac{[\mathrm{In}]_\mathrm{T}}{K_\mathrm{X}} \tag{9}$$

by reference to tables of EDTA stability constants (*e.g.* refs. 7, 10).

When compared with common rock abundances of the elements (*e.g.* ref. 11), these calculations show that indium must be separated completely from iron, bismuth, scandium, thorium, thallium and zirconium; aluminum and gallium interfere to a lesser extent. The greatest problem is iron which is about 10^6 times more abundant than indium and interferes at concentrations of 10^{-3} times that of indium, which implies that a separation factor of about 10^9 is required.

The bromide extraction of indium removes aluminium, gallium, thorium, scandium, and zirconium while greatly reducing the concentration of iron. The cupferron extracts iron, bismuth, and some of the thallium with indium; iron and

bismuth are retained in the organic phase while indium is stripped. Acetylacetone extraction and stripping separates indium from the last traces of iron, thallium, and bismuth.

An important advantage of acetylacetone for the final separation is the yellow color that appears if microgram amounts of iron are present. A visible yellow implies that previous separations were insufficient and the analysis will not be reliable. Experience with routine use of the procedure suggests that visible iron in the acetylacetone is rare and is usually attributable to insufficient care in performing the previous separations.

With manual or even machine shaking of the funnels, the separations are lengthy and tedious. In this procedure separatory funnels are placed in a rack contained in a fume hood. Mixing of the phases is accomplished by an air stream. A 1-mm i.d. capillary tube connected to a compressed air source with plastic tubing is inserted through the open funnel top to the bottom of the funnel. The air stream intimately mixes the phases, and extractions are complete within 1 min. After extraction the capillary tubes are raised above the liquid level permitting the phases to separate. Some loss of solvent though the open funnel top does occur by volatilization; this is of no importance if a fume hood is used.

In the recommended procedure, the phase to be discarded is generally the lower one, thus facilitating the operations. Operating with 18 separatory funnels simultaneously, the separations are completed within 2 h. Despite the many extraction steps the procedure is suitable for routine analysis of many samples.

RESULTS

The precision and accuracy of the method were estimated by determining indium in four splits from three bottles of each of four U.S.G.S. standard rocks and in three splits from a single bottle of G-1 and W-1. The various splits were randomized and analyzed over a period of a week to preclude any correlation of errors. These results are given in Table I. The replicate analyses of different bottles

TABLE I

INDIUM IN U.S.G.S. STANDARD ROCKS

(Results in ng g^{-1})

Rock	*Bottle "A"*	*Bottle "B"*	*Bottle "C"*
AGV-1	43, 44	42, 46	48, 43
	43, 45	46, 45	46, 45
G-2	31, 28	30, 30	28, 29
	29, 32	29, 30	27, 30
GSP-1	46, 47	48, 51	45, 51
	46, 46	48, 59	47, 47
BCR-1	88, 89	89, 87	87, 95
	81, 100	88, 92	98, 89
G-1	26, 27, 23		
W-1	66, 61, 58		

of the standard rocks were used to test for bottle-to-bottle homogeneity by a one-way analysis of variance. The F-test showed that the variation among bottles was not significantly (95% confidence limit) greater than the variation within bottles and thus that different bottles of these standard rocks are homogeneous with respect to indium content.

In Table II the mean and an estimate of the analytical precision derived from the analysis of variance are compared with previous neutron activation analyses. These data show that the accuracy and precision of the method are adequate for most geochemical problems.

TABLE II

COMPARISON OF INDIUM DETERMINATIONS BY THIS METHOD WITH NEUTRON ACTIVATION ANALYSES

Rock	*Mean from Table I* ($ng\ g^{-1}$)	*Analytical precision* (%)[a]	*Neutron activation* ($ng\ g^{-1}$)
G-2	29	4.5	30, 28
AGV-1	45	3.8	45, 44
GSP-1	48	6.9	55, 53
BCR-1	90	6.2	109, 94
G-1	25	—	26, 24
W-1	62	—	67, 66

[a] Analytical precision was derived from an analysis of variance of the Table I data; it is the square root of the mean sum of squares variance within bottles with 9 degrees of freedom expressed as percent of the mean. Neutron activation results are from ref. 2 and ref. 3 except G-1 and W-1 data which are cited in ref. 12.

We are grateful to F. Flanagan for advice and assistance with the analysis of variance experiment and to R. Meyrowitz and D. Norton for helpful comments on the manuscript.

SUMMARY

Rocks containing 10–140 ng of indium per g are decomposed with hydrofluoric and nitric acids in the presence of ^{114}In. Indium is separated from other constituents by sequential extractions of the bromide, cupferronate, and acetylacetonate, and is then reacted with a substoichiometric amont of EDTA. Excess of indium is removed by acetylacetone extraction and the specific activity of the complexed fraction is determined by counting ^{114}In. Analyses of the U.S.G.S. standard rocks are reported. These show good agreement with previous neutron activation analyses. Repetitive rock analyses indicated an analytical precision of ± 4–7%.

RÉSUMÉ

Des roches contenant 10 à 140 ng d'indium par g sont décomposées par un

mélange acide fluorhydrique—acide nitrique, en présence de ^{114}In. L'indium est séparé des autres constituants par une série d'extractions au bromure, au cupferronate et à l'acétylacétonate. Il est traité ensuite par une quantité substroechiométrique d'EDTA. L'excès d'indium est éliminé par une extraction à l'acétylacétone. L'activité spécifique de la fraction complexée est déterminée par comptage. On indique les résultats obtenus avec des roches étalons; ils concordent bien avec ceux des analyses par activation neutronique. On arrive à une précision de ±4–7%.

ZUSAMMENFASSUNG

Gesteine mit einem Gehalt von 10–140 ng Indium pro g werden mit Fluorwasserstoff- und Salpetersäure in Gegenwart von ^{114}In zersetzt. Das Indium wird von anderen Bestandteilen durch aufeinanderfolgende Extraktionen des Bromids, Kupferronates und Acetylacetonates abgetrennt und dann mit einer unterstöchiometrischen Menge EDTA umgesetzt. Der Überschuss des Indiums wird durch Acetylaceton-Extraktion entfernt und die spezifische Aktivität der komplexierten Fraktion durch Zählung des ^{114}In bestimmt. Analysen von U.S.G.S.-Standardgesteinen werden beschrieben. Sie zeigen eine gute Übereinstimmung mit vorher ausgeführten Neutronenaktivierungsanalysen. Bei wiederholten Gesteinsanalysen ergab sich eine analytische Reproduzierbarkeit von ±4–7%.

REFERENCES

1 L. R. Wager, J. van R. Smit and H. Irving, *Geochim. Cosmochim. Acta*, 13 (1958) 81.
2 O. Johansen and E. Steinnes, *Talanta*, 13 (1966) 1177.
3 P. A. Baedecker, R. Schaudy, J. L. Elzie, J. Kimberlin and J. T. Esson, *Geochim. Cosmochim. Acta*, Suppl. no. 2, Proc. 2nd Lunar Sci. Conf., 2 (1971) 1037.
4 J. Ružička and J. Stary, *Substoichiometry in Radiochemical Analysis*, Pergamon Press, Oxford, 1968.
5 J. Stary and J. Ružička, *Talanta*, 18 (1971) 1.
6 J. Ružička and J. Stary, *Talanta*, 11 (1964) 691.
7 J. Stary, *The Solvent Extraction of Metal Chelates*, Pergamon Press, Oxford, 1964.
8 G. B. Briscoe and A. Dodson, *Talanta*, 14 (1967) 1051.
9 L. P. Greenland and E. Y. Campbell, *Anal. Chim. Acta*, 60 (1972) 159.
10 H. A. Flaschka and A. J. Barnard, Jr., in C. L. Wilson and D. W. Wilson, *Comprehensive Analytical Chemistry*, Vol. 1B, Elsevier, Amsterdam, 1960.
11 F. J. Flanagan, *Geochim. Cosmochim. Acta*, 33 (1969) 81.
12 M. Fleischer, *Geochim. Cosmochim. Acta*, 33 (1969) 65.

Analytica Chimica Acta, 67 (1973) 37–53

DETERMINATION OF TRACE ELEMENTS IN UNFUSED ROCK AND MINERAL SAMPLES BY X-RAY FLUORESCENCE

ENVER MURAD

Abteilung Geochemie, Mineralogisch-Petrographisches Institut der Universität, Tübingen (Germany)

(Received 1st January 1973)

The determination of trace elements in rocks and minerals by X-ray fluorescence presents various problems not encountered during the investigation of major constituents. The concentrations of the minor elements are such that the intensity of secondary radiation is frequently low, and the peak-to-background ratio unfavourable. Interferences between the characteristic lines that are to be measured and tube spectra or other lines originating from the sample, are considerably more pronounced than for major elements. High resolution is therefore desirable; this can be achieved by the use of narrow collimators and, if necessary, analyzing crystals with smaller d-spacing than the commonly employed LiF (200). Such collimators and crystals, however, suffer from a lower reflection efficiency.

Mechanical dilution or fusion procedures are often applied to decrease inter-element, grain size and mineralogical effects in analysis for major elements. Such procedures are, however, time-consuming, and decrease the signal intensities, thereby raising the limit of detection. Furthermore, as shown by Czamanske *et al.*[1], fusions involving moderate dilution of the sample still leave an appreciable matrix effect. The use of dilution methods in trace analysis should therefore be restricted to cases where their application is unavoidable (an example is given below). If undiluted samples are to be analyzed, a correction for matrix effects is imperative. In the present paper a simple and rapid method of preparation of samples for analysis is described, and different techniques of correction for matrix effects are tested.

To obtain an unbiassed indication of which methods offer optimal results, the concentrations of seven trace elements in the atomic number range from 24 (chromium) to 82 (lead) were determined in standard rock and mineral samples. The values obtained can be compared not only among themselves, but also with results obtained by other workers. Such comparisons must nevertheless be done carefully, for most of the investigated standards have been distributed only recently, and many of the published averages have not yet been fully established.

The elements chosen for analysis were chromium, zinc, rubidium, strontium, zirconium, barium and lead. The techniques recommended for the determination of these elements can readily be extended to many others.

EXPERIMENTAL

The finely ground material (4 g) is intimately mixed with 0.800 g of ultra-fine

wax C (Hoechst) in a glass beaker. This mixture is then placed between flat plexiglas discs in a die of 30-mm diameter and pressed at 6 tons, giving a pellet 3–4 mm thick. The wax not only serves as a binder, but also makes the pellet relatively impervious to water vapour. Both sides of such a pellet can be irradiated in the course of replicate measurements.

All measurements were carried out with a Philips PW 1212 automatic X-ray spectrometer in conjunction with an Olivetti Programma 101 desk computer. The above-named elements were determined by measurement of the Cr Kα, Zn Kα, Pb Lβ_{1+2}, Rb Kα, Sr Kα, Zr Kα and Ba Kα count rates. For excitation of the Cr Kα, Zn Kα, Sr Kα, Zr Kα and Ba Kα spectra, the samples were irradiated by a tungsten target tube, whereas a molybdenum tube served to excite the Pb Lβ and Rb Kα spectra. To obtain optimal resolution the fine entrance collimator of 160 μm spacing, and a LiF (220) analyzing crystal (2d = 2.848 Å), were used throughout. For the determination of chromium and zinc, the gas flow and scintillation counters were applied in series; the Pb, Rb, Sr, Zr and Ba lines were measured with the scintillation counter only.

The spectrometer offers the possibility of automatic pulse-height selection through the incorporation of sine law and crystal attenuator units. This external window was used during measurements of Zn Kα, Ba Kα and the scattered W Lα and Mo Kα tube lines which served as internal standards. For the determination of Cr, Pb, Rb, Sr and Zr, the pulse-height analyzer was set individually for each element; a narrower window than that offered by the automatic selector was used, so that second and higher order radiation was minimized.

For all the described elements except barium, the background was measured on both sides of the peak. The Ba Kα line (0.387 Å) lies very close to the iodine absorption edge (0.374 Å), which is prominent because of the use of a NaI(Tl) crystal as detector in the scintillation counter. The background for barium was therefore measured on the long wavelength side of Ba Kα only; a correction for the slope of the background was effected by determining the quotient of the count rates at the barium peak and background positions for barium-free samples ("Specpure" silica, Johnson Matthey Chemicals, and silica/Fe_2O_3 mixtures).

The short wavelength background of lead and, to a lesser extent, the Pb Lβ peak itself may suffer interference from the neighbouring Rb Kα line. To counteract this effect, the background positions for lead were placed asymmetrically with respect to the peak, the short wavelength background being chosen closer to the Pb Lβ peak than the long wavelength background. A further correction for such an interference can be effected by attaching more weight to the background position further from the interfering line than to that nearer this line. Because interference of Sr Kα with the rubidium background and the Rb Kα peak may occur at high strontium contents, similar procedures were adopted for rubidium. Such techniques require the determination of a correction factor for the mean background by a procedure similar to that for barium.

All determinations were carried out by the "absolute-ratio" method, in which both the samples used for calibration and the unknown samples are referred to one standard (whose content of the test element should be high enough to give a reasonable count rate, but need not necessarily be known). The time required for this standard to accumulate a pre-set number of counts is electronically stored, and the

succeeding samples are measured for the same period of time. This procedure is repeated for every investigated series of standard plus three samples, so that the determinations are practically independent of long-term variations of the apparatus.

Details of the procedure are summarized in Table I.

ILE I

TAILS OF OPERATING CONDITIONS AND PRECISION OF DETERMINATION

(220) and fine collimator (160 μm) were used throughout; samples were spun during analysis)

nent	Line	X-ray tube			Path	Detector	Av. counting time (s)	Counts per p.p.m. element	Precision[a] content ± s	
		Target	kV	mA						
omium	Kα	W	60	32	Vacuum	F+S	123	58	66	3
:	Kα	W	60	32	Vacuum	F+S	94	445	41	1
idium	Kα	Mo	60	32	Air	S	44	458	348	3
ntium	Kα	W	60	32	Air	S	86	452	160	2
onium	Kα	W	60	32	Air	S	62	472	219	5
um	Kα	W	80	24	Air	S	110	165	820	6
d	$L\beta_{1+2}$	Mo	60	32	Air	S	116	321	41	2

determine the precision 12 pellets of a granite were prepared, and measurements were carried out on each. The n standard deviations include errors of preparation, apparatus drift and counting statistics.

CORRECTION FOR MATRIX EFFECTS

Matrix effects may have several causes: absorption or enhancement of the radiation by other elements in the sample (inter-element effect), dependence of the intensity of X-ray emission on the grain size of the sample and occasionally on the orientation of the mineral grains ("mica effect"), and influence of the mineral species in which the element is bound.

Methods of correction for matrix effects can be divided into four major categories:

1. dilution or fusion procedures with or without a heavy absorber;
2. addition of known amounts of the investigated element to the sample;
3. internal standard procedures:

(*a*) addition of a suitable element, or use of an element of known concentration in the sample,

(*b*) use of a scattered tube line or of the background radiation as an internal standard;

4. computation of correction factors on the basis of mass absorption or empirically determined coefficients.

Discussion of these methods in the present paper is restricted to their applicability in trace element analysis.

Dilution and fusion procedures

Dilution procedures, regardless of whether the sample is only mechanically diluted or fused with the diluent, will raise the limit of detection. Such procedures should therefore be applied only if the standards used for calibration and the

samples differ considerably. Fusions involving moderate dilution (high dilutions are out of the question) would, while not totally eliminating inter-element effects, overcome grain size, textural and mineralogical effects.

Dilution methods were tested on two of the standards studied in this paper: the CRPG biotite Mica iron and the SSC sulfide ore. Because of the exotic composition of the latter, the diluted material (1 part ore plus 4 parts quartz) was used throughout.

Addition of known amounts of required element

Addition of the element in question in a series of known steps to the sample, thereby producing a calibration curve for this sample, will in general lead to excellent results. The method is, however, too time-consuming to find extensive application in practice.

Calibration in this investigation was effected by addition of different amounts of simple compounds (preferably oxides) of the investigated elements to geological samples, exclusively rocks of aplite–granitic composition and low content in the corresponding elements. The use of a geochemical end-member of the igneous rock family enabled the influence of inter-element effects on the emitted X-ray intensity, and the degree of compensation of matrix effects by application of the different correction methods to be studied systematically.

Internal standard methods

Internal standards are frequently used to correct for matrix effects; a suitable standard that has been admixed to a sample can serve for various determinations[2]. The addition of an internal standard to every sample is, however, tedious, requiring accurate weighing and thorough mixing to ensure uniform distribution. The reliability of internal standard procedures based on a constituent of known concentration in the sample[3] will be limited by the precision of determination of that element.

The use of scattered X-ray tube spectra as internal standards eliminates the time-consuming procedures of the above method, while offering a more or less similarly effective tool for the correction of matrix effects. This makes the method particularly attractive if many samples must be analyzed. Several examples involving this technique are described below; the coherently (Rayleigh) scattered W Lα and Cr Kα lines of tungsten and chromium target tubes, the Rayleigh and Compton scattered portions of the Mo Kα line of a molybdenum tube, and the coherently scattered continuous background radiation, all served as internal standards. Owing to the relatively long wavelength of W Lα and Cr Kα, scattering of these lines by silicate samples will be mainly coherent. Reynolds[4] preferred the Compton scattered portion of the Mo Kα line as an internal standard to the coherently scattered portion.

The simplest method of correction for matrix effects is that first described by Andermann and Kemp[5], who used the background as an internal standard; no further measurements are required other than those essential to determine the net peak of the element. When this method is used, pulse-height selection is essential to ensure that the registered background radiation is exclusively of the same wavelength as the investigated peak. One limitation of the method is that the background radiation may be falsified by some overspill from the peak. Although this can be

corrected for, experience shows that the quality of the results obtained tends to decrease above the 1000-p.p.m. level. Similarly, all other interferences with the background will result in a significantly larger error than when other techniques of correction for matrix effects are applied.

Which of the described internal standard methods—coherently or incoherently scattered tube line or background—will find application in practice depends largely on the wavelength of the analytical line and on the nature of the X-ray tube used for excitation, the target material determining the internal standard lines at the analyst's disposal.

Computation of correction factors

The computation of correction factors for inter-element effects on the basis of mass absorption or empirically determined coefficients requires a knowledge of the major element composition of the sample. On the assumption that only trace elements heavier than calcium were to be determined, Hower[6] divided the X-ray spectrum of silicate rocks into three regions: wavelengths shorter than the K absorption edge of iron, wavelengths between the K absorption edges of iron and titanium, and wavelengths between the K absorption edges of titanium and calcium. In the first region, which includes the K lines of all elements heavier than cobalt, trace elements are not excited by the fluorescent radiation from the normal major elements in silicate rocks; absorption of X-rays is therefore the controlling factor. A correction coefficient for matrix effects can be determined at any point of this region, and remains valid for the whole region. The spectra of elements lighter than cobalt are not only absorbed by the major elements of the sample, but also intensified by those major elements whose characteristic radiation is of shorter wavelength than the K absorption edge of the required element (or the corresponding L edge if the line belongs to the L series). This renders a correction for matrix effects on the grounds of mass absorption alone insufficient. Such enhancement effects can be compensated for by empirical factors.

The calculation of correction factors has the advantage that it is applicable to a wide range with relative ease, and without additional measurements or admixture of internal standards.

RESULTS

The X-ray spectrum of silicate rocks was divided into three major wavelength regions, each presenting different problems and possibilities. These regions cover the following wavelengths: (1) longer than 1.9 Å, (2) between 1.9 and 0.6 Å, and (3) shorter than 0.6 Å.

Region (1)

The absorption edges of lines belonging to this region lie at a wavelength longer than Fe Kβ, which is the line of highest energy emitted by the major elements normally present in silicate rocks and minerals. All elements lighter than iron are included here, as well as the elements cadmium (atomic number 48) to neodymium (60) if L lines are used. The fluorescent lines in this region have wavelengths longer than 1.9 Å. These will be excited not only by radiation emanating from the X-ray

TABLE II

CHROMIUM CONTENT OF GEOCHEMICAL STANDARDS COMPUTED BY DIFFERENT CORRECT TECHNIQUES

Sample		*Uncorrected value*	*Values corrected by application of*			*Publis value*[b]
			Mass absorption coefficients	*Mass absorption coefficients* μ_{Fe} *empirical*	*Cr Kα as internal standard*[a]	
USGS	G-1	16	17	17	17	(20)
	G-2	11	12	12	11	(7)
	GSP-1	13	14	13	13	12.5
	AGV-1	13	14	13	13	12
	BCR-1	25	27	26	24	18
	W-1	139	157	152	140	114
	PCC-1	3660	2980	2860	2600	2730
	DTS-1	5240	4380	4210	3780	4000
CRPG	GH	2	2	2	2	(6)
	GA	10	10	10	10	(10)
	BR	382	454	435	390	*420*
	Mica Fe	102	110	99	85	*90*
	Mica Fe (dil.)[c]	106	108	105	100	*90*
	Mica Mg	110	118	114	102	
ANRT	DR-N	48	51	49	46	*45*
	UB-N	3640	2800	2680	2670	*2200*
	DT-N	367	328	329	320	
	BX-N	473	378	332	315	
	VS-N	742	869	859	796	*684*
SSC	Sulfide ore (dil.)[d]	632	573	559	608	374
	Syenite 1	46	52	51	48	56
	Syenite 2	7	8	8	7	
MRT	T-1	24	25	24	24	(24)
NBS	99	5	5	5	5	
ZGI	GM	14	15	15	15	*10*
	BM	182	181	174	163	*123*
NIM	G	10	10	10	10	12
	S	10	12	12	11	13
	L	9	10	9	8	20
	N	40	45	44	41	40
	P	28200	25600	24100	20600	
	D	3990	3360	3080	2860	2900
QMC	I1[e]	—	—	—	—	
	M2	68	73	70	66	
	M3	63	72	71	70	
	I3	40	45	42	38	
GSJ	JG-1	57	58	58	58	50
	JB-1	431	477	462	437	417

[a] The values in this column are those obtained by the recommended routine procedure.

[b] Recommended values are in italics, orders of magnitude in brackets; other values are averages without indicati quality.

[c] 1 part biotite Mica Fe diluted with 3 parts granite.

[d] 1 part sulfide ore diluted with 4 parts SiO_2.

[e] Not detected, less than 3 p.p.m. chromium.

tube, but also by fluorescent radiation from at least one of the major elements of the sample.

Two of the correction methods described in the previous section were tested in this region: the internal standard and the mass absorption/empirical coefficient techniques. When the former is applied, there is one important limitation: the wavelength of the absorption edge of the required element and that of the internal standard must lie on the same side of all characteristic lines of the major elements in the sample. For manganese, chromium, vanadium and titanium, and for the elements iodine to neodymium, the intensity of the scattered Cr Kα line of a chromium target tube may serve as an internal standard.

Inter-element effects can be corrected for on the basis of the major element composition of the sample. If such methods are to be successful, the correction coefficients must include the enhancement of the fluorescent radiation by major elements that emit lines of sufficient energy to excite the required trace element; these coefficients replace mass absorption coefficients.

The chromium content of geochemical standards was determined, the results being adjusted by different correction techniques. A comparison of these values with published results is shown in Table II. The uncorrected values are often considerably in error, as is particularly evident for the ultramafic rocks. A correction based on mass absorption brings improvement in some cases, but gives inferior results for samples with high iron content. An empirical coefficient that takes into consideration the enhancement of Cr Kα by the Fe Kα and Fe Kβ radiation induced in the sample, has a magnitude of 39 for Fe_2O_3, compared to a mass absorption coefficient of 91. The results obtained when this empirical coefficient is substituted for the mass absorption coefficient of Fe_2O_3, show a considerable improvement over the values determined using mass absorption only, and are approximately equivalent to, though frequently somewhat higher than those obtained when Cr Kα was applied as an internal standard.

Both of the latter methods of correction can be recommended. The mass absorption/empirical coefficient technique can be applied in the whole region, and has the further advantage of making a change of the X-ray tube and subsequent measurement of Cr Kα unnecessary. Because a full analysis is frequently not available, the internal standard method is preferred for routine determination of the appropriate elements.

Region (2)

The energy required for excitation of the lines in this region is too high for enhancement by fluorescent radiation of the major elements constituting silicate rocks; mass absorption is therefore the major factor controlling matrix effects. All elements whose characteristic radiation is of shorter wavelength than the limiting wavelength of region (1), but long enough that at least 90% of the incident radiation at the wavelength of the K edge will be absorbed in the sample are included here. This region covers the K spectra of the elements cobalt (27) to molybdenum (42) and the L spectra of gadolinium (64) to uranium (92).

For measurements in this region, Hower[6] suggested the determination of correction factors at one wavelength, and their application for the K spectra of all elements heavier than cobalt. Correction factors calculated on the basis of mass

TABLE III

ZINC CONTENT OF GEOCHEMICAL STANDARDS COMPUTED BY DIFFERENT CORRECTION TE NIQUES

Sample		*Uncorrected value*	*Value corrected by application of*					*Publish value*[b]
			Internal standard procedures				*Mass absorption coefficients*[a]	
			Background	*Mo Kα/ Rayleigh*	*Mo Kα/ Compton*	*W Lα*[a]		
USGS	G-1	39	41	39	41	43	41	*45*
	G-2	77	83	80	85	87	84	*85*
	GSP-1	86	97	94	104	105	102	*98*
	AGV-1	62	77	72	83	80	80	*84*
	BCR-1	70	100	92	120	107	115	*120*
	W-1	49	68	62	80	72	77	*86*
	PCC-1	37	43	44	44	47	43	*36*
	DTS-1	39	45	46	47	47	46	*45*
CRPG	GH	57	58	57	56	62	58	*80*
	GA	53	56	55	57	60	58	*75*
	BR	80	120	106	148	128	137	*160*
	Mica Fe	595	975	910	1460	1130	1310	(1350)
	Mica Fe (dil.)[c]	1034	1250	1300	1380	1290	1340	(1350)
	Mica Mg	203	273	251	318	297	295	
ANRT	DR-N	100	130	123	149	139	145	*150*
	UB-N	71	80	83	81	90	78	(85)
	DT-N	28	25	26	23	28	24	
	BX-N	44	66	64	83	78	79	
	VS-N	568	538	570	820	686	770	803
SSC	Sulfide ore (dil.)[d]	196	222	228	245	239	223	294
	Syenite 1	168	208	204	262	230	246	219
	Syenite 2	180	232	211	255	239	260	
	Syenite 3	166	210	197	241	221	230	
MRT	T-1	152	175	172	187	186	187	(190)
NBS	99	16	14	15	13	15	13	(15)
ZGI	GM	39	41	40	40	43	41	40
	BM	92	119	113	129	127	127	107
NIM	G	46	47	46	46	50	48	60
	S	6	8	7	8	8	8	21
	L	257	297	317	424	353	383	(320)
	N	39	52	48	59	55	57	80
	P	64	89	85	104	96	100	100
	D	55	76	76	92	83	87	90
QMC	I1	10	10	10	10	11	10	(20)
	M2	117	156	143	175	171	168	(150)
	M3	32	39	37	42	42	41	(40)
	I3	52	79	73	100	86	94	(100)
GSJ	JG-1	39	41	40	40	44	41	36
	JB-1	52	70	64	79	74	76	83

[a] The boxed values are those obtained by the recommended routine procedure.

[b–d] As for Table II.

absorption data indeed remain practically unchanged at different wavelengths; however, internal standard procedures, and particularly the background variety, tend to give results not totally independent of the wavelength. A subdivision of this region therefore proved necessary.

Region 2A. This region includes lines of wavelength between 1.9 and about 1.25 Å (K lines of cobalt to germanium, Lα lines of gadolinium to gold, $L\beta_1$ lines of europium to tungsten). To compare the efficiency of different correction techniques for matrix effects in this region, the zinc content of geochemical standards was determined. The following methods were tested: background, Mo Kα (Rayleigh and Compton scattered lines) and W Lα as internal standards, and mass absorption coefficients. The results showed considerable discrepancies between the values obtained by different correction methods. The Rayleigh scattered portion of Mo Kα gave the poorest results, these being frequently only little better than the uncorrected values. The results were improved somewhat when the background was used as internal standard. The low background count rates in this region, however, render this procedure imprecise. Considerably better values were produced by application of the scattered W Lα line or the Compton scattered portion of Mo Kα, the latter giving the higher degree of compensation. Best results, however, were achieved by computing the mass absorption coefficients, and using these to correct for inter-element effects. This method gave very good results for the zinc-rich samples, *e.g.* the CRPG Mica Fe and the ANRT synthetic glass VS-N. The values computed by the mass absorption method correspond quite well to the average values of the results corrected by the W Lα and Mo Kα Compton scattered lines.

The results of all zinc determinations are shown in Table III.

Region 2B. This region includes wavelengths between 1.25 and 0.6 Å (K lines of arsenic to molybdenum, Lα lines of mercury to uranium and Lβ lines of tungsten to uranium). Of the investigated elements lead, zirconium, strontium and rubidium lie in this range. The efficiency of different correction techniques was tested for strontium (Table IV).

As for the zinc determinations, the coherently scattered Mo Kα line gave totally inadequate results. Values obtained by using the W Lα peak as an internal standard were somewhat better. Considerable improvement resulted by using the background as an internal standard, or by correcting on the basis of mass absorption. Maximum compensation for matrix effects was obtained by using the Compton scattered Mo Kα peak as internal standard; the resulting values, however, appear to be rather high.

To compare the efficacy of the described correction techniques at higher concentrations, rubidium was determined in the CRPG mica standards and the ANRT glass VS-N, and the results were adjusted by different methods. Investigation of the micas led to conclusions similar to those for strontium. The background measurement for the synthetic glass was impeded by the presence of considerable quantities of lead and bismuth in the sample, so that the background could not be used as internal standard. Only the Compton scattered Mo Kα line and the mass absorption coefficients gave acceptable results (Table IV).

In a recent paper, Fairbairn and Hurley[7] noted that when rubidium and strontium are determined by X-ray fluorescence, the Compton scattered Mo Kα line yields a higher degree of compensation for matrix effects than the background.

TABLE IV

STRONTIUM AND RUBIDIUM CONTENTS OF GEOCHEMICAL STANDARDS COMPUTED BY I FERENT CORRECTION TECHNIQUES

Sample		*Uncorrected value*	*Value corrected by application of*					*Publish value*[b]
			Internal standard procedures				*Mass absorption coefficients*[a]	
			Background[a]	*Mo Kα/ Rayleigh*	*Mo Kα/ Compton*	*W Lα*		
Strontium								
USGS	G-1	255	274	257	271	281	273	*250*
	G-2	463	502	483	516	524	509	*479*
	GSP-1	205	243	225	249	247	246	*233*
	AGV-1	526	677	609	705	686	692	*657*
	BCR-1	206	330	270	354	315	348	*330*
	W-1	124	194	157	202	183	200	*190*
	PCC-1[c]	—	—	—	—	—	—	*0.4*
	DTS-1[c]	—	—	—	—	—	—	*0.3*
CRPG	GH	9	9	9	9	9	9	*10*
	GA	296	326	309	323	335	326	*305*
	BR	786	1280	1050	1460	1260	1380	*1350*
	Mica Fe	1	2	2	3	2	3	*6*
	Mica Mg	18	26	22	28	26	27	(25)
ANRT	DR-N	283	405	350	422	393	419	*400*
	UB-N	7	9	9	9	9	8	(10)
	DT-N	41	36	37	33	40	35	
	BX-N	62	112	92	118	110	115	
	VS-N	559	707	561	806	678	765	(846)
SSC	Sulfide ore (dil.)[d]	81	100	94	101	99	93	105
	Syenite 1	139	185	169	217	191	208	286
	Syenite 2	205	271	240	289	271	300	
	Syenite 3	218	287	259	316	290	306	
MRT	T-1	324	395	366	398	398	403	(410)
NBS	99	169	143	155	134	159	140	(120)
ZGI	GM	135	141	137	140	148	143	*133*
	BM	167	233	205	236	232	235	*230*
NIM	G	10	11	10	10	11	11	13
	S	54	64	56	66	65	66	76
	L	3040	3610	3750	5010	4190	4620	4480
	N	184	263	226	279	261	276	254
	P	22	35	29	36	33	35	40
	D	2	3	2	3	2	3	5
QMC	I1	189	182	183	178	197	183	(175)
	M2	135	190	165	202	198	197	(200)
	M3	405	510	464	537	528	530	(410)
	I3	158	269	220	301	258	291	(255)
GSJ	JG-1	189	199	192	196	212	201	*184*
	JB-1	318	450	392	480	455	472	*438*

ILE IV

ple		Uncorrected value	Value corrected by application of					Published value[b]
			Internal standard procedures				Mass absorption coefficients[a]	
			Background[a]	Mo Kα/ Rayleigh	Mo Kα/ Compton	W Lα		
idium								
PG	Mica Fe	893	1740	1390	2230	1730	2020	*2300*
	Mica Mg	827	1270	1040	1310	1230	1220	
RT	VS-N	566	422	578	831	698	775	(915)

ıe boxed values are those obtained by the recommended routine procedure.
ıs for Table II.
rontium was not detected, less than 1 p.p.m.

They recommended averaging the results obtained by these two methods, the mean values corresponding more or less to those corrected by mass absorption. The observations made in this work confirm the discrepancy between the Compton scatter and background methods in sign and magnitude. The preferred values of Fairbairn and Hurley are in good agreement with those obtained here by the background method (Tables IV and V).

TABLE V

RUBIDIUM, LEAD AND ZIRCONIUM CONTENTS OF SOME STANDARDS

Sample		Rubidium values		Lead values		Zirconium values	
		XRF[a]	Published[b]	XRF[a]	Published[b]	XRF[a]	Published[b]
USGS	G-1	207	*220*	45	48	208	*210*
	G-2	165	*168*[c]	31	31	324	*300*
	GSP-1	239	*254*	47	51	496	*500*
	AGV-1	64	*67*	34	35	248	*225*
	BCR-1	44	*47*	14	18	191	(190)
	W-1	20	*21*	6	8	92	*105*
	PCC-1	<1	*0.06*	10	13	<1	(7)
	DTS-1	<1	0.05	9	14	<1	(3)
CRPG	GH	380	*390*	41	*50*	132	*160*
	GA	172	*175*	29	*26*	134	*140*
	BR	41	*45*	4	16	268	*240*
	Mica Fe	2020[d]	2300	7	17	648	
ANRT	VS-N	887[d]	914	885	928	687	740
SSC	Sulfide ore[e]	20	60	249	249	88	110
	Syenite 1	159[d]	195	405[d]	495	3360[d]	3030
GSJ	JG-1	181	*185*	27	24	122	(160)
	JB-1	38	41	5	14	140	(300)

[a] This investigation, corrections for matrix effects by the background method unless stated otherwise.
[b,c] As for Table II.
[d] Correction for matrix effects using the mass absorption coefficients.
[e] 1 part sulfide ore diluted with 4 parts SiO_2.

Lead was determined by measurement of the practically coincident Pb $L\beta_1$ and Pb $L\beta_2$ peaks. The net radiation intensity (counts per p.p.m.) of the lead peak is lower than that of the neighbouring rubidium and strontium $K\alpha$ lines by a factor of four, but is nevertheless sufficient to give a limit of detection of about 2 p.p.m.

Several important X-ray lines in this region cannot be completely separated from neighbouring lines. Prominent examples are the coincidences of Zr $K\alpha$ with Sr $K\beta$ and of Y $K\alpha$ with Rb $K\beta$; the line couples Nb $K\alpha$/Y $K\beta$ and Mo $K\alpha$/Zr $K\beta$ also cannot be totally resolved. If one of these lines is to be used for the determination of an element, a correction for the interfering peak is essential. The zirconium values of Table V were therefore corrected for the strontium content of the samples.

These examples show that the determination of trace elements by means of moderately weak lines or lines that suffer interference does not necessarily present an insurmountable problem. In Table V the lead and zirconium values determined on some geochemical standards are compared with published averages. The results were corrected by the background method with few exceptions, notably the SSC syenite 1, the high thorium content of which considerably falsified the background in this region. Corrections for this and the rubidium-rich standards of Table IV were effected by using the mass absorption coefficients.

For routine work in the long wavelength part of this region (1.9 to 1.25 Å), matrix effects at concentrations below 500 p.p.m. can be corrected for successfully by using W $L\alpha$ as an internal standard if a tungsten tube is used for excitation. If the samples and the standards serving for calibration differ considerably, and also at higher concentrations, mass absorption coefficients should be used for correction. In the short wavelength range between 1.25 and 0.6 Å, the scattered background can serve as internal standard, the results being of sufficient accuracy up to a concentration of 1000 p.p.m. This technique has the further advantage of making additional measurements superfluous. Other methods, *e.g.* mass absorption, should be applied at concentrations above 1000 p.p.m. or if extraneous radiation originating from other elements interferes with the background.

Region (3)

This region includes wavelengths shorter than 0.6 Å. It is well known that the penetrative power of X-rays increases with decreasing wavelength. At a wavelength of 0.5 Å (this corresponds approximately to the K absorption edge of palladium, Pd $K\alpha$ having a wavelength of 0.587 Å), about 90% of the radiation falling on a pellet of silicate rock powder prepared as described, is absorbed; the remaining 10% that passes through the pellet does not contribute to the excitation of secondary radiation. The absorption of 90% of the incident radiation, resulting in a limiting wavelength of about 0.6 Å for this region, was chosen to define the border between the regions (2) and (3). At longer wavelengths, the absorption of radiation striking the sample was high enough for application of correction techniques described for region (2). For X-rays of shorter wavelength the thickness of the pellet must be increased if maximum fluorescent yield is desired. The dependence of the intensity of fluorescent Ba $K\alpha$ emission (0.387 Å, absorption edge at 0.332 Å) on the thickness of the irradiated pellet for the standards GA and BCR-1 is shown in Fig. 1. As it is preferable to use the same pellet for all trace element determinations, it may be necessary to dispense with maximum fluorescent yield at short wavelengths if the

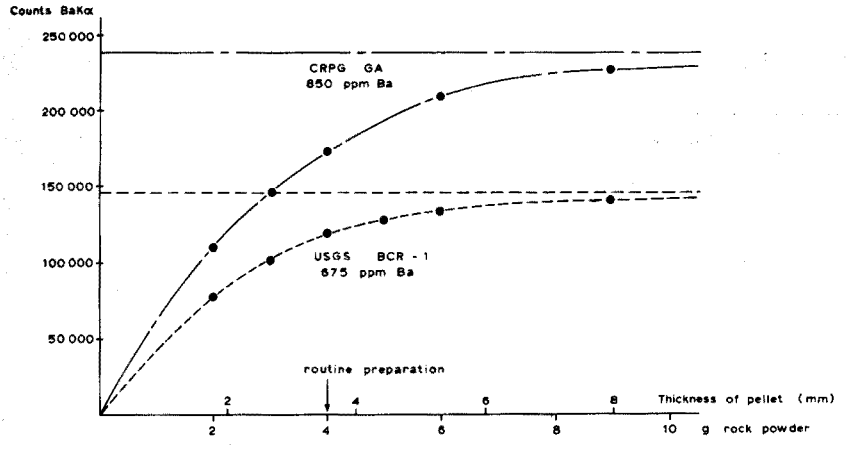

Fig. 1. Relation of Ba Kα counts to the thickness of the pellet (rock powder + 20% wax).

amount of sample is limited. If the described method of preparation (4.000 g of sample + 0.800 g of wax) is adopted, all pellets will comprise the same amount of material; nevertheless, the incomplete absorption of strongly penetrating incident X-rays will only be balanced out if all samples have the same mass absorption coefficient. Accordingly, the direct relationship $I = K[C]/\mu$ (where I is the fluorescent intensity, K an instrumental constant, $[C]$ the concentration of the investigated element and μ the mass absorption coefficient of the sample) that held previously will no longer be valid in this region.

Liebhafsky *et al.*[8] gave the following simplified equation for the dependence of the fluorescent intensity on the thickness d of a thin sample with mass absorption coefficients μ_1 and μ_2 for the incident and fluorescent radiation:

$$I = \frac{k \cdot \csc \vartheta_1 \cdot I_0 [1 - e^{-(\mu_1 \cdot \csc \vartheta_1 + \mu_2 \cdot \csc \vartheta_2) \cdot \rho \cdot d}]}{(\mu_1 \cdot \csc \vartheta_1 + \mu_2 \cdot \csc \vartheta_2) \cdot \rho}$$

where ϑ_1 and ϑ_2 are the angles made by the incident and emergent beams with the sample surface, I_0 is the intensity of X-rays striking the sample, ρ is the density of the sample and k a proportionality factor for the absorption and conversion of incident to fluorescent radiation (this factor contains the concentration of the element that is to be determined). Unfortunately, in practice, the radiation falling on the sample is normally polychromatic, so that μ_1 can be only roughly estimated. In order to test this formula, the mass absorption value at the wavelength of maximum intensity was substituted for μ_1. This wavelength is only little shorter than the K absorption edge of the element investigated in this region (barium—K edge at 0.332 Å, maximum intensity of a tungsten tube operated with 80 kV at 0.26 Å).

Barium was also determined in routine analysis by measurement of Ba Kα, which was preferred to the L lines because an effective separation of the L lines and the interfering spectra of other elements proved impossible. To obtain satisfactory resolution of the Ba Kα and the neighbouring La Kα and Cs Kα lines a secondary collimator of 10 cm length and 140 μm spacing was inserted between the analyzing crystal and the scintillation counter.

TABLE VI

BARIUM CONTENT OF GEOCHEMICAL STANDARDS COMPUTED BY DIFFERENT CORRECTION TECHNIQUES

Sample		*Uncorrected value*	*Value corrected by application of*			*Published value*[b]
			Background[a]	*Mass absorption coefficients*	*Modified mass absorption method*	
USGS	G-1	1080	1120	1160	1110	(1200)
	G-2	1870	1970	2060	1950	*1870*
	GSP-1	1270	1400	1520	1380	*1300*
	AGV-1	1160	1360	1550	1320	*1208*
	BCR-1	587	811	1000	765	*675*
	W-1	162	217	263	206	*160*
	PCC-1	19	20	22	20	1
	DTS-1	24	28	29	27	*2*
CRPG	GH	25	25	25	25	*22*
	GA	865	907	955	902	*850*
	BR	856	1260	1520	1140	*1050*
	Mica Fe	116	211	262	183	(140)
	Mica Mg	3540	4380	5210	4260	(4700)
ANRT	DR-N	369	466	549	446	*360*
	UB-N	39	42	44	41	(40)
	DT-N	148	135	128	140	
	BX-N	51	79	96	71	
	VS-N	707	834	940	807	896
SSC	Sulfide ore (dil.)[d]	303	347	350	322	221
	Syenite 1	258	367	387	313	282
	Syenite 2	427	530	626	513	
	Syenite 3	412	526	578	483	
MRT	T-1	574	644	718	634	(640)
NBS	99	105	94	88	94	(110)
ZGI	GM	345	360	364	353	*328*
	BM	247	301	349	291	*263*
NIM	G	130	132	136	132	179
	S	2520	2750	3070	2750	2590
	L	335	511	599	452	448
	N	92	117	138	112	90
	P	55	73	88	69	56
	D	27	36	44	34	20
QMC	I1	510	495	493	503	(480)
	M2	1240	1540	1800	1480	
	M3	130	152	170	147	
	I3	540	811	1000	743	
GSJ	JG-1	517	525	551	531	450
	JB-1	468	595	696	566	(400)

[a,b,d] See Table II.

In Table VI the uncorrected barium values obtained by X-ray fluorescence and those corrected by the background, mass absorption and modified mass absorption methods are compared with published averages. The previously successful conventional mass absorption method does not improve the values; in fact, the results are frequently worse. Although the uncorrected values are acceptable, the influence of inter-element effects is apparent. Best results are obtained by use of the background as an internal standard, or by application of the mass absorption method as modified for thin samples. In this region, as in the previous one, the background method is preferred because of its simplicity.

The barium values obtained during this investigation for the ultramafic rock standards of the U.S. Geological Survey are rather high. This may be due to the lack of linearity in the background radiation at this wavelength.

CONCLUSIONS

Reasonably accurate determinations of trace elements heavier than calcium at concentrations upward from a few p.p.m. can be carried out on unfused samples by X-ray fluorescence. By dispensing with the fusion procedure a simple and rapid preparation of samples for analysis is possible. For the 38 investigated rock and mineral standards, inter-element effects were found to be present at all wavelengths, and required corrections.

At wavelengths above 1.9 Å, correction for matrix effects can be effected by a combined mass absorption/empirical coefficient method or, for some elements, by using the scattered Cr Kα radiation of a chromium target tube as an internal standard. In the wavelength range from 1.9 to 1.25 Å, corrections are best carried out by using the scattered W Lα line of a tungsten tube as an internal standard or, at concentrations over 500 p.p.m., on the basis of mass absorption. Between 1.25 and 0.6 Å, the background as an internal standard is recommended up to 1000 p.p.m.; at higher concentrations the mass absorption procedure is to be preferred.

Conventional mass absorption methods become increasingly unsuitable at wavelengths under 0.6 Å. In this region the background technique can be applied to correct for matrix effects at all concentrations. For samples of considerably divergent matrix an advance correction can be effected by diluting the sample with a suitable matrix. Such a procedure, however, requires a sufficiently high primary concentration of the element under investigation.

The mass absorption coefficients that were applied to correct for inter-element effects at wavelengths over 0.7 Å are based on a paper by Heinrich[9]; for lines of shorter wavelength a table published by Philips[10] was used. For the organizations issuing the standards the designation of Flanagan[11] was applied. Published averages are from Flanagan[12] for the USGS, CRPG and ANRT, SSC, ZGI, NIM and GSJ standards. Some values for the CRPG and ANRT standards have been taken from de la Roche and Govindaraju[13]; values for ANRT VS-N are from de la Roche and Govindaraju[14]. Values for T-1 are from Thomas and Kempe[15], for the albite NBS 99 from a compilation by Schneider[16] and for the QMC samples from compilations by Poole[17]. Several major element analyses for the calculation of mass absorption coefficients were carried out at the Geochemistry Department of the University of Tübingen.

The support of the Stiftung Volkswagenwerk who supplied the apparatus and provided a personal grant to the author is gratefully acknowledged. Thanks are also extended to Dr. H. Puchelt, Tübingen, for a critical review of the manuscript.

SUMMARY

The wavelength range in which trace elements are commonly determined by X-ray fluorescence has been divided into three major regions: wavelengths longer than 1.9 Å, between 1.9 and 0.6 Å, and shorter than 0.6 Å. The factors controlling matrix effects differ somewhat in each of these regions; the methods that can be applied to compensate for these effects also differ. The least laborious correction method is the internal standard technique involving scattered X-ray tube spectra. The results are discussed in the light of trace element determinations carried out on geochemical standards.

RÉSUMÉ

L'échelle des longueurs d'ondes où se fait généralement le dosage de traces d'éléments par fluorescence aux rayons-X est divisée en trois principales régions: longueurs d'ondes supérieures à 1.9 Å, entre 1.9 et 0.6 Å et inférieures à 0.6 Å. Les facteurs contrôlant l'influence de la matrice diffèrent dans chacune de ces régions, de même que les méthodes utilisées pour compenser ces effets. La technique de l'étalon interne est la plus simple. Les résultats sont examinés en fonction de dosages de traces d'éléments effectués sur des échantillons géochimiques de référence.

ZUSAMMENFASSUNG

Der Wellenlängenbereich, in dem Spurenelemente durch Röntgen-Fluoreszenz-Analyse üblicherweise bestimmt werden, wurde in drei wesentliche Bereiche unterteilt: Wellenlängen oberhalb 1.9 Å, zwischen 1.9 und 0.6 Å und unterhalb 0.6 Å. Die Faktoren, die die Matrixeffekte bestimmen, sind in diesen Bereichen verschieden; die Methoden, die zur Kompensation dieser Effekte angewendet werden, unterscheiden sich ebenfalls. Die einfachste Methode ist das Verfahren des inneren Standards, bei dem die gestreuten Röntgenröhren-Spektren berücksichtigt werden. Die Ergebnisse werden hinsichtlich der Bestimmungen von Spurenelementen diskutiert, die an geochemischen Standards ausgeführt worden sind.

REFERENCES

1 G. K. Czamanske, J. Hower and R. C. Millard, *Geochim. Cosmochim. Acta*, 30 (1966) 745.
2 K. H. Wedepohl, *Z. Anal. Chem.*, 180 (1961) 246.
3 J. Hower and T. W. Fancher, *Science*, 125 (1957) 498.
4 R. C. Reynolds, *Amer. Mineral.*, 48 (1963) 1133.
5 G. Andermann and J. W. Kemp, *Anal. Chem.*, 30 (1958) 1306.
6 J. Hower, *Amer. Mineral.*, 44 (1959) 19.
7 H. W. Fairbairn and P. M. Hurley, *Geochim. Cosmochim. Acta*, 35 (1971) 149.

8 H. A. Liebhafsky, H. G. Pfeiffer, E. H. Winslow and P. D. Zemany, *X-Ray Absorption and Emission in Analytical Chemistry*, Wiley, New York, 1960.
9 K. F. J. Heinrich, in T. D. McKinley, K. F. J. Heinrich and D. B. Wittry (Eds.), *The Electron Microprobe*, Wiley, New York, 1966, p. 296.
10 *X-Ray Mass Absorption Coefficients*, Application Data 53, Philips, Eindhoven, 1962.
11 F. J. Flanagan, *Geochim. Cosmochim. Acta*, 34 (1970) 121.
12 F. J. Flanagan, *Geochim. Cosmochim. Acta*, 37 (1973) 1189.
13 H. de la Roche and K. Govindaraju, *Revue GAMS*, 7 (1971) 314; personal communication, 1972, *A.N.R.T. Groupe 35 A*, Circulaire 3962.
14 H. de la Roche and K. Govindaraju, *Analysis*, 2 (1973) 59.
15 W. K. L. Thomas and D. R. C. Kempe, *Standard Geochemical Sample T-1*, Suppl. No. 1, Government Printer, Dar Es Salaam, Tanzania, 1963.
16 G. Schneider, *Neues Jahrb. Mineral. Monatsh.*, (1969) 504.
17 A. B. Poole, Unpublished reports on the standard rocks QMC I1, QMC I3, QMC M2 and QMC M3, 1968, 1970.

Analytica Chimica Acta, 67 (1973) 55–67

STUDIES IN ATOMIC FLUORESCENCE SPECTROMETRY

PART I. INEXPENSIVE METHODS OF IMPROVING SIGNAL-TO-NOISE RATIOS

D. P. HUBBARD* and R. G. MICHEL

Department of Chemistry and Biology, Sheffield Polytechnic, Sheffield S1 1WB (England)

(Received 14th April 1973)

Atomic fluorescence spectrometry has some potential advantages over atomic absorption spectrometry in the determination of trace elements. One such advantage is the possibility of increased sensitivity owing to the direct proportionality of the intensity of fluorescence radiation to the intensity of the light source. Another advantage is the greater linear range of fluorescence intensity *vs.* concentration curves shown by some elements. Winefordner and Elser[1] and Kirkbright and West[2] have discussed these and other considerations.

In addition to increasing the magnitude of the atomic fluorescence signal it is also extremely important to decrease the noise level associated with this signal, *i.e.* the signal-to-noise ratio needs to be maximized. This paper describes the adaptation of a Jarrell-Ash atomic absorption/atomic emission flame spectrometer to obtain the maximum fluorescence signal-to-noise ratio that was possible within a relatively small budget. The basic components of a flame spectrometer such as the premix burner and gas handling arrangements, monochromator and photomultiplier tube with its associated power supply have all been retained. However, the a.c. tuned amplifier used in the Jarrell-Ash instrument was found to be incapable of discriminating sufficiently between the very weak atomic fluorescence signals and the associated flame noise. Hieftje[3] has reviewed the electronic techniques available for improving signal-to-noise ratios including filtering, narrow-band amplifiers, lock-in amplifiers, signal averaging, boxcar integration and correlation techniques. Correlation techniques[4] and the lock-in amplifier[5] have both been discussed in more detail. An inexpensive lock-in amplifier has been described by Caplan and Stern[6]. The design of this amplifier has been adapted with slight modification and evaluated in this work by investigating the atomic fluorescence of tin. This paper also describes the application of high-frequency modulation of electrodeless discharge tubes, flame separation and a suitable optical system to the improvement of signal-to-noise ratios.

EXPERIMENTAL AND RESULTS

A simplified block diagram of the system described is shown in Fig. 1.

* Present address: Department of Chemistry, University of Otago, Box 56, Dunedin, New Zealand.

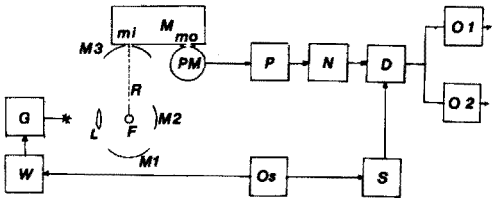

Fig. 1. Block diagram of the atomic fluorescence system described. (M1, M2, M3, and L) Optical arrangement (Fig. 2); (R) fluorescence emission; (M) monochromator; (mi and mo) entrance and exit slits respectively; (PM) photomultiplier tube; (P) pre-amplifier; (N) narrow-band amplifier; (D) mixer (often called a demodulator or synchronous detector); (S) phase shifter; (Os) oscillator; (W) EMS modulator; (G) EMS microwave generator; (01 and 02) output filters 1 and 2 respectively. Either one or the other of these outputs taken to the chart recorder.

TABLE I

APPARATUS

Sources	Tin electrodeless discharge tube (EDT Supplies Ltd.) was operated in a 3/4-wave cavity and powered by microwave generator in conjunction with either a modified 400 Hz modulator or a 50/100 Hz modulator (all from Electromedical Supplies, Ltd.). Reflected power meter (EDT Supplies).
Burner	Beckman RIIC with modified provision for flame separation. Pye–Unicam premix nebulizer and cloud chamber fitted with impact bead assembly. Gases supplied through Gallenkamp type FL-420 flowmeters with interchangeable jets. Air supplied by a Binks–Bullows PR303E portable rotary air-comp Mk V.
Optical components	Concave spherical front-silvered mirror 62 mm diameter, 60 mm focal length (M2). Concave spherical front-silvered mirror 90 mm diameter, 57.5 mm focal length with a rectangular slit in the vertex (5 × 20 mm) (M3). Concave rectangular front-silvered mirror 48 × 87 mm, focal length 69 mm (M1). Silica lens, 30 mm diameter, 50 mm focal length (L).
Basic spectrometer	A Jarrell–Ash Maximum Versatility atomic absorption/atomic emission spectrometer model 82-529.
Monochromator	Jarrell–Ash ½-m Ebert grating, 52 × 52 mm with 1180 lines per mm blazed at 300 nm. Fixed slits (25 and 100 μm) provided.
Detector	Hamamatsu T.V. R106 photomultiplier tube operated at 900 V using Jarrell–Ash stabilized power supply of the 82-529 spectrometer (variable from 270 to 1100 V).
Amplifiers	Homebuilt pre-amplifier and lock-in amplifier.
Recorder	Honeywell Electronik 194, chart recorder.
Signal generator	Sine-square oscillator Type LFM2 (Farnell Instruments Ltd.).

Details of the individual components are given in Table I. The lock-in amplifier consists of the narrow-band amplifier (N), mixer (D), output low-pass filters (01 and 02), and phase-shifter (S), and was built almost exactly to the design of Caplan and Stern[6] with monolithic integrated circuit operational amplifiers. A regulated power supply was built for the amplifier capable of delivering about 1 A at each of the two voltages, +14.5 and −7.5 V. The circuit for this can be obtained by applying to one of the authors (R.G.M.).

Flame noise or flicker is approximately inversely proportional to the frequency. A noise spectrum plotted by observing the distribution of the frequency

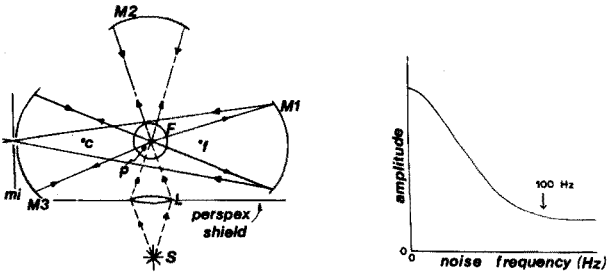

Fig. 2. Optical arrangement. (F) Flame; (S) source; (mi) monochromator entrance slit; (c and f) centre of curvature and focal point of mirror M1; (P) centre of curvature of mirror M3 at flame position. Mirror to flame distances are: (M1–F) 145 mm; (M2–F) 120 mm; (M3–F) 115 mm. Source and lens positioned to give best fluorescence signal, the lens being *ca.* 50 mm from the flame.

Fig. 3. The distribution of the frequencies of the noise from a typical flame.

of the flame noise would have the characteristics shown in Fig. 3, which indicates that d.c. measurements are to be avoided whenever flame noise dominates other noise such as photomultiplier shot noise. Most of the flicker noise is concentrated at the low frequency end of the curve, *i.e.* around d.c. This low-frequency noise or drift, inherent with d.c. amplifiers can be virtually eliminated by using an a.c. amplifier and modulating the light signal at a chosen frequency. It can be seen from Fig. 3 that frequencies in excess of 100 Hz should be employed to minimize flame noise. Dagnall *et al.*[7] have shown that the optimal frequency for the operation of a microwave-excited electrodeless discharge tube is 10 kHz. However, this frequency is favourable not only because of the noise considerations but also because of an increase in intensity of the light output from the discharge tube which occurs as the modulation frequency is increased.

A simple a.c. amplifier will have a wide frequency response and therefore, no matter which modulation frequency is used, the flame noise will still be obtained at the output. Such an amplifier is therefore, usually modified to give a reduction in response at all frequencies except a moderately narrow-band around the signal frequency. This modified type of amplifier is often called a tuned a.c. amplifier or a narrow-band amplifier. The centre frequency and bandwidth of the lock-in amplifier designed by Caplan and Stern can be selected by the operator.

The output from the photomultiplier is amplified by a pre-amplifier (P) and further amplified by the narrow-band amplifier (N). Much of the noise at frequencies far removed from the modulation frequency is eliminated by N. The signal is then fed into a mixer (D) into which a reference signal is fed. The reference derived from the oscillator (Os), switches the signal on and off at every half cycle of the reference frequency, and, when both the reference and required signal are of the same frequency and phase, the mixer–output filter combination (D and 01 or 02) gives a mean direct voltage output proportional to the amplitude of the signal voltage. The phase of the reference can be adjusted to that of the signal by means of the phase-shifter (S). This is necessary if there is anything causing a phase shift in the signal somewhere in the system before the mixer. The out-of-phase noise signals appear as an a.c. voltage fluctuating about the mean output d.c. signal voltage, and attenuated, partially, by the output low-pass filter.

The pre-amplifier

Because the input impedance of the lock-in amplifier is low relative to the high output impedance of the photomultiplier, poor matching of the two can place a potential divide across the output of the photomultiplier and a percentage of the signal will be lost. This loss is undesirable since the lock-in amplifier functions most effectively with larger signals. To overcome this problem a voltage amplifier, with an input impedance at least 100 times greater than the output impedance of the photomultiplier[8], is normally placed between the photomultiplier and the lock-in amplifier. This amplifier is usually either a buffer amplifier with a gain of unity or a pre-amplifier with fixed or variable gain greater than unity. Also, instead of using a voltage amplifier, measurements can be made with a field effect transistor–input operational amplifier as a current amplifier[9]. As well as reducing problems associated with the capacitance of the lead from the photomultiplier output, the current amplifier can also be used to obtain very high sensitivities. The voltage amplifier described in this paper is, however, a compromise between high sensitivity and the cost of components.

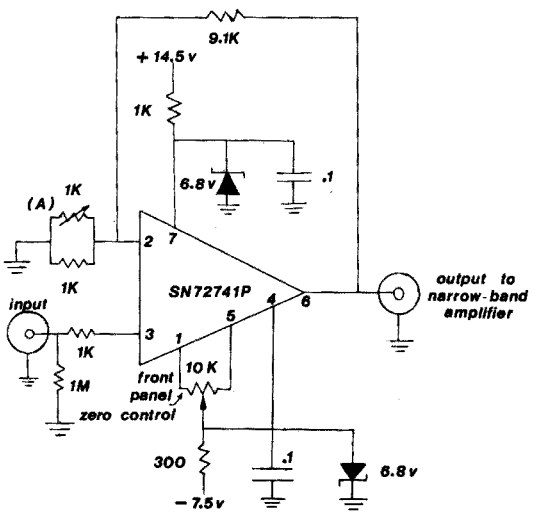

Fig. 4. The pre-amplifier. Resistance in ohms, capacitance in microfarads. Input via 100 mm, 50 Ω coaxial cable from photomultiplier tube. (2) Inverting input; (3) non-inverting input.

A pre-amplifier (Fig. 4) was built from a Texas Instruments SN72741P linear integrated circuit operational amplifier. This device, when used in the non-inverting configuration, has the high input impedance required. When the 1 kΩ preset potentiometer (A) is varied, the closed loop gain varies between some high value and a value around 20. However, this is accompanied by a variation in input impedance, which falls from just less than 400 MΩ at gain 20 to lower values as the gain is increased, and by a decrease in bandwidth[10]. If it is assumed that initially the input impedance of the amplifier is high enough, at 400 MΩ, to prevent signal loss, any increase in gain would give an increased signal at the pre-amplifier output only as long as the input impedance remains high. As soon

as the impedance drops sufficiently to attenuate the signal, further increase in gain will result in overall signal decrease.

The pre-amplifier was connected to the photomultiplier and the gain optimized by varying the preset potentiometer (A) until a maximum in the output signal had been obtained.

A low input impedance at this first stage, however, is not the only factor which can attenuate the signal at the output of the photomultiplier. The Jarrell-Ash instrument has a 1-m long 50 Ω coaxial cable at the photomultiplier output which has an inherent capacitance between the inner and outer conductors; this, in conjunction with the resistance of the cable, can attenuate high-frequency signals. As the relatively high frequency of 10 kHz was being used, attenuation was suspected, and therefore the cable was cut in half to reduce its resistance and capacitance. This resulted in an increase in output of 40%. The length of the lead was finally reduced to 100 mm to minimize the signal loss.

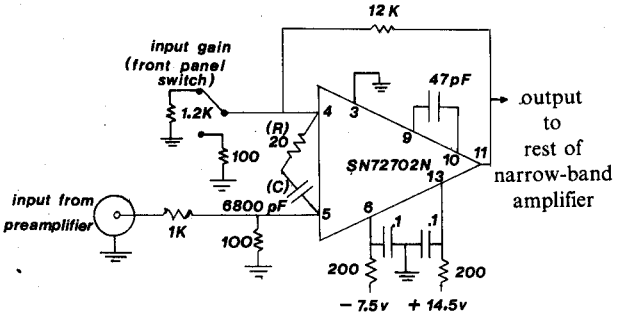

Fig. 5. Modified input amplifier. The SN72702N device is equivalent to the μA-702 used by Caplan and Stern[6]. (4) Inverting input; (5) non-inverting input.

As similar impedance matching problems occurred between the output of the pre-amplifier and the input amplifier of the narrow-band amplifier, the non-inverting input of the SN72702N input amplifier was used (Fig. 5) rather than the lower impedance inverting input which is used in the original design. The position here was not as serious as in the photomultiplier–pre-amplifier situation because the output impedance of the SN72741P is fairly low. However, use of the non-inverting input decreased the stability of the SN72702N sufficiently to cause it to go into self-oscillation. By changing the frequency compensation components (R and C, Fig. 5) oscillation was prevented, but the effective maximum bandwidth of the lock-in amplifier was consequently reduced at the same time. However, the bandwidths of the lock-in amplifier and of the pre-amplifier were both still wide enough to permit measurements of signals at frequencies between 10 and 30 kHz without significant attenuation.

A switch was used to change the gain of the input amplifier rather than the two separate BNC connectors used by Caplan and Stern. The symmetrical power supply for the pre-amplifier was derived from the supply built for the lock-in amplifier. The pre-amplifier circuit board was built into a diecast metal box to provide electrical shielding and to allow placing of the lock-in amplifier remote from the photomultiplier.

The output low-pass filters

The output low-pass filter can be thought of as a d.c. narrow-band amplifier. It is not normally possible to reduce the frequency response bandwidth of narrow-band amplifiers too much, because the signal frequency can and does drift to a position where the response of the amplifier may be low, resulting in loss of signal level. However, the lock-in amplifier, since the reference is derived from the same source as the signal, maintains the centre of the amplifier's response at the signal frequency. Consequently, the bandwidth of the output low-pass filter can be made very small because it comes after the mixer. The degree by which the low-pass filter attenuates noise depends on the time constant of the filter, which in this case is part of the negative feedback loop of a high-gain operational amplifier. The noise in fact decreases as the square-root of the time constant. Thus compared to a 1-s time constant, a 100-s constant gives only a factor of 10 reduction in noise but it takes 100 times longer for the signal to appear[8].

The filter designed by Caplan and Stern uses the same SN72741P operational amplifier as used in the pre-amplifier described above. When this filter was built, the d.c. output stability of the lock-in amplifier at a bandwidth of 0.034 Hz and a time constant of 4.7 s was satisfactory at 0.02% V^{-1}. However, a change to a bandwidth of 0.0031 Hz and a time constant of 51.7 s resulted in a stability of only 3% V^{-1}. This degraded the detection limits for atomic fluorescence. To improve the situation, a second output filter was built (Fig. 6). This circuit uses a μA-727B, SGS-Fairchild amplifier which is kept at a constant temperature by active regulator circuitry incorporated into the same monolithic integrated circuit chip as the amplifier[10]. Drift in d.c. amplifiers is caused predominantly by changes in ambient temperature, hence the advantages of an amplifier which is held at constant temperature. The μA-727B is a pre-amplifier designed to drive a standard linear integrated circuit amplifier, in this case an SN72741P.

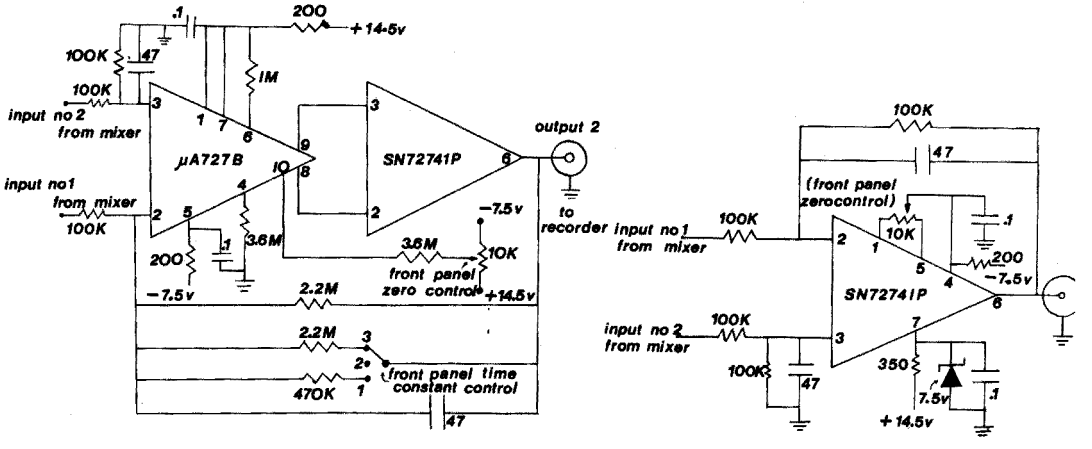

Fig. 6. Output filter 2. Switch positions give time constants of (1) 18.2 s, (2) 103.4 s, and (3) 51.7 s. Connections to pins 1, 4, 5 and 7 of the SN72741P device are identical to those in Fig. 7.

Fig. 7. Modified output filter 1. The SN72741P device is equivalent to the μA-741 device used by Caplan and Stern[6]. Time constant fixed at 4.7 s.

The output stability of the lock-in amplifier with the second filter (output 2) with a bandwidth of 0.0031 Hz and a time constant of 51.7 s was 0.02% V^{-1}. This large improvement was sufficient to allow the use of an even longer time constant of 103.4 s without further significant loss in stability. The circuitry associated with the 51.7 s time constant of the original filter was removed. The resulting circuit is shown in Fig. 7. The output (output 1) was provided with a separate BNC connector.

The time constant and bandwidth details of both filter circuits are given in Table II together with the improvements in signal-to-noise ratio which are obtained with increasingly long time constants.

The offset-null circuits, power supply decoupling, etc., were all as recommended by the device manufacturers[9].

TABLE II

PERFORMANCE OF THE OUTPUT LOW-PASS FILTERS AND ATOMIC FLUORESCENCE DETECTION LIMITS FOR TIN

(Experimental conditions outlined in the section on the a.f.s. of tin. An aqueous 1-p.p.m. tin solution was nebulized into an argon-separated air–acetylene flame and the fluorescence measured at 303.4 nm)

Output filter	*Time constant T(s)*	*Bandwidth f (Hz)*[a]	*Signal (arbitrary units)*	*Noise*	*Signal-to-noise ratio*	*Detection limit (p.p.m.)*[b]	s_r (%)[c]
1	4.7	0.034	8.0	1.5	5.3	0.38	2.3
2	18.2	0.0056	24.0	2.5	10.0	0.20	—
2	51.7	0.0031	61.5	4.5	13.6	0.15	4.6
2	103.4	0.0015	92.0	3.0	30.6	0.065	—

[a] $f = 1/2\pi T$.
[b] Signal-to-noise ratio of 2.
[c] 10 results.

High-frequency modulation of electrodeless discharge tubes

Various methods of electronically modulating electrodeless discharge tubes have been described. Thompson and Wildy[11] transformer-coupled a small a.c. voltage into the anode circuit of the magnetron which powers the discharge tube. Dagnall *et al.*[7] injected the modulation waveform directly at the reference point of the stabilizing element of the magnetron power supply. Alger *et al.*[12] used switched resistor modulation which depends on the value of the magnetron anode load resistor being repetitively changed at the modulation frequency.

The switched resistor method, although potentially more versatile in that it could be developed for pulsing the light output from the discharge tube, cannot be applied to the EMS Microtron microwave generator which has been used to power electrodeless discharge tubes for atomic fluorescence spectrometry in many laboratories. The microwave generator modified by Alger *et al.*, an Evans Electroselenium Model 245, has its anode load resistor in the d.c. side of the power supply. This resistor controls the power to the magnetron. It is therefore possible, by means of a power transistor which can withstand a large collector-to-emitter voltage, to switch at the modulation frequency, a second resistor in parallel with the anode

load resistor. However, the EMS generator has its power control in the a.c. side of its power supply. A transistor, therefore, cannot be used to achieve switched resistor modulation, the alternative being the more complicated thyristor or triac control of the power.

Stabilization modulation is not easy to apply because a voltage amplifier with a 200-V peak-to-peak output is necessary, and the power supply has to be current-stabilized[12].

In view of the above difficulties in modifying the EMS generator, it was decided to retain transformer-coupled modulation. EMS Ltd supply modulators, for use with their microwave generators, which use this method of modulation at a spot frequency variable by about 10%. A 400-Hz modulator was obtained, the internal circuit which provides the required small a.c. voltage at the frequency of 400 Hz was disconnected, and an oscillator was substituted. The square-wave signal from the oscillator, which is variable in frequency between 1 Hz and 1 MHz, is boosted to a higher voltage and transformer-coupled into the anode circuit by the EMS modulator. The reference for the lock-in amplifier was taken from the appropriate socket on the oscillator. This simple modification allowed the modulation frequency to be varied between 200 Hz and 40 kHz. Modulation at 50 Hz and 100 Hz was obtained by using another EMS modulator. Incidentally, this 50/100-Hz modulator takes the modulation signal from the mains a.c. and does not therefore incorporate the boosting circuitry necessary for the 400-Hz modulator. Suitable modification for modulation over a large range of frequencies is therefore more difficult to apply.

The frequency of modulation which gave the best signal-to-noise ratio for the atomic fluorescence spectrometry of tin in an air–acetylene flame was determined. The results, obtained with an aqueous 10-p.p.m. tin solution and an output time constant of 4.7 s, are plotted in Fig. 8. These results agree in general with those of Dagnall *et al.*[7]. Their conclusions that the discharge tube intensity increases with increasing modulation frequency and that 10.0 kHz is the frequency that gives the best signal-to-noise ratio, are confirmed. At higher frequencies, up to 20 kHz, the discharge tube intensity does increase further but unfortunately short-term noise degrades the signal-to-noise ratio to below that at 10 kHz. The minimum at 3.5 kHz in the plot of Fig. 8 probably appears because the bandwidth

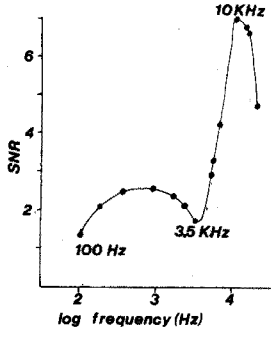

Fig. 8. Plot of frequency of modulation applied to a tin electrodeless discharge tube *vs.* the fluorescence signal-to-noise ratio obtained from the 303.4-nm tin step-wise transition. No flame separation or mirrors were used.

of the particular amplifier used was wide around this frequency compared to the bandwidths at all the other chosen frequencies. Consequently, noise was not being reduced as effectively, and the signal-to-noise ratio was poor.

When the modulation frequency is optimized, it is best to consider a plot such as Fig. 8 rather than a plot of source intensity *vs.* modulation frequency. The signal-to-noise ratio depends on lamp intensity, flame and other noise and on the characteristics of the particular amplification system used.

Optical arrangement

The purpose of a suitable arrangement of mirrors and lenses is to maximize the signal reaching the detector. The arrangement should be able to focus as much of the resonance radiation from the source onto the flame, and to collect as much of the resulting fluorescence as possible and focus this onto the entrance slit of the monochromator.

A diagram of the optics employed in this work is shown in Fig. 2. This system was based on that of Benetti *et al.*[13] except that the rather expensive ellipsoidal mirror was replaced by a concave mirror (M1). The alternative optical systems available are discussed at length by Benetti *et al.* The mirror M3 has its radius of curvature equal to the mirror–flame distance; some radiation from the flame is therefore collected by this mirror, and the image that is formed is focused back onto the flame. The mirror M1 also collects radiation from the flame but focuses both this and the image formed by mirror M3, through the slot in M3, onto the monochromator slit. The mirror M2 gives the conventional double pass, through the flame, of the source radiation. The lens allows the source to be placed in such a way as to prevent stray light entering the monochromator slit as well as focusing the source radiation onto the flame.

For the atomic fluorescence of tin in an argon-separated air–acetylene flame, this optical arrangement gave a factor of 4.4 improvement in signal-to-noise ratio made up of the factors detailed in Table III. Details of the mirror dimensions are given in Table I. Better quality and larger diameter mirrors M1 and M2 might have improved the light-gathering power of the optics, but mirror M3 was

TABLE III

IMPROVEMENT IN SIGNAL-TO-NOISE RATIO CAUSED BY OPTICAL ARRANGEMENT

(An aqueous 10-p.p.m. tin solution was nebulized into an argon-separated air–acetylene flame. Fluorescence was measured at 303.4 nm with a 4.7-s output time constant. Optimal flame conditions were not used; the discharge tube was modulated at 10 kHz)

Mirrors in use	*Signal (arbitrary units)*	*Noise*	*Signal--to-noise ratio*	*Improvement factor due to individual mirrors*	
				Mirror	*Factor*
None	14.0	2.0	7.0	M1	1.79
M1	25.0	2.0	12.5	M2	1.12
M1 and M2	38.0	2.0	14.0	M3	2.21
M1, M2 and M3	62.0	2.0	31.0	All three	4.43

of adequate diameter and reflectance. The ability of the lock-in amplifier to discriminate between signal and noise is demonstrated by the fact that no significant increase in noise is observed when the mirrors M1 and M3 are in use. When a simple tuned amplifier is used, some increase in noise is usually observed because these two mirrors must focus both the noisy flame emission and the wanted fluorescence into the monochromator.

Flame separation

Separated pre-mixed flames have been studied extensively because of the often very effective reduction in background emission which does give improvements in signal-to-noise ratio when used in conjunction with both d.c. and a.c. amplifiers. A lot of the unwanted emissions from a flame originate from the secondary diffusion zone caused by the flame gases reacting with entrained oxygen from the surrounding air to produce mostly carbon dioxide and water. The secondary zone can be lifted 3–4 cm up above the analytically useful region of the flame, which is normally just above the primary cones, by allowing nitrogen or argon to flow around the burner head parallel to the flame to form an inert shield between the atmosphere and the flame. Hobbs *et al.*[14] used coiled steel strip around the burner head to direct the inert gas, and later Aldous *et al.*[15] described the use of stainless steel hypodermic needles around the burner head to effect separation with a much smaller flow-rate of gas. This capillary separator was used by Browner and Manning[16] in conjunction with lock-in amplification for the atomic fluorescence of tin in an argon separated air–acetylene flame. These authors, using a hollow-cathode lamp as source, quote an improvement in detection limit, on separation, by a factor of 4.0. In the present work, the most sensitive conditions in the separated flame gave a factor of 3.8 improvement over the best conditions in the unseparated flame (Table IV), which indicates that the improvement factor of *ca.* 7 obtained by using 10 kHz instead of 50 Hz modulation of the discharge tubes (Fig. 8) can be still further improved by flame separation. However, this factor of 3.8 is due not only to a reduction in noise by about 1/3, but also to an increase in fluorescence emission, probably because of an increase in atomic population on separation of the flame, as observed by Dagnall *et al.*[17] for the

TABLE IV

IMPROVEMENT IN SIGNAL-TO-NOISE RATIO CAUSED BY FLAME SEPARATION

(Conditions as specified for Table III except for flame separation)

Fuel flow ($l\ min^{-1}$)	*Air flow* ($l\ min^{-1}$)	*Signal (arbitrary units)*	*Noise*	*Signal-to noise ratio*	
1.25[a]	3.7	24.0	3.0	8.0	Unseparated
0.90	3.7	9.0	3.0	3.0	Unseparated
0.90[b]	3.7	60.5	2.0	30.3	Argon-separated

[a] Fuel-rich flame giving most sensitive conditions for tin determinations.

[b] Fuel flow was the maximum possible consistent with preventing the argon from extinguishing the flame.

atomic fluorescence determination of silicon in the separated nitrous oxide–acetylene flame. Moreover, quenching of fluorescence by diatomic species in air is probably reduced by argon shielding, so that more radiation reaches the monochromator.

A water-cooled capillary separator, built to a design similar to that of Aldous *et al.*[15], was used in this work; it gave very efficient separation and required an argon flow rate of only 6 l min^{-1}. A Beckman RIIC Meker burner with 13 holes supported the air–acetylene flame.

The atomic fluorescence determination of tin

The performance of the system described above was evaluated in the first instance by looking at the signal-to-noise ratios obtained from the atomic fluorescence emissions of tin in the air–acetylene flame. The tin electrodeless discharge tube was operated at an incident microwave power of 43 W and a reflected power of 25 W, in a 3/4-wave Broida cavity with modulation at 10 kHz. The first discharge tube used was air-cooled and operated satisfactorily at the maximal percentage modulation that the equipment could deliver; it lasted several hundred hours. A second lamp would only operate at 10% of the maximal modulation depth and also required cooling. However, the fluorescence intensities obtained with the two lamps were identical.

The monochromator entrance and exit slits were set at 100 and 150 μm respectively, the maximum available, for both fixed wavelength and wavelength scanned results.

The mirrors M1 and M3 were set up with a tungsten filament lamp at the flame position by focusing the two images of the filament onto the slit. The image of the source was focused onto the flame position with the lens and the mirror M2 was placed to focus the image back onto the flame position. A perspex shield with a hole for the passage of light through the lens, and painted matt black, was placed in front of the cavity to reduce the amount of stray light reaching the monochromator.

A photomultiplier voltage of 900 V was the maximum that could be used without saturation of the narrow-band amplifier. Without flame separation, noise reaching the photomultiplier was greater and 800 V became the maximum.

The narrow-band amplifier was set at maximal gain and the smallest bandwidth possible around the 10-kHz signal frequency. The lock-in amplifier was set up as described by Caplan and Stern[6].

Fuel and oxidant flows were as given in Table IV for the argon-separated flame; the argon flow of 6.0 l min^{-1} was the minimal flow required to lift the secondary diffusion zone and produced the best signal-to-noise ratio.

The atomic fluorescence spectrum of tin was obtained and showed similar characteristics to the spectrum obtained by Browner *et al.*[18]. The detection limits calculated from the signal-to-noise ratio of an aqueous 1-p.p.m. tin solution are listed in Table II. The 303.4-nm tin line was used for the reasons discussed by Browner *et al.*[18], being the most intense of the fluorescence emissions from tin in the air–acetylene flame.

CONCLUSIONS

The detection limit of about 0.6 p.p.m. for tin in an air–acetylene flame

obtained by Browner *et al.*[18], has been improved upon by applying high-frequency modulation to the electrodeless discharge tube. It is possible to obtain a detection limit of 0.065 p.p.m. However, some analytical applications may preclude the use of the rather long time constant of 103.4 s. A separated argon–oxygen–hydrogen flame should provide a further improvement in detection limit. Browner *et al.* achieved a value of 0.1 p.p.m. for tin in this flame.

The modifications to the conventional flame spectrometric set-up described in this paper appear to give a worthwhile improvement in signal-to-noise ratio and the changes in instrumentation suggested are well within the budget of most laboratories; the lock-in amplifier and its associated electronics was built for less than £100.

The authors acknowledge with thanks the Science Research Council for the provision of an S.R.C. (CAPS) Studentship for one of us (R.G.M.). Our thanks are also due to BISRA, the Corporate Laboratories of the British Steel Corporation, for the loan of the 400-Hz modulator and the 3/4-wave cavity, and to colleagues who contributed much valuable advice during the early stages of the building of the lock-in amplifier.

SUMMARY

The simple inexpensive adaptation of a conventional flame spectrometer for sensitive measurements of atomic fluorescence signals is described. The modifications include a home-built lock-in amplifier and pre-amplifier, high-frequency modulation of electrodeless discharge tubes, an optical system with 3 mirrors and a lens, and argon separation of an air–acetylene flame. The detection limits for the atomic fluorescence of tin range from 0.38 to 0.065 p.p.m. for time constants of 4.7 and 103.4 s, respectively. These figures compare favourably with both atomic fluorescence and atomic absorption detection limits obtained previously.

RÉSUMÉ

On décrit une adaptation simple, et non coûteuse d'un spectromètre de flamme conventionnel pour des mesures sensibles de signaux de fluorescence atomique. Cette modification comprend: amplificateur et préamplificateur, modulation à haute fréquence de tubes à décharge sans électrode, système optique avec 3 miroirs et une lentille, séparation argon d'une flamme air–acétylène. Les limites de détection pour la fluorescence atomique de l'étain vont de 0.38 à 0.065 p.p.m. pour des temps de 4.7 et 103.4 s respectivement. Ces valeurs sont intéressantes comparées avec celles obtenues précédemment avec la fluorescence atomique et l'absorption atomique.

ZUSAMMENFASSUNG

Eine einfache, billige Anpassung eines konventionellen Flammenspektrometers für empfindliche Messungen von Atomfluoreszenz-Signalen wird beschrieben. Hierzu gehören ein selbstgebauter phasenempfindlicher Verstärker und ein Vorverstärker, Hochfrequenz-Modulation von elektrodenlosen Entladungsröhren, ein

optisches System mit 3 Spiegeln und einer Linse und die Isolierung einer Luft–Acetylen-Flamme mittels Argon. Die Nachweisgrenzen für die Atomfluoreszenz von Zinn liegen zwischen 0.38 und 0.065 p.p.m. bei Zeitkonstanten von 4.7 bzw. 103.4 s. Diese Werte sind günstig im Vergleich zu den bisher bei Atomfluoreszenz und Atomabsorption erhaltenen Nachweisgrenzen.

REFERENCES

1 J. D. Winefordner and R. C. Elser, *Anal. Chem.*, 43 (1971) No. 4, 24A.
2 G. F. Kirkbright and T. S. West, *Chem. Br.*, 8 (1972) 428.
3 G. M. Hieftje, *Anal. Chem.*, 44 (1972) No. 6 81A and No. 7 78A.
4 G. M. Hieftje, R. I. Bystroff and R. Lim, *Anal. Chem.*, 45 (1973) 253.
5 T. C. O'Haver, *J. Chem. Educ.*, 49 (1972) No. 3 A131 and No. 4 A211.
6 L. C. Caplan and R. Stern, *Rev. Sci. Instrum.*, 42 (1971) 689.
7 R. M. Dagnall, M. D. Silvester and T. S. West, *Talanta*, 18 (1971) 1103.
8 C. Veillon, in J. A. Dean and T. C. Rains, *Flame Emission and Atomic Absorption Spectrometry*, Vol. 2, Marcel Dekker, New York, Ch. 6, p. 163–173.
9 J. D. Winefordner, S. G. Schulman and T. C. O'Haver, *Luminescence Spectrometry in Analytical Chemistry*, Vol. 38 in Chemical Analysis, Wiley–Interscience, New York, 1972.
10 J. Keen (Editor), *The Application of Linear Microcircuits*, Vols. 1 and 2, SGS (UK) Ltd. 1971.
11 K. C. Thompson and P. C. Wildy, *Analyst*, 95 (1970) 562.
12 D. Alger, R. M. Dagnall, M. D. Silvester and T. S. West, *Anal. Chem.*, 44 (1972) 2255.
13 P. Benetti, N. Omenetto and G. Rossi, *Appl. Spectrosc.*, 25 (1971) 57.
14 R. S. Hobbs, G. F. Kirkbright, M. Sargent and T. S. West, *Talanta*, 15 (1968) 997.
15 K. M. Aldous, R. F. Browner, R. M. Dagnall and T. S. West, *Anal. Chem.*, 42 (1970) 939.
16 R. F. Browner and D. C. Manning, *Anal. Chem.*, 44 (1972) 843.
17 R. M. Dagnall, G. F. Kirkbright, T. S. West and R. Wood, *Anal. Chim. Acta*, 47 (1969) 407.
18 R. F. Browner, R. M. Dagnall and T. S. West, *Anal. Chim. Acta*, 46 (1969) 207.

Analytica Chimica Acta, 67 (1973) 69–77

DETERMINATION OF EIGHT METALS IN THE INTERNATIONAL BIOLOGICAL STANDARD BY FLAMELESS ATOMIC-ABSORPTION SPECTROMETRY

P. SCHRAMEL

Gesellschaft für Strahlen- und Umweltforschung mbH., 8042-Neuherberg-München (German Federal Republic)

(Received 20th December 1972)

Owing to its high sensitivity and precision, the flameless atomic-absorption spectrometric method should be useful for investigations of the behaviour of trace elements in biological material. This method could also be a valuable complement to neutron activation analysis in the medical and biological research laboratory, for it should solve some practical clinical problems in the determination of trace elements. Various elements, such as lead, vanadium and aluminium cannot be determined easily in biological materials by neutron activation analysis.

However, before this technique can be applied with confidence in routine work, basic investigations are necessary. In the work described here, the influence of some major components in wet-ashed biological material, *i.e.* Ca, K, Na, P and S, on the accuracy of flameless atomic-absorption analysis was studied. The experiments were carried out on the International Biological Standard (IBS) of Bowen[1] as a reference material. The elements mentioned were selected because they were to be investigated subsequently in studies of trace element behaviour in some human tissues as a complement to neutron activation analysis.

EXPERIMENTAL

Instrumentation

The instruments used were a double-beam Perkin-Elmer Model 403 spectrometer, a graphite furnace, Model HGA 72, and a laboratory recorder. The spectrometer had a deuterium-arc background corrector as an accessory. This device is designed to remove the effect of unwanted absorption or light scattering, mostly caused by fumes from the destruction of the biological material or by evaporation of the solvent.

The normal Perkin-Elmer graphite tubes were used for the determinations of all the elements mentioned.

Wet-ashing of the samples

For the destruction of the biological material, a wet-ashing method with concentrated sulphuric acid and 50% hydrogen peroxide was used. This method is well known and is applied for radiochemical processing in this laboratory for neutron activation analysis[2]. In the case of flameless atomic-absorption spectro-

metry, it is desirable to work with low concentrations of acids in order to minimize fumes during the thermal treatment and atomization of the sample. Accordingly, the minimal amount of concentrated sulphuric acid necessary to ash a sample of about 100–150 mg (dry weight) was tested; this was found to be 100 μl of sulphuric acid and 1.5–2 ml of 50% hydrogen peroxide. It is also important in flameless atomic absorption work, to use the minimal amounts of added chemicals to the sample because of the "background effect". All chemicals are contaminated with trace elements, and hydrogen peroxide is particularly difficult to obtain in a very pure form. It was therefore necessary to use as little peroxide as possible to reduce the "background effect", and, to use the small amount effectively, it was necessary to add it in a controlled manner to the hot sulphuric acid sample solution. If the peroxide was added in one step, there was an excessive dilution of the sulphuric acid solution and the time for the destruction of the biological material became much longer.

In order to reduce further the contamination of the sample, quartz flasks must be used for the ashing procedure. The dropwise addition of the peroxide was done by a small peristaltic pump (Fig. 1). The time for ashing one sample was 3–5 min. Up to 10 samples could be ashed simultaneously by a suitable device for routine work.

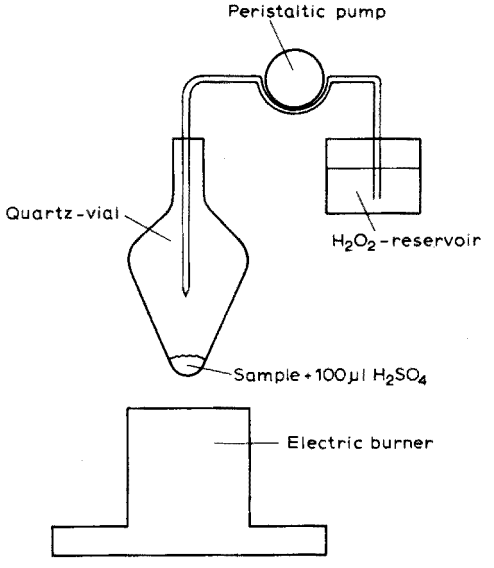

Fig. 1. Schematic drawing of the wet-ashing device.

The final wet-ashing procedure, applied in the present work, was as follows: cover 100–150 mg of dry sample with 100 μl of concentrated sulphuric acid, and heat until fumes of sulphur trioxide appear. Then add dropwise 1.5–2 ml of 50% hydrogen peroxide until a clear solution is reached. Cool and dilute to 10 ml with twice-distilled water.

Solutions prepared in this way were suitable for all the elements studied. Ten sample solutions of the IBS were prepared. All sample weights were in the range of

100–150 mg. Because this standard material is slightly hygroscopic, it contains about 5% of water when despatched. It is recommended that samples of the material should be dried for 20 h at 90° and subsequently cooled in a desiccator for determination of the dry weight[3].

Various other acid mixtures, with and without peroxide, were tested for wet-ashing, but none was as satisfactory as the mixture described above.

Preparations of standard solutions

In the first step, standard solutions of all the elements investigated were prepared in the range 0.1–10 ng per 10 μl in 0.18 *M* sulphuric acid. These solutions were stored in quartz flasks.

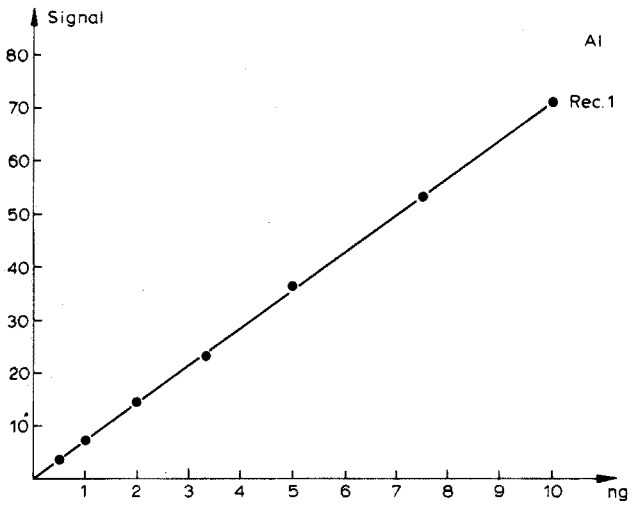

Fig. 2. Calibration curve for aluminium.

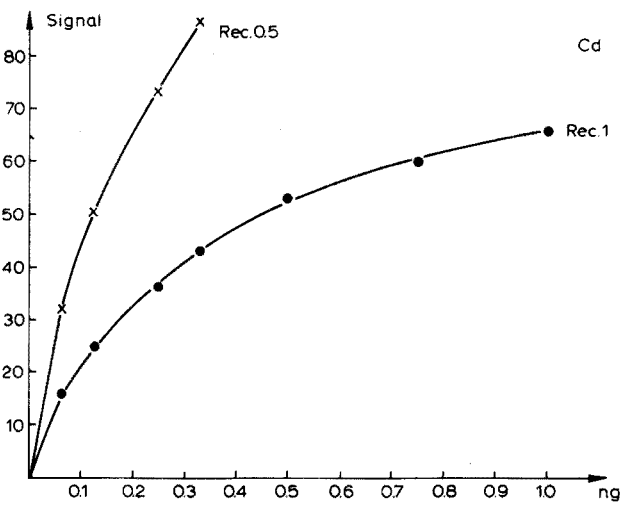

Fig. 3. Calibration curves for cadmium.

Calibration curves

All calibration curves were obtained with 10-μl amounts of each "pure" standard solution prepared in 0.18 *M* sulphuric acid (Figs. 2–9). The temperature programmes applied are presented in Table I; these programmes were worked out for each element by applying the new gradient temperature programme of the HGA-72 for optimizing the three steps: drying, thermal treatment and atomization.

Subsequently, the effects of the matrix elements, calcium, potassium, sodium and phosphorus were investigated. The interference of sulphur was taken into consideration by applying a 0.18 *M* sulphuric acid standard solution. For these

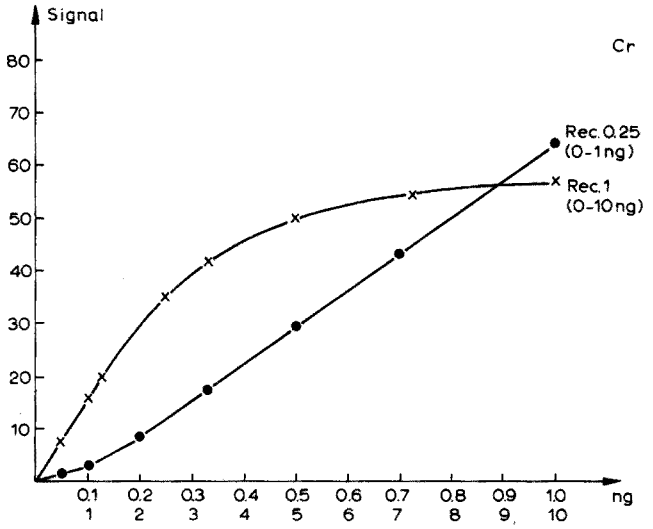

Fig. 4. Calibration curves for chromium.

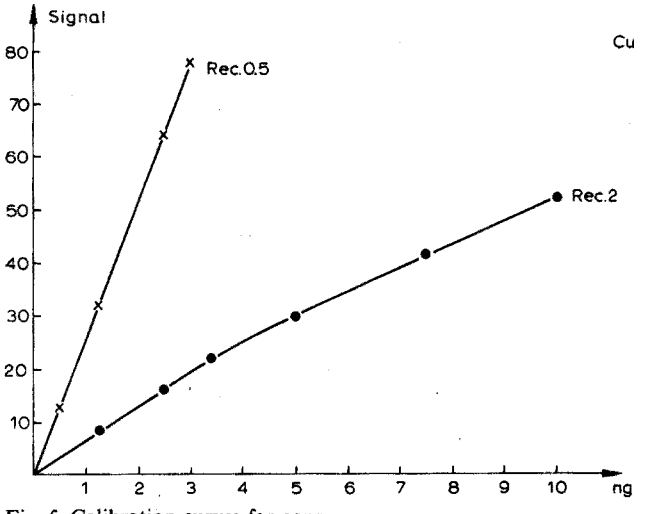

Fig. 5. Calibration curves for copper.

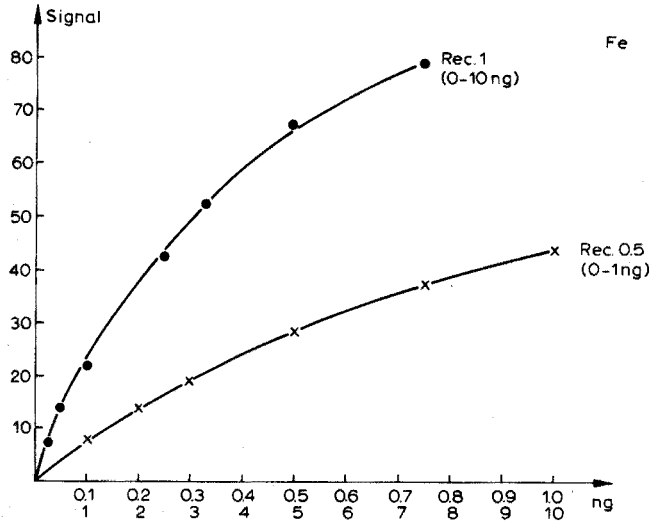

Fig. 6. Calibration curves for iron.

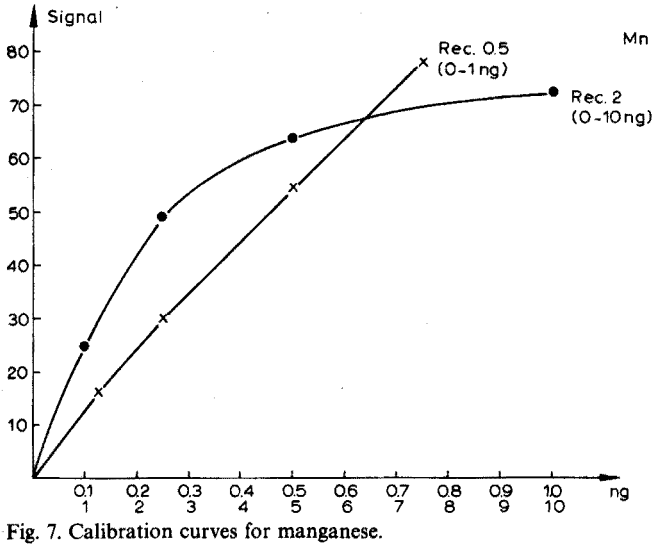

Fig. 7. Calibration curves for manganese.

experiments, known amounts of Ca, K, Na and P were added to the "pure" standard solutions to give concentrations of these elements equal to those in the IBS, as shown in Table II. The amounts added to the "pure" standard solutions were calculated for 100-mg samples in 10 ml of solution. The results showed that there were no interferences for the elements Al, Cd, Cu, Cr, Fe and Mn; for all these metal ions, the calibration curves found were the same as with "pure" standard solutions (Figs. 2–7).

The results for lead and vanadium are shown in Figs. 8 and 9. Further calibration curves for lead and vanadium were prepared with different concentrations of these matrix elements; the concentrations used correspond to muscle

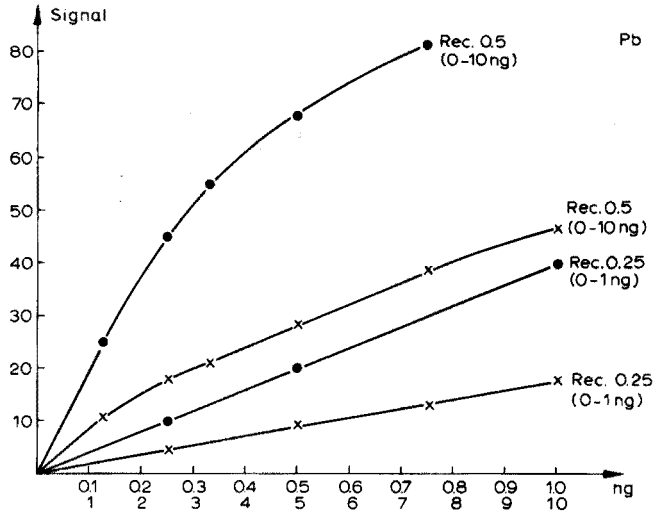

Fig. 8. Calibration curves for lead. (●) In 0.18 *M* sulphuric acid medium. (×) IBS matrix.

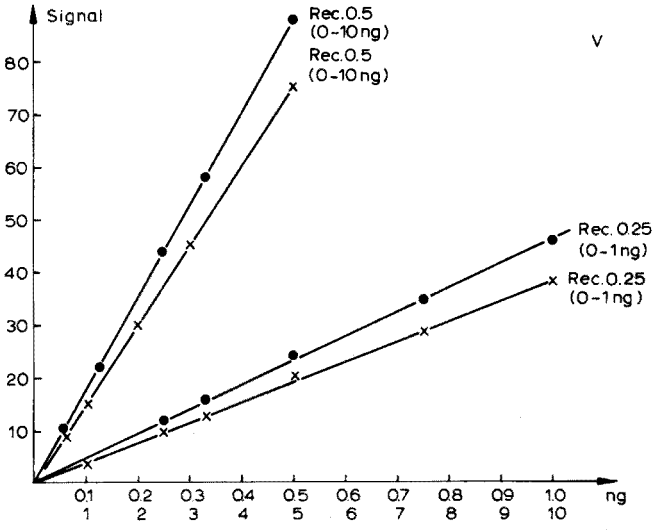

Fig. 9. Calibration curves for vanadium. (●) In 0.18 *M* sulphuric acid medium. (×) IBS matrix.

tissue (tissue matrix 2) and placenta tissue (tissue matrix 1), and details are given in Table II. The different calibration curves obtained for lead in the three matrices are shown in Figs. 8 and 10. In the case of vanadium, there were no significant differences in the curves for the three matrices mentioned. With regard to the IBS matrix, it is clear that there are very strong interferences with the absorbance signal in the case of lead. The "pure" standard solutions of this element gave absorbance signals which were about three times higher than the signals in the case of the IBS matrix. Interferences were less significant in the case of vanadium.

TABLE I

TEMPERATURE PROGRAMMES FOR THE GRAPHITE FURNACE

Element (10-μl solutions)	*Drying temperature /time*	*Thermal treatment /time*	*Atomization /time*
Al	100°/30 s	900°/15 s	2500°/5 s
Cd	100°/30 s	450°/30 s	2500°/5 s
Cr	100°/30 s	1350°/10 s	2500°/5 s
Cu	100°/30 s	700°/10 s	2500°/5 s
Fe	100°/30 s	1000°/10 s	2500°/5 s
Mn	100°/30 s	700°/15 s	2500°/5 s
Pb	100°/30 s	600°/20 s	2500°/5 s
V	100°/30 s	1700°/10 s	2500°/7 s

TABLE II

CONCENTRATIONS OF THE MATRIX ELEMENTS IN INTERNATIONAL BIOLOGICAL STANDARD, DRY MAMMALIAN MUSCLE TISSUE AND FRESH HUMAN PLACENTA TISSUE

Element	*Concentration (p.p.m.)*		
	IBS[3]	*Muscle*[4]	*Placenta*[5]
Ca	40000	105	250
K	25000	10500	1560
Na	2500	4000	2250
P	4500	6300	930
S	16000	6800	–

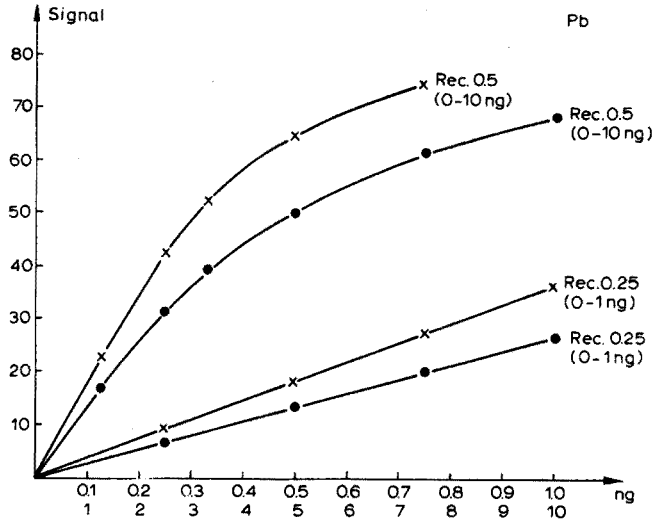

Fig. 10. Calibration curves for lead. (×) Tissue matrix 1. (●) Tissue matrix 2.

RESULTS

Table III shows the results of the determinations of the above-mentioned elements in the IBS. In the last column of the Table, the grand means given by Bowen[1] are presented. The elements Al, Cd, Cr, Cu, Fe and Mn were determined by applying the calibration curves obtained with "pure" solutions; the determinations of lead and vanadium were done by means of the matrix-corrected curves shown in Figs. 8 and 9.

TABLE III

CONCENTRATIONS OF SOME TRACE ELEMENTS IN THE IBS

(All results in mg kg^{-1}. In each case, 10 samples were analysed)

Element	*Mean value*	*Standard deviation*	*Mean value*[1]
Al	39.3	±1.8	38.2
Cd	0.75	±0.18	0.80
Cr	0.34	±0.19	0.308
Cu	4.8	±0.6	4.99
Fe	106	±5	118.3
Mn	14.8	±1.3	14.73
Pb	2.6	±0.3	2.645
V	0.33	±0.004	0.36

DISCUSSION

The results obtained, which are in good agreement with those given by Bowen, indicate that the applied wet-ashing procedure with concentrated sulphuric acid and 50% hydrogen peroxide is a useful and quick method for destroying biological material for determinations of trace elements by flameless atomic-absorption spectrometry. Furthermore, one can say that the flameless method is a good technique for analyzing biological material for the elements investigated in this study. Only for the determinations of lead and vanadium is it necessary to know the concentrations of the matrix elements in order to avoid systematic errors. In general, however, in the current state of knowledge of the flameless method, it is desirable to have the standard solutions for calibrating the instrument always in the matrix of the investigated samples. Ebdon *et al.*[6] have shown that there can be strong interferences from some ions on the absorbance signal of manganese in aqueous solutions. However, in the present experiments with a weak sulphuric acid solution, no interference on manganese by the mentioned elements was found.

SUMMARY

Concentrations of the elements Al, Cd, Cr, Cu, Fe, Mn, Pb and V were investigated in the International Biological Standard (IBS) of Bowen, by means of atomic-absorption spectrometry with a graphite furnace. An established wet-ashing method with concentrated sulphuric acid and hydrogen peroxide was applied. For

each element, a temperature programme for the graphite furnace was worked out. The influence on the absorbance of the matrix elements Ca, K, Na, P and S was tested. Considerable interferences were found in determinations of lead and vanadium.

RÉSUMÉ

On propose un dosage de huit métaux (Al, Cd, Cr, Cu, Fe, Mn, Pb et V) par spectrométrie par absorption atomique, avec four de graphite. L'échantillon à analyser est d'abord minéralisé par l'acide sulfurique concentré et le peroxyde d'hydrogène. Les conditions de température sont déterminées pour chaque métal. On examine l'influence des éléments de matrice (Ca, K, Na, P et S). Les interférences sont considérables lors du dosage du plomb et du vanadium.

ZUSAMMENFASSUNG

Die Konzentrationen der Elemente Al, Cd, Cr, Cu, Fe, Mn, Pb und V im Internationalen Biologischen Standard (IBS) von Bowen wurden mittels Atomabsorptionsspektrometrie unter Verwendung eines Graphitofens untersucht. Es wurde eine bekannte Nassveraschungsmethode mit konzentrierter Schwefelsäure und Wasserstoffperoxid angewendet. Für jedes Element wurde ein Temperaturprogramm für den Graphitofen ausgearbeitet. Der Einfluss der Matrixelemente Ca, K, Na, P und S auf die Extinktion wurde geprüft. Erhebliche Störungen wurden bei der Bestimmung von Blei und Vanadin festgestellt.

REFERENCES

1 H. J. M. Bowen, *C.N.R.S. Int. Colloq. on Activation Analysis, C.E.N. Saclay, France, 2nd–6th Oct. 1972.*
2 K. Samsahl, *Anal. Chem.*, 39 (1967) 1480.
3 J. M. A. Lenihan and S. J. Thomson, *Advances in Activation Analysis*, Vol. 1, Academic Press, London, 1969, pp. 101–113.
4 H. J. M. Bowen, *Trace Elements in Biochemistry*, Academic Press, London, 1968.
5 Documenta Geigy, *Wissenschaftliche Tabellen*, J. R. Geigy A.G., Pharma, Basel, 1968.
6 L. Ebdon, G. F. Kirkbright and T. S. West, *Anal. Chim. Acta*, 58 (1972) 39.

Analytica Chimica Acta, 67 (1973) 79–87

THE DETERMINATION OF GERMANIUM BY ATOMIC ABSORPTION SPECTROMETRY WITH A GRAPHITE TUBE ATOMIZER

D. J. JOHNSON and T. S. WEST

Chemistry Department, Imperial College of Science and Technology, London SW7 2AY (England)

R. M. DAGNALL

Biochemistry Division, Huntingdon Research Centre, Huntingdon (England)

(Received 25th April 1973)

The determination of germanium by atomic spectrometric methods is difficult, owing to the formation of a highly stable oxide species which precludes the efficient production of germanium atoms. Amos and Willis[1] reported a sensitivity of only 120 μg Ge ml^{-1} for 1% absorption at the germanium 256.12, 256.16-nm doublet in a fuel-rich air–acetylene flame, and almost identical results in an air–hydrogen flame. Using nitrogen–oxygen–acetylene and nitrous oxide–acetylene flames, the same authors obtained sensitivities (by atomic absorption spectrometry) of 5.5 and 1.5 μg Ge ml^{-1}, respectively. Manning[2], using a nitrous oxide–acetylene flame found a sensitivity of 2.5 μg Ge ml^{-1} and a limit of detection of 1 μg Ge ml^{-1}. Popham and Schrenk[3] found a limit of detection of 0.5 μg Ge ml^{-1} with the same flame system, but with a (1 + 1) acetone–water solvent system. With a reducing oxy/acetylene flame, the limit of detection was 5 μg Ge ml^{-1}. The low background of the argon-separated nitrous oxide–acetylene flame has enabled the limit of detection to be lowered to 0.2 μg Ge ml^{-1} (for a signal–noise ratio of 2)[4].

Other workers[5–8] have measured the thermal emission at the 256.2-nm doublet of germanium in nitrogen–oxygen–acetylene and nitrous oxide–acetylene flames, Pickett and Koirtyohann[5,6] finding a detection limit of 0.5 μg Ge ml^{-1}.

Bratzel *et al.*[9] demonstrated the feasibility of determining germanium by atomic fluorescence spectrometry, and Dagnall *et al.*[8] using a germanium electrodeless discharge lamp light source and an argon-separated nitrous oxide–acetylene flame obtained a limit of detection of 0.13 μg Ge ml^{-1} (S/N = 2). A non-dispersive atomic fluorescence system has also been used[10].

The graphite tube atomizer and the carbon filament atom reservoir have been used by numerous workers[11–14]. The detection limits (in terms of concentration) by this method have generally been as good as or better than those found for flame methods, with the advantage that only very small (μl) quantities of sample are required. These systems are also able to atomize such refractory elements as vanadium[11,15], molybdenum[11,16,17] and titanium[11], and it would seem that this technique would lend itself to the determination of germanium.

In this work, a study is made of the use of both the graphite tube and the carbon filament reservoir as methods for the determination of germanium.

EXPERIMENTAL

Apparatus

The carbon filament assembly used was, apart from minor modifications to the cooling water supply, identical to that described by Maines[18] and by West *et al.*[19–22]. The graphite tube atomizer was designed to fit directly on top of the stainless steel pillars of the carbon filament reservoir, in place of the normal filament clamps. These two assemblies were easily interchanged. The graphite tube assembly is shown in Figs. 1 and 2. The graphite tube was machined from Ringsdorff 6-mm spectrographic graphite rod. The internal diameter was 4.8 mm (no. 12 drill) and the overall length 20 mm. A 2-mm hole, drilled at the mid-point, enabled a sample to be introduced into the tube. Two transverse slots *ca.* 1 mm deep, were cut in the tube 4 mm from the mid-point; the effect of these was to produce a localized heating at the centre of the tube. The ends of the tube were supported in graphite (Morganite EY 110) split rings (6 mm i.d., 9 mm o.d. $\times 3$ mm long), which were clamped firmly in the stainless steel end-supports by means of two pinch bolts. The split rings were found necessary, in order that good electrical contact was made at the tube ends, and also to prevent overheating and melting of the end-supports at the point of contact. Only one of the supports was screwed to the pillar; the other was free-floating, electrical connection being made via flexible copper braiding (not shown). This arrangement prevented breakage of the tube by misalignment or expansion on heating.

The tube assembly was enclosed in a pyrex cell, which rested on the base plate. Two diametrically opposed holes ($\frac{1}{2}$-in. diameter) allowed transmission of the light beam. The cell top was removable, enabling a sample to be placed easily in the tube. The cell was flushed with nitrogen via the gas box normally used for the carbon filament, and also via a second gas inlet in the base plate. A total nitrogen flow rate of *ca.* 3 l min^{-1} ensured that the tube operated in an inert atmosphere.

Power was supplied by a 20:1 stepdown transformer, the primary voltage of which was controlled by a Variac transformer from the mains supply. This supply was originally designed for use with the carbon filament and was rated at 1.2 kW (continuous). Current and voltage measurements made with the graphite tube indicated that the power dissipated by the tube was *ca.* 3.5 kW but, as the tube was generally only switched on for 2 s or less, it was felt that this overload was acceptable.

A Southern Analytical A1740 grating photometer, fitted with an EMI 9662B photomultiplier, was used. The slit-width was 0.06 mm, corresponding to a band-pass of 0.35 nm. The normal integration and readout facilities of this instrument were by-passed and the output was taken directly from the photomultiplier to the Y-axis input of a Telequipment DM53A Storage Oscilloscope, fitted with a "K" type amplifier. A 22,000 pF capacitor was connected across the input terminals, in order to reduce high-frequency noise; this increased the effective response time of the oscilloscope to *ca.* 75 ms f.s.d.

A germanium electrodeless discharge lamp was used as a spectral source. This was made from germanium metal and iodine (amounts estimated as less than 1 mg) sealed under a pressure of 3 Torr of argon. Microwave power was provided

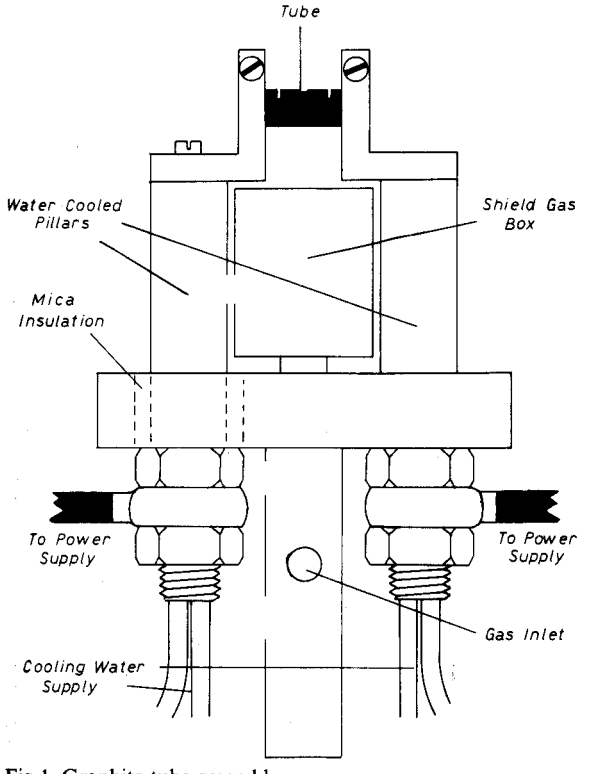

Fig 1. Graphite tube assembly.

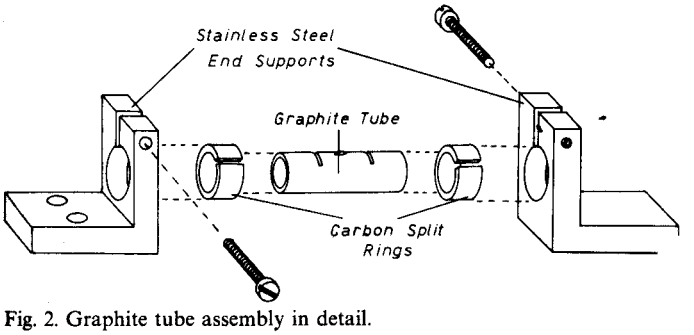

Fig. 2. Graphite tube assembly in detail.

by a Beckman "Microgen" (2450 MHz) unit, and coupling was via a fore-shortened $\frac{3}{4}$-wave cavity. The source was initiated by a spark from the EHT supply of the "Microgen".

In order to obtain good rejection of radiation emitted from the heated tube, the following optical arrangement was found satisfactory. The radiation from the source was focused by a lens at the mid-point of the tube, and a second lens focused the radiation onto the monochromator slit. Two light stops (in the form of 2-mm diameter holes) were placed either side of the tube, so that only a narrow "pencil" of radiation was transmitted.

Solutions

A 1000-p.p.m. germanium stock solution was made by dissolving 0.380 g of germanium dioxide in the minimum of 1 *M* sodium hydroxide. This was acidified with 1 *M* hydrochloric acid and diluted to 250 ml with deionized water. All other solutions were made from AnalaR-grade materials.

PRELIMINARY STUDY

Carbon filament atom reservoir

With the carbon filament, the germanium atomic absorption at 265.2 nm was investigated. A 1000-p.p.m. solution (1 μl) gave a large (>99% absorption) signal, but no signal at all was observed with a 500-p.p.m. solution. Absorption signals could be obtained from a 100-p.p.m. solution, provided that the filament was pre-treated by heating to red heat in air before each sample was placed on the filament. However, the reproducibility of the signals was extremely poor (typically > 50%), and the filament had a lifetime of only about ten such treatments. It was concluded that the carbon filament did not provide a usable technique for the determination of germanium.

Workers who have studied the $Ge/GeO_2/C$ systems[23–25] indicate that the reaction

$$GeO_2 + C \rightarrow GeO + CO$$

predominates when germanium dioxide is heated in the presence of carbon. Germanium monoxide is volatile at the temperature of the reaction, and sublimes as such without undergoing further reduction. If a thermal degradation of the germanium sample to GeO_2 first occurs, then it would be expected that germanium will be largely lost as volatile GeO; little atomization will occur and hence little absorption will be observed.

Graphite tube

One of the major differences between the carbon filament and the graphite tube is the residence time of atoms in a high-temperature environment. With the carbon filament, this time is of the order of 10^{-2} s, whereas with a tube it can be of the order of seconds. It was thought that the use of a tube would facilitate the formation of germanium atoms by retaining the GeO species within the tube until the temperature had risen sufficiently for breakage of the Ge–O bond to occur. Preliminary investigations confirmed this; a reproducible germanium atomic absorption signal was observed from samples containing less than 10 ng of germanium. It was decided, therefore, to evaluate fully the graphite tube technique for the determination of germanium.

OPTIMIZATION OF OPERATING PARAMETERS

The germanium electrodeless discharge lamp emitted 23 germanium lines between 204.3 and 422.7 nm. Of these 12 were resonance lines. The absorbances of a 10-ng germanium sample at some of the most intense of these lines are shown in Table I. The unresolved 265.12, 265.16-nm line pair was chosen as the most

TABLE I

WAVELENGTHS, SOURCE INTENSITIES AND ATOMIC ABSORPTION SENSITIVITY FOR GERMANIUM IN A HEATED GRAPHITE TUBE ATOMIZER

Wavelength (nm)	*Relative intensity of line*	*Absorbance (10 ng Ge)*	*Sensitivity (1% absorption) (g)*
209.4	3	0.155	$2.8 \cdot 10^{-10}$
249.8	7	0.013	$3.4 \cdot 10^{-9}$
253.3	7	0.000	
258.9 } 259.2 }	53	0.180	$2.4 \cdot 10^{-10}$
265.12 } 265.16 }	100	0.305	$1.5 \cdot 10^{-10}$
269.1	41	0.123	$3.6 \cdot 10^{-10}$
270.9	49	0.178	$2.5 \cdot 10^{-10}$
275.5	47	0.129	$3.4 \cdot 10^{-10}$

useful because of its high sensitivity and high signal–background ratio. This line pair is subsequently referred to as the 265.2-nm "line".

Electrodeless discharge lamp power

The absorbance of a germanium sample at 265.2 nm was measured at various microwave powers. This indicated that a low power was desirable. The absorbance was approximately constant below a microwave generator current of 10 mA but dropped by *ca.* 25% at 20 mA and *ca.* 35% at 25 mA. A current of 10 mA was normally used.

Variac setting

The shape of the germanium absorption signal varied with Variac setting. Below *ca.* 70% power (*ca.* 8 V), no absorption peak was observed although the sample was lost from the tube, as was evidenced by the lack of an absorption peak on re-heating the tube at maximal power. This supports the view that loss of germanium as GeO is important; in this instance, the temperature was too low to effect atomization of the oxide. Above this power setting, an absorption signal was observed which increased in peak height and decreased in width as the power was increased. As all measurements were made from the peak height, the maximal power available was used in order to obtain maximal sensitivity. At the highest power setting, the tube reached maximal temperature (*ca.* 3200°) in less than 2 s. The germanium absorption peak commenced 0.14 s after the power was switched on and reached a maximum within 0.2 s. The overall peak-width was *ca.* 1 s. After the tube had been used a number of times, a second absorption peak occurred which commenced *ca.* 1 s after the power had been switched on. This was also observed at the germanium 303.9-nm (non-resonance) line and at 253.6 nm when a mercury electrodeless discharge lamp was substituted as light source; it was concluded that this peak was due to scattering of the light by carbon particles, produced by sublimation from the tube walls.

Recommended procedure

In order to obtain good reproducibility of results, the following timing procedure was employed.

(*i*) $t=0$ s. Switch on power at *ca.* 5% and set nitrogen shield gas at 3 l min^{-1}. This "pre-heat" of the tube to 70–80° helps to prevent the sample spreading excessively.

(*ii*) $t=45$ s. Place sample in tube. Increase power to *ca.* 7% to evaporate water. Check oscilloscope traces *viz.* 100% and 0% absorption levels.

(*iii*) $t=75$ s. Switch power off. Set Variac to 100% power. Switch on power for *ca.* 1.5 s, to volatilize sample. Measure height of absorption peak.

(iv) $t=5$ min. Repeat procedure. This long period was necessary to allow the tube and end-supports to cool; particularly the support which was "free-floating" and which made poor thermal connection with the water-cooled pillar. In order to reduce the time for one measurement, it would be preferable to water-cool the end-supports directly.

Results

A summary of results is shown in Table II. The calibration curves for 1-, 10- and 20-μl samples, except for a slight curvature at the lower end, were linear as far as useful measurements could be made (*ca.* 95% absorption). This corresponded to a maximum sample of *ca.* 50 ng ($5\cdot10^{-8}$ g). A slight dependence of sensitivity upon sample size was observed. The maximal absorbance from 10 ng of germanium was observed with a 1-μl sample (10 p.p.m.); the absorbance of a 5-μl sample (2 p.p.m.) was less by 4%, a 10-μl sample (1 p.p.m.) by 6%, and a 20-μl sample (0.5 p.p.m.) by 10%. A 50-μl (0.2 p.p.m.) sample showed an approximately 15% reduction in signal, but this size of sample was difficult to use because of "bumping" and consequent loss of sample on evaporation. The standard deviation (15 consecutive measurements) for a 10-ng sample (1 μl × 10 p.p.m.) was 2.7% and for a 2-ng sample (20 μl × 0,1 p.p.m.) was 6.5%.

TABLE II

SENSITIVITY AND DETECTION LIMIT DATA FOR GERMANIUM

Sample volume (10 ng Ge)	*Sensitivity (for 1% absorption)*		*Limit of detection*		*Range (p.p.m.)*
	g	*p.p.m.*	*g*	*p.p.m.*	
1 μl	$1.5\cdot10^{-10}$	0.15	$3\cdot10^{-10}$	0.3	0.3–50
10 μl	$1.7\cdot10^{-10}$	0.017	$3\cdot10^{-10}$	0.03	0.03–5
20 μl	$1.8\cdot10^{-10}$	0.009	$3\cdot10^{-10}$	0.015[a]	0.015–2.5

[a] Scale expansion (× 3) used.

Interferences

The effects of a number of foreign anions and cations on the absorbance of a 10-ng (1 p.p.m. × 10 μl) germanium sample are summarized in Table III. In the tests given as "Interference", the germanium absorption signal was superimposed on a highly irregular background absorption caused by either molecular absorption

or light scatter by the interfering species (confirmed by using the mercury 253.6-nm line, when the background was still observed). It was not possible to resolve the germanium absorption peak from this high background absorption. Attempts to remove the interfering species by selective volatilization failed, because of the high volatility of germanium oxide which resulted in the sample being lost when more than 35% power was used. However, to remove, *e.g.* sodium chloride, it was necessary to use *ca.* 60% power.

TABLE III

INTERFERENCE DATA

(10 ng Ge in 10 μl containing foreign ions at specified level)

Element	*Molecule*	*Interference (%)*	
		1000-fold excess over Ge	*100-fold excess over Ge*
Na	NaCl	Interf.[a]	0
Ca	$CaCl_2$	Interf.[a]	0
Mg	$MgSO_4$	Interf.[a]	−45
Mn	$MnCl_2$	Interf.[a]	0
Co	$CoCl_2$	−30	0
Zn	$Zn(NO_3)_2$	+25	+25
Cd	$CdSO_4$	0	0
Hg	$HgCl_2$	−70	−25
Pb	$Pb(NO_3)_2$	0	0
Sn	Sn/6 *M* HCl	−85	—
S	H_2SO_4	0	0
P	Na_2HPO_4	—	−10
Cl	HCl	−10	0

[a] Interference caused by non-resolution of signal from background absorption.

DISCUSSION

It has been shown that the determination of germanium with a carbon filament atom reservoir is not feasible, because of the poor efficiency of atom formation. Other workers[17] have reported similar results where volatile oxide species are present, *e.g.* silica. As mentioned previously, a heated tube facilitates atomization owing to the longer residence time of species in it. However, the rate of increase in temperature of the tube is also important. If, say, germanium oxide is volatilized at *ca.* 1000°, but no germanium atoms are produced below *ca.* 3000°, then it is important that the time taken for the tube temperature to rise from 1000° to 3000° should be as short as possible to prevent loss of sample as germanium oxide. For this reason, the small slots were cut in the tube. A more rapid temperature rise, and an improvement in sensitivity were found with larger slots, but the higher localized temperature attained reduced the lifetime of a tube considerably. The normal useful life of a tube was 50–80 "flashes", although it would be expected to be considerably longer for those elements not requiring such high temperatures as germanium.

A further advantage of the graphite tube technique over the carbon filament, is the possibility of using a larger sample. An often-quoted advantage of the carbon filament is the small sample required, but when the sensitivity (in p.p.m.) is insufficient for an analysis as in this instance, it is not possible to improve it by increasing the sample size. The tube does not suffer so severely from this limitation and even the largest sample volumes used (50 μl) are small compared with the requirements of many other techniques.

One of us (D.J.J.) wishes to thank Imperial Chemical Industries Limited, Agricultural Division, Billingham, Teeside for the award of a research grant to carry out this work.

SUMMARY

A carbon filament atom reservoir and a graphite tube atomizer are compared as methods for the determination of germanium by atomic absorption spectrometry. It is shown that the filament technique is not applicable, probably because of loss of the sample as a volatile oxide species which results in inefficient atomization. The design of a small graphite tube atomizer is described; with this, a limit of detection for germanium of $3 \cdot 10^{-10}$ g was found. For a 20-μl sample, this corresponds to a concentration of 0.015 p.p.m. The interfering effect of 13 anions and cations is studied.

RÉSUMÉ

Une comparaison entre réservoir atomique à filament de carbone et atomiseur à tube de graphite est faite, en vue du dosage du germanium par spectrométrie d'absorption atomique. La technique du filament n'est pas applicable, probablement en raison de pertes dues à la formation d'un oxyde volatile. L'atomiseur à petit tube de graphite est décrit. Il permet d'arriver à une limite de détection de $3 \cdot 10^{-10}$ g de germanium. Ce qui correspond à une concentration de 0.015 p.p.m. pour un échantillon de 20 μl. On examine également l'influence de 13 anions et cations.

ZUSAMMENFASSUNG

Eine Kohlenstoff-Heizfaden-Küvette und ein Graphitrohr-Verdampfer werden als Methoden für die Bestimmung von Germanium durch Atomabsorptions-Spektrometrie verglichen. Es wird gezeigt, dass das Heizfaden-Verfahren nicht anwendbar ist, wahrscheinlich weil Probenverluste in Form einer flüchtigen Oxid-Spezies auftreten und die Atomisierung unwirksam werden lassen. Der Aufbau eines kleinen Graphitrohr-Verdampfers wird beschrieben; hiermit wurde eine Nachweisgrenze für Germanium von $3 \cdot 10^{-10}$ g erhalten. Für eine Probe von 20 μl entspricht dies einer Konzentration von 0.015 p.p.m. Der störende Einfluss von 13 Anionen und Kationen wird untersucht.

REFERENCES

1 M. D. Amos and J. B. Willis, *Spectrochim. Acta*, 22 (1966) 1325.

2 D. C. Manning, *At. Absorption Newslett.*, 6 (1967) 35.
3 R. E. Popham and W. G. Schrenk, *Spectrochim. Acta*, 23B (1968) 543.
4 G. F. Kirkbright, M. Sargent and T. S. West, *Talanta*, 16 (1969) 1467.
5 E. E. Pickett and S. R. Koirtyohann, *Spectrochim. Acta*, 23B (1968) 235.
6 E. E. Pickett and S. R. Koirtyohann, *Spectrochim. Acta*, 24B (1969) 325.
7 R. M. Dagnall, K. C. Thomson and T. S. West, *Anal. Chim. Acta*, 41 (1968) 551.
8 R. M. Dagnall, G. F. Kirkbright, T. S. West and R. Wood, *Analyst*, 95 (1970) 425.
9 M. P. Bratzel, J. M. Mansfield, J. D. Winefordner and K. E. Zacha, *Anal. Chem.*, 40 (1968) 1733.
10 P. L. Larkins and J. B. Willis, *Spectrochim. Acta*, 26B (1971) 491.
11 B. V. L'Vov, *Spectrochim. Acta*, 24B (1969) 53.
12 H. Massman, *Spectrochim. Acta*, 23B (1968) 215.
13 T. S. West and X. K. Williams, *Anal. Chim. Acta*, 45 (1969) 27.
14 M. D. Amos, *Amer. Lab.*, August (1970) 33.
15 K. W. Jackson, T. S. West and L. Balchin, *Anal. Chem.*, 45 (1973) 249.
16 R. M. Dagnall, D. J. Johnson and T. S. West, *Anal. Chim. Acta*, (1973) in press.
17 H. M. Donega and T. E. Burgess, *Anal. Chem.*, 42 (1970) 1521.
18 I. S. Maines, *Ph.D. Thesis*, University of London, 1970.
19 R. G. Anderson, I. S. Maines and T. S. West, *Anal. Chim. Acta*, 51 (1970) 355.
20 J. F. Alder and T. S. West, *Anal. Chim. Acta*, 51 (1970) 365.
21 J. Aggett and T. S. West, *Anal. Chim. Acta*, 55 (1971) 349.
22 L. Ebdon, G. F. Kirkbright and T. S. West, *Anal. Chim. Acta*, 58 (1972) 39.
23 N. F. Turkalov, R. L. Magunov and A. V. Zagorodnyuk, *Ukr. Khim. Zh.*, 38 (1972) 215.
24 V. I. Davydov, B. V. Teplyakov and G. K. Romanov, *Zh. Prikl. Khim.*, 35 (1962) 1625.
25 L. Barton and C. A. Heil, *J. Less-Common Met.*, 22 (1970) 11.

Analytica Chimica Acta, 67 (1973) 89–98

FLUORIMETRIC DETERMINATIONS BY ION-PAIR EXTRACTION

PART V. STUDIES ON ION-PAIR EXTRACTION WITH THE FLUORESCENT ANION 9,10-DIMETHOXYANTHRACENE-2-SULPHONATE

DOUGLAS WESTERLUND and KARL OLOF BORG

Department of Analytical Chemistry, Farmaceutiska Fakulteten, University of Uppsala, Box 6804, S-113 86 Stockholm (Sweden)

(Received 26th February 1973)

Fluorimetric measurements are often used in the determination of drugs in biological material, mainly because of the high sensitivity that can be obtained. Since most substances are nonfluorescent or weakly fluorescent, it is necessary to develop methods for transformation of these molecules into fluorescent forms. A general principle applicable to ionizable organic compounds, *e.g.* amines, is ion-pair extraction with fluorescent counter ions.

In previous papers[1–4], the highly fluorescent anion of anthracene-2-sulphonic acid was used as counter ion in studies on ion-pair extraction and fluorimetric determination of non-fluorescent amines and quaternary ammonium compounds in low concentrations ($10^{-7} - 10^{-8}$ *M*). This anion was found to be reasonably suitable as a counter ion with respect to both its fluorescence and its extraction properties. Those studies indicated, however, that modifications of the chemical structure of the anion should yield a reagent with improved extraction and solubility properties.

9,10-Dimethoxyanthracene-2-sulphonate proved to be such a compound, which still retained the advantageous fluorescence properties of the anthracene fluorophore. The aim of the present investigation was to study the properties of this anion in ion-pair extraction in the low concentration range by means of fluorimetric measurements.

In a subsequent paper, dimethoxyanthracenesulphonate is applied to the determination of an anticholinergic drug, propantheline, in blood plasma[5].

EXPERIMENTAL

Apparatus

The fluorimetric measurements were performed with an Aminco-Bowman spectrophotofluorimeter 4-8202 B calibrated as described by Chen[6]. The fluorimeter was equipped with a Hanovia 200 W xenon–mercury lamp and an IP 21 photomultiplier.

A band-width of 36 nm was generally used for both exciting and emitted radiation. The measurements were performed at 20.0° and variations in the instrumental sensitivity were compensated for by calibration with known aqueous

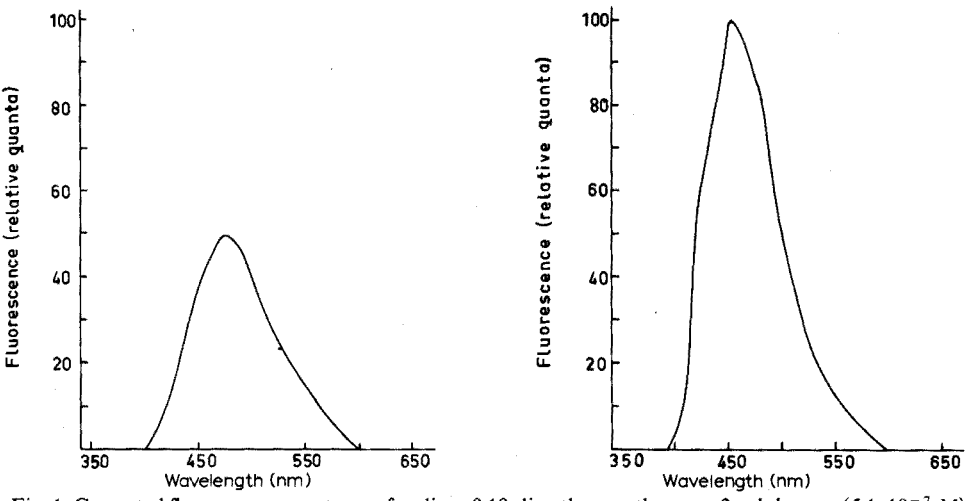

Fig. 1. Corrected fluorescence spectrum of sodium 9,10-dimethoxyanthracene-2-sulphonate ($5.1 \cdot 10^{-7}$ *M*) in 0.1 *M* sulphuric acid. Excitation wavelength, 370 nm; bandwidth of emission light, 12 nm.

Fig. 2. Corrected fluorescence spectrum of the ion pair between tetrabutylammonium and 9,10-dimethoxyanthracene-2-sulphonate ($5.1 \cdot 10^{-7}$ *M*) in methylene chloride. Excitation wavelength, 370 nm; bandwidth of emission light, 12 nm.

solutions of sodium 9,10-dimethoxyanthracene-2-sulphonate. The corrected wavelengths of excitation and emission maxima were 383/479 nm in aqueous solutions and 383/452 nm in methylene chloride. Corrected emission spectra are given in Figs. 1 and 2.

The photometric measurements were performed with a Zeiss Spektralphotometer PMQ II and the pH determinations with a Radiometer pH Meter 4.

Chemicals and reagents

Sodium 9,10-dimethoxyanthracene-2-sulphonate was synthesized by reduction of sodium anthraquinone-2-sulphonate and subsequent methylation with dimethyl sulphate[7]. The product was recrystallized three times from water. Its identity was checked by elemental analysis and i.r. spectroscopy. The purity of the material was controlled by ion-pair extraction as described previously[8].

Commercial amitriptyline and protriptyline were used without further purification. All other chemicals were of analytical grade.

Methylene chloride (Fisher Certified quality) was used after distillation. All organic phases were equilibrated with water before use.

Sulphuric acid (0.1 *M*) and sodium phosphate buffer solutions ($I=0.1$) were used as aqueous phases.

Tetrabutylammonium hydroxide in ethanol or isopropanol was obtained from the iodide by treatment with silver oxide.

Partition studies

The partition experiments were done in centrifuge tubes in a thermostated

bath at 20.0°. The tubes were shaken until equilibrium was achieved (30 min); after centrifugation the phases were separated with a capillary siphon, and the organic phase was collected in flasks containing tetrabutylammonium hydroxide in ethanol or isopropanol. The concentration of tetrabutylammonium hydroxide in the final solution was 10^{-3} M^2. The concentrations of 9,10-dimethoxyanthracene-2-sulphonate in the aqueous phase and its ion pair in the organic phase were determined by fluorimetry or photometry.

The pipettes were washed twice with the solutions before the final pipetting to avoid changes of the concentrations by adsorption losses.

THEORETICAL

Basic ion pair extraction

Cations, *e.g.* protolyzed amines and quaternary ammonium ions, can be extracted from an aqueous solution to an organic solvent as ion pairs with anions:

$$HA^+_{aq} + X^-_{aq} = HAX_{org}$$

The extraction constant, E_{HAX}, is:

$$E_{HAX} = [HAX]_{org}/([HA^+][X^-]) \quad (1\ \text{mole}^{-1}) \tag{1}$$

When side reactions, *e.g.* protolysis, polymerizations, occur, it is convenient to use a conditional extraction constant, E^*_{HAX}, defined by:

$$E^*_{HAX} = C'_{HA(X)org}/(C'_{HA(X)}C'_{X(HA)}) \tag{2}$$

where $C'_{HA(X)org}$ = total concentration of HA^+ present as ion pair with X^- in organic phase, $C'_{HA(X)}$ = total concentration of HA^+ not present as ion pair with X^- in organic phase, and $C'_{X(HA)}$ = total concentration of X^- not present as ion pair with HA^+ in organic phase.

This conditional constant can be related to the extraction constant by means of α-coefficients[9,10] with the following definitions:

$$E^*_{HAX} = E_{HAX}\alpha_{HAX}(\alpha_{HA(X)}\alpha_{X(HA)})^{-1} \tag{3}$$

where $\alpha_{HAX} = C'_{HA(X)org}/[HAX]_{org}$, $\alpha_{HA(X)} = C'_{HA(X)}/[HA^+]$, and $\alpha_{X(HA)} = C'_{X(HA)}/[X^-]$

In the low concentration range, dissociation of the ion pair in the organic phase is an important side reaction; this equilibrium is characterized by the dissociation constant:

$$k_{diss(HAX)} = ([HA^+]_{org}[X^-]_{org})/[HAX]_{org}\ (\text{mole}\ 1^{-1}) \tag{4}$$

The distribution of HA^+ as an ion pair with X^- is given by the distribution ratio, $D_{HA(X)}$:

$$D_{HA(X)} = C'_{HA(X)org}/C'_{HA(X)} = E^*_{HAX}\ C'_{X(HA)} \tag{5}$$

Quantitative extraction (>99%) is obtained when the distribution ratio $D_{HA(X)} > 100$ (equal phase volumes).

Back-extraction of the anionic component of the ion pair

A quantitative back-extraction to an aqueous phase of the fluorescent anion component of the ion pairs can be made by equilibrating an aqueous solution of a competitive non-fluorescent anion with the organic phase containing the ion pair[9]. This method can be used whether the cationic component is an amine or a quaternary ammonium ion. With amines, quantitative back-extraction can also be made by using the partition of the amine as a base.

Competitive anion addition method

Addition of an anion, Z^-, which is distributed as the ion pair HAZ increases $\alpha_{HA(X)}$ (eqn. 6). E_{HAZ} is the extraction constant of the HAZ ion pair.

$$\alpha_{HA(X)} = ([HA^+] + [HAZ]_{org})/[HA^+] = 1 + E_{HAZ}[Z^-] \quad (6)$$

The distribution ratio of the fluorescent anion, X^-, is given by:

$$D_{X(HA)} = E^*_{HAX} C'_{HA(X)} \quad (7)$$

Quantitative back-extraction of the anion is obtained when $D_{X(HA)} < 0.01$. The necessary decrease in E^*_{HAX} is accomplished by the addition of the competitive anion, its concentration being calculated from eqns. (3), (6) and (7).

Base partition method

For this method the increase in $\alpha_{HA(X)}$ is given by eqn. (8).

$$\alpha_{HA(X)} = ([HA^+] + [A] + [A]_{org})/[HA^+] = 1 + K'_{HA}[(1 + k_{d(HA)})(a_{H^+})^{-1}] \quad (8)$$

The pH necessary for quantitative back-extraction is calculated from eqns. (3), (7) and (8).

RESULTS AND DISCUSSION

Optical properties

Optical data for anthracene-2-sulphonate (AS) and 9,10-dimethoxyanthracene-2-sulphonate (MAS) in water and for their ion pairs with tetrabutylammonium ion in methylene chloride are given in Table I. The two reagents have intense absorption peaks at 260–270 nm which make precise photometric determinations in the 10^{-6} *M* range possible.

Quantum yields of fluorescence were determined as described by Parker and Rees[11] and Chen[12]. Quinine hydrogensulphate in 0.05 *M* sulphuric acid was used as reference standard ($\phi = 0.55$). The excitation of quinine and sample was performed at the same wavelength (335 nm) and the absorbance at this wavelength was less than 0.01 absorbance units. When different solvents were used for quinine and sample, the fluorescence intensity was multiplied by the squared refractive indices for the solvents in calculating quantum yields[13]. The shapes of the emission spectra were unchanged by excitation between 260 nm and 390 nm.

A comparison of the fluorescence properties of the reagents can be based on the fluorescence sensitivity index $\varepsilon\phi/H$, where ε is the molar absorptivity, ϕ the quantum yield of fluorescence, and H half the bandwidth of the emission

TABLE I

MOLAR ABSORPTIVITY, QUANTUM YIELD AND FLUORESCENCE SENSITIVITY

Substance[a]	*Excitation maximum (nm)*	*log ε*	*Emission maximum (nm)*	*Half band width of emission spectrum (μm^{-1}) = H*	*Quantum yield = φ*	*Fluorescence sensitivity index = log εφ/H*
Solvent: water						
NaMAS	263	5.20	479	0.44	0.36	5.11
NaMAS	383	3.80	479	0.44	0.36	3.71
NaAS[b]	257	5.27	415	0.34	0.40	5.22
NaAS[b]	359	3.69	415	0.34	0.40	3.76
Solvent: methylene chloride						
TBA–MAS	267	5.23	452	0.42	0.69	5.45
TBA–MAS	383	3.84	452	0.42	0.69	4.05
TBA–AS	260	5.20	410	0.36	0.10	4.74
TBA–AS	359	3.80	410	0.36	0.10	3.22

[a] NaMAS = sodium 9,10-dimethoxyanthracene-2-sulphonate; TBA–MAS = ion pair of MAS and tetrabutylammonium; NaAS = sodium anthracene-2-sulphonate; TBA–AS = ion pair of AS and tetrabutylammonium.
[b] From ref. 1.

spectrum[1,11]. From the index it can be concluded that the two anions give about the same sensitivity in water. In methylene chloride the ion pairs TBA–MAS and TBA–AS have highly different quantum yields and TBA–MAS gives theoretically 5–6 times higher sensitivity than TBA–AS depending on excitation wavelength.

In practical work the wavelength 267 nm cannot be used for excitation of TBA–MAS with the xenon–mercury lamp, because the fluorescence then rapidly declines. Furthermore, the excitation maximum at about 360 nm for anthracene-2-sulphonate and its ion pairs has a limited practical value, because Rayleigh- and Raman-scattering will interfere at the emission maximum. Owing to the variation of the lamp intensity with wavelength (about 35 times higher at 380 nm than at 260 nm), the ion pair TBA–MAS when excited at about 380 nm will have about seven times the fluorescence intensity of TBA–AS excited at 260 nm and twice the fluorescence intensity of 9,10-dimethoxyanthracene-2-sulphonate or anthracene-2-sulphonate in water.

Extraction and dissociation constants

The extraction and dissociation constants of the ion pairs of two quaternary ammonium compounds and two monovalent amines with anthracene-2-sulphonate and 9,10-dimethoxyanthracene-2-sulphonate are given in Table II. The constants and standard errors were calculated on an Olivetti Programma 101 calculator, by the method of least squares; it was assumed that the relative errors were normally distributed.

The difference between the extraction constants for the 9,10-dimethoxyanthracene-2-sulphonate and anthracene-2-sulphonate ion pairs is about 0.4–0.5 units, which is in agreement with the difference (0.52 units) for chloride constants in

TABLE II

EXTRACTION AND DISSOCIATION CONSTANTS OF ION PAIRS WITH 9,10-DIMETHOXY-ANTHRACENE-2-SULPHONATE AND ANTHRACENE-2-SULPHONATE

(Organic phase, methylene chloride; aqueous phase, 0.1 *M* NaH_2PO_4 (quaternary ions) or 0.1 *M* H_2SO_4 (amines))

Cation	*Anion*	$-Log\ C'_{HA(X)org}$	$Log\ E_{HAX} \pm s.e.$	$-Log\ k_{diss(HAX)} \pm s.e.$
Tetrapropyl-ammonium	MAS	4.68–5.39	3.77 ± 0.02	4.78 ± 0.04
	AS	3.31–5.76	3.44 ± 0.01	4.89 ± 0.03
Tetrabutyl-ammonium	MAS	4.03–5.08	5.85 ± 0.03	4.38 ± 0.06
	AS	4.66–6.62	5.45 ± 0.03[a]	4.96 ± 0.04[a]
Amitriptyline	MAS	5.77–6.85	7.16 ± 0.02	6.78 ± 0.06
	AS	—	6.61[b]	6.6[b]
Protriptyline	MAS	6.41–7.86	5.93 ± 0.03	8.01 ± 0.08
	AS	—	5.50[b]	7.8[b]

[a] The difference between these constants and those reported earlier (ref. 1) is due to differences in the computation technique and those given in this paper must be considered as the more accurate.
[b] From ref. 3.

chloroform with the two alkaloids brucine and strychnine; these alkaloids also differ by two methoxy groups in chemical structure.

The maximal concentration of sodium 9,10-dimethoxyanthracene-2-sulphonate in the aqueous phase is limited by its solubility to about $3 \cdot 10^{-3}$ *M*, which means that cations with conditional extraction constants higher than $10^{4.5}$ can be quantitatively extracted (see eqn. 5).

The blank

In ion-pair extractions with an anionic reagent, the blank is usually caused by the distribution of the reagent as an ion pair with hydronium and buffer cations. It has been found[1] that methylene chloride is advantageous for use in extractions with anthracene-2-sulphonate, and 9,10-dimethoxyanthracene-2-sulphonate also gives a low blank with this solvent. The addition of an alcohol (1-pentanol) raises the distribution of such ion pairs[1]; hence the blank will be higher and the final method will be less sensitive.

Determination of amines and quaternary ammonium ions

The determination can be based on the fluorescence of the ion pair in the organic phase or of the anion in an aqueous phase after back-extraction. The optical data above indicate that measurement of the dimethoxyanthracene-sulphonate ion pair in methylene chloride gives the highest sensitivity. Methylene chloride is however sensitive to temperature changes and adsorption of ion pair compounds to phase boundaries is also more pronounced than in aqueous solution.

Determinations in the range 10^{-7}–10^{-8} *M* were made fluorimetrically in the organic phase (Table III) and in the aqueous phase after back-extraction

TABLE III

FLUORIMETRIC DETERMINATION OF AMINES AND QUATERNARY AMMONIUM IONS BY ION-PAIR EXTRACTION WITH 9,10-DIMETHOXYANTHRACENE-2-SULPHONATE

(Organic phase, methylene chloride; aqueous phase, 0.1 M H_2SO_4

Method	$-Log\ C^{\circ}_{HA}$	$-Log\ C^{\circ}_{MAS}$	*Recovery (%)*	s_r *(%)*	*No. of detns.*
Tetrabutylammonium					
Standard curve	6.70	6.00	95.8	2.6	5
	6.82	6.00	97.7	1.6	6
	7.00	6.00	96.7	1.7	6
	7.30	6.00	96.7	2.0	8
Reference solution	6.82	6.00	100.1	3.4	9
	7.30	6.00	101.0	3.1	10
Standard curve	6.00[a]	7.00	100.3	1.1	5
	6.00[a]	7.30	100.4	2.2	5
Amitriptyline					
Standard curve	7.00	5.00	99.5	1.7	11
	7.30	5.00	100.5	5.1	10
	7.60	5.00	99.3	5.9	9
Reference solution	6.70	5.00	102.7	1.3	7
	7.00	5.00	97.4	4.7	8

[a] Tetrabutylammonium ion used in excess.

(Table IV). Photometric determinations in the range 10^{-5}–10^{-6} M were also made for comparison of recovery and precision (Table IV).

The fluorimetric evaluation was based on references prepared in two different ways[4]. The first type (referred to as "standard curve") was made from solutions of dimethoxyanthracenesulphonate or its ion pair, which were photometrically determined and then diluted and measured fluorimetrically. The second type (referred to as "reference solution") was made from solutions which after dilution to a suitable concentration were extracted simultaneously with the samples.

Measurements of ion pairs in the organic phase. Determinations of tetrabutylammonium ion and amitriptyline as ion pairs with dimethoxyanthracenesulphonate are reported in Table III. Studies on extractions with anthracenesulphonate[4] have indicated that a quantitative recovery could not be obtained when results were evaluated by the "standard curve" method. With the dimethoxy reagent, almost quantitative recoveries were obtained with both tetrabutylammonium and amitriptyline but the precision was lower for the amine. The lower precision might be due to adsorption, and attempts were made to decrease this by silanization of the centrifuge tubes and other glass vessels in contact with the organic phases. This gave, however, still lower precision and also low recoveries for amitriptyline (17–39%), the yield decreasing with decreasing concentration.

Quantitative recoveries were also obtained when dimethoxyanthracenesulphonate was extracted with tetrabutylammonium ion in excess.

TABLE IV

DETERMINATION OF CATIONS AFTER BACK-EXTRACTION OF 9,10-DIMETHOXY-ANTHRACENE-2-SULPHONATE

(Organic phase, methylene chloride. Aqueous phase: 1, anion addition method, 0.1 *M* $NaClO_4$; 2, base partition method, 0.001 *M* NaOH)

Cation	*Back-extraction*	$-Log\ C^{\circ}_{HA}$	$-Log\ C^{\circ}_{MAS}$	*Recovery (%)*	s_r *(%)*	*No. of detns.*
Fluorimetric method[a]						
Tetrabutyl-ammonium	Anion addition	6.82	6.00	99.00	3.9	12
		7.00	6.00	103.0	3.7	13
		7.30	6.00	99.4	3.8	10
		7.70	6.00	101.7	5.0	17
Amitrip-tyline	Base partition	6.70	5.00	92.0	2.7	8
		6.82	5.00	92.5	0.7	8
		7.00	5.00	92.8	2.4	5
	Anion addition	6.70	5.00	100.0	2.2	8
		6.82	5.00	99.8	2.3	7
		7.30	5.00	99.6	2.0	8
Photometric method						
Tetrabutyl-ammonium	Anion addition	5.70	4.30	100.6	1.0	5
Amitriptyline	Base partition	5.60	4.60	99.3	0.9	5

[a] Evaluation by standard curve.

Measurements in the aqueous phase after back-extraction. Determinations after back-extraction of the reagent to an aqueous phase are given in Table IV. The observed recovery comprises both the yield from extraction of the ion pair to organic phase and the yield of the back-extraction. Two different principles were used for the back-extractions[4]: in the "anion addition" method a competitive anion (perchlorate) is used for the transfer of the reagent anion to the aqueous phase; in the "base partition" method the cation of the ion pair is removed by transformation to base.

The back-extraction by means of 0.1 *M* sodium perchlorate gave a yield of about 100% for both tetrabutylammonium ion and amitriptyline, whereas base partition of amitriptyline with 0.001 *M* sodium hydroxide (the amine being quantitatively transferred as base to the organic phase, according to calculations) gave recoveries of only about 90%.

In the concentration range 10^{-5}–10^{-6} *M* (photometric measurements) both back-extraction methods gave recoveries of about 100% with a standard deviation of 1% (Table IV).

CONCLUSION

This study has shown that amines and quaternary ammonium ions can be

determined by ion-pair extraction with the fluorescent 9,10-dimethoxyanthracene-2-sulphonate as counter ion. Quantitative recoveries and good precisions are obtained in the low concentration range (10^{-7}–10^{-8} *M*) when the ion pair is determined either in the organic phase or after back-extraction with measurements in the aqueous phase.

In comparison with anthracenesulphonate, dimethoxyanthracenesulphonate has about three times higher extraction ability and a higher solubility in aqueous solutions. Those properties of dimethoxyanthracenesulphonate allow a quantitative extraction and determination of more hydrophilic cations than when anthracenesulphonate is used as counter ion. In determinations of amines and quaternary ammonium compounds, dimethoxyanthracenesulphonate has the advantage of giving almost quantitative recoveries.

The two anions have about the same fluorescence sensitivity in aqueous phases. In an organic phase (methylene chloride) ion pairs containing dimethoxyanthracenesulphonate give about seven times higher fluorescence sensitivity than those with anthracenesulphonate.

We are indebted to Professor Göran Schill for his kind interest in the work and his valuable help with the manuscript, and to Mrs Ulla Tjärnlund for her skillful technical assistance. This work was supported by a grant from the Swedish Medical Research Council (Project No B71-13X-3136 and B71-13X-2056).

SUMMARY

The fluorescent anion 9,10-dimethoxyanthracene-2-sulphonate has been studied in ion-pair extractions. Its ability to extract amines and quaternary ammonium compounds was investigated by fluorimetric determination of extraction and dissociation constants with methylene chloride as organic phase for two amines (amitriptyline and protriptyline) and two quaternary ammonium ions (tetrabutyl- and tetrapropylammonium). The optical properties of the anion and its ion pairs were characterized by quantum yield of fluorescence and a fluorescence sensitivity index. The determination of two of the ion pairs was studied, both after extraction to an organic phase and after a subsequent back-extraction of the anion component to an aqueous phase. Recoveries and standard deviations are given.

RÉSUMÉ

Une étude est effectuée sur les extractions à paires ioniques, en utilisant l'anion fluorescent diméthoxy-9,10-anthracènesulfonate-2. On examine sa capacité d'extraction de composés d'amines et d'ammonium quaternaire par fluorimétrie et détermination des constantes de dissociation au moyen de chlorure de méthylène, comme phase organique. On a utilisé deux amines (amitriptyline et protriptyline) et deux ions ammonium quaternaire (tétrabutyl- et tétrapropylammonium).

ZUSAMMENFASSUNG

Die fluoreszierende Anion 9,10-Dimethoxiantracen-2-sulfonat war in Ionen-

paarextraktionen erforschet. Das Vermögen der Anion Ammonium Verbindungen zu extrahieren war durch Bestimmung von Extraktion- und Dissoziationskonstanten für zwei Amine (Amitriptyline und Protriptyline) und zwei quartäre Ammonium Ione (Tetrabutyl- und Tetrapropylammonium) untersucht. Als organische Phase diente Methylenchlorid und die Messungen waren mit Fluorimetrie ausgeführt.

Die optische Eigenschaften der Anion und seine Ionenpaaren waren mit Quantenausbeuten der Fluoreszenz und ein Index von der Empfindlichkeit der Fluoreszenz kennzeichnet.

Die quantitative Bestimmung war mit zwei Ionenpaaren, sowohl nach Extraktion zu organische Phase als auch nach einem nachfolgender Zurückextraktion von der Anion an die wässrige Phase, studiert.

Ausbeuten und Standardabweichungen sind präsentiert.

REFERENCES

1 D. Westerlund and K. O. Borg, *Acta Pharm. Suecica*, 7 (1970) 267.
2 K. O. Borg and D. Westerlund, *Z. Anal. Chem.*, 252 (1970) 275.
3 D. Westerlund, K. O. Borg and P.-O. Lagerström, *Acta Pharm. Suecica*, 9 (1972) 47.
4 P.-O. Lagerström, K. O. Borg and D. Westerlund, *Acta Pharm. Suecica*, 9 (1972) 53.
5 D. Westerlund and K. H. Karset, *Anal. Chim. Acta*, 67 (1973) 99.
6 R. F. Chen, *Anal. Biochem.*, 20 (1967) 339.
7 K. H. Meyer, *Ann. Chem.*, 379 (1911) 37.
8 K. O. Borg, R. Modin and G. Schill, *Acta Pharm. Suecica*, 5 (1968) 299.
9 R. Modin and G. Schill, *Acta Pharm. Suecica*, 4 (1967) 301.
10 A. Ringbom, *J. Chem. Educ.*, 35 (1958) 282.
11 C. A. Parker and W. T. Rees, *Analyst*, 85 (1960) 587.
12 R. F. Chen, *Science*, 150 (1965) 1593.
13 J. J. Hermans and S. Levinson, *J. Opt. Soc. Amer.*, 41 (1951) 460.

Analytica Chimica Acta, 67 (1973) 99–106

FLUORIMETRIC DETERMINATION OF PROPANTHELINE IN HUMAN BLOOD PLASMA BY AN ION-PAIR EXTRACTION METHOD

DOUGLAS WESTERLUND and KARI HELENE KARSET*

Department of Analytical Chemistry, Farmaceutiska Fakulteten, University of Uppsala, Box 6804, S-113 86 Stockholm (Sweden)

(Received 26th February 1973)

Propantheline has been used for about twenty years in clinical practice but only a few data on biological concentration levels are available. Beermann *et al.*[1] used ^{14}C-propantheline and measured total radioactivity of intestinal aspirates, plasma, urine and feces. Their results indicated an absorption of less than 50% after oral administration of the drug. Pfeffer *et al.*[2] measured propantheline in urine by ion-pair extraction with tropaeolin 00 and photometric measurements.

This paper introduces a selective and sensitive analytical method for propantheline in blood plasma. The selectivity is obtained by ion-pair extraction under conditions calculated from extraction and dissociation constants of the ion pairs. High sensitivity is achieved by use of a strongly fluorescent anion, 9,10-dimethoxyanthracene-2-sulphonate as the ion-pair reagent[3].

EXPERIMENTAL

Apparatus

The fluorimetric measurements were performed with an Aminco-Bowman spectrophotofluorimeter 4-8202 B calibrated as described by Chen[4]. The fluorimeter was equipped with a Hanovia 200 W xenon–mercury lamp and an IP 21 photomultiplier.

A bandwidth of 36 nm was used for both exciting and emitted light. The measurements were performed at 20.0° and variations in the instrumental sensitivity were compensated for by calibration with known aqueous solutions of sodium 9,10-dimethoxyanthracene-2-sulphonate. The uncorrected wavelengths of excitation and emission maxima were 368/462 nm in aqueous solutions and 368/448 nm in methylene chloride.

The photometric measurements were performed with a Zeiss spektralphotometer PMQ II and the pH determinations with a Radiometer pH meter 4.

Chemicals and reagents

Sodium 9,10-dimethoxyanthracene-2-sulphonate was synthesized and checked for purity as described elsewhere[3].

The hydrolysis product of propantheline, 2-hydroxyethyldiisopropylmethyl-

* Present address: Apothekernes Laboratorium for Specialpraeparater, Skøyen, Oslo 2, Norway.

ammonium ion, was synthesized by hydrolysis of propantheline with 1 *M* sodium hydroxide for 24 h; after acidification with 1 *M* hydrochloric acid and extraction with ether to remove the xanthene-9-carboxylic acid, the aqueous phase was evaporated under vacuum. The residue was recrystallized in ethanol and finally dried over phosphorus pentoxide. The identity was checked by i.r. and n.m.r. spectroscopy and the purity by thin-layer chromatography.

Commercial propantheline bromide (I) was used without further purification. All other chemicals were of analytical grade.

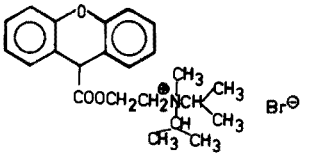

I

Methylene chloride (Fisher Certified quality) was used after distillation and equilibration with water. Perchloric acid, sodium phosphate buffers (ionic strength = 0.1) and sodium hydroxide solutions were used as aqueous phases.

Tetrabutylammonium hydroxide in isopropanol was obtained from the iodide by treatment with silver oxide.

Partition studies

The partition experiments were performed in centrifuge tubes in a thermostated bath at 20.0°, with an equilibration time of 5–30 min. After centrifugation and separation of the phases with a capillary siphon, the concentration of the ion pairs in the organic phase and of the cation or anion in the aqueous phase were determined photometrically or fluorimetrically. The organic phases meant for fluorimetric measurements were collected in flasks containing tetrabutylammonium hydroxide in isopropanol[5].

Method for determination of propantheline in blood plasma

Propantheline is extracted from acidified plasma to methylene chloride as the ion pair with perchlorate. The organic phase is purified by extraction with 0.01 *M* sodium perchlorate at pH 13. In the third step the organic phase is equilibrated with $2 \cdot 10^{-5}$ *M* 9,10-dimethoxyanthracene-2-sulphonate (MAS) at pH 11, the perchlorate ion being quantitatively replaced by MAS. Finally the MAS ion pair is determined fluorimetrically.

Procedure. Extract at 20° in mechanically shaken centrifuge tubes. After centrifugation, separate the phases by a capillary siphon. The following extractions are needed. Extract 3.00 ml of plasma and 3.00 ml of 0.1 *M* perchloric acid with 10.00 ml of methylene chloride for 10 min. Then extract 5.00 ml of the organic phase with 5.00 ml of 10^{-2} *M* sodium perchlorate in 0.1 *M* sodium hydroxide for 5 min. Transfer the organic phase quantitatively to another tube and extract with 5.00 ml of $2 \cdot 10^{-5}$ *M* MAS in 10^{-3} *M* sodium hydroxide for 10 min. Siphon the organic phase to a small flask containing 0.05 ml of 0.1 *M* tetrabutylammonium hydroxide in isopropanol and measure fluorimetrically. Use an excitation wavelength of 368 nm, with an emission wavelength of 448 nm (uncorrected wavelengths).

The calibration of the fluorimetric measurements can be done in two ways. In one method, used only for the determination of unknown concentrations of the drug in plasma, a standard curve is prepared by adding known amounts of propantheline to plasma samples (collected before administration of the drug) which are treated as in the Procedure simultaneously with the unknown samples. In the second method, used for evaluating the yields, a standard curve is prepared with solutions of the MAS ion pair which are assayed by photometry, diluted to suitable concentrations and measured fluorimetrically.

RESULTS AND DISCUSSIONS

Determination of constants

A computation of extraction conditions for propantheline in the concentration ranges expected in plasma requires a knowledge of the extraction and dissociation constants of the ion pairs. The extraction constants were determined as discussed by Modin and Schill[6] and the dissociation constants were determined simultaneously by slope analysis[7]. The constants of the propantheline ion pairs with bromide, perchlorate, β-naphthalenesulphonate and MAS are given in Table I.

TABLE I

EXTRACTION AND DISSOCIATION CONSTANTS OF PROPANTHELINE ION PAIRS

(Aqueous phase: phosphate buffer solutions, $I=0.1$; organic phase: methylene chloride. Fluorimetric measurements, bromide constants by photometry)

Anion	$-\log C'_{Q(X)\,org}$ [a]	$\log E_{QX} \pm s$ [b]	$-\log k_{diss} \pm s$ [c]
MAS	7.11–6.10	6.27±0.20	5.59±0.10
Perchlorate	5.93–4.84	4.25±0.05	4.62±0.06
β-Naphthalene-sulphonate	6.83–5.61	4.28±0.05	6.00±0.05
Bromide	4.00–3.05	1.43±0.01	4.59±0.07

[a] Negative logarithm of the total concentration of quaternary ammonium ion (Q^+) as an ion pair with X^- in the organic phase.
[b] $E_{QX}=[QX]_{org}/[Q^+][X^-]$ in l mole^{-1} (extraction constant); s=standard deviation.
[c] $k_{diss}=[Q^+]_{org}[X^-]_{org}/[QX]_{org}$ in mole l^{-1} (dissociation constant of ion pair in organic phase).

The extraction and dissociation constants of the ion pairs and the standard deviations of these constants were calculated on an Olivetti Programma 101 calculator, by the method of least squares, on the assumption that the relative errors are normally distributed.

Conditions for quantitative extractions

Concentration of anions. Propantheline can be extracted quantitatively from plasma as an ion pair with perchlorate. The extraction constant is rather large and the dissociation of the ion pair in the organic phase will give a further increase of the distribution ratio. The initial concentration of perchlorate ( ) necessary for quantitative extraction of propantheline (10^{-8}–10^{-7} M) in the Procedure can be

calculated to be $2.3–23 \cdot 10^{-6}$ *M*. However, a quantitative extraction from a complex sample like plasma requires a higher perchlorate concentration owing to different side reactions (*e.g.* protein binding of drug or reagent, coextraction of other perchlorate ion pairs, etc.).

Coextracted impurities can be removed by back-extractions, which are done with a concentration of the reagent (counter ion) such that propantheline is quantitatively retained in the organic phase. The first back-extraction is done with 0.01 *M* sodium perchlorate in 0.1 *M* sodium hydroxide and the final purification is obtained by equilibrating the organic phase with $2 \cdot 10^{-5}$ *M* MAS in 10^{-3} *M* sodium hydroxide. By this procedure a quantitative transformation of propantheline to the fluorescent MAS ion pair is obtained. The MAS concentrations necessary for a quantitative transformation at different propantheline concentrations are given in Fig. 1. The curve was computed from the extraction and dissociation constants of the MAS and perchlorate ion pairs under the following conditions:

$$D_Q = C_{Qorg}/C_{Qaq} = 100;\ C'_{MAS(Q)org}/C'_{ClO_4(Q)org} = 100;\ C^0_Q = C^0_{ClO_4}$$

where C_Q is the total concentration of Q^+ in the organic or aqueous phase, C' is the total concentration of the respective anion as ion pair with Q^+ in the organic phase, and C^0 is the initial concentration of Q^+ or perchlorate.

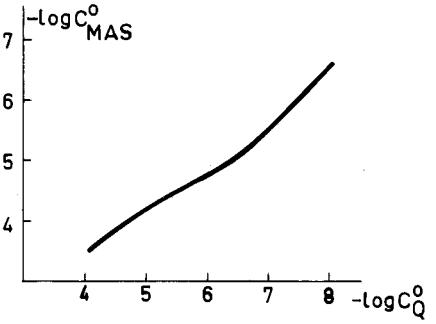

Fig. 1. Initial concentration of sodium 9,10-dimethoxyanthracene-2-sulphonate (MAS) giving quantitative transformation of the propantheline (Q)–perchlorate ion pair into the fluorescent MAS ion pair.

TABLE II

YIELD DEPENDENCE ON THE pH OF PLASMA

(Sample: Propantheline bromide added to plasma ($C^0_Q = 1.5 \cdot 10^{-7}$ *M*). The recommended method was followed, except that in the initial extraction the diluent was either phosphate buffer ($I = 0.1$) containing sodium perchlorate (0.1 *M*) or perchloric acid)

Diluent	*pH*[a]	*Yield*
Buffer pH 11	8.4	0
Buffer pH 7	7.0	65
Buffer pH 3	5.7	85
$HClO_4$ 0.1 *M*	3.7	90
$HClO_4$ 1.0 *M*	0.7	20

[a] Measured after the addition of buffer.

The magnitude of the blank in ion-pair extractions with an anionic reagent depends mainly on the distribution of the anion as ion pair with hydronium and buffer cations[3]. The blank in this method can be kept low by using 10^{-3} *M* sodium hydroxide as solvent.

pH effects on the recovery from plasma. Experiments with propantheline added to plasma showed that the yield was strongly pH dependent (Table II). The low yields from alkaline solutions probably reflect a combination of hydrolysis and protein binding of the drug. The losses of propantheline when a high concentration of perchloric acid was used may be due to occlusion of the drug in the very heavy precipitate formed at this pH.

Purification of the extract. It is known that propantheline is quite stable at pH below 5[1,8] but is hydrolyzed in more alkaline media. Experiments have shown that a back-extraction with a strongly alkaline aqueous phase is necessary to remove coextracted impurities so that satisfactory blanks and recoveries are obtained. The hydrolysis of propantheline can be eliminated by using a high distribution ratio.

The recoveries in model experiments with pure solutions of propantheline perchlorate in methylene chloride and aqueous phases of different perchlorate concentrations at pH 12 and 13 are given in Table III. A perchlorate concentration of 10^{-3} *M* was adequate in this case. However, in experiments with propantheline extracted from plasma samples, it was found that 10^{-2} *M* perchlorate must be used to give an acceptable yield. Losses caused by hydrolysis in the alkaline aqueous phase in the final step of the Procedure also necessitated the use of a higher MAS concentration ($2 \cdot 10^{-5}$ *M*) than that theoretically calculated (see Fig. 1).

TABLE III

YIELD DEPENDENCE ON THE PERCHLORATE CONCENTRATION IN THE FIRST BACK-EXTRACTION

(Sample: 1.10^{-7} *M* propantheline perchlorate in methylene chloride; aqueous phase: $NaClO_4$ in NaOH. Equilibration time: 5 min)

Concentration of perchlorate (M)	*Recovery (%)*[a] *in*	
	0.1 M NaOH	*0.01 M NaOH*
10^{-4}	72	86
10^{-3}	96	98
10^{-2}	93	95

[a] Average of three samples.

The removal of cationic impurities which are more hydrophilic than propantheline from the organic phase is less efficient when too high concentrations of perchlorate and MAS are used. In this case, however, the risk of hydrolysis of the drug must determine the concentration of the reagent.

Stability of propantheline in plasma

When test samples prepared by adding a known amount of propantheline to plasma were analyzed after storage at $-20°$ for one and two weeks, recoveries of only 74% and 36%, respectively, of the initial value were found. An improvement

in the drug stability was obtained by addition of an equal amount of 0.1 *M* perchloric acid to the plasma before freezing. With this treatment no decrease of the drug concentration was observed within one week at −20°.

Selectivity and sensitivity

The main metabolites of propantheline are its hydrolysis product, xanthene-9-carboxylic acid, and one unidentified compound which is also found when xanthene-9-carboxylic acid is administered[1]. The alcoholic hydrolysis product, 2-hydroxyethyldiisopropylmethylammonium ion, is also a probable metabolite, and extraction and dissociation constants for this quaternary ammonium ion as the ion pair with MAS and perchlorate are given in Table IV. Calculations based on these constants show that the extraction of this metabolite in the Procedure is too low to interfere in the determination of propantheline even if it is present in very high initial concentrations (10^{-3} *M*).

The sensitivity of the analytical method is determined by the magnitude of the blank; a measurement of twice the blank value gives an acceptable precision. In the experiments with plasma (3 ml), the typical blank value corresponded to a propantheline concentration of 20–30 ng ml^{-1}, which is 10–15% higher than the blanks obtained from pure aqueous buffer solutions. The sensitivity was improved when a larger amount of plasma was taken for analysis, because the blank value was affected very little by the larger plasma volume.

TABLE IV

EXTRACTION AND DISSOCIATION CONSTANTS OF ION PAIRS OF 2-HYDROXYETHYLDIISOPROPYLMETHYLAMMONIUM ION

(Aqueous phase: phosphate buffer solution ($I=0.1$); organic phase: methylene chloride)

Anion	$-\log c'_{Q(X)\,org}$ [a]	$\log E_{QX} \pm s$ [b]	$-\log k_{diss} \pm s$ [c]
MAS	6.09–5.49	1.00 ± 0.04	5.25 ± 0.08
Perchlorate	—	−1.2 [d]	4.6 [d]

[a] Total concentration of the hydrolysis product as its ion pair in the organic phase.
[b] Extraction constant.
[c] Dissociation constant of the ion pair in the organic phase.
[d] Estimated constants.

Yield and precision

The results from recovery experiments by the recommended procedure with propantheline added to buffer and plasma are given in Table V. The yields from plasma decrease with decreasing concentration. This might depend on protein binding of the drug or on its adsorption to the protein precipitate.

Application

The method was applied to determinations of propantheline in human plasma samples after an oral administration of two 15-mg doses of propantheline bromide in tablets. The plasma levels of five persons were followed for 6 h and were in all cases found to be less than 40 ng ml^{-1}.

TABLE V

DETERMINATION OF PROPANTHELINE IN AQUEOUS SOLUTION AND IN PLASMA

Concentration of propantheline (ng ml^{-1})	*Yield (ng ml^{-1})*	*s (ng ml^{-1})*	*n*
Aqueous solution[a]			
157	150.1	4.4	6
78	74.6	2.6	6
39	38.1	2.6	6
Plasma			
134	119.4	2.6	5
72	61.9	3.3	5
13[b]	10.4	0.6	8

[a] Propantheline in phosphate buffer pH 7.
[b] 5.0-ml samples.

We are indebted to Prof. Göran Schill and Dr. Karl Olof Borg for their valuable help with the manuscript and to Mrs. Ulla Tjärnlund for skillful technical assistance. This work was supported by a grant from the Swedish Medical Research Council (Project No. B71-13X-3136 and B71-13X-2056).

SUMMARY

Propantheline bromide, an anticholinergic quaternary ammonium compound, was determined in human blood plasma by an ion-pair extraction method. The extraction and dissociation constants of the ion pairs involved were determined. In the method, the drug is extracted as the perchlorate ion pair to methylene chloride, the extract is purified and the propantheline is quantitatively converted to a fluorescent ion pair with the highly fluorescent anion 9,10-dimethoxyanthracene-2-sulphonate; 10–15 ng of propantheline per ml can be determined with a standard deviation of 0.6 ng ml^{-1}.

RÉSUMÉ

Le bromure de propanthéline, un compesé d'ammonium quaternaire anticholinergique, a été dosé dans le plasma de sang humain par une méthode d'extraction, "de paires ioniques". On a déterminé les constantes d'extraction et de dissociation. On procède à une extraction comme perchlorate–chlorure de méthylène. L'extrait est purifié. La propanthéline est transformée quantitativement en un produit fluorescent à l'aide de l'anion 9,10-diméthoxyanthracène-2-sulfonate. On peut ainsi doser 10 à 15 ng de propanthéline par ml, avec une déviation standard de 0.6 ng ml^{-1}.

ZUSAMMENFASSUNG

Propanthelinbromid, eine quaternäre Ammoniumverbindung mit anticholi-

nergischer Wirkung, wurde in menschlichem Blutplasma nach einer Ionenpaarextraktionsmethode bestimmt. Die Extraktions- und Dissoziationskonstanten der Ionenpaare wurden ermittelt. Das Heilmittel wird als Ionenpaar mit Perchlorat mittels Methylenchlorid extrahiert, der Extrakt gereinigt und das Propanthelin quantitativ mit dem intensiv fluoreszierenden Anion 9,10-Dimethoxyanthracen-2-sulfonat in ein fluoreszierendes Ionenpaar umgewandelt. 10–15 ng Propanthelin pro ml können mit einer Standardabweichung von 0.6 mg ml^{-1} bestimmt werden.

REFERENCES

1 B. Beermann, K. Hellström and A. Rosen, *Clin. Pharm. Ther.*, 13 (1972) 212.
2 M. Pfeffer, J. M. Schor, S. Botton and R. Jacobsen, *J. Pharm. Sci.*, 57 (1968) 1375.
3 D. Westerlund and K. O. Borg, ACA preceeding paper.
4 R. F. Chen, *Anal. Biochem.*, 20 (1967) 339.
5 K. O. Borg and D. Westerlund, *Z. Anal. Chem.*, 252 (1970) 275.
6 R. Modin and G. Schill, *Acta Pharm. Suec.*, 7 (1970) 285.
7 B.-A. Persson and G. Schill, *Acta Pharm. Suec.*, 3 (1966) 281.
8 J. Kracmar, *Pharm.*, 21 (1966) 224.

Analytica Chimica Acta, 67 (1973) 107–112

SPECTROPHOTOMETRIC DETERMINATION OF INDIUM AND GALLIUM WITH CHROME AZUROL S AND CETYLTRIMETHYLAMMONIUM BROMIDE

B. EVTIMOVA and D. NONOVA

Department of Analytical Chemistry, University of Sofia, Sofia-26 (Bulgaria)

(Received 18th October 1972)

The sensitivity of colour reactions between metal ions and some metallochromic indicators, used as reagents, has recently been greatly increased by the sensitizing action of cetyltrimethylammonium bromide (cetrimide). It has been found that on addition of cetrimide a considerable bathochromic shift of the maximal absorption wavelength takes place, accompanied by an appreciable increase in the reaction sensitivity. Consequently, some very sensitive spectrophotometric methods for determining traces of metals have been developed[1–5].

The reagents which are commonly applied in conjunction with cetrimide, are triphenylmethane dyestuffs. Of these, chrome azurol S has been used for spectrophotometric determinations of indium and gallium; the indium complex has been measured at 555 nm, and at 530 nm with a reaction sensitivity of 0.057 μg In cm^{-2} for $A=0.001$ [7], whereas the wavelength of maximal absorption for the gallium complexes is at 547 nm [6]. Chrome azurol S and cetrimide have been proposed for the spectrophotometric determination of gallium and beryllium[5], the molar absorptivities quoted being $1.15 \cdot 10^5$ and $9.1 \cdot 10^4$, respectively.

In the work described here, the colour reactions obtained with indium and gallium were studied with respect to specificity and sensitivity, and it was found that cetrimide produced a very pronounced bathochromic shift of about 100 nm for both metal ions. Blue water-soluble complexes were formed and the sensitivity of the reactions was very high. Despite this high sensitivity, a reasonable selectivity could also be achieved.

EXPERIMENTAL

Reagents

Indium, $1.000 \cdot 10^{-2}$ M stock solution. Dissolve 0.1148 g of pure metallic indium in 1 ml of concentrated nitric acid (Merck) and dilute to 100 ml in a volumetric flask. Prepare working solutions by dilution with 10^{-2} *M* nitric acid.

Gallium, $0.987 \cdot 10^{-2}$ M stock solution. Dissolve 0.0688 g of high-purity metallic gallium in 2 ml of concentrated nitric acid and dilute to 100 ml in a volumetric flask. Dilute as required with 10^{-2} *M* nitric acid.

Chrome azurol S (Merck). Prepare 10^{-3} or 10^{-4} *M* solutions in distilled water.

Cetyltrimethylammonium bromide, $2 \cdot 10^{-3}$ *M*. Dissolve with warming 0.0728 g of the reagent (Merck) in 100 ml of distilled water. Prepare a $2 \cdot 10^{-4}$ *M* solution as required.

Buffers. An aqueous 2% (w/v) hexamine solution, and a phthalate buffer comprising 0.1 *M* potassium hydrogen phthalate and 0.1 *M* sodium hydroxide adjusted to the required pH, were used.

Apparatus

A VSU-1 universal spectrophotometer, a Specord u.v. vis. recording spectrophotometer and a L. Seibold, type GLD, pH meter were employed.

RESULTS AND DISCUSSION

To study the spectral properties of the coloured complexes, the absorption spectra of the chrome azurol S–cetrimide systems with indium and gallium as well as these ones without cetrimide were recorded (Fig. 1). The absorption maxima of the ternary complexes occur at 630 nm (In) and 640 nm (Ga). Since the reagent absorbance is very small at the absorption maxima of the ternary complexes, the conditions are almost ideal for analytical measurements.

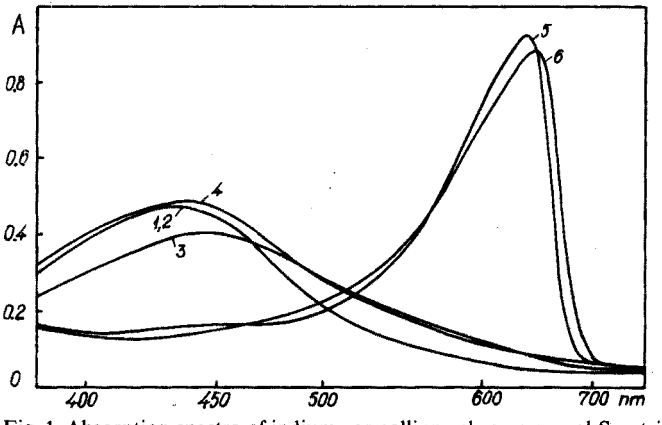

Fig. 1. Absorption spectra of indium– or gallium–chrome azurol S–cetrimide systems. (1), (2) $2 \cdot 10^{-5}$ *M* Chrome azurol S, pH 5.5 and 6.0; (3) $4 \cdot 10^{-6}$ *M* indium and $2 \cdot 10^{-5}$ *M* chrome azurol S, pH 6.0; (4) $4 \cdot 10^{-6}$ *M* gallium and $2 \cdot 10^{-5}$ *M* chrome azurol S, pH 5.5; (5) $4 \cdot 10^{-6}$ *M* indium, $2 \cdot 10^{-5}$ *M* chrome azurol S and $4 \cdot 10^{-5}$ *M* cetrimide, pH 6.0; (6) $4 \cdot 10^{-6}$ *M* gallium, $2 \cdot 10^{-5}$ *M* chrome azurol S and $4 \cdot 10^{-5}$ *M* cetrimide, pH 5.5. 2-cm cells.

Effect of chrome azurol S and cetrimide concentrations

The influence of the chrome azurol S concentration was established by measuring the absorbances of solutions containing $4 \cdot 10^{-6}$ *M* indium (or gallium), $3.2 \cdot 10^{-5}$ *M* cetrimide ($4 \cdot 10^{-5}$ *M* for gallium), 0.5 ml of hexamine solution (2 ml of phthalate buffer pH 5.5 for gallium) and increasing concentrations of chrome azurol S. The curves in Fig. 2 indicate that in the presence of up to 5-fold molar amounts of chrome azurol S, the absorbance gradually increased; above this amount no further effect was observed. However, above 7-fold molar amounts of reagent, turbidity appeared.

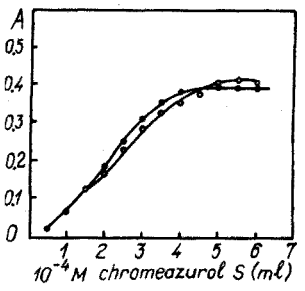

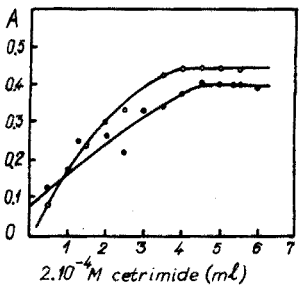

Fig. 2. Variation of absorbance with chrome azurol S concentration. (○) Indium, 1-cm cell, 630 nm; (●) gallium, 1-cm cell, 640 nm. Other conditions as in text.

Fig. 3. Variation of absorbance with cetrimide concentration. (○) Indium, 1-cm cell, 630 nm; (●) gallium, 1-cm cell, 640 nm. Other conditions as in text.

The effect of cetrimide concentration was investigated in solutions containing $4 \cdot 10^{-6}$ *M* of indium or gallium, and the established 5-fold molar concentration of chrome azurol S ($2 \cdot 10^{-5}$ *M*) at the pH values given above. Figure 3 shows that maximal absorbance was reached with an 8-fold molar amount of cetrimide in the indium reaction and a 9-fold molar amount in the gallium reaction. Further increase in the cetrimide concentration did not affect the absorbance. At lower cetrimide concentrations the solutions of indium and gallium (as well as the reagent blanks) tended to become turbid; accordingly, a larger excess of cetrimide, *viz.* a 10-fold molar amount ($4 \cdot 10^{-5}$ *M*), was selected for further studies.

Effect of pH

The optimal ratio of the components Me:chrome azurol S:cetrimide = 1:5:10 (established as described above) was used in studies of the effect of pH. The pH values of solutions containing $4 \cdot 10^{-6}$ *M* indium or gallium were carefully adjusted with dilute nitric acid or sodium hydroxide solution. On account of the difficulty of adjusting the pH of the reagent blanks, absorbances here were measured against distilled water; in any case, the absorption of the reagent was negligible at the wavelengths used. The reactions were found to be pH-dependent: maximal absorbance for the indium complex occurred at pH 5.2–6.2, and that for the gallium complex at pH 4.7–6; outside these limits, absorbances decreased gradually.

Preliminary investigations showed that hexamine was the most suitable buffer for the indium reaction, and phthalate (or acetate) the most favorable for the gallium reaction.

The amount of phthalate buffer added was of no importance, because the buffer components did not form complexes with gallium(III). With phthalate buffers the optimal pH was 4.75–5.75, and a buffer of pH 5.50 was selected. For the reaction with indium 1.5 ml of 2% hexamine solution was always introduced into a 25-ml volumetric flask, the pH being thus adjusted to 5.80–6.00.

Total effect of chrome azurol S and cetrimide

In the above investigations, the solutions were prepared with arbitrarily chosen constant concentrations of the components, varying the concentration of only one

of them. However, a turbidity appeared at certain ratios of chrome azurol S to cetrimide, hence the optimal correlation between the two ligands and the amount of metal had to be established. For this purpose, the effect of increasing concentrations of the reagents at a constant 1:2 ratio between chrome azurol S and cetrimide, was studied. The absorption maxima of the complexes were shifted about 30 nm towards shorter wavelengths with a Me:chrome azurol S:cetrimide ratio of 1:20:40, but the absorbances were not changed significantly. A small shift of the wavelength of maximal absorbance was observed in studying the dependence between the absorbance and the concentration of metal ion because the ratio of metal to reagents changed slightly (Fig. 4). The curves in Fig. 4 pass through an isosbestic point, which indicates that there is a simple complexation equilibrium and that only one complex is formed under the various conditions. The solutions remained pure blue with a constant wavelength of maximal absorbance at 630 nm (In) or 640 nm (Ga) at all metal concentrations if the correlation Me:chrome azurol S:cetrimide was 1:5:10.

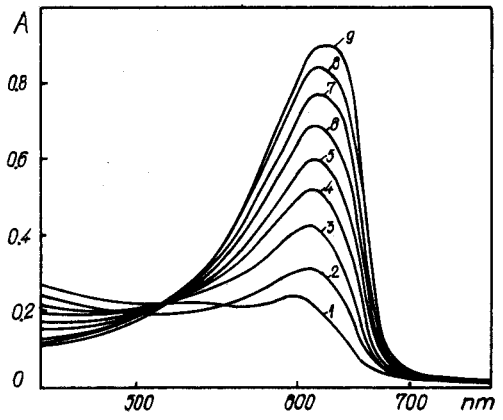

Fig. 4. Variation of absorbance with metal concentration. $2 \cdot 10^{-5}$ *M* chrome azurol S, $4 \cdot 10^{-5}$ *M* cetrimide, pH 6.0, 2-cm cell. Concentration of indium: (1) $8 \cdot 10^{-7}$ *M*; (2) $1.2 \cdot 10^{-6}$ *M*; (3) $1.6 \cdot 10^{-6}$ *M*; (4) $2.0 \cdot 10^{-6}$ *M*; (5) $2.4 \cdot 10^{-6}$ *M*; (6) $2.8 \cdot 10^{-6}$ *M*; (7) $3.2 \cdot 10^{-6}$ *M*; (8) $3.6 \cdot 10^{-6}$ *M*; (9) $4.0 \cdot 10^{-6}$ *M*.

Effect of time and of addition of reagents

The maximal absorbance of the complexes developed immediately and remained constant for about 1 h; a gradual decrease in absorbance was then observed. The order of addition of the reagents was not critical, provided that the buffer was added last.

Beer's law

Calibration graphs were prepared by mixing the standard solutions containing $4 \cdot 10^{-6}$–$4 \cdot 10^{-7}$ *M* metal ion, 5 ml of 10^{-4} *M* chrome azurol S solution, 5 ml of $2 \cdot 10^{-4}$ *M* cetrimide and the appropriate amount of buffer (see above). The solution was then diluted with distilled water in a 25-ml volumetric flask. Absorbances were measured in 1-cm cells against reagent blanks at 630 nm (In) or 640 nm (Ga). Beer's law was obeyed in the ranges 0.046–0.46 μg In ml^{-1} and 0.027–0.27 μg Ga ml^{-1}.

A molar absorptivity of $1.23 \cdot 10^5$ l mole^{-1} cm^{-1} was obtained for the indium complex, and $1.14 \cdot 10^5$ l mole^{-1} cm^{-1} for the gallium complex. According to Sandell's expression, the sensitivities of the reactions are respectively 0.00093 μg In cm^{-2} and 0.00061 μg Ga cm^{-2} for log $A = 0.001$. The molar absorptivity for the gallium complex is in good agreement with the earlier value[5], although it appears that different conditions were used. No information on the indium complex seems to be available in the literature.

Interference study

In order to assess possible analytical applications of the reactions, the effects of some ions which often accompany indium and gallium were studied, as well as the effect of some common metal ions. For these studies, the solutions contained 6 μg of indium (or 3.5 μg of gallium), 5 ml of 10^{-4} *M* chrome azurol S, 5 ml of $2 \cdot 10^{-4}$ *M* cetrimide and 1.5 ml of 2% hexamine solution (or 2 ml of phthalate buffer) in 25-ml volumetric flasks. Ni(II), Co(II), Mn(II), Ag(I), Bi(III), Pb(II), Cd(II), Zn(II) and Tl(III) did not react with chrome azurol S and cetrimide under these conditions, but caused only a faint red coloration, the intensity of which slightly increased with metal ion concentration. The results are listed in Table I. Al(III), Fe(II), Fe(III) and Cu(II) reacted under the same conditions with chrome azurol S and cetrimide, and in equivalent quantities strongly interfered with the determinations of indium and gallium.

TABLE I

EFFECT OF DIVERSE IONS ON THE DETERMINATION OF INDIUM AND GALLIUM

Ion added	Tl(III)	Bi(III)	Ag(I)	Ni(II)	Pb(II)	Mn(II)	Co(II)	Zn(II)	Cd(II)
Amount tolerated for 6 μg In	20	220	550[a]	300	1050	2750[a]	2400[a]	2800[a]	5600[a]
Amount tolerated for 3.5 μg Ga	40	220	550[a]	600	1450	2750[a]	3000[a]	3500[a]	5600[a]

[a] Larger amounts were not investigated.

Conclusions

The bathochromic shift in the absorption spectra of the complexes formed between chrome azurol S and indium or gallium caused by the addition of cetrimide, provides a basis for highly sensitive determinations of these ions. The methods described are simple and precise, and when combined with preliminary separations to improve selectivity, should simplify the determination of traces of indium and gallium in many materials. Studies of applications are now in progress.

SUMMARY

Spectrophotometric methods are described for the determination of microgram amounts of indium and gallium based on the formation of a ternary complex

between the metal, chrome azurol S and cetyltrimethylammonium bromide (cetrimide). A considerable bathochromic shift (100 nm) of the wavelength of maximal absorption accompanies the sensitizing action of cetrimide. The complexes have absorbance maxima at 630 nm and 640 nm, respectively, with molar absorptivities of $1.23 \cdot 10^5$ (In) and $1.14 \cdot 10^5$ l mole^{-1} cm^{-1} (Ga). The sensitivities are 0.00093 μg In cm^{-2} and 0.00061 μg Ga cm^{-2} for $A = 0.001$. The effects of pH, reagent concentrations and rate of complex formation are discussed. Reasonable amounts of many metal ions can be tolerated, but aluminium, iron and copper interfere.

RÉSUMÉ

Une méthode spectrophotométrique est décrite pour le dosage de microquantités d'indium et de gallium; elle est basée sur la formation d'un complexe ternaire entre métal, chromazurol-S et bromure de cétyltriméthylammonium (cétrimide). Ces complexes ont une absorption maximum à 630 et 640 nm, respectivement, avec des coefficients d'extinction molaires de $1.23 \cdot 10^5$ et $1.14 \cdot 10^5$ l mole^{-1} cm^{-1}. Les sensibilités sont de 0.00093 μg In cm^{-2} et 0.00061 μg Ga cm^{-2} pour $A = 0.001$. On examine l'influence du pH, des concentrations en réactif et de la vitesse de formation des complexes. Le dosage peut se faire en présence de nombreux ions métalliques; cependant aluminium, fer et cuivre gênent.

ZUSAMMENFASSUNG

Es werden spektrophotometrische Methoden für die Bestimmung von Mikrogramm-Mengen von Indium und Gallium beschrieben. Sie beruhen auf der Bildung eines ternären Komplexes zwischen dem Metall, Chromazurol S und Cetyltrimethylammoniumbromid (Cetrimid). Eine erhebliche bathochrome Verschiebung (100 nm) der Wellenlänge der maximalen Absorption begleitet die empfindlichkeitssteigernde Wirkung von Cetrimid. Die Komplexe haben Extinktionsmaxima bei 630 nm bzw. 640 nm mit molaren Extinktionskoeffizienten von $1.23 \cdot 10^5$ (In) und $1.14 \cdot 10^5$ l mol^{-1} cm^{-1} (Ga). Die Empfindlichkeiten sind 0.00093 μg In cm^{-2} und 0.00061 μg Ga cm^{-2} für $A = 0.001$. Der Einfluss des pH-Wertes, der Reagenzkonzentrationen und der Komplexbildungsgeschwindigkeit wird diskutiert. Mässige Mengen vieler Metallionen können toleriert werden, jedoch stören Aluminium, Eisen und Kupfer.

REFERENCES

1 R. M. Dagnall, T. S. West and P. Young, *Analyst*, 92 (1967) 27.
2 C. L. Leong, *Analyst*, 19 (1970) 1018.
3 Y. Shijo and T. Takeuchi, *Jap. Anal.*, 17 (1968) 1519.
4 Y. Shijo and T. Takeuchi, *Jap. Anal.*, 17 (1968) 61.
5 Y. Shijo and T. Takeuchi, *Jap. Anal.*, 20 (1971) 137.
6 Y. Horiuchi and H. Nishida, *Z. Anal. Chem.*, 242 (1968) 49; *Anal. Abstr.*, 16 (1969) 1167.
7 S. P. Sangal, *Z. Anal. Chem.*, 239 (1968) 48; *Anal. Abstr.*, 16 (1969) 78.

Analytica Chimica Acta, 67 (1973) 113–118

COULOMETRIC DETERMINATION OF IRON(II)–1,10-PHENANTHROLINE WITH CERIUM(IV)*

SHARON W. McCLEAN and WILLIAM C. PURDY

Department of Chemistry, University of Maryland, College Park, Md. 20742 (U.S.A.)

(Received 14th March 1973)

Iron has been titrated coulometrically in aqueous solution in both the oxidized and reduced form of the ion and in the oxidized and reduced forms of the cyanide complex. All the titrants normally used for determinations of iron have been adapted for electrogeneration, including unstable or volatile titrants such as tin(II) or bromine, and difficult-to-prepare titrants such as manganese(III). Since iron is usually found in matrices containing substances which could interfere with an oxidation–reduction titration, the present study was undertaken to develop a titration for iron which could be compatible with a separation.

Solvent extraction is probably the most efficient means of separating iron before a titration. Solvent extraction of iron has been accomplished by formation of both coordination and ion-association complexes. To coordinate a separation and titration, it was desirable to select a separation procedure which would involve iron in a form easily usable in or adaptable to a titration. In addition, iron has to be in a stable form, one which can be titrated and one which will not change during the separation process.

Separation of iron by the well-known ether–hydrochloric acid extraction was a possibility. The extraction is efficient and hydrochloric acid is the electrolyte for the electrogeneration of chlorine. Chlorine has been used to titrate iron in amounts of 12 μg and above[1,2]. However, the use of this system suffers from the disadvantages of the easy volatility of chlorine and the necessity of reducing iron after the extraction rather than before. Although iron cyanide is a stable complex and has been titrated coulometrically[3,4], solvent extraction would probably necessitate the formation of a mixed ligand complex which, even if easily formed, would mean an alteration in the titration. Ferroin, the 1,10-phenanthroline complex of iron, appeared a good choice for analysis since it has been used both for iron separations and as an indicator in redox titrations. Vydra and Pribil[5] have titrated milligram amounts of the iron–phenanthroline complex volumetrically with cerium, using visible and potentiometric end-points.

The present work describes the development of a coulometric titration of ferroin with electrogenerated cerium(IV) and a modified amperometric indicating system of the type devised by Cooke *et al.*[6]

* Taken in part from the Ph.D. Dissertation of Sharon W. McClean, University of Maryland, 1972.

EXPERIMENTAL

Apparatus

Coulometric titrations were performed with the CrisFeld Microcoulometric Quantalizer, Model B. A Sargent Model XV Polarograph with Microrange Extender was used to maintain a constant voltage across the indicating electrodes and to monitor the current passing between them. A Hamilton 10-μl syringe was used to deliver the iron solutions.

The titration cell was equipped with two side-arms which were isolated from the body of the cell by fritted glass discs. The central compartment was made from a weighing bottle of *ca.* 12 ml volume. The use of the two isolated side-arms for holding the indicating reference electrode and the auxiliary generating cathode made possible greater freedom of choice in selection of the two electrodes internal to the cell. Both generating electrodes were platinum. A saturated calomel electrode and a platinum electrode were used for the indicating system.

Reagents

The iron powder used was electrolytic grade; all other chemicals were reagent grade.

The generating solution was prepared by saturating a 3 *M* sulfuric acid solution with cerium(III) sulfate.

Iron–1,10-phenanthroline solution was prepared by dissolving 0.1003 g of iron(II) ammonium sulfate hexahydrate and 0.600 g of 1,10-phenanthroline in 1 l of water.

Procedure

About 8 ml of generating solution was added to the titration cell. The potential of this solution was usually lower than the reference voltage, 1.025 V. The solution was then brought to the reference voltage by generating the required amount of cerium(IV). After the potential was adjusted, the unknown solution of ferroin was added. The timer was reset and cerium(IV) was generated until the current indicator showed less than 0.0001 μA.

RESULTS AND DISCUSSION

To find the best end-point potential for the ferroin–cerium(IV) titration, the changes in the potential of the titration solution were followed during several coulometric titrations. Since the standard potentials of the ferroin/ferriin and cerium(III)/cerium(IV) couples are relatively close, a well-formed S-shaped curve is not achieved by plotting the potential of the solution as a function of titration time. By plotting the derivative of this curve, the inflection-point potential of the titration curve can be found. In a coulometric titration the inflection-point and the end-point potentials are not identical; but if an arbitrary end-point is chosen close to the point of maximal slope and used for both pretitration and actual titration, the effect on accuracy of the potential difference is eliminated. For this method, an end-point potential of about 1.024 V *vs.* N.H.E. was selected.

To determine the effect of the applied voltage on the titration system, titra-

tions were performed at several voltages. The generating solution was changed with each voltage change, but for a given voltage the titrations were carried out repetitively without solution change. Table I shows that titration times tended to increase with increasing voltage. Although this trend is not shown in the Table, the greater the applied voltage, the greater was the tendency for the times to increase with each successive titration. The titration times for an applied potential within 5 mV of 1.025 V were most accurate. The rest of the work was done with an applied potential of 1.025 V across the indicating electrodes.

TABLE I

EFFECT OF APPLIED VOLTAGE ON TITRATION TIME

(In all cases, 0.570 μg of iron was taken)

Applied voltage (V)	*Time (s)*	*Trials*
1.020	101.1	4
1.028	102.2	14
1.029	101.8	11
1f034	104.6	7
1.038	104.8	6
1.044	105.8	5
1.050	106.6	5
1.055	106.2	4
1.060	105.8	3

The current efficiency for the electrogeneration of cerium(IV) was checked against electrolytic iron. With the method of Lingane[7], the current efficiency was found to be 97.0–98.9%. The variance in current efficiency was attributed to differences in current density. Lingane *et al.*[8] have shown current efficiency to be dependent on current density for electrogenerated cerium(IV). Because attempts to obtain reasonable results with generating electrodes smaller than 0.1 cm^2 were unsuccessful, the current density obtained with the smallest current used was slightly low for optimal current efficiency. However, since ferroin can react at a platinum electrode, the titration efficiency was expected and, in fact, found to be closer to 100% than would have been predicted from the current efficiency.

As long as the iron(II) ion remains bound to 1,10-phenanthroline, oxidation by the air is not a problem. But with increasing acidity, the dissociation of the ferroin complex increases and the formal potential of the ferroin/ferriin couple decreases. Since the generating solution is 3 *M* in sulfuric acid, the necessity for deaeration was investigated. Deaeration was always carried out with nitrogen gas bubbled through the solution for 5 min before the titration. During the titration, a nitrogen atmosphere was maintained above the sample solution. If some of the ferroin were oxidized by oxygen, it would be expected that the deaerated samples would have longer titration times than the non-deaerated samples. In fact, no such trend was noted. Deaeration was thus considered unnecessary.

Titrations were performed in which generation was stopped for 1 min after

about 80% of the sample had been titrated. No significant differences were observed between these titrations and those run with no delay.

With a constant voltage impressed across the indicating electrodes, some electrolysis of the analyte will occur. For larger samples the extent of the electrolysis can cause results to be low by 1–2%. This electrolysis can be lessened by (*a*) decreasing the area of the platinum indicating electrode, (*b*) introducing a large resistor in series with the indicating electrodes for the first part of the titration, or (*c*) leaving the indicating circuit open for the major portion of the titration. With very small samples the indicating current is so small that the electrolysis is usually not appreciable. Titrations were carried out with 6.00-μg samples in which the indicating circuit was not activated until about 75% of the sample had been titrated. Titrations performed in this manner were found to give no lower results than those in which the indicator voltage was applied throughout the titration.

The condition of the three platinum electrodes became increasingly important with decreasing amounts of analyte. If the electrodes were used at least once a day and stored between use in distilled water, they usually responded as desired. If the electrodes were left unused for a period of a week, or if one of the electrodes had to be replaced, the titration times would be erratic. In the former case, usually the performing of a series of 5–10 titrations followed by a change in generating solution was sufficient treatment to start the electrodes performing properly. Introduction of a new electrode, particularly a new indicating electrode, presented more of a problem. Preconditioning with concentrated nitric acid, with 10% nitric acid, with hot 50% aqua regia, and with silver polish, was tried. Silver polish was found to be just as effective as the others. Whatever was used to clean the electrode, it was usually necessary to perform about 15 titrations to zero current with the indicator electrode, and change the generating solution two to three times, before reproducibility of the results was acceptable.

TABLE II

COULOMETRIC TITRATION OF FERROIN

Fe^{2+} taken (μg)	Fe^{2+} found (μg)	Trials	*s*	Relative error (%)	s_r (%)
131.4	131.7	7	±2.7	0.2	±2.1
65.7	65.5	5	0.8	−0.3	1.2
2.63	2.65	4	0.1	0.8	3.8
10.00	10.00	4	0.23	0.0	2.3
8.00	8.06	3	0.22	0.8	2.7
6.00	6.05	8	0.11	0.8	1.8
5.00	5.13	2		2.6	
3.00	3.06	2		2.0	
1.00	1.12	4	0.05	12.0	5.0
0.915	0.912	6	0.022	−0.3	2.4
0.712	0.700	6	0.005	−1.6	0.7
0.508	0.500	26	0.009	−1.6	1.8
0.305	0.307	10	0.006	0.6	2.0
0.102	0.106	8	0.003	4.0	3.0

For this work no drift was observed in the solution potential over a 5-min period following the titration of a 0.5-μg sample, if the applied indicator voltage was shut off after the titration. If, however, the applied voltage was maintained for 5 min after a titration, the next titration performed would be about 5% high. This increase in time may be caused by the reduction of excess of cerium(IV) at the indicator electrode.

Table II presents the accuracy and precision for amounts of iron ranging from 0.1 to 130 μg. The samples in the 1–130 μg range were titrated without benefit of the Sargent Microrange Extender in the indicating system. Thus, the current sensitivity was 0.003 μA mm^{-1}. The 1–10 μg range was titrated at a generating current of 96.50 μA. At this current a 1.00-μg sample required a generation time of about 20 s. It would be expected that a large error would result from this low generation time, and, in fact, when samples in the 0.1–0.9 μg range were titrated at 9.65 μA, the errors were lower. The 0.102-μg sample again had a 20-s titration time and a relatively high error. A smaller generating current would probably increase the accuracy here as well. Problems involved in titrating smaller amounts than 0.1 μg would include (*a*) a small initial indicating current which would be difficult to monitor even at a current sensitivity of 0.0001 μA mm^{-1}, and (*b*) a decrease in current efficiency resulting from decreased current density with a smaller current.

SUMMARY

Iron bound to 1,10-phenanthroline is determined with electrogenerated cerium(IV). Iron samples in the range 0.1–130 μg were titrated with a relative standard deviation of 0.7–5.0% and a relative error of 0–4.0% with the greatest inaccuracies and imprecision being at the lower end of the range, where titration times were shortest. The end-point detection system consists of a platinum and a saturated calomel electrode across which a constant voltage is impressed. This voltage is such that the platinum electrode is 1.025 V *vs.* N.H.E. The current between the indicating electrodes is monitored with a current-sensing device possessing a sensitivity of 0.0001 μA mm^{-1}.

RÉSUMÉ

Une méthode est proposée pour le dosage du fer combiné à la 1,10-phénanthroline, par coulométrie au moyen de cérium(IV). La déviation standard relative est de 0.7 à 5.0% et l'erreur relative de 0 à 4.0% pour des échantillons contenant 0.1 à 130 μg de fer. L'erreur est maximum lorsque les temps de titrage sont les plus courts. Le point final est décelé à l'aide d'un système d'électrodes platine/calomel saturé (1.025 V *vs.* NHE). Le courant est de l'ordre de 0.0001 μA mm^{-1}.

ZUSAMMENFASSUNG

An 1,10-Phenanthrolin gebundenes Eisen wird mit elektrochemisch erzeugtem Cer(IV) bestimmt. Eisenproben im Bereich 0.1–130 μg wurden mit einer relativen Standardabweichung von 0.7–5.0% und einem relativen Fehler von 0–4.0% titriert, wobei sich die grösste Ungenauigkeit und die schlechteste Reproduzierbarkeit am

unteren Ende des Bereiches ergaben, bei dem die Titrationszeiten am kürzesten sind. Das System zur Endpunktsbestimmung besteht aus einer Platin- und einer gesättigten Kalomelelektrode, an die eine konstante Spannung angelegt wird, so dass das Potential der Platinelektrode 1.025 V gegen NHE beträgt. Der Strom zwischen den Indikatorelektroden wird mit einer Anordnung gemessen, die eine Empfindlichkeit von 0.0001 μA mm^{-1} besitzt.

REFERENCES

1 P. S. Farrington, W. P. Schaefer and J. M. Dunham, *Anal. Chem.*, 33 (1961) 1318.
2 V. K. Khakimova and P. K. Agasyan, *Zavod. Lab.*, 27 (1961) 263.
3 R. V. Dilts and N. H. Furman, *Anal. Chem.*, 27 (1955) 1275.
4 B. Miller and D. N. Hume, *Anal. Chem.*, 32 (1960) 524.
5 F. Vydra and R. Pribil, *Talanta*, 5 (1960) 44.
6 W. D. Cooke, C. N. Reilley and N. H. Furman, *Anal. Chem.*, 23 (1951) 1662.
7 J. J. Lingane, *Electroanalytical Chemistry*, Interscience, New York, 2nd Ed., 1958, p. 485.
8 J. J. Lingane, C. H. Langford and F. C. Anson, *Anal. Chim. Acta*, 16 (1957) 165.

Analytica Chimica Acta, 67 (1973) 119–127

A UNIVERSAL SOLVENT EXTRACTION–TITRATION METHOD FOR THE RAPID AND ACCURATE DETERMINATION OF URANIUM IN COMPLEX SOLUTIONS*

C. R. WALKER and O. A. VITA

Chemical Analysis Department, Technical Division, Goodyear Atomic Corporation, P.O. Box 628, Piketon, Ohio 45661 (U.S.A.)

(Received 13th February 1973)

A wide variety of complex solutions is produced in the recovery of uranium from nuclear fuels. These solutions ordinarily contain 0.1–20 g of uranium per liter and high concentrations of aluminum nitrate in addition to a variety of cations and anions associated with fuel-element constituents and dissolution media. Several analytical procedures, each intended for a particular type of solution, are available for the determination of uranium, but none can give satisfactory results universally. Thus, there is the need for a method that would be applicable to all types of material and also give accurate results, be rapid, and require no expensive equipment or skilled personnel.

Although accurate determinations of uranium can be made with combinations of such techniques as cupferron precipitation, sulfide precipitation, hydroxide precipitation, solvent extraction, and electrolytic separations of impurities, such procedures which must be tailored to the sample are extremely long, require careful sample preparation, and demand great skill and patience from the analyst. Ion-exchange separations, which have the advantages of being more universal and adaptable to handling a large number of samples, are slow and usually require a preliminary sample preparation to convert uranium to the ionic form required for adsorption on the resin.

The chemistry of uranium makes it particularly adaptable to solvent-extraction separations. Two of the best known solvent-extraction systems for uranium use tri-isooctyl amine (TIOA) and tributyl phosphate (TBP), but they both have disadvantages. In the TIOA system, the uranium must be in a chloride solution which is not a usual reactor fuel dissolution medium. In the TBP system, uranium is extracted from the more common nitrate solution, but the TBP must be diluted with an inert solvent to prevent extraction of other elements such as the lanthanides, niobium, and zirconium. Since dilution decreases the extraction coefficient of uranium, as many as four extractions with diluted TBP may be required for complete recovery of uranium. The TBP system is also subject to interferences from phosphate and large quantities of sulfate; both substances inhibit the extraction of uranium.

* Presented in part at the Twelfth Annual Conference on Analytical Chemistry in Nuclear Technology, Gatlinburg, Tenn., October 8–10, 1968.

Maeck *et al.*[1] proposed an extraction system in which uranium is extracted as its tetrapropylammonium nitrate (TPAN) complex from acid-deficient aluminum nitrate. With several major modifications, this system has been adapted to a universal procedure for the quantitative separation of 1–300 mg of uranium from large quantities of diverse ions. Back-extraction of 75–300 mg uranium with phosphoric acid then transfers the uranium into a medium in which it can be determined directly by the titration method of Davies and Gray[2]. For lower concentrations of uranium a colorimetric determination is made[3]. In developing this procedure, several parameters and variables in the solvent extraction system had to be evaluated. Among these were the stability and extraction efficiencies of organic solvents, and the effects of various anions and cations on uranium extraction.

Evaluation of solvents

Extraction efficiencies of solvent were determined with a dibenzoylmethane colorimetric method to determine uranium in the extraction raffinates. Hexone, the solvent suggested by Maeck *et al.*[1], was used to extract the uranium–TPAN complex in the preliminary experiments. The uranium was extracted satisfactorily, but hexone was unsuitable as a solvent because of its miscibility with the phosphoric acid used to recover the uranium from the organic layer. Undiluted TBP, as an extractant for the TPAN–uranium complex, formed emulsions with solutions containing zirconium and niobium, but when diluted with inert solvents, such as hexane or carbon tetrachloride, the uranium extraction was incomplete even after two equilibrations. Emulsions continued to be a problem particularly with zirconium and niobium solutions. Butyl acetate was an excellent solvent for extracting the TPAN–uranium complex, but small quantities of butyl acetate, which were carried through the extraction process, interfered with the uranium determination by consuming oxidant in the titration to give high results and indistinct end-points.

Amyl acetate, which is less soluble in aqueous media, was evaluated, and in a single equilibration, with a standard zirconium–uranium solution added to 200 ml of 2.8 *M* aluminum nitrate containing 0.5% TPAN, extracted 98.5% of the uranium with no evidence of decomposition. Repeated equilibrations, however, did not extract any further amounts of uranium. Increasing the amount of the TPAN–salting agent solution to 300 ml improved the uranium extraction to 99.8%, but again the last portion of uranium could not be extracted even after adding tartrate to the aqueous layer to help complex the zirconium. This led to the assumption that uranium was forming a complex with zirconium at low acidities. Further experiments to investigate this effect with both zirconium and niobium are summarized in Table I.

As shown in Table I, under certain conditions, zirconium and niobium apparently form complexes with uranium to prevent their complete extraction. Also, sulfate ion is a good complexing agent for zirconium but not niobium, while phosphoric acid is an excellent complexing agent for niobium but not zirconium.

Since increasing the amount of TPAN solution did not give the quantitative uranium recovery desired, TBP, an additional uranium complexing agent, was added to the amyl acetate, and a series of extractions were made, in which varying amounts of TBP were added to the amyl acetate. The addition of only 2% TBP gave a system that could extract 99.97–99.98% of the uranium from all types

TABLE I

AMYL ACETATE EXTRACTION OF 300 mg OF URANIUM FROM Zr AND Nb SOLUTIONS

Element	*Wt.(g)*	*Complexing agent added*	*Uranium recovery (%)*
Zr	2.0	Tartrate	0.0
Nb	2.0	Tartrate	0.0
—	—	Tartrate	100
Mo	2.0	Tartrate	100
Zr	2.0	10 ml H_2SO_4	100
Nb	2.0	10 ml H_2SO_4	Precipitate
Zr	2.0	10 ml H_3PO_4	Precipitate
Nb	2.0	10 ml H_3PO_4	100

of solutions after two equilibrations; 5–10% TBP extracted the uranium efficiently, but again emulsions were troublesome. Thus, amyl acetate containing 2% TBP was selected as the organic extraction medium.

Effect of cations on extraction efficiency

Several tests were run to evaluate the effect of various cations on the extraction efficiency of amyl acetate–tributyl phosphate mixtures. The results of this evaluation using 300 ml of 2.8 *M* aluminum nitrate–0.5% TPAN are shown in Table II.

TABLE II

CATION EFFECT ON EXTRACTION EFFICIENCY

Sample type	*Solvent system*	*100-ml equilibrations*	*Av. % U extracted*
U–Zr	AA–2% TBP	1	99.30
U–Zr	AA–1% TBP	2	99.98
U–Zr	AA–2% TBP	2	99.98
U–Zr	AA–5% TBP	2	99.97
U–Zr	AA–10% TBP	2	Emulsion formed
U–Mo	AA–2% TBP	2	99.97
GAE[a]	AA–2% TBP	2	99.98

[a] These are representative samples from the General Analytical Evaluation program administrated by the New Brunswick Laboratory for the Atomic Energy Commission. The solutions include a variety of known standards and production material from nuclear fuel scrap recovery programs.

Effect of acids on extraction efficiency

Most scrap recovery solutions contain high concentrations of various acids or a mixture of acids—often more than the TPAN–acid-deficient aluminum nitrate solution can neutralize. Thus, the extraction efficiency was studied as a function of varying quantities of the acids that might be encountered in typical samples. The effect of the addition of various acids on extraction efficiencies with the

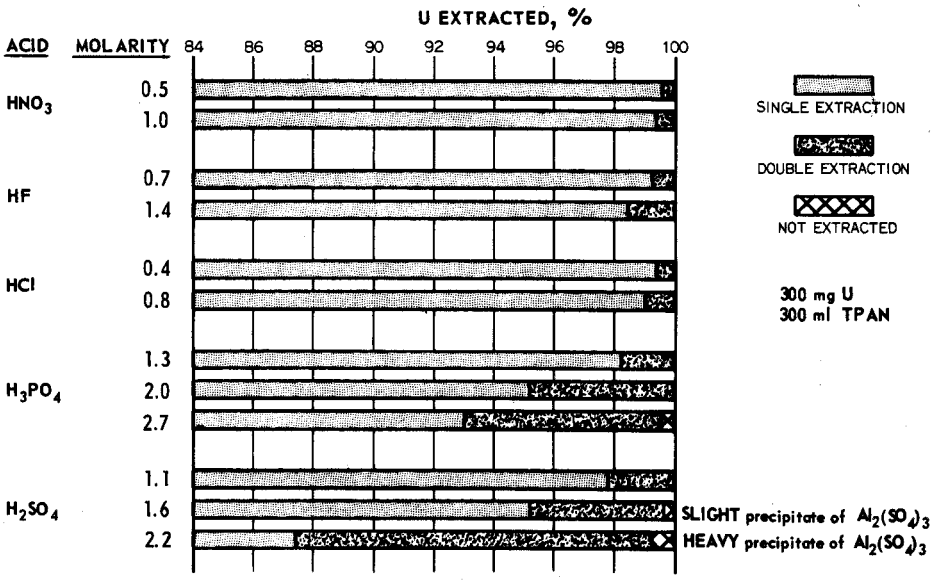

Fig. 1. Effect of acids on extraction efficiency.

TPAN–AA–TBP system is shown in Fig. 1. Acid concentrations, which are presented as molarities, represent 10 and 20 ml of nitric acid, 10 and 20 ml of hydrofluoric acid, 10 and 20 ml of hydrochloric acid, 10, 15 and 20 ml of phosphoric acid, and 10, 15, and 20 ml of sulfuric acid, all added as concentrated reagents. Precipitates that form with 15 and 20 ml of sulfuric acid prevent a clean separation of the organic and aqueous phases. Thus, large amounts of sulfuric acid should be removed by evaporation before the extraction.

Titration of the uranium

Uranium separated by the solvent extraction procedure is determined by the Davies and Gray[2] titration method. Since the uranium is removed from the organic layer with strong phosphoric acid solution, it is in the proper medium for starting the analysis, which is outlined as follows: (1) uranium(VI) is reduced to uranium(IV) with iron(II) sulfate in the strong phosphoric acid medium; (2) excess of iron(II) ion is oxidized with nitric acid using molybdate as a catalyst; (3) nitrite ion, a potential interference, formed during the oxidation of iron(II) ion is destroyed with sulfamic acid; and (4) the uranium(IV) is titrated to uranium(VI) with standard potassium dichromate. This method is used for concentrations of 1.5–20 g of uranium per liter.

Accuracy and precision of titration

The evaluation of the accuracy and precision of the proposed procedure was based on the analysis of a standard solution containing uranium and zirconium (as prepared according to Reid[4]), and samples from the General Analytical Evaluation (GAE) program. GAE samples include both known standard samples and typical unknown production samples. The limits of error at the 95% confidence

TABLE III

PRECISION STUDIES

Sample type	*No. of samples*	*Limit of error (%)*
U–Zr standard	9	0.23
GAE knowns	5	0.74
GAT production	8	0.64

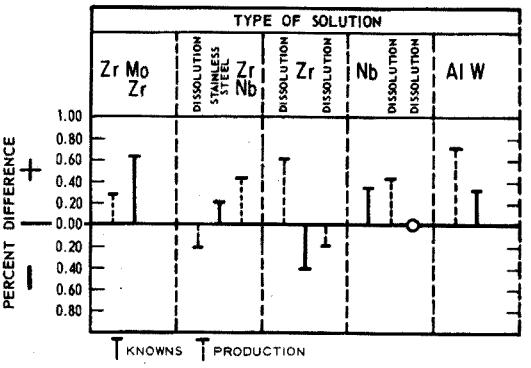

Fig. 2. Analysis of General Analytical Evaluation (GAE) solutions.

interval for the analysis of the various types of solutions are shown in Table III. The results obtained with individual GAE samples are shown graphically in Fig. 2. Percent differences for known samples are based on the prepared value supplied by New Brunswick Laboratory, while for the production samples the differences are based on average values from seven or more participating laboratories. The values for the GAE samples are limited by the fact that the amounts of samples received were insufficient to perform more than one determination by this new procedure. Occasionally, the one determination had to be performed on a quantity of uranium somewhat less than the desired amount.

Analysis of unknown samples

Further evaluation was made by several different methods on unknown samples submitted to this laboratory for referee analysis. The results of these analyses (Table IV) indicate the efficiency of the described method for the accurate determination of uranium in impure samples. The main advantage over other methods is that, in general, no prior sample preparation is necessary (sample weights up to 50 g can be analyzed). The method is rapid, requiring only 1.5 h for a duplicate analysis.

EXPERIMENTAL

Equipment

Separatory funnels. 500-ml pear-shaped fitted with Teflon stopcock. (An

TABLE IV

ANALYSIS BY DIFFERENT METHODS

(Results are given as mg U g^{-1} solution)

Sample	*Mass spectrometry*	*γ-Spectrometry*	*Ion-exchange titration*	*Solvent ext. colorimetric*	*Proposed method*
1	1.500	1.495	—	1.496	1.512
2	6.317	6.249	6.295	—	6.339
3	5.829	5.813	5.789	—	5.855
4	6.658	6.608	6.653	—	6.668
5	—	—	5.501	—	5.535
6	—	—	5.388	—	5.395
7	—	—	4.254	—	4.291

improved separatory funnel has been developed which is fitted with a flared top similar to that on an iodine flask; the modified extraction funnel can be purchased from Kimble Products or Fisher Scientific Company.)

Reagents

Aluminum nitrate–0.5% tetrapropylammonium nitrate (TPAN) solution. Dissolve 1050 g of aluminum nitrate nonahydrate in a minimum amount of water with the aid of heat. Add 135 ml of ammonia liquor and 50 ml of 10% tetrapropylammonium hydroxide. Stir until solution is complete with the temperature below 50° to prevent decomposition of TPAN. Dilute to 1 l with distilled water.

Phosphoric acid solution. Dilute 783 ml of concentrated phosphoric acid to 1 l with distilled water and add 1 ml of 1 *N* potassium dichromate solution.

n-Amyl acetate–2% tributyl phosphate. Dissolve 80 ml of TBP in 3920 ml of n-amyl acetate. Purify by equilibrating with three 100-ml portions of phosphoric acid solution and then washing with three 200-ml portions of distilled water. An alternative purification system for an impure amyl acetate is to equilibrate with 100 ml of 10% potassium hydroxide before adding phosphoric acid solution.

Diphenylamine sulfonate indicator. Add 0.32 g of barium diphenylamine sulfonate to 90 ml of water. Stir and add 0.5 g of sodium sulfate. Allow to stand overnight and filter. Dilute filtrate to 100 ml with distilled water.

Sulfamate solution—3 M. Add 300 g of sulfamic acid to 800 ml of water. Then add concentrated ammonia liquor slowly with stirring until all the solid dissolves; about 30 ml is usually required. Dilute the solution to 1 l with distilled water.

Iron(II) sulfate—1.25 M. Dissolve 348 g of iron(II) sulfate heptahydrate in 700 ml of water containing 100 ml of (1+1) sulfuric acid. Dilute to 1 l with distilled water. Add 30–50 g of mossy cadmium metal to prevent oxidation.

Ammonium molybdate $[(NH_4)_6Mo_7O_{24}\cdot 4\ H_2O]$, *1%.* Dissolve 10 g of ammonium molybdate in distilled water and add 10 ml of 1 *M* sodium hydroxide. Dilute the solution to 1 l with distilled water.

Potassium dichromate, 0.05 N. Dissolve 4.90266 g of National Bureau of Standards (NBS Lot 136b) potassium dichromate in water and dilute to 1 l with

distilled water. (The weight given is corrected for air buoyancy and for the 99.98% oxidizing power stated for the material by NBS.) One ml of this solution is equivalent to 5.951 mg of normal uranium.

Nitric acid–sulfamic acid. Dilute 250 ml of concentrated nitric acid to about 950 ml with distilled water; then add 20 ml of 3 *M* sulfamate solution and dilute to 1 l with distilled water.

Procedure

Weigh to the nearest 0.1 mg duplicate sample aliquots containing 100–300 mg U into plastic graduates. (Note: For samples containing large quantities of Zr, add 10 ml concentrated sulfuric acid, and for samples containing large quantities of Nb, add 10 ml of concentrated phosphoric acid.) Transfer the aliquots to 500-ml separatory funnels, washing the graduates three or more times with aluminum nitrate–TPAN solution; add the washings to the separatory funnels. Dilute the solutions in the funnels to 330 ml with aluminum nitrate–TPAN solution. Add 100 ml of n-amyl acetate–TBP solution in a graduate to the separatory funnel. At this point the analysis should be completed without delay.

Wet the stopper and neck of the flask with aluminum nitrate–TPAN solution. Stopper the funnel and shake it vigorously for 3 min. *Do not twist the stopper in the funnel.* Allow the layers to separate completely (*ca.* 10 min) and transfer the aqueous phase to a second separatory funnel. Add 100 ml of n-amyl acetate–TBP solution to the second funnel, stopper, and shake it for 2 min. Allow the layers to separate and discard the aqueous layer. Transfer the second organic fraction to the first funnel, washing with an additional 30–40 ml of purified n-amyl acetate to complete the transfer. Equilibrate the combined organic phase four times—twice with 25 ml of phosphoric acid and twice with 15 ml. After equilibrating for 30 s each time, allow the mixture to stand 5 min and then carefully transfer the phosphoric acid solution containing the uranium to a 600-ml beaker. The stopper and the neck of the funnel must be washed thoroughly each time with phosphoric acid solution. *Do not twist the stopper in the funnel.*

The following techniques are recommended to obtain a quantitative recovery of the uranium. After the first equilibration, drain the phosphoric acid solution down the side of the beaker. Before the second equilibration, add phosphoric acid solution, lift the funnel, touch the tip to the side of the beaker and then invert the funnel. Allow the tip to drain for 30 s and then equilibrate in an inverted position. Treat the third equilibration the same as the second, except when draining the phosphoric acid solution, flick the stopcock backward and forward to promote complete washing of the stem. Repeat this procedure to obtain the fourth equilibration.

Wash the tip of the funnel with two 3-ml portions of phosphoric acid solution and wash down the sides of the beaker with 20 ml of concentrated phosphoric acid. If the sample is known or suspected to contain some easily oxidizable material (*e.g.*, an organic compound like an alcohol) that will consume the dichromate titrant, the combined phosphoric acid solutions should be treated with 5 ml of nitric acid and 1 ml of perchloric acid, and heated to 210° on a hot plate. After cooling, 20 ml of water is added. Start stirring the sample and, while stirring, add 5 ml of 3 *M* sulfamate solution, using the solution to wash down the inside of the beaker.

Add 4 ml of iron(II) sulfate solution directly to the sample solution taking care not to touch the sides of the beaker or splash any of the sample solution. Add 5 ml of nitric acid–sulfamic acid solution from a pipet, again using the solution to rinse the inside of the beaker. Add 2 ml of ammonium molybdate solution to the beaker. At this point a dark color is formed more slowly than in the normal Davies and Gray method and persists up to 10 min. The sample is then allowed to stand an *additional* 10 min after the brown color appears. Add 35 ml of (1+1) sulfuric acid and 230 ml of water. Add 11 drops of diphenylamine sulfonate indicator and titrate to a purple end-point. Accurate detection of the visual end-point, however, requires some practice and experience. The end-point is taken at the last addition of 0.02–0.04 ml of titrant that produces a visible deepening of the purple color in the solution. Another such addition made after the solution has stirred for 1 min produces no visible color change.

Calculations

Calculate the g of uranium per g of sample using the following equation.

$$\text{g U/g solution} = \frac{(\text{ml } 0.05\ N\ K_2Cr_2O_7 - \text{blank}) \cdot 5.951}{\text{wt. sample}}$$

The blank may vary occasionally which is attributable to several factors including the reagents used. An accurate method for determining a true blank requires a titration of 4 or 5 weighed portions of a standard uranium solution. The weights taken should be selected to give titers ranging from 10–45 ml of standard dichromate solution. Using the method of least squares, fit the titration volumes and corresponding solution weights to a straight line and determine the blank by extrapolating the titration volume to zero uranium solution weight. When new reagents are prepared, a single determination of about 120–130 mg U will determine the validity of the blank in use. The factor 5.951 applies to normal uranium. For other isotopic compositions of uranium, the factor is obtained by the following calculation: (0.025·atomic weight uranium).

SUMMARY

A rapid and accurate method has been developed for the determination of uranium in complex solutions produced in the recovery of uranium from nuclear fuels. These solutions usually contain 0.1–20 g $U\,l^{-1}$ and high concentrations of aluminum nitrate in addition to a variety of cations and anions associated with fuel-element constituents and dissolution media. The method involves the solvent extraction of uranium from an acid-deficient aluminum nitrate–tetrapropylammonium nitrate solution into 2% tributyl phosphate in n-amyl acetate. The uranium is then back-extracted with a concentrated phosphoric acid solution, and titrated by the method of Davies and Gray. The uranium extraction efficiency for sample solutions weighing up to 50 g is 99.9% or better, and the limit of error per analysis with 95% confidence is ±0.6%. No prior sample preparation is necessary, no expensive equipment is required, and even unskilled personnel can do duplicate analyses in 1.5 h.

RÉSUMÉ

Une méthode rapide et précise est proposée pour le dosage de l'uranium dans des solutions complexes provenant de sa récupération dans des combustibles nucléaires. Ces solutions renferment ordinairement 0.1 à 20 g U l^{-1} et de fortes concentrations de nitrate d'aluminium. On procède par extraction dans un solvant. L'uranium est ensuite extrait en retour dans une solution concentrée d'acide phosphorique et titré par la méthode de Davies et Gray. L'erreur est de $\pm 0.6\%$. Cette méthode présente les avantages suivants: pas de préparation préliminaire de l'échantillon, pas d'équipement coûteux, même une personne non entraînée peut effectuer ces analyses, à double, en 1.5 h.

ZUSAMMENFASSUNG

Es wurde eine schnelle und genaue Methode entwickelt für die Bestimmung von Uran in komplexen Lösungen, die bei der Wiedergewinnung von Uran aus Kernbrennstoffen anfallen. Diese Lösungen enthalten üblicherweise 0.1–20 g U l^{-1} und hohe Konzentrationen an Aluminiumnitrat sowie eine Vielfalt von Kationen und Anionen, die in Brennelementbestandteilen und in den zur Auflösung verwendeten Medien vorkommen. Bei der Methode wird das Uran aus einer Aluminiumnitrat–Tetrapropylammoniumnitrat-Lösung mit 2% Tributylphosphat in n-Amylacetat extrahiert. Das Uran wird dann mit konzentrierter Phosphorsäure zurückextrahiert und nach der Methode von Davies und Gray titriert. Das Uran wird bei Probelösungen von bis zu 50 g Gewicht zu 99.9% oder besser extrahiert, und die Fehlergrenze für eine Analyse bei 95% Vertrauensbereich ist $\pm 0.6\%$. Es ist weder eine vorherige Probenvorbereitung noch eine aufwendige Einrichtung erforderlich, und eine Doppelanalyse kann selbst von unerfahrenem Personal in 1.5 h ausgeführt werden.

REFERENCES

1 W. J. Maeck, G. L. Booman, M. C. Elliott and J. E. Rein, *Anal. Chem.*, 31 (1959) 1130.
2 W. Davies and W. Gray, *TRG Report 716 (D)*, 1964.
3 C. A. Francois, *Anal. Chem.*, 30 (1958) 50.
4 D. G. Reid, *2nd Conf. Peaceful Uses At. Energy*, 17 (1958) 145.

Analytica Chimica Acta, 67 (1973) 129–134

A SOLVENT-EXTRACTION METHOD FOR THE DETERMINATION OF MANGANESE-54 IN SEA WATER

W. W. FLYNN

Chemical Technology Division, Australian Atomic Energy Research Division, Lucas Heights, N.S.W. 2232 (Australia)

(Received 21st March 1973)

Manganese-54 is an artifical isotope produced as a by-product of nuclear technology. It is also found in very small amounts in meteorites as a result of bombardment by cosmic rays. Decay is by electron capture to give a γ-ray of 0.835-MeV energy, which enables the isotope to be detected by γ-ray spectrometry relatively easily.

However, the determination of manganese-54 in the environment is difficult, owing to the low efficiency of γ-ray spectrometers for most isotopes, and because the amounts found in environmental materials are usually small.

Few methods are available for the determination of manganese-54 in sea water, and those in use require large volumes of sea water to obtain any degree of accuracy. Schmitt[1] used 100 l of sea water to determine cobalt-60, zinc-65, and manganese-54 by a series of precipitations involving numerous manipulations. Silker and Rieck[2] operated a filtration–sorption system with many litres of sea water to obtain *in situ* measurements of manganese-54 and other isotopes in the Pacific Ocean. Agreement with a precipitation method, with manganese dioxide as scavenging agent[3,4], was unsatisfactory.

Davis *et al.*[5] used di(2-ethylhexyl)phosphoric acid (HDEHP) in hexane for the extraction of manganese-54 from 10-g samples of food ash. Two extractions were required, each using 150 ml of 60% HDEHP solution. The manganese was back-extracted into an EDTA buffer, which was washed twice with 70 ml of a 1.0% 8-hydroxyquinoline solution in chloroform before counting with a γ-ray spectrometer.

The present method was developed for the routine determination of manganese-54 in sea water contaminated by reactor effluent. An investigation of the use of HDEHP as an extractant for manganese(II) showed that good recovery could be obtained from 1 l of sea water with one extraction, when n-heptane was used as a diluent. After the organic phase had been stripped with 1.0 *M* hydrochloric acid, and evaporated to dryness, the manganese-54 with carrier was precipitated as manganese dioxide to improve the decontamination from other isotopes. Dissolution of the precipitate in 10 *M* hydrochloric acid allowed the sample to be counted in a γ-ray well-scintillation counter. The efficiency, for a 5-ml aliquot of standard manganese-54 solution, was 24%.

The overall recovery was determined colorimetrically after oxidation of manganese carrier to permanganate. Average recovery was 70–75%.

EXPERIMENTAL

Apparatus

An Ekco scintillation counter type N664A, with automatic scaler type M530F, a Hilger-Spekker absorptiometer, and a M.S.E. centrifuge were used.

Reagents

^{54}Mn standard solution. This was obtained from the Radioisotopes Standards Section, AAEC, as an aqueous solution of manganese(II) chloride in 0.1 *M* hydrochloric acid. It was diluted to give a working solution of about 5000 dis min^{-1} ml^{-1}

Manganese carrier stock solution. Dissolve 22.9 g of manganese(II) chloride in demineralized water and dilute to 1.0 l. Standardize by pipetting 2.0 ml into a 40-ml centrifuge tube. Add 0.2 ml of 10 *M* hydrochloric acid and 3 ml of 1.5 *M* diammonium hydrogenphosphate, then add ammonia solution to make the solution basic. Heat to boiling and let stand for 10 min. Filter into a weighed sintered glass crucible, and wash with 0.1 *M* ammonia solution and then with alcohol. Dry at 110° and weigh as $MnNH_4PO_4 \cdot H_2O$.

Manganese carrier working solution (ca. 0.5 mg Mn^{2+} ml^{-1}). Dilute 25 ml of standardized stock solution to 500 ml.

Buffer solution. To 240 g of sodium acetate trihydrate, add about 400 ml of demineralized water and stir to dissolve. Add 100 ml of glacial acetic acid and dilute to 1.0 l with demineralized water.

Di(2-ethylhexyl)phosphoric acid (HDEHP). Use a 40% solution in n-heptane.

Bismuth hold-back carrier (10 mg Bi^{3+} ml^{-1}). Dissolve 2.3 g of bismuth nitrate pentahydrate in 5 ml of 15 *M* nitric acid. Dilute to 100 ml with demineralized water.

Cerium hold-back carrier (10 mg Ce^{4+} ml^{-1}). Dissolve 2.9 g of cerium(IV) sulphate tetrahydrate in 5 ml of 36 *M* sulphuric acid. Dilute to 100 ml with demineralized water.

Chromium hold-back carrier (10 mg Cr^{6+} ml^{-1}). Dissolve 3.1 g of sodium chromate in 50 ml of demineralized water and dilute to 100 ml.

Recommended procedure

Collect sea-water samples in polythene containers to which hydrochloric acid has been added. Allow for about 2 ml of 10 *M* hydrochloric acid per litre.

To a 1.0-l aliquot of sea water add 5.0 ml of manganese carrier working solution, evaporate to about 300 ml, and cool. Transfer to a 500-ml separating funnel and add 2.0 ml of bismuth, 1.0 ml of cerium, and 1.0 ml of chromium hold-back carrier solutions. Then add 2.0 ml of aqueous 10% (w/v) ascorbic acid solution, 50 ml of buffer solution, and 100 ml of 40% HDEHP solution. Shake for 2 min and allow to settle. Discard the aqueous phase.

Add 50 ml of 1.0 *M* hydrochloric acid to the organic phase, shake for 2 min, and allow to settle. Run the aqueous phase into a 100-ml beaker and discard the organic phase.

Evaporate to dryness, add 20 ml of 15 *M* nitric acid, cover with a watch glass and heat to boiling until all brown fumes are expelled and the solution is almost colourless. Cool.

Add about 0.5 g of solid potassium chlorate, cover, and heat to near boiling to precipitate manganese dioxide. Digest for 10 min, and then cool.

Transfer to a 40-ml centrifuge tube, stir with a glass rod, and centrifuge for 5 min. Discard the supernatant liquid and wash the precipitate with 15 ml of demineralized water. Centrifuge and discard the supernate.

Add 3 ml of 10 *M* hydrochloric acid to dissolve the precipitate, then transfer to a 5-ml graduated counting tube, make up to the mark, mix, and count in a γ-ray well-scintillation counter.

After counting, transfer a 2.0-ml aliquot to a 100-ml beaker, add 2.5 ml of 36 *M* sulphuric acid and evaporate to fumes. Cool, add 2.5 ml of syrupy phosphoric acid, and dilute to about 40 ml with demineralized water. Add about 0.1 g of potassium periodate, cover, and heat to boiling for 20 min. Cool, transfer to a 50-ml volumetric flask and make up to the mark with demineralized water. Measure the absorbance at 525 nm in a 1-cm cell.

DISCUSSION

In environmental surveys carried out to determine whether sea water has been contaminated with reactor effluent, it is often necessary to do radiochemical analyses to determine the nature and amounts of the various isotopes present. It is desirable that the methods used be rapid and suitable for routine laboratory operation, and that the sample volumes required for the determination of low levels of radioisotopes are not excessive.

The analysis for ^{54}Mn in the environment, if carried out by γ-ray spectrometry alone, is difficult because of low efficiency and high counter background which limit the sensitivity of the method. To overcome this handicap, very large sample aliquots are normally used, combined with heavy shielding to reduce the background count.

The method described here is designed for routine analysis, with 1-l aliquots of sea water and a simple well-scintillation counter. For a counting time of 4 h, and a background of about 400 c.p.m., the minimum detectable limit is less than $1.0 \cdot 10^{-8}$ μCi ml^{-1}. This is well within the limit of $1.0 \cdot 10^{-7}$ μCi ml^{-1} for ^{54}Mn set down by the International Committee for Radiological Protection for estuarine water.

The only other isotope of manganese likely to be found in reactor effluent is ^{56}Mn, with a half-life of 2.6 h. By setting the sample aside for 24 h, interference from this source can be avoided.

Davis *et al.*[5] investigated six diluents for HDEHP, before choosing hexane because it gave better phase separation. HDEHP is used in this laboratory for ^{90}Sr analysis[6] with n-heptane as a diluent, and the extraction of ^{54}Mn from sea water was therefore investigated with the same diluent.

Experiments with 500 ml of sea water and 50 ml of 40% HDEHP in n-heptane showed that over 90% of ^{54}Mn was extracted in the pH range 3.3–6.0. Phase separation was satisfactory, but deteriorated at higher pH values. Increasing the HDEHP concentration yielded only a small increase in extraction, so a 40% solution was used for all further work.

To obtain an equilibrium pH suitable for extraction it was necessary to

TABLE I

DECONTAMINATION FACTORS FOR VARIOUS RADIONUCLIDES

Radionuclide	*Decontamination factor*	*Radionuclide*	*Decontamination factor*
^{133}Ba	> 1000	^{131}I	> 1000
^{207}Bi	> 100[a]	^{99}Mo–^{99}Tc	> 1000
^{144}Ce	> 1000[b]	^{22}Na	> 4000
^{60}Co	> 5000	^{106}Ru	> 5000
^{51}Cr	> 750[c]	^{90}Sr–^{90}Y	> 20000
^{137}Cs	> 2000	^{238}U	> 2000
^{203}Hg	> 2000	^{95}Zr–^{95}Nb	> 4000

[a] 20 mg of Bi^{3+} added as hold-back carrier.
[b] 10 mg of Ce^{4+} added as hold-back carrier.
[c] 10 mg of Cr^{6+} added as hold-back carrier.

TABLE II

EFFECT OF VARIOUS ELEMENTS ON ^{54}Mn RECOVERY FROM 500 ml OF SEA WATER

(10 mg of each metal ion was added; 500 mg of ascorbic acid, nitrate or sulphate were added, and 200 tartaric acid)

Foreign ion	*Added as*	*Carrier recovery (%)*	*^{74}Mn recovery (%)*	*Foreign ion*	*Added as*	*Carrier recovery (%)*	*^{54}Mn recovery*
Al^{3+}	$AlCl_3$	70.6	99.9	Ni^{2+}	$NiSO_4$	74.0	100.0
As^{3+}	As_2O_3	69.2	99.1	Sb^{3+}	$SbCl_3$	74.3	100.3
Ba^{2+}	$BaCl_2$	76.2	97.1	Sc^{3+}	Sc_2O_3	76.2	100.5
Bi^{3+}	$Bi(NO_3)_3$	71.3	98.5	Si^{4+}	SiO_2	79.7	101.7
Ca^{2+}	$CaCl_2$	74.2	99.6	Sr^{2+}	$SrCl_2$	75.3	99.9
Co^{2+}	$Co(NO_3)_2$	66.2	99.4	Te^{4+}	K_2TeO_3	76.4	100.7
Cr^{3+}	$CrCl_3$	77.6	100.8	Th^{4+}	$Th(NO_3)_4$	73.6	100.4
Cs^{+}	CsCl	70.4	100.8	U^{6+}	$UO_2(NO_3)_2$	77.2	99.2
Cu^{2+}	$Cu(NO_3)_2$	69.1	101.0	V^{5+}	Na_3VO_4	77.3	100.7
F^{-}	NH_4F	75.0	100.0	Y^{3+}	$Y(NO_3)_3$	77.6	103.5
Fe^{3+}	$FeCl_3$	73.4	99.2	Zn^{2+}	$ZnCl_2$	78.5	99.9
Hg^{2+}	$HgCl_2$	69.2	101.8	Zr^{4+}	$Zr(SO_6)_2$	71.0	102.0
La^{3+}	$La(NO_3)_3$	75.5	102.3	Ascorbic acid		74.3	101.0
Mg^{2+}	$MgCl_2$	70.4	96.7	Nitrate	$NaNO_3$	71.8	102.0
Mo^{6+}	$(NH_4)_6Mo_7O_{24}$	73.6	98.7	Sulphate	Na_2SO_4	80.8	101.3
Pb^{2+}	$Pb(NO_3)_2$	75.6	99.5	Tartaric acid		69.9	101.4
Nb^{5+}	NbF_5	75.9	99.3				

increase the pH of the sea water to counteract the acid release from HDEHP. Consequently, precipitation occurred before extraction. This was avoided by using a sodium acetate–acetic acid buffer to obtain an equilibrium pH of 3.8, and this method was preferable to neutralization of the HDEHP.

The addition of 20 mg of manganese(II) carrier had no effect on the extraction. Ascorbic acid, which was added to ensure that manganese was in the manganese(II) form, which was essential for extraction, did not interfere.

Extraction from volumes of sea water larger than 500 ml showed that more HDEHP was necessary to maintain a high recovery. Experiments indicated that 100 ml of 40% HDEHP was necessary to obtain over 90% extraction from a 1-l aliquot which had been evaporated to 300 ml.

Stripping the organic phase with 1.0 *M* hydrochloric acid carried most of the ^{54}Mn with manganese(II) carrier into the aqueous phase, but decontamination factors for some radionuclides were unsatisfactory. However, the precipitation of added Mn^{2+} carrier from 15 *M* nitric acid as manganese dioxide was very selective. Good decontamination from most of the radioisotopes possibly present in reactor effluent was obtained (Table I). Holdback carriers were necessary for ^{207}Bi, ^{51}Cr and ^{144}Ce. The presence of 10-mg quantities of various ions did not influence the extraction (Table II).

The precipitated manganese dioxide was dissolved, counted, and then oxidised to permanganate for colorimetric determination of the overall recovery. The average recovery was 73%.

TABLE III

RECOVERY FROM 1.0 l OF SEA WATER SPIKED WITH ^{54}Mn[a] AND HELD FOR SIX WEEKS IN POLYTHENE BOTTLES UNDER VARYING CONDITIONS

Acid added	*Manganese added (mg)*	*Mn^{2+} carrier recovery (%)*	*^{54}Mn recovery (%)*
0	0	72.0[b]	19.8
0	2.5	57.4	96.2
0	5.0	62.8	100.6
10 *M* HCl, 2 ml	0	78.0[b]	98.7
10 *M* HCl, 5 ml	0	71.8[b]	99.3
15 *M* HNO_3, 2 ml	0	68.0[b]	99.8
15 *M* HNO_3, 5 ml	0	71.8[b]	96.8
11 *M* $HClO_4$, 2 ml	0	73.5[b]	98.0
11 *M* $HClO_4$, 5 ml	0	75.9[b]	104.5

[a] 5200 d.p.m.
[b] 2.5 mg Mn carrier added before extraction.

The determination of ^{54}Mn in samples of sea water spiked with a standard solution and left for six weeks in polythene bottles under various conditions showed that the method was quantitative (Table III).

The time taken for the analysis, excluding counting, was about 6 h for six samples.

SUMMARY

A solvent-extraction procedure for the determination of manganese-54 in sea water is described. The water (1 l) is buffered to pH 3.8, and extracted with di(2-ethylhexyl)phosphoric acid in n-heptane. The manganese-54 with carrier is stripped from the organic phase, and eventually precipitated as the dioxide; the precipitate is dissolved in hydrochloric acid and counted in a scintillation counter. Chemical recovery is determined colorimetrically. Samples spiked with

manganese-54 showed quantitative recovery from 1 l of sea water with a typical recovery of 70–75% of carrier.

The method is applicable to sea water containing many other ions, and decontamination factors for a wide range of radionuclides are reported. The limit of detection is *ca.* 10^{-8} μCi ml^{-1}.

ZUSAMMENFASSUNG

Es wird ein Extraktionsverfahren für die Bestimmung von Mangan-54 in Meerwasser beschrieben. Das Wasser (1 l) wird auf pH 3.8 gepuffert und mit Di-(2-äthylhexyl)-phosphorsäure in n-Heptan extrahiert. Das Mangan-54 mit Träger wird aus der organischen Phase reextrahiert und schliesslich als Dioxid gefällt; der in Salzsäure wieder aufgelöste Niederschlag wird mit einem γ-Szintillationszähler gemessen. Der chemisch erfasste Anteil wird kolorimetrisch bestimmt. Proben, die mit Mangan-54 versetzt worden waren, zeigten, dass dieses aus 1 l Meerwasser quantitativ erfasst wird bei einer typischen Wiedergewinnung von 70–75% vom Träger. Die Methode ist auf Meerwasser mit einem Gehalt an vielen anderen Ionen anwendbar; die Dekontaminationsfaktoren für eine ganze Reihe von Radionukliden werden angegeben. Die Nachweisgrenze ist *ca.* 10^{-8} μCi ml^{-1}.

REFERENCES

1 D. E. Schmitt, *Dtsch. Hydrogr. Z.*, 1 (1966) 28.
2 W. D. Silker and H. E. Rieck, *U.S.A.E.C. Rep. BNWL-1051, Part 2*, 1969.
3 J. Rosinski and C. T. Nagamoto, *Ind. Eng. Chem.*, 52 (1960) 429.
4 W. B. Silker, *U.S.A.E.C. Rep. HW 73337*, 1962.
5 S. Davis, A. Arnold and A. Jordan, *J. Radioanal. Chem.*, 2 (1969) 161.
6 W. W. Flynn, *Aust. At. Energy Comm. Rep. AAEC/TM421*, 1967.

Analytica Chimica Acta, 67 (1973) 135–144

STUDIES WITH DITHIZONE

PART XXX*. COMPLEXES OF METALS WITH S-METHYLDITHIZONE AND THE METHYLATION OF METAL DITHIZONATES

H. M. N. H. IRVING, A. H. NABILSI and S. S. SAHOTA

Department of Inorganic and Structural Chemistry, The University of Leeds, Leeds LS2 9JT (England)

(Received 11th January 1973)

S-Methyldithizone (3-methylmercapto-1,5-diphenylformazan, HMeDz; I) was originally prepared by Irving and Bell[1] in the hope of deciding by the classical procedure which of the two bands (at *ca.* 450 and 620 nm) in the visible spectra of solutions of dithizone in organic solvents should be ascribed to the thiol form (IIa) and which to the thioketone form (IIb).

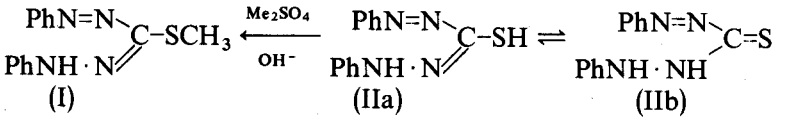

Unfortunately, the solution spectrum of (I) did not comprise a single band; indeed, a freshly prepared solution has two bands at 270 and 550 nm ($\varepsilon = 12{,}250$ in chloroform) and it undergoes a first-order photochemical isomerization to a form with three bands at 280, 420 ($\varepsilon = 17{,}750$) and 540 nm, with a concomitant change in colour from permanganate pink to yellow[2–4].

Since S-methyldithizone does not yield extractable metal complexes under conditions where dithizone itself is effective, it follows that the formation of extractable complexes must involve the replacement of the thiol proton of (IIa) rather than that of an imino-hydrogen in (IIb), as envisaged by Fischer[5]. However, red crystals of m.p. 144° were formed on mixing solutions of S-methyldithizone and mercury(II) acetate in acetone–ethanol; the metal : ligand ratio was not stoicheiometric (1 : 1.7) and the loose adduct was completely dissociated into its components on dissolution in chloroform. Similar addition compounds to which no definite molecular formulae could be ascribed, were formed with copper(II) and palladium(II)[1].

We now find that, under different conditions, stoicheiometric compounds can be formed from several metals in which the reagent acts as a monobasic acid, a cation replacing the imino-hydrogen of (I). In certain cases (notably with nickel(II) and palladium(II)), the same compounds can be obtained by methylating the corre-

---

* *J. Inorg. Nucl. Chem.*, 34 (1972) 109 and *Anal. Chim. Acta*, 65 (1973) 202 are regarded as Parts XXVIII and XXIX.

sponding metal dithizonates. Since dithizone does not itself methylate under comparable conditions, this provides an example of the now familiar increase in the reactivity of coordinated ligands[6].

The complexes formed by treating S-methyldithizone with a metallic salt in ethanol and in the presence of sodium acetate fall into two categories. With the chlorides of copper(II), mercury(II) and phenylmercury(II), 1:1 complexes are formed in which the imino-hydrogen of the ligand is replaced to give deeply coloured chelates which can be formulated as (III):

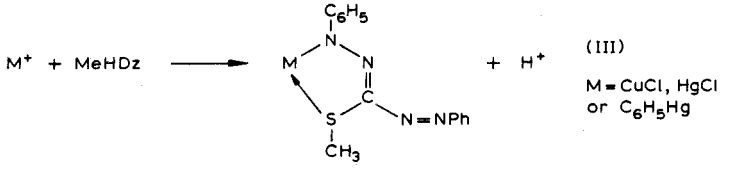

With nickel(II) the reaction with S-methyldithizone proceeds further to give a 1:2 complex which can be formulated as (IV). Cobalt(II), manganese(II) and zinc(II) did not form similar complexes under any conditions, and no definite complexes were obtained from copper(II) or mercury(II) acetates or nitrates.

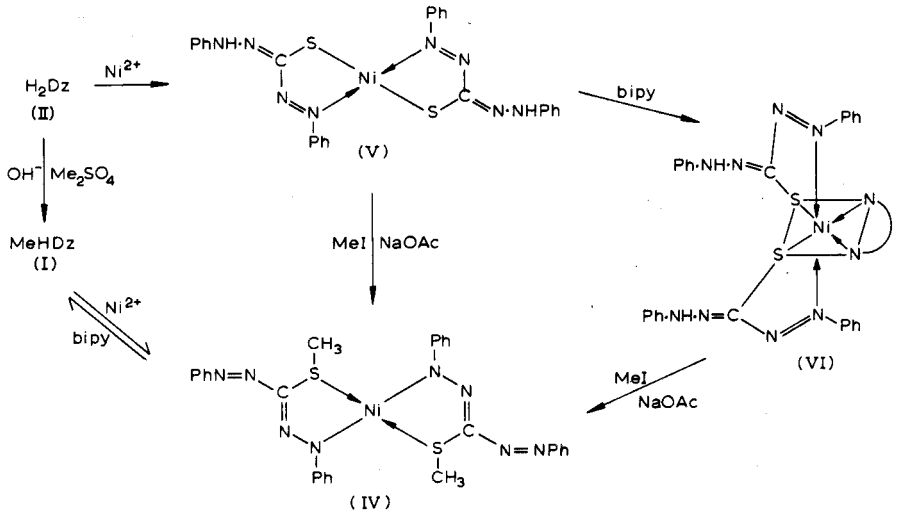

Although insoluble in water the S-methyldithizonate complexes dissolve in most organic solvents. Typical absorption parameters are listed in Table I (*cf.* Fig. 1). It is very likely that the copper and mercury chlorocomplexes (as III) are dimerized through metal–chlorine bridges.

The nickel(II)–S-methyldithizone complex

The bis-chelate (IV) of nickel(II) forms glistening black crystals (m.p. 235°) which dissolve in chloroform to give a yellow solution with peaks at 290 and 440 nm (ε_{max} 33,000 and 12,200) as shown in Fig. 1, curve 1. There is no change in spectrum after 4 days if the solution is kept in the dark. Slow changes which

TABLE I

ABSORPTION MAXIMA AND MOLAR ABSORPTIVITIES OF S-METHYLDITHIZONE ($C_{14}H_{14}N_4S$) AND ITS METAL COMPLEXES IN CHLOROFORM

Compound	*Absorption maxima*[a]		
$C_{14}H_{14}N_4S$ (I)			
Pink form	270 (18,500)	550 (12,250)	
Yellow form	280 (13,250)	420 (17,750)	540 (5,800)
$(C_{14}H_{13}N_4S)CuCl$ (III)	275 (13,200)		520 (21,300)
$(C_{14}H_{13}N_4S)HgCl$ (III)	262 (18,000)	430 (22,200)	
$(C_{14}H_{13}N_4S)HgC_6H_5$ (III)	260 (14,700)	425 (20,900)	610
$(C_{14}H_{13}N_4S)_2Ni$ (IV)	290 (33,000)	440 (12,200)	
$(C_{14}H_{13}N_4S)_2Pd$ (as IV)	270 (29,500)	380 (20,500)	490 (60,500)

[a] Molar absorptivity in parentheses. The absorption spectra of S-methyldithizone complexes of nickel(II), palladium(II) and chloromercury(II), are shown in Fig. 1, curve 1, Fig. 2, curve 2, and Fig. 3, curve 3, respectively.

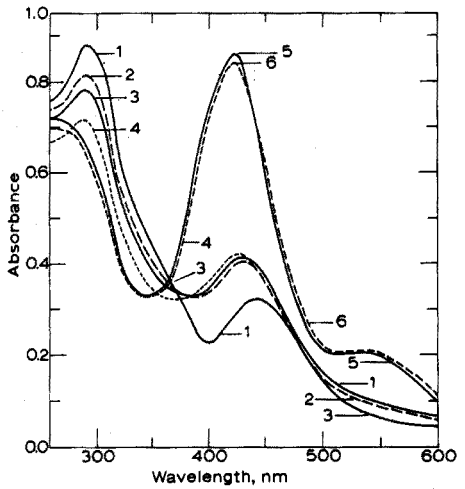

Fig. 1. Changes in the absorption spectrum of nickel(II) bis-S-methyldithizonate in chloroform. (1) Spectrum immediately after preparation and after 4 days in the dark; (2, 3 and 4) spectra obtained by heating the original solution (curve 1) for 1 h and then standing for 1, 14 and 20 h, respectively; (5) spectrum obtained by heating the original solution (curve 1) for 7 h; (6) spectrum of the same sample after standing for 2 days and also that obtained by adding a drop of concentrated hydrochloric acid to solution 1.

take place when the solution is allowed to stand in the light, could be accelerated by heating (Fig. 1, curves 2–6). The colour changes from yellow to red and the peak at 290 nm disappears while that at 440 nm is replaced by a much more intense absorption peak at 430 nm and a subsidiary maximum appears at 540 nm. The final spectrum is identical with that of the yellow form of S-methyldithizone (I) and is identical with that obtained by adding a drop of concentrated hydrochloric acid to a solution of the original nickel complex or by treating a pink solution of S-methyldithizone with a catalytic trace of acid (Fig. 1, curve 6).

There are many examples of the enhanced reactivity of sulphur atoms coordinated to a metal. The reactions of coordinated mercaptide groups with alkyl halides was first studied by Blomstrand[7]. Later, Ewens and Gibson[8] demonstrated the reaction of diethyl-β-mercaptoethylaminogold(II) with methyl iodide and ethylbromide:

$$Et_2Au(NH_2 \cdot CH_2 \cdot CH_2S) + RX \rightarrow [Et_2Au(NH_2 \cdot CH_2 \cdot CH_2S\text{–}R)X]$$

Busch and Jicha[9] reported detailed studies of the reactions of methyl iodide and benzyl halides with β-mercaptoethylamine complexes of nickel(II) and palladium(II) in dimethylformamide solvent.

It was found that dithizone (II) can be recovered unchanged after heating in ethanol under reflux with a large excess of methyl iodide, even in the presence of a large excess of sodium acetate. In contrast, there is an obvious change in colour when a solution of nickel(II) dithizonate (V) is heated with methyl iodide in the presence of a base such as sodium acetate, and the bis-chelate (IV) can be separated from the reaction mixture in excellent yield. The presence of sodium acetate was found to be essential: in its absence the components were recovered unchanged.

The preparation of adducts of nickel(II) dithizonate with heterocyclic nitrogen bases was first reported by Math and Freiser[10]. The analytical potential of the adduct with 1,10-phenanthroline was reported by Freiser *et al.*[11,12] and the crystal structure of the adduct with 2,2′-bipyridyl, $Ni(HDz)_2 \cdot bipy$, was determined by Math and Freiser[13], who showed that the two dithizone residues were coordinated through sulphur atoms in the *cis*-position as shown in (VI). The location of the iminohydrogen atom was not determined, though at the stage of refinement reached ($R = 13.6\%$) the evidence favours a double bond between the nitrogen atoms in the chelate ring as shown in (VI).

Attempts to methylate this octahedral complex (VI) gave nickel(II) bis-S-methyldithizonate (IV) as the sole product. This result could be explained if S-methylation of the dithizone residues had produced a situation in which, for steric reasons, the bipyridyl could no longer be accommodated. Certainly an attempt to synthesize an adduct of bipyridyl with (IV) under conditions where nickel dithizonate (V) and bipyridyl react very rapidly failed completely. When attempts were made to force the reaction by heating the S-methyldithizonate(IV) with excess of bipyridyl, there were successive changes in the absorption spectrum which showed that (IV) had been decomposed to give (presumably) the colourless stable cation $Ni(bipy)_3^{2+}$, while the S-methyldithizone (II) set free had isomerized under the influence of excess base to the yellow form. Since heating methyl iodide and the adduct (VI) produced no reaction unless sodium acetate was present, it seems to be likely that the large excess of methyl iodide first alkylates the bipyridyl to give the bication $[bipy(CH_3)_2]^{2+}$ which would no longer be able to chelate, leaving nickel dithizonate (V) which has been shown to methylate only in the presence of sodium acetate.

The palladium(II)–S-methyldithizone complex

Palladium(II) resembles nickel(II) in forming a bis-chelate (as IV) with S-methyldithizone. This consisted of fine greenish needles which gave a yellow

solution in chloroform (λ_{max} 270, 380 and 490 nm with ε_{max} 29,500, 20,500 and 60,500, respectively), in which it is more soluble than the parent dithizonate. Unlike the corresponding nickel complex (IV), its solution is stable to light.

When the dark green solution of palladium bis-dithizonate (as V) was heated under reflux in ethanol for 3 h with a slight excess of methyl iodide and sodium acetate, a brownish-red solution resulted which deposited on concentration a violet solid admixed with some light green crystals. On standing, the mother liquor deposited more green crystals which were identified as pure palladium S-methyldithizonate (as IV) by spectral and elemental analysis. The violet solid proved to be the less soluble, unchanged palladium dithizonate (as V), and despite many variations in the reaction conditions, it did not prove possible to achieve complete methylation and a homogeneous product. On chromatography on alumina, the S-methyldithizonate travelled faster than the parent palladium dithizonate so that separation was possible. However, chromatography of crude reaction mixtures revealed the presence of another component, possibly the partially methylated product Pd(HDz)(MeDz). In this connection, it is noteworthy that the spectrum of an equimolar solution of pure palladium dithizonate, $Pd(HDz)_2$, and of pure palladium S-methyldithizonate, $Pd(MeDz)_2$, did not exactly correspond to the spectrum calculated from those of the pure components (Fig. 2). This surprising result suggested the possibility of ligand exchange leading to a greater or less amount of the intermediate species, Pd(HDz)(MeDz). The possibility of the reaction between methyl iodide and (V) leading to a salt or compound with coordinated iodine, was excluded by elemental analyses; indeed, the spectrum of palladium S-methyldithizonate in chloroform (Fig. 2, curve 2) was unchanged by the addition of excess of methyl iodide both in the cold and after heating with or without sodium acetate.

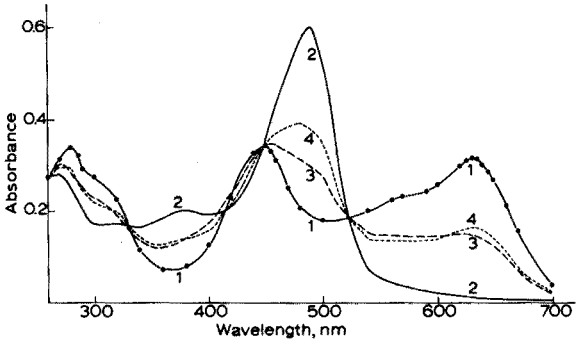

Fig. 2. The absorption spectra in chloroform of $5 \cdot 10^{-6}$ *M* solutions of palladium dithizonate, palladium S-methyldithizonate and their admixture. (1) Palladium dithizonate; (2) palladium S-methyldithizonate; (3) equimolar mixture of palladium dithizonate and palladium S-methyldithizonate; (4) spectrum of mixture computed from curves 1 and 2.

Attempted methylation of chloromercury(II) dithizonate

No reaction took place even after 3 h when chloromercury(II) dithizonate[14], ClHg(HDz), was heated with methyl iodide and sodium acetate in chloroform solution. In ethanol, however, there was a striking change of colour from orange-yellow to dark red and the bands at 260 and 485 nm ($\varepsilon = 37{,}100$) (Fig. 3, curve 1)

gave place to bands of lower intensity at 425 and 480 nm (Fig. 3, curve 2) which were clearly distinguishable from the spectrum of chloromercury(II) S-methyldithizonate (Fig. 3, curve 3). On heating with excess of methyl iodide the spectrum became clearly identified with that of the yellow form of S-methyldithizone (II; λ_{max} 420 and 540 nm); on the addition of water, this substance separated as a black solid whose composition was established by elemental analysis. Since dithizone alone cannot be methylated, it must be supposed that the change ClHg(HDz) to ClHg(MeDz) was followed by the replacement of chlorine by acetate to give $CH_3 \cdot CO \cdot O \cdot Hg(MeDz)$ and thence $Hg(O \cdot CO \cdot CH_3)_2$ and MeHDz. The impossibility of making a stable complex of mercury(II) acetate and S-methyldithizone (II) has already been mentioned, and the special stability of the complexes ClHg(MeDz) and ClCu(MeDz) must be due to their existence as bridged dimers.

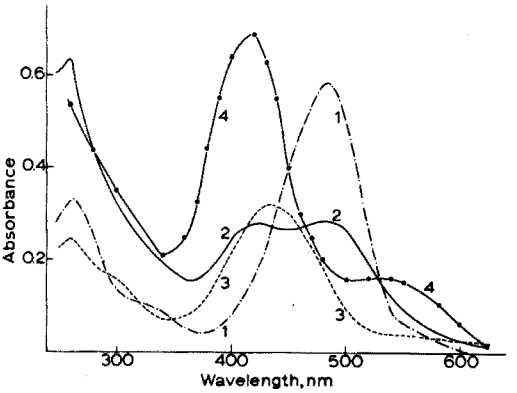

Fig. 3. The attempted methylation of chloromercury(II) dithizonate. (1) Spectrum of $1.584 \cdot 10^{-5}$ *M* chloromercury(II) dithizonate in chloroform; (2) spectrum after heating for 1 h with methyl iodide; (3) spectrum of $1.488 \cdot 10^{-5}$ *M* chloromercury(II)–S-methyldithizonate; (4) spectrum after heating the mixture (curve 2) further with excess sodium acetate and methyl iodide: also that of the solid obtained.

EXPERIMENTAL

Preparation of complexes of S-methyldithizone

(a) From mercury(II) chloride. S-Methyldithizone (0.5 g) in ethanol (100 ml) was mixed with a solution of mercury(II) chloride (3 g) in ethanol (50 ml), and sodium acetate (1 g) was added. After stirring for 10 min, distilled water (200 ml) was added slowly and the precipitated complex was collected and washed free from mercury(II) ions. The residue was dried over calcium chloride *in vacuo* and taken up in chloroform, and the complex was precipitated as dark blue-black needles by adding light petroleum (60–80°). Yield 0.82 g. (Found: 33.2% C, 2.5% H, 11.0% N, 6.6% S, 6.5% Cl, 38.9% Hg; $C_{14}H_{13}N_4SHgCl$ requires 33.3% C, 2.6% H, 11.1% N, 6.3% S, 7.0% Cl, 39.7% Hg.)

(b) From phenylmercury(II) chloride. The complex was prepared similarly from S-methyldithizone (0.2 g) and phenylmercury(II) chloride (0.8 g) as a deep

blue solid (0.35 g). (Found: 43.8% C, 3.3% H, 10.4% N, 6.1% S, 36.1% Hg; $C_{14}H_{13}N_4SHgC_6H_5$ requires 43.9% C, 3.3% H, 10.2% N, 5.9% S, 36.7% Hg.)

(c) From copper(II) chloride. S-Methyldithizone (0.2 g) in ethanol (70 ml) was well stirred and copper(II) chloride (0.7 g) and sodium acetate (1 g) in water (20 ml) were added dropwise. After 30 min, water (150 ml) was added slowly, and the complex (0.085 g) separated as a black crystalline solid. (Found; 45.7% C, 3.6% H, 14.9% N, 8.8% S, 9.5% Cl, 17.4% Cu; $C_{14}H_{13}N_4SCuCl$ requires 45.6% C, 3.6% H, 15.2% N, 8.7% S, 9.6% Cl, 17.3% Cu.)

(d) From nickel(II) acetate. Nickel acetate (0.4 g), S-methyldithizone (0.2 g) and anhydrous sodium acetate (0.2 g) were heated under reflux with absolute ethanol (50 ml) for 2 h. When cold the black crystalline residue was collected, washed in turn with ethanol, *M* hydrochloric acid, ethanol and ether, and dried *in vacuo* over calcium chloride (yield: 0.155 g, m.p. 235°). (Found: 56.45% C, 4.45%H, 19.0% N, 10.6% S; $(C_{14}H_{13}N_4S)_2Ni$ requires 56.3% C, 4.4% H, 18.8% N, 10.7% S.)

(e) From palladium(II) chloride. Palladium chloride dihydrate (0.076 g), S-methyldithizone (0.152 g) and sodium acetate (0.2 g) were heated in ethanol (100 ml) under reflux for 3 h. The complex that separated as well formed greenish crystals was isolated as described for the nickel complex. (Found: 52.15% C, 4.1% H, 17.5% N; $(C_{14}H_{13}N_4S)_2Pd$ requires 52.1% C, 4.1% H, 17.4% N.)

Preparation of nickel(II) dithizonate

A filtered solution of dithizone (0.4 g) in dilute isopiestic ammonia (100 ml) was brought to pH 9.25 by the addition of hydrochloric acid and mixed with a solution of nickel(II) chloride (0.19 g) in water; nickel dithizonate separated as a violet precipitate which was collected and dissolved in chloroform (100 ml). After concentration to a syrupy consistency, ethanol (40 ml) was added and the mixture was stirred mechanically for 3 h. The greenish black microcrystalline product was collected, washed with ethanol and dried *in vacuo* over anhydrous magnesium perchlorate. (Found: 54.6% C, 3.9% H, 19.5% N; $Ni(C_{13}H_{11}N_4S)_2$ requires 54.9% C, 3.9% H, 19.7% N.) A solution of this complex, $Ni(HDz)_2$, in chloroform was violet-blue and the absorption spectrum showed three peaks at 290, 480 ($\varepsilon = 26{,}000$) and 560 nm.

Methylation of nickel(II) dithizonate

Nickel dithizonate (0.1 g) suspended in absolute ethanol (150 ml) was heated under reflux with a slight excess of methyl iodide (0.2 ml) and sodium acetate (0.2 g). On cooling, the nickel complex of S-methyldithizone separated as a black crystalline solid (yield, *ca.* 80%) and was purified as described above. The identity with the product synthesized directly from nickel acetate and S-methyldithizone was confirmed by comparison of absorption spectra and by analysis. (Found: 56.2% C, 4.45% H, 19.05%, N, 10.6% S; $(C_{14}H_{13}N_4S)_2Ni$ requires 56.3% C, 4.4% H, 18.8% N, 10.7% S.)

If the sodium acetate is omitted, no reaction takes place and the spectrum of the original nickel dithizonate remains unaltered. In many cases, the use of dimethylformamide is said to promote methylation even in the absence of added base[6,9]. Used here in place of ethanol only uncrystallizable oils resulted.

Preparation of palladium dithizonate

Palladium(II) dithizonate separated as a violet-blue solid on concentrating the deep green organic phase obtained after equilibrating palladium(II) chloride dihydrate (0.104 g) in 0.4 *M* hydrochloric acid (100 ml) with dithizone (0.198 g) in chloroform (150 ml) for 3 h. The product was recrystallized from chloroform and dried *in vacuo* over phosphorus pentoxide. (Found: 50.5% C, 3.6% H, 18.35% N; $C_{26}H_{22}N_8S_2Pd$ requires 50.6% C, 3.6% H, 18.15% N.)

Methylation of palladium dithizonate

A suspension of palladium dithizonate (0.05 g) in ethanol (150 ml) was heated under reflux for 3 h with anhydrous sodium acetate (0.2 g) and a slight excess of methyl iodide (0.2 ml). The colour changed from dark green to brownish-red and after concentration a violet-red solid admixed with green crystals separated. After standing for 3 days, the mother liquors deposited a green solid identified as palladium bis(S-methyldithizonate) (as IV) by its absorption spectrum (λ_{max} 270, 380 and 490 nm) and elemental analysis.

Spectrum of a synthetic mixture of $Pd(HDz)_2$ and $Pd(MeDz)_2$

Solutions (10^{-5} *M*) in chloroform of purified palladium dithizonate and of pure palladium S-methyldithizonate were separately prepared. Portions (10 ml) of each were mixed to give a violet-blue solution, whose spectrum showed three peaks at 270, 460 and 630 nm (Fig. 2, curve 3). The spectra of the separate components were also recorded after dilution with an equal volume of chloroform (curves 1 and 2). The calculated absorption spectrum for the mixture (Fig. 2, curve 4) assuming no interaction was not coincident with the experimental curve. All spectra were measured in matched 1-cm silica cells with a Unicam SP 500 spectrophotometer.

Changes in the absorption spectrum of nickel(II)–bis(S-methyldithizonate)

A solution (25 ml of $2.645 \cdot 10^{-5}$ *M*) of the nickel complex (IV) in chloroform was made up to 50 ml after standing in the dark or heating and standing for various times as detailed in the text and in the legend to Fig. 1.

The action of methyl iodide on the adduct of 2,2'-bipyridyl with primary nickel dithizonate (VI)

A suspension of the adduct (VI) (0.1 g) prepared according to Math and Freiser[10] was heated in ethanol (100 ml) under reflux for 3 h with excess of methyl iodide (0.3 ml) and sodium acetate (0.3 g). On cooling a black solid separated which was identified as nickel S-methyldithizonate (IV) by its absorption spectrum and elemental analysis.

Attempted methylation of chloromercury(II) dithizonate

The named complex[14] ClHg(HDz) was prepared by shaking dithizone (0.2 g) in chloroform (150 ml) with mercury(II) chloride (0.3 g) and potassium chloride (0.5 g) dissolved in water (200 ml) for 15 min. The complex separated as a red solid and was collected by centrifugation after rejecting the organic layer, washed with water and dried *in vacuo* over calcium chloride. (Found: 31.75% C, 2.3% H,

11.5% N, 6.45% S; ($C_{13}H_{11}N_4S$)HgCl requires 31.8% C, 3.2% H, 11.4% N, 6.5% S.)

When chloromercury(II) dithizonate (0.15 g) suspended in ethanol (100 ml) was heated under reflux for 3 h with anhydrous sodium acetate (0.2 g) and a slight excess of methyl iodide (0.2 ml), the colour changed from orange-yellow to dark red (Fig. 3). The spectrum suggested a mixture of products from an incomplete reaction. More sodium acetate and methyl iodide were added and the heating was continued; the final spectrum (Fig. 3, curve 4) corresponded to the yellow form of S-methyldithizone which could be isolated from the reaction mixture. No reaction occurred in chloroform.

SUMMARY

S-Methyldithizone (5-methylmercapto-1,5-diphenylformazan) reacts with the chlorides of copper(II), mercury(II) and phenylmercury(II) to give the 1:1 chelates [CuCl(MeDz), HgCl(MeDz) and C_6H_5Hg(MeDz)] and with nickel(II) and palladium(II) to give the 1:2 chelates, M(MeDz)$_2$. All these complexes are intensely coloured in chloroform solution. No complexes are formed from cobalt(II), manganese(II) or zinc(II) or from the nitrates or acetates of copper and mercury. Coordination increases the reactivity of the sulphur atom in dithizone. Whereas dithizone is unaffected by methyl iodide, nickel dithizonate, Ni(HDz)$_2$, gives Ni(MeDz)$_2$ when heated with methyl iodide in ethanol in the presence of sodium acetate; palladium dithizonate behaves similarly. The 1:1 adduct of nickel dithizonate with 2,2′-bipyridyl gave only Ni(MeDz)$_2$ on treatment with methyl iodide, and this complex would not form an adduct with bipyridyl. On standing in the light, Ni(MeDz)$_2$ reacted photochemically to give the yellow isomer of S-methyldithizone.

RÉSUMÉ

La S-méthyldithizone (5-méthylmercapto-1,5-diphénylformazan) réagit avec les chlorures de cuivre(II), mercure(II) et phénylmercure(II) pour donner les chélates 1:1 [CuCl(MeDz), HgCl(MeDz) et C_6H_5Hg(MeDz)] et avec nickel(II) et palladium(II) pour donner les chélates 1:2 M(MeDz)$_2$. Ces complexes dans le chloroforme sont très colorés. Aucun complexe n'est formé par le cobalt(II), le manganèse(II) ou le zinc(II) ou encore par les nitrates ou acétates de cuivre et de mercure. La coordination augmente la réactivité de l'atome de soufre dans la dithizone. La dithizone n'est pas affectée par l'iodure de méthyle; cependant Ni(HDz)$_2$ donne Ni(MeDz)$_2$ par chauffage avec l'iodure de méthyle dans l'éthanol en présence d'acétate de sodium. Le dithizonate de palladium se comporte de la même façon. A la lumière, Ni(MeDz)$_2$ se transforme photochimiquement en son isomère jaune, la S-méthyldithizone.

ZUSAMMENFASSUNG

S-Methyldithizon (5-Methylmercapto-1,5-diphenylformazan) reagiert mit den Chloriden von Kupfer(II), Quecksilber(II) und Phenylquecksilber(II) unter Bildung der 1:1-Chelate [CuCl(MeDz), HgCl(MeDz) und C_6H_5Hg(MeDz)] und mit Nickel-

(II) und Palladium(II) unter Bildung der 1:2-Chelate, $M(MeDz)_2$. Diese Komplexe sind alle in Chloroformlösung intensiv gefärbt. Mit Kobalt(II), Mangan(II) und Zink(II) sowie den Nitraten und Acetaten von Kupfer und Quecksilber werden keine Komplexe gebildet. Die Koordination erhöht die Reaktivität des Schwefelatoms im Dithizon. Während Dithizon durch Methyljodid nicht angegriffen wird, ergibt Nickeldithizonat, $Ni(HDz)_2$, beim Erwärmen mit Methyljodid in Äthanol in Gegenwart von Natriumacetat $Ni(MeDz)_2$; Palladiumdithizonat verhält sich ähnlich. Das 1:1-Addukt von Nickeldithizonat mit 2,2'-Bipyridyl ergab bei Behandlung mit Methyljodid nur $Ni(MeDz)_2$; dieser Komplex bildete mit Bipyridyl kein Addukt. Beim Stehenlassen im Licht reagierte $Ni(MeDz)_2$ photochemisch unter Bildung des gelben Isomeren von S-Methyldithizon.

REFERENCES

1 H. Irving and C. F. Bell, *J. Chem. Soc.*, (1954) 4253.
2 C. F. Bell, *D. Phil. Thesis*, Oxford, 1952.
3 W. Furguson, *B.Sc. Thesis*, Oxford, 1967, and refs. therein.
4 P. S. Pel'kis and R. G. Dubenko, *Proc. Acad. Sci. USSR*, 88 (1953) 999; 110 (1956) 615.
5 H. Fischer, *Angew. Chem.*, 47 (1934) 685.
6 *Cf.* Reactions of Coordinated Ligands, in *Adv. Chem.*, Ser. 37, Amer. Chem. Soc., 1963, pp. 125–141.
7 C. W. Blomstrand, *Z. Prakt. Chem.*, 38 (1888) 529.
8 R. V. G. Ewens and C. S. Gibson, *J. Chem. Soc.*, (1949) 431.
9 D. H. Busch and D. C. Jicha, *Inorg. Chem.*, 1 (1962) 878, 884.
10 K. S. Math and H. Freiser, *Anal. Chem.*, 41 (1969) 1682.
11 K. S. Math, K. S. Bhatki and H. Freiser, *Talanta*, 16 (1969) 412.
12 B. S. Freiser and H. Freiser, *Talanta*, 17 (1970) 540.
13 K. S. Math and H. Freiser, *Chem. Commun.*, (1970) 110.
14 G. B. Briscoe and B. G. Cooksey, *J. Chem. Soc.*, (1969) 205.

Analytica Chimica Acta, 67 (1973) 145–153

THE DETERMINATION OF SULPHUR BY COMBUSTION IN IRON, STEEL AND ASSOCIATED MATERIALS

T. S. HARRISON and R. J. SPIKINGS

Group Chemical Laboratories, British Steel Corporation, P.O. Box 1, Scunthorpe, Lincs (England)

(Received 12th March 1973)

The combustion method for the determination of sulphur has been in operation in iron and steelworks laboratories for many years[1,2]. As a rapid routine technique for a wide range of materials it has been of immeasurable benefit to the industry despite its non-stoichiometry and consequent dependence on standards prepared gravimetrically.

Considerable work has been done by individuals and by research committees, *e.g.* in B.C.I.R.A. and B.I.S.R.A. for iron, steel and "oxide" materials, and in B.C.R.A. for coke, and many modifications have been introduced, mainly to improve the yield of sulphur and, if possible, attain 100%.

The purpose of this paper is to describe developments with the modern high-frequency induction heating technique which eventually led to a simple innovation, appropriate for routine use, whereby complete recovery of sulphur can be obtained.

Methods of combustion

The combustion method may be classified according to the mode of heating, *viz.* resistance heating[1,2] or the more modern high-frequency induction heating[3]. In either case, combustion of a sulphur-bearing material in the oxygen stream yields a mixture of sulphur dioxide and trioxide. Oxidation of sulphur dioxide to the trioxide is reversible so that, with oxygen, an equilibrium is established in the apparatus. Sulphur trioxide is completely dissociated at 1300°, which is exceeded in the hot zone, but some reformation occurs subsequently in cooler parts of the tube. Here it may be absorbed by fine particles of iron(III) oxide, similarly formed in the hot zone, carried over and deposited, to form the stable sulphate.

With the optimal oxygen flow rate to restrict formation of the trioxide and transfer the gases to the absorbent rapidly, the final determination is usually based on absorption in water followed by an iodimetric titration of the sulphur dioxide, or absorption in hydrogen peroxide solution followed by an alkalimetric titration of sulphur dioxide and part of the sulphur trioxide; the remainder of the sulphur trioxide may be absorbed by iron oxide particles, condense in the tube or escape as a fine mist above the absorbent. In either case, the method is empirical and is based, for each material under examination, on the appropriate standard, prepared gravimetrically and similarly treated.

From these considerations, the problem of obtaining a 100% yield of sulphur

depends upon: (*i*) a good burn at a sufficiently high temperature to produce the maximum ratio of sulphur dioxide to sulphur trioxide, (*ii*) the retention of iron and other oxides in the boat or crucible, and (*iii*) the complete absorption of the oxides of sulphur. This applies to either mode of heating.

On this basis, routine methods involving resistance heating were developed some years ago and have given satisfaction in daily use for iron and steel, "oxide" materials and solid fuels. Condition (*ii*) is aided by preheating the sample before combustion, whilst (*iii*) is met by using standards. For coke, however, a British Standard method[4] based on the procedure of Beet and Belcher[5] is used in which the absorption conditions in hydrogen peroxide yield 100% of sulphur[6].

More recently, commercial apparatus comprising a high-frequency induction furnace linked to a manual titration device[3] (Leco Model 517) has become available. In this method, the sample is heated in a refractory crucible with a porous lid, the upward oxygen flow is automatically controlled, and an iodimetric or alkalimetric titration may be used. Iron, or sometimes nickel, must be present to act as a coupler in order to initiate combustion, and a little powdered tin may also be added. Preliminary work in this laboratory established suitable parameters for iron, steels and cokes, and also ferro-alloys, scale and manganese ore. Reproducibilities and accuracies, based on the appropriate standards, were satisfactory although yields on a range of BCS materials varied from 82 to *ca.* 100%. Yield tests on small calculated amounts of sulphur-bearing pure chemical reagents gave an average of 93.9%, and application of the factor 100/93.9 then gave results within routine tolerances of the standard values. Reproducibility tests, evaluated on this basis on further materials, were again very satisfactory[7]. However, solid fuels in the presence of a suitable coupling agent and accelerator showed a delay in combustion and gave erratic, unreliable results. Results for lime were also variable, and so the resistance heating method was retained for these materials.

Recently, an intensive investigation of the optimal conditions for combustion consistent with the available power and furnace geometry, as well as with retention of material within the crucible, has been made, and an attempt to trap all the sulphur liberated has eventually met with success.

Initially, to avoid the formation of sulphur trioxide, the sample was burned in a minimum of oxygen and the products swept away by nitrogen in a specially designed combustion unit. However, as the yield was not improved, it was concluded that the trioxide was still formed. Heating with iron and mixed metal oxides in a stream of nitrogen did not ignite the sample. Carbon dioxide was similarly unsuitable. To accelerate combustion, a downward oxygen flow was tried, but without success for this type of apparatus; this method was rejected mainly because the exit tubing and glassware had to be lengthened, and so presented a larger area for the deposition of trioxide mist. The conventional mode of combustion in a stream of oxygen flowing upwards over the crucible was therefore adopted.

The burn must be closely controlled to give maximum heating of the crucible and evolution of sulphur from a fluid melt, without ejection of any material or splashing on to the lid. Experiments in which the combustion of

various weights of sample and flux material was modified by Variac control of the plate (anode) current favoured the conditions given below. Vanadium pentoxide, prepared by heating ammonium vanadate, gave a burn more easily controlled than the commercial "vanodisc" which also contains iron.

Rinsing of the combustion and delivery tubes with the peroxide absorbent solution – to trap both sulphur dioxide and trioxide—after a run of tests, followed by titration with sodium borate solution showed an average loss of sulphur in the "plumbing" of *ca.* 5%.

Attempts were then made to prevent this by heating the delivery tube during the combustion, first with a hair dryer—which improved the sulphur yield—and secondly by winding with a coil of nichrome wire and heating electrically to 200°[8]. The improved yield was maintained and the sulphur loss was further reduced to 2% by introducing a curved delivery tube and heating to 350° in a coil insulated with asbestos tape. Further modification produced the apparatus shown in Fig. 1, which was specially designed and made of transparent silica. With the aid of a device to permit rinsing of the cooler tip of the tube, complete absorption and measurement of sulphur was achieved.

The recommended method is detailed below. It may also be applied to nickel-base alloys.

EXPERIMENTAL

Instrumental

To the Leco high frequency furnace, attach the apparatus shown in Fig. 1. This comprises a combustion tube and curved delivery tube, heated electrically to 350°, made in one piece of transparent silica and connected by a ground-glass joint to a silica bubbler which is immersed in the absorbent solution. The apparatus is well insulated with asbestos tape and string, as shown.

A glass "T" piece in the oxygen supply line carries a sleeve-operated safety pipette which provides a means of rinsing the extreme portion "A" of the delivery tube.

Induction coil geometry. Length 38 mm; mean diameter 44 mm; 5 turns; power input, 1.5 kVA. Variac current controller in the heating coil circuit.

Ceramic pedestal. Length 70 mm; ext. diameter 20 mm; the platform below is adjusted to bring the crucible contents into the centre of the coil.

The combustion section of the tube has a length of *ca.* 140 mm with an internal diameter of 35 mm. The delivery tube has a mean diameter of *ca.* 210 mm, and is wound with a nichrome wire heating coil, controlled by a transformer. The silica bubbler (length *ca.* 120 mm) leads to an absorption cylinder with a capacity of 200 ml.

The H.F. pots or crucibles (depth 25 mm, int. diameter 19 mm, ext. diameter 25 mm) with their lids (diameter 25 mm, thickness 3 mm) were preheated for 1 h in a muffle furnace at 1000°.

The oxygen flow rate is 1.5 l min^{-1}, with a 2-l supply reservoir. The gas is purified before use by passage through a tube, 200 mm long by 20 mm internal diameter, charged with anhydrone, soda asbestos (8–14 mesh) and again with anhydrone, the layers being separated by glass wool.

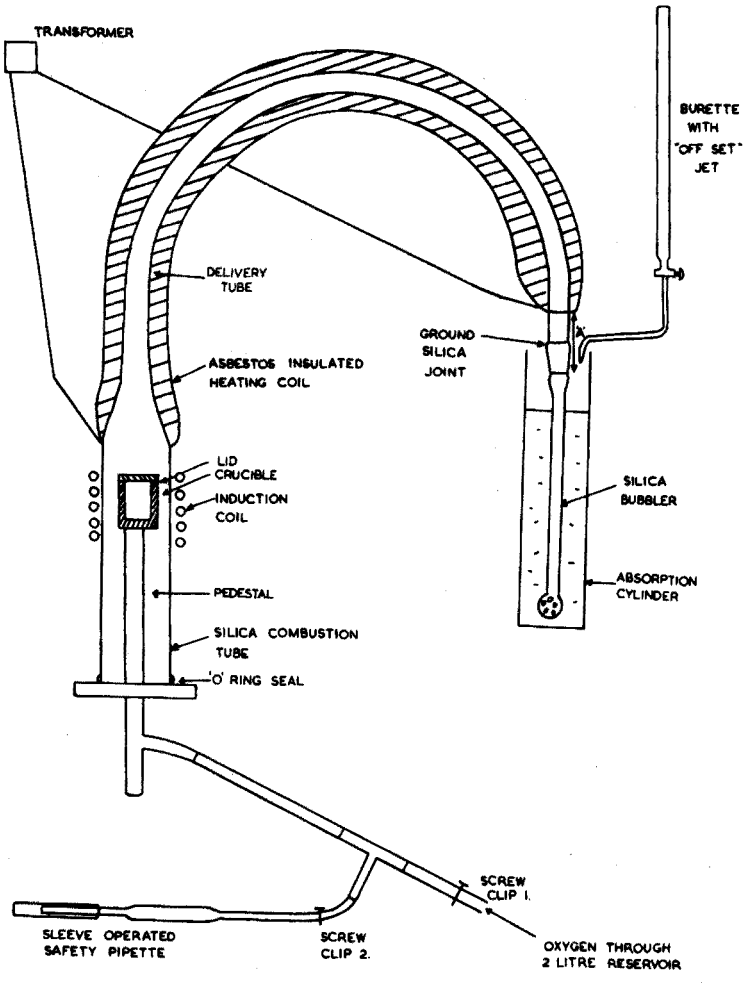

Fig. 1. Transparent silica apparatus for the absorption and measurement of sulphur.

Reagents

Vanadium pentoxide. Prepare by heating ammonium vanadate, G.P.R. grade.

Sodium borate solution. Dissolve 2.3850 g of recrystallized disodium tetraborate monohydrate in 200 ml of water and dilute to 2 l. Standardize against the sulphuric acid. (1 ml $\equiv$ 0.010% sulphur on a 1-g sample.)

Bulk absorbent. Dilute 50 ml of 20-vol. hydrogen peroxide to 2 l, add 10 ml of conventional methyl red–methylene blue mixed indicator solution, and adjust to the given end-point with 10^{-2} *M* sulphuric acid and the borate solution (Note 1).

Procedure

Switch on the power supplies to the furnace and the heating coil. Transfer 100 ml of the bulk absorbent to the cylinder, immerse the bubbler and clamp

in position below the burette, as shown. Transfer 1 g of sample to a ceramic crucible, add 1 g of vanadium pentoxide, cover with a high porosity lid (Note 2) and place on the furnace pedestal in the lowered position. Operate the mechanism to raise and lock the pedestal into the ignition position and, by means of the Variac control, adjust the plate current to 250 mA. As combustion proceeds and the crucible commences to glow, increase the current gradually to 300 mA and maintain there for the final 2 min of the 5-min cycle, to maintain fluidity and release residual sulphur.

When combustion is complete, titrate the blue solution back to the original green colour, maintaining the oxygen flow to agitate the solution.

Switch off the current and oxygen supply, close screw clip 1 and open clip 2 (Fig. 1). By means of the safety pipette draw up absorbent into the tip of the heated tube (section A). Readjust the clips, turn on the oxygen supply to complete the rinse, titrate the residual sulphur and add to the previous reading.

Determine the blank on the apparatus, at the same time, by running duplicate 1-g samples of high-purity iron (BCS 260/3), and calculate the mean. Deduct 0.4 ml to allow for the sulphur content (Note 3).

Then calculate the % sulphur from $(A-B)\cdot 0.010$, where A = ml of titrant used for test sample, and B = ml of titrant used for the blank, after correction.

Notes

1. Use of a pre-neutralized bulk absorbent ensures standard initial conditions and reduces end-point errors.

2. Provided that efficient covers are used, the iron oxide deposited in the delivery tube is negligible and the usual plugs of glass wool may be omitted. Covers may be used several times until oxide deposit or metal spatter affects the porosity.

3. The glassware should be rinsed with distilled water and dried after each series of tests.

RESULTS AND DISCUSSION

In initial tests of this method, a synthetic sulphur solution of strength 2 g/100 ml was made from micro-analytical reagent sulphamic acid (33.02% S) and standardized gravimetrically. Nickel (1.5 g) and vanadium pentoxide (1 g) were transferred to a lidded Leco crucible, and a 0.1-ml aliquot of the sulphamic acid solution was introduced by means of an Agla syringe. The crucible was immediately admitted to the furnace and the liberated sulphur determined. This was repeated several times and a blank on the crucible and contents, without sulphamic acid, deducted in each case. Compared with the theoretical value of 0.66 mg, the mean of ten determinations was 0.6595 mg, with a standard deviation of 0.007 mg.

The sulphur contents of a series of BCS iron and steel and a Nimonic alloy standard were then determined as proposed, a freshly neutralized bulk absorbent being used. For high sulphur steel BCS 152/3, 0.5 g of sample was heated with 0.5 g of nickel and 1 g of vanadium pentoxide. The results obtained are shown in Table I. The theoretical weight of sulphur was calculated from

TABLE I

RESULTS FOR STANDARD IRONS AND STEELS

BCS standard	*S (%)*		
	Value	*Found*	
Steel 224/1	0.008	0.006	0.0065
Steel 235/2	0.018	0.019	0.020
Nimonic alloy	0.0185	0.0205	0.020
Steel 218/3	0.036	0.035	0.036
Steel 220/2	0.029	0.0285	0.0305
Steel 239/3	0.052	0.0535	0.0525
Steel 234/7	0.125	0.124	0.1245
Steel 152/3	0.28	0.274	0.274
Theoretical wt. of sulphur (g)		0.004355	0.004355
Recovered wt. of sulphur (g)		0.00432	0.00436
Recovered % of sulphur		99.2	100
Deposited in apparatus		Nil	Nil
Iron 173/1	0.020	0.018	0.019
Iron 206/2	0.039	0.041	0.040
Iron 234/7	0.125	0.127	0.127
Iron 172/1	0.096	0.097	0.096
Theoretical wt. of sulphur (g)		0.00280	0.00280
Recovered wt. of sulphur (g)		0.00283	0.00282
Recovered % of sulphur		100	100
Deposited in apparatus		Nil	Nil

BCS values with the addition of sulphur from duplicate high-purity iron (BCS 260/3) blank determinations run concurrently. Recovered weight of sulphur was calculated from total volume of titrant used after deduction of ten average blank determinations.

Recovery tests were then made on a high sulphur steel in which sulphur equivalent to a total of 125 ml of titrant was determined, an unheated delivery tube being used for greater deposition. Rinsing tests with the absorbent for the iodine–iodate titration procedure, which traps all the sulphur dioxide, failed to detect sulphur. But a deposit could reasonably be expected in the system from such a large amount of sulphur. This test therefore, coupled with the earlier work using the peroxide absorbent and alkalimetric titration, showed that the sulphur retained in the tube is the trioxide. Possibly moisture from the sample combines with the sulphur trioxide produced to give a deposit of sulphuric acid on the glass or silica ware.

A study of the distribution of sulphur deposition in cold or inadequately heated tubes showed that the amounts deposited decreased in the order: neck of combustion tube > delivery tube to titrant > middle portion. It therefore seemed that the abrupt restriction in diameter of the usual combustion tube favoured sulphur deposition; to avoid this, as well as problems with coil winding and the usual silicone rubber joints, the apparatus shown in Fig. 1 was designed with a tapered shoulder and in one piece, connection to the bubbler being made via a

ground-glass joint. A larger proportion of the tube could then be heated, as shown. The smooth curved shape was also an improvement over earlier systems with right-angled bends where sulphur tended to accumulate.

When two runs of BCS steels were made, no measurable sulphur was deposited anywhere with the exception of the unheated tip "A". Total losses of 0.86% and 0.56% were recorded, showing the need for rinsing for which the suction device was subsequently introduced.

The sulphur contents of a series of BCS iron ore and slag samples were then determined. Three foreign ore samples were also included. Crucible additions were 1 g of nickel and 1 g of vanadium pentoxide plus a suitable fraction sample weight for Tests 1 and 2, with 1 g of Leco iron and 1 g of tin plus the sample for Test 3. The results are shown in Table II. No sulphur was detected in the dismantled apparatus after rinsing with the neutralised absorbent.

TABLE II

RESULTS FOR IRON ORES AND SLAGS

Standard sample	*Sulphur (%)*				
	Cert. value	*Test 1*	*Test 2*	*Test 3*	*Iodimetric detn.*[a]
Nimba iron ore BCS 175/2	0.007	0.011	0.010	0.009	—
Iron ore sinter BCS 378	0.031	0.030	0.029	0.028	—
Iron ore sinter BCS 303	0.22	0.226	0.224	0.224	0.204
Lincolnshire iron ore BCS 301	0.47	0.44	0.45	0.44	—
Northamptonshire iron ore BCS 302	0.12	0.15	0.15	0.14	—
Basic slag BCS 174/2	0.11	0.089	0.096	0.110	—
Blast furnace slag BCS 367	0.94	0.99	0.99	0.94	—
Kiruna ore	0.020	0.094	0.097	0.094	0.019
Japan hematite ore	0.075	0.081	0.080	0.079	0.074
Japan magmetite ore	0.251	0.285	0.285	0.287	0.244

[a] The iodimetric method was applied only to fluorine-bearing materials (see text).

Enhanced sulphur values were observed for some ore samples, probably caused by acid-forming elements in the presence of combined water. Kiruna ore, for example, contains 0.3% of fluorine. Sinter 303, however, contains 0.1% of fluorine with little enhancement.

Interference tests were then carried out with the Japanese hematite ore, a Krivoj Rog ore and sinter BCS 303 with additions of 0.3% and 0.15% of fluorine, as sodium fluoride; 0.5 g of sample was used, together with 1 g of Leco iron and 1 g of tin. The results (Table III) prove that the acid–alkali titration is unsuitable for fluorine-bearing materials. The iodimetric finish, which is not affected, should therefore be used, with reference to the appropriate standard similarly treated (see Table II). Chlorine would show a similar effect.

Conclusion

In the high-frequency induction heating technique, optimal combustion con-

TABLE III

INTERFERENCE OF FLUORIDE

Sample	*Sulphur (%) (cert. value)*	*Fluoride addition (%)*	*Sulphur found (%)*
Hematite	0.075	Nil	0.078, —
Hematite	0.075	0.15	0.121, 0.130
Hematite	0.075	0.3	0.188, 0.192
Krivoj Rog	—	Nil	0.037
Krivoj Rog	—	0.15	0.082
Krivoj Rog	—	0.30	0.167
Sinter BCS 303	0.22	0.30	0.250

ditions have been achieved, and the use of a specially designed heated silica delivery tube system, coupled with a rinsing operation, collects the total sulphur from each determination. Good results are shown for BCS irons and steels.

The method is also suitable for oxide materials such as slags, but not for iron ores or materials containing combined water and acid-forming elements where enhanced sulphur values occur.

For routine operation it compares favourably in convenience and time with the previous non-stoichiometric method, and the modification is simpler than a device recently published[9].

Resistance heating is still used for lime and solid fuels.

The authors thank Messrs. Bell, Jeffery, Stamp and Wilkinson of these laboratories for their co-operation at various stages of this work and the management of the Scunthorpe Group, British Steel Corporation for permission to publish this paper.

SUMMARY

The principles of combustion techniques suitable for the determination of sulphur in irons, steels, slags, etc. and their application to a range of materials are outlined. Conditions which give a 100% yield by high-frequency induction heating are established. Deposition of sulphur trioxide on the walls of the delivery train is obviated by heating electrically, giving total sulphur absorption in hydrogen peroxide. Good results for BCS irons, steels, slags and iron ores are given but the presence of fluorine causes a positive interference, unless the alkalimetric titration is replaced by an iodimetric procedure. Resistance heating is still used for lime and solid fuels.

RÉSUMÉ

Une étude est effectuée sur les techniques de combustion pour le dosage du soufre dans le fer, l'acier, les scories, etc. On indique les conditions permettant d'obtenir un rendement de 100% par chauffage à induction-haute-fréquence. On

évite un dépôt de trioxyde de soufre sur les parois, par chauffage électrique, et on arrive à une absorption totale de soufre dans le peroxyde d'hydrogène. De bons résultats sont obtenus; cependant en présence de fluor, le titrage alcalimétrique doit être remplacé par un procédé iodimétrique. Ce système de chauffage peut être aussi utilisé pour la chaux et les combustibles solides.

ZUSAMMENFASSUNG

Die Grundlagen von Verbrennungsverfahren für die Bestimmung von Schwefel in Eisen, Stählen, Schlacken etc. und deren Anwendung auf eine Reihe von Stoffen werden dargelegt. Es werden die Bedingungen festgestellt, unter denen durch Hochfrequenz-Induktionsheizung eine 100%ige Ausbeute erhalten wird. Einer Abscheidung von Schwefeltrioxid an den Wandungen des Ableitungsrohrs wird durch elektrisches Heizen entgegengewirkt, so dass der gesamte Schwefel in Wasserstoffperoxid absorbiert wird. Es werden gute Ergebnisse bei BCS Eisen, Stählen, Schlacken und Eisenerzen erhalten; jedoch verursacht die Gegenwart von Fluor eine positive Abweichung, wenn nicht die alkalimetrische Titration durch ein jodometrisches Verfahren ersetzt wird. Für Kalk und feste Brennstoffe wird stets Widerstandsheizung angewendet.

REFERENCES

1 *Standard Methods of Analysis of Iron, Steel and Associated Materials*, The United Steel Cos., Ltd., 5th Ed., 1961, p. 113.
2 *Standard Methods of Chemical Analysis of Iron and Steel*, B.S.C. Midland Group Analytical Panel, 1970, p. 175.
3 Ref. 2, p. 178.
4 *British Standard 1016: Part 7: 1959.*
5 A. E. Beet and R. Belcher, *Fuel*, 19 (1940) 92.
6 F. A. B. Jeffery, *Intern. Rep.*, October, 1963.
7 C. Stamp, A. Wilkinson and T. S. Harrison, *Intern. Rep.*, November, 1969.
8 P. B. Dunnill, private communication.
9 R. Kajiyama and K. Hoshino, *Analyst*, 96 (1971) 835.

Analytica Chimica Acta, 67 (1973) 155–178

SELECTRODE—THE UNIVERSAL ION-SELECTIVE ELECTRODE

PART VI. THE CALCIUM(II) SELECTRODE EMPLOYING A NEW ION EXCHANGER IN A NONPOROUS MEMBRANE AND A SOLID-STATE REFERENCE SYSTEM

J. RŮŽIČKA, E. H. HANSEN and J. CHR. TJELL

Chemistry Department A, The Technical University of Denmark, Building 207, 2800 Lyngby (Denmark)

(Received 2nd May 1973)

It is seldom appreciated how much is owed to workers in the biological sciences for their contributions in establishing means for pH determination[1]. Today, half a century later, a similar situation is occurring, except that the emphasis has shifted from measurements of hydrogen ion activities to metal ion activities. In particular, the important role of calcium ion activities in medicine, has long been appreciated, yet reliable calcium electrodes did not emerge until very recently. Many unsuccessful attempts have been made since Luther[2] in 1898 described the first calcium electrode, until Ross[3]—only six years ago—suggested the ingenious liquid membrane electrode. The fair selectivity of this new sensor towards typical components of blood serum has led to numerous applications in biomedical sciences and eventually also to its use in analytical, inorganic and physical chemistry. This type of electrode became manufactured by the Orion Company[4], soon followed by Beckman, Corning and Philips[5–7]. The liquid membranes of all these electrodes employ calcium salts of dialkylphosphates (with 8–10 membered carbon chains) as the electroactive material, dissolved in an organophosphonate, serving as the water-immiscible solvent.

During extensive use of these electrodes, however, certain drawbacks as well as peculiarities in their function have been observed[8,9]. Some of these may be ascribed to the rather complicated construction of the Orion electrode body[8], which comprises both reservoir of the organic ion exchanger as well as an inner aqueous reference system, plus a membrane-holding device. The chemical properties of the calcium alkylphosphate based membranes also create certain problems in the use of these electrodes for indication during complexometric determinations of calcium in, *e.g.* serum or sea water[10], where the sodium level is so high that it impairs the electrode performance. In addition, the response to hydrogen ions makes the electrode useful only above pH 6, while below pH *ca.* 5, a characteristic "dip" appears in the potential–pH diagram[4,8,9].

Various attempts have been made to overcome these drawbacks of the construction by modifying it (Philips[7], Corning[6], Beckman[5,11] and Hisel[12,13]). Different electroactive materials have also been suggested, but all attempts have fallen short of, or at best have only equalled the performance of the Orion electrode. The only notable exception is the electrode of Moody *et al.*[14,15], in which the

original Orion ion exchanger is incorporated into a nonporous PVC membrane. Use of such membranes results in substantially prolonged electrode lifetime, and allows the reservoir of ion exchanger within the electrode body to be discarded.

After some initial experience with the Orion electrode (used for calcium measurements in a flowing stream[16]), the authors also made an unsuccessful attempt to simplify the electrode construction[17]. This experience, however, led to the introduction of selectrodes[18]; and after further preliminary studies on various organophosphate systems[19], a new calcium sensor has finally been developed.

THEORETICAL

A system consisting of two phases α (electrode) and β (sample solution) in contact, both containing the i'th component, is considered. If the system is in equilibrium, the phase-boundary potential, π, can be computed from the electrochemical potential, $\bar{\mu}_i$, of component i in the respective phases, *i.e.*:

$$\pi = \varphi(\alpha) - \varphi(\beta) = \frac{\mu_i^0(\beta) - \mu_i^0(\alpha)}{z_i F} - \frac{RT}{z_i F} \ln a_i(\alpha) + \frac{RT}{z_i F} \ln a_i(\beta) \qquad (1)$$

where the symbols have their usual meaning[20]. If it is assumed that the distribution of component i is the main process determining the phase-boundary potential (*i.e.*, other components *g*, *f*, etc., are absent or do not enter the phase α), the changes of π will therefore selectively reflect the changes in $a_i(\beta)$ so that eqn. (1) may be transformed into:

$$\pi = \text{const.} + \frac{RT}{z_i F} \ln a_i(\beta) \qquad (2)$$

providing that the factor $(RT/z_i F) \ln a_i(\alpha)$ remains constant and unaffected by changes in $a_i(\beta)$. This would, however, be the case if the number of sites occupied by i within α remains constant, *i.e.*, phase α has to be loaded by i at least up to 99% of available capacity even at low $a_i(\beta)$ values.

The value π is, of course, not accessible to direct measurement, and the phases α and β have to be part of an electrochemical cell, the components of which are chosen according to the properties of i and α. The simplest case is that of a cation i in reversible equilibrium with its metallic form constituting phase α, but this combination is unfortunately not suited to serve as the basis for a calcium electrode. An appropriate phase α such as a solution of a calcium chelate in water, immiscible with an organic solvent requires a more complicated cell arrangement:

$$\overbrace{\underset{\beta'}{\text{REF}_1} \,||\, \underset{\beta'}{0.01\ M\ \text{CaCl}_2} \,|\, \underset{\pi'\alpha'}{\text{membrane}} \,|\, \underset{\alpha\pi}{\text{Ca}^{2+}\ \text{sample}} \,||\, \underset{\beta}{\text{REF}_2}}^{\text{ISE}} \qquad \text{(cell A)}$$

where phase α is placed symmetrically between two aqueous solutions β' and β. The half of the cell marked ISE is the ion-selective electrode, while REF_2 presents a reference electrode placed in the sample solution. In the case of complete symmetry, *i.e.*, $\text{REF}_1 = \text{REF}_2$ and $\beta' = \beta$, the electromotive force of cell A

will at equilibrium be equal to zero, unless an asymmetric potential is formed within the membrane (*i.e.*, $\alpha' \neq \alpha$). The obvious advantages of this arrangement are:

(*a*) well defined (and stable) values of the inner reference potential (REF_1);

(*b*) fixed a_i within β' which not only secures stability of π', but also helps to stabilize the activity of i within phase α;

(*c*) no transport of water across the membrane.

On the other hand, the actual construction of a cell A with a liquid membrane is complicated and therefore electrodes of this type have many disadvantages of practical and mechanical character[8]. Consequently, various attempts have been made to simplify the construction by eliminating the inner aqueous reference system. This led to the conception of an asymmetrical cell:

$$\overbrace{\text{CONDUCTOR} \mid \text{membrane} \mid \text{Ca}^{2+}\ \text{sample}}^{\text{ISE}} \mid\mid \text{REF}_2 \qquad \text{(cell B)}$$
$$\pi'\ \alpha' \qquad \alpha\ \pi \qquad \beta$$

Here the ion-selective electrode may simply be a platinum wire coated by a layer of organic ion exchanger in PVC (coated wire electrode[21]) or graphite coated by a layer of organic solvent (liquid-state electrode[17,22,23]). Unless phase α contains a compound which can participate in reversible redox equilibria and thus furnish stable (and predictable) values of π', cell B is objectionable from a theoretical viewpoint, because it relies on an unknown and ill-defined redox system. However, in potentiometric measurements the currents passing through the electrode are so small that even easily polarizable systems might remain sufficiently stable and hence furnish reliable although not entirely predictable E^0_{ISE} (eqn. 3) values. Unfortunately, any organic solvent dissolves a certain amount of water; therefore, during electrode use, increasing quantities of humidity enter the membrane phase, thus altering the composition of phase α and in particular the π' value. Consequently, even minute but gradual transport of water will cause large potential drifts of the coated wire electrode and the measurements will become unreliable.

The selectrode concept[18], however, offers an alternative, combining all the advantages of cell A with those of a simple and robust electrode construction, without either a reservoir of organic ion exchanger or a bulky aqueous inner reference system (see Fig. 4). Thus the electrochemical cell composed of a calcium selectrode with a solid-state calomel-based inner reference system:

$$\overbrace{\text{TG} \mid \text{Hg} \mid \text{Hg}_2\text{Cl}_2,\ \text{KCl(s)},\ \text{CaSO}_4 \cdot 2\text{H}_2\text{O(s)}}^{\text{Selectrode}} \mid \text{membrane} \mid \text{Ca}^{2+}\ \text{sample} \mid\mid \overbrace{\text{KCl(s)},\ \text{Hg}_2\text{Cl}_2 \mid \text{Hg}}^{\text{SCE}} \quad \text{(cell A1)}$$

operates, like the reference-selectrode[18], on humidity contained within the calomel paste, which has been applied onto the teflon graphite conductor (TG) and tightly pressed against a nonporous PVC membrane. From the solubility product of calcium sulphate, which compound is mixed into the calomel paste, the inner calcium activity can be calculated, in turn allowing the computation of E^0_{ISE} and the asymmetry potential (see Results and discussion). In addition to cell A1, the following cells were used in the present investigation:

$$\overbrace{\text{Ag}|\text{AgCl, 0.01 } M \text{ CaCl}_2\text{, 0.1 } M \text{ NaCl}|\text{membrane}}^{\text{Orion}}|\text{Ca}^{2+}\text{ sample}\overbrace{||\text{KCl(s), Hg}_2\text{Cl}_2|\text{Hg}}^{\text{SCE}} \quad \text{(cell A2)}$$

where the original Orion construction, Orion inner reference solution (see Electrodes) as well as Orion ion exchanger were used. Additionally, the electrode construction suggested by Moody *et al.*[14,15] was used in two alternative versions, *i.e.*:

$$\overbrace{\text{Ag}|\text{AgCl, 0.005 M CaCl}_2|\text{membrane}}^{\text{ISE}}|\text{Ca}^{2+}\text{ sample}\overbrace{||\text{KCl(s), Hg}_2\text{Cl}_2|\text{Hg}}^{\text{SCE}} \quad \text{(cell A3)}$$

and

$$\overbrace{\text{Hg}|\text{Hg}_2\text{Cl}_2\text{, KCl(s)}||\text{0.01 } M \text{ CaCl}_2|\text{membrane}}^{\text{ISE}}|\text{Ca}^{2+}\text{ sample}\overbrace{||\text{KCl(s), Hg}_2\text{Cl}_2|\text{Hg}}^{\text{SCE}} \quad \text{(cell A4)}$$

According to the Nernst equation, the electromotive force, E, of all these cells may be expressed by the equation:

$$E = E^0_{\text{ISE}} + (RT/2F)\ln(a_{\text{Ca}^{2+}}) \tag{3}$$

where the constant E^0_{ISE} comprises all phase boundary (and diffusion) potentials except π', expressed against the saturated calomel electrode.

The electroactive material

The sensitivity and selectivity of an electrode which is based on an organic liquid immiscible with water, can be evaluated by means of extraction data[22,23]. This is done by computing the degree of saturation of the organic phase by the ion to be measured from the values of extraction constants or distribution coefficients at the particular pH. Furthermore, by assuming that any foreign ion would interfere only when occupying more than 1% of the sites available within the organic phase (*i.e.*, in the immediate vicinity of phase boundaries), the influence of various ions on the electrode potential can be predicted.

The calcium electrode of Ross[3] is said to employ a 0.1 M solution of calcium di-(n-decyl)phosphate (DDP)* in dioctylphenylphosphonate (DOPP-n) held by a porous membrane[3,8,24]. The reason for choosing this particular combination was never quite revealed, but very likely was based on reference to the extensive literature dealing with the extraction of organophosphate compounds. These compounds, although often referred to as ion exchangers, differ from cation-exchange resins in that their individual extraction reactions very seldom are stoichiometrically equivalent. The reason is a strong dimerization of dialkylester molecules even when diluted by carrier solvent, and as they are monoionized, one of the hydrogens is not replaceable. This is true for extractions by an excess of reagent in an organic solvent such as benzene or toluene, where the following type of chelate is formed[25]:

* The systems DDP and DOPP, as used in this paper, denote the calcium chelates of the respective acids, regardless of the degree of loading.

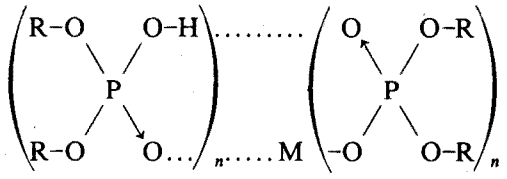

according to the reaction:

$$M^{n+} + n(H_2A_2)_o \rightleftarrows [M(HA_2)_n]_o + nH^+$$

with the extraction constant:

$$K = \frac{[M(HA_2)_n]_o [H^+]^n}{[M^{n+}] [H_2A_2]_o^n} = q \frac{[H^+]^n}{[H_2A_2]_o^n} \tag{4}$$

where $[M^{n+}]$ is the equilibrium concentration of uncomplexed metal ion; $[H_2A_2]$ is the equilibrium concentration of unreacted dimer; $[M(HA_2)_n]$ is the equilibrium concentration of chelate formed; and subscript o denotes the organic phase, while q is the distribution coefficient.

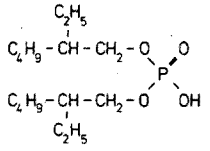

HDEHP

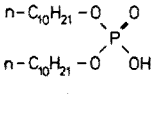

HDDP

HDEHP = di-(2-ethylhexyl)phosphoric acid; HDDP = di-(n-decyl)phosphoric acid.

This means that the higher the q (or K) value, the better electrode selectivity will be obtained, also towards hydrogen ions, and therefore electrodes containing compounds with higher K values will be applicable in more acidic solutions. Thus for di-(2-ethylhexyl)phosphoric acid (HDEHP[25,26]) in toluene, the K value decreases in the order: $Sc^{3+} \gg In^{3+} \approx Fe^{3+} \approx Be^{2+} \gg Zn^{2+} > Ca^{2+} > Cu^{2+} > Sr^{2+} > Ba^{2+} > Na^+ > K^+$, and, consequently, so does the selectivity of the corresponding electrodes. With regard to the influence of the alkyl chain R, it can be predicted that the K value will increase with chain length, linear chains being preferable, as branched chains are less effective owing to steric hindrance. Therefore HDDP (R = n-decyl) as used by Ross[3] gives better extraction than HDEHP (branched), yet the order of selectivities remains the same. Measurements with any organophosphate-based calcium electrode can therefore be expected to be strongly affected by any cation of higher q than calcium(II). Indeed, zinc(II) interference on the Orion electrode is well known and so is that caused by beryllium(II) ions.

Equation (4) represents, however, only an approximation, valid for an excess of extractant, where the total number of extractant molecules in the chelate depends on the charge and coordination number of the metal ion. In the case of calcium, species like $Ca(HA_2)_2$, $Ca(HA_2)_2HA$, and $Ca(HA_2)_2(HA)_2$ (some of them dimerized or polymerized) may be present in the organic phase, depending on the conditions of extraction, solvent and nature of R. Thus according to Peppard *et al.*[27], for low loading and HDEHP in xylene, the species $Ca(HA_2)_2(HA)_2$

is extracted, while with branched dioctylphenylphosphate, $Ca(HA_2)_2HA$ is predominant.

The extraction equilibria at high loadings, when an excess of calcium is present in the aqueous phase, have not been much studied. It is known that here the charge of the cation determines the number of molecules chelating the extracted metal ion[28]. At ultimate loadings, CaA_2 is formed to which, however, both HA and NaA still can be attached.

Thus when the pH of a solution containing high concentrations of calcium and sodium is varied, $(H_2A_2)_n$ will prevail in very acidic media as all calcium is replaced by protons, while with increasing pH, $CaA_2 \cdot 4HA$, $CaA_2 \cdot 2HA$ and finally CaA_2 will be formed in the organic phase—which at the same time might contain various amounts of $NaA \cdot xHA$ adducts[29]. Along with these changes, the distribution coefficient of calcium, q_{Ca}, will also change. In acidic solutions, low q values will be observed, owing to competition of protons, and an increase in q with increasing pH will reflect progressive formation of $Ca(HA_2)nHA$ in the organic phase. If higher loaded complexes such as CaA_2 are less extractable, the q value will, after reaching a maximum (most likely corresponding to $Ca(HA_2)_2$) decrease, and finally stabilize when maximum loading (corresponding to CaA_2) has been obtained. The position of this maximum will be pH- and $[Ca^{2+}]$-dependent, and in presence of sodium the height of the maximum will decrease because of Na^+–Ca^{2+}

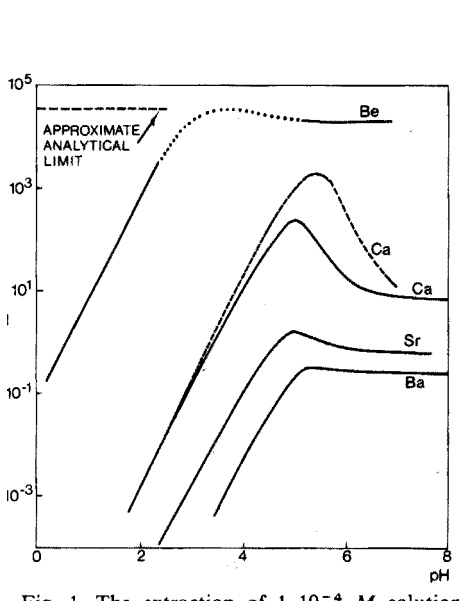

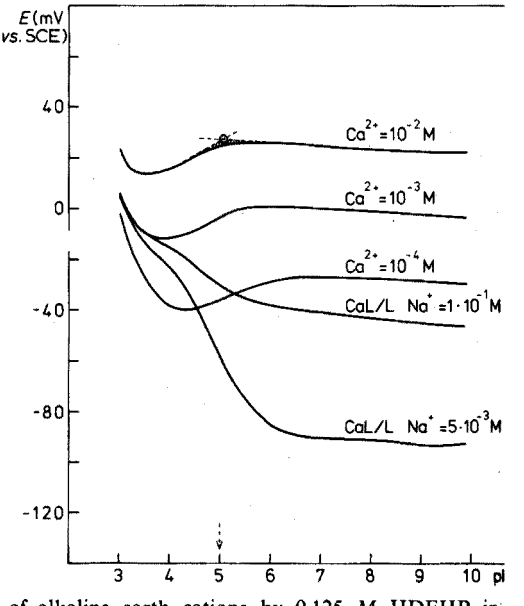

Fig. 1. The extraction of $1 \cdot 10^{-4}$ *M* solutions of alkaline earth cations by 0.125 *M* HDEHP in benzene[29]. Owing to the limit imposed by the analytical method used, the maximum on the beryllium curve cannot be measured. All curves depict extractions from 4.0 *M* $NaNO_3$ solutions, except the curve denoted by the broken line, which represents the extraction of calcium from a 0.5 *M* $NaNO_3$ solution. All data were obtained by radioactivity measurements.

Fig. 2. The potential–pH diagram of the Orion electrode, recorded at various pCa and pNa levels in absence and presence (CaL/L) of EDTA.

competition. This form of the extraction curves of alkaline earths with HDEHP has been described by McDowell and Coleman[29] (Fig. 1) and can be expected to occur similarly with other organophosphates (see *e.g.* Shevcenko *et al.*[30]).

It has been shown[22] that an increase of the q (or K) value is reflected in a decrease of the electrode potential. Therefore, the potential–pH diagram should exhibit a minimum at that pH where the extraction curve shows a maximum. Comparison of Figs. 1 and 2 shows that this indeed is the case, except that the position of the extreme on the electrode curve is situated *ca.* 1.2 pH units lower than that on the extraction curve. This is, however, due to the less acidic nature of the proton of HDEHP compared with that of HDDP. It is then reasonable to assume that by introducing groups of even more electrophilic character into the substituent R, the proton would be less firmly bound, and the region of existence of HA and its associates would be shifted to even lower pH values. This in turn would lead to increased selectivity towards calcium(II) over hydrogen ion, resulting in improved stability of the electrode potential as the available sites within the membrane would be fully calcium-occupied over a wider pH range. In order to test this hypothesis, di-(n-octylphenyl)phosphoric acid (HDOPP) was synthesized and its calcium chelate used as an electroactive material. For the sake of close comparison, di-(n-octylphenyl)phosphonate (DOPP-n) was used to dissolve the calcium chelate of HDOPP, as the same solvent was used by Ross in combination with the calcium chelate of didecylphosphate (HDDP) in a porous membrane of the Orion electrode, and by Moody and Thomas in a nonporous PVC membrane. The role of this solvent will be considered in the Discussion.

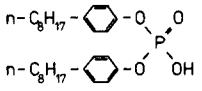

HDOPP

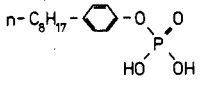

HOPP

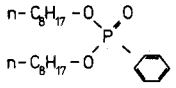

DOPP-n

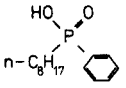

HOPP-n

HDOPP = di-(n-octylphenyl)phosphoric acid; HOPP = mono-n-octylphenylphosphoric acid; HOPP-n = mono-n-octylphenylphosphonic acid; DOPP-n = di-(n-octyl)phenylphosphonate.

Calcium buffers

It has been suggested by Bates and Alfenaar[31] that calcium-responsive electrodes should be standardized in solutions of completely dissociated calcium chloride salts, and for this purpose standard reference dilutions encompassing a range of pCa 1.11–3.54 have been proposed. This range is unfortunately too narrow to be useful for the present purpose; an analogous situation would be a set of pH standards based solely on dilutions of hydrochloric acid, by means of which the glass electrode never could be properly tested for its H^+ sensitivity and selectivity towards Na^+ and other alkaline metal ions.

Accordingly, the concepts described previously[32] were developed further, and

a series of calcium buffers was prepared and used throughout this study to ascertain the maximum sensitivity, selectivity and time stability of selectrodes activated by DDP and by DOPP, these characteristics being compared with those of the Orion electrode. Based on the principles of conditional stability constants and side-reaction coefficients, it has been shown that, at constant ionic strength, the pM value in a solution of the metal ion M^{n+} and the ligand L^{m-} forming the 1:1 complex $ML^{(n-m)+}$, at equilibrium can be expressed by the equation:

$$pM = -\log[M^{n+}] = \log K'_{ML} + \log \alpha_M + \log([L']/[ML']) \quad (5)$$

where the conditional stability constant K'_{ML} is given by $\alpha_{ML} \cdot K_{ML}/\alpha_M\alpha_L$, [L'] is the total concentration of uncomplexed ligand, [ML'] is the total concentration of complex formed, and α_i denotes the side-reaction coefficient for the i'th component.

From the definition of the conditional stability constant, eqn. (5) may be rearranged to read:

$$pM = \log K_{ML} + \log(\alpha_{ML}/\alpha_L) + \log([L']/[ML']) \quad (6)$$

Thus, for a given metal/ligand system, the pM may be varied by varying the [L']/[ML'] ratio and the α values. The side-reaction coefficients are inherently functions of all the side reactions in which the individual species participate. Often, however, side reactions with H^+ (or OH^-) are dominant, so that other side reactions may be neglected. Consequently, by addition of an appropriate pH buffer system any desired pM value may be obtained.

All the calcium buffers prepared were computed so as to contain a total 0.1 *M* concentration of sodium ion and to be of ionic strength *ca.* 0.1. These two prerequisites are, however, reciprocally dependent. As a consequence, it was not always feasible to prepare buffers of exactly 0.10 ionic strength.

A convenient mode of estimating the pCa values obtainable for a given calcium–ligand system may be achieved from a diagram such as Fig. 3, where pCa values as a function of pH are shown for L=NTA (nitrilotriacetic acid) and L=EDTA (ethylenediaminetetraacetic acid), the two ligands used for preparing the buffers here. The [L']/[CaL'] ratio is varied between 1/10 and 10/1, *i.e.*, within this region it is directly seen which ratio should be chosen in order to obtain a given pCa value for a given pH.

Calibration curves

By applying calcium solutions of constant ionic strength, the activities are directly proportional to the concentration of calcium ions, $[Ca^{2+}]$, thus furnishing the basis for an operational pCa scale defined by $pCa = -\log[Ca^{2+}]$, *i.e.*, the contribution from activity coefficients are incorporated into the E^0_{ISE} value. Hence the true position of the calibration curve may remain virtually unknown, yet well fixed in calcium solutions adjusted to constant ionic strength. In addition, by retaining a constant ionic strength, any variation in the junction potential, E_j, of the reference electrode is avoided, the term being incorporated into E^0_{ISE}. For these reasons, all calcium standard solutions, buffered as well as those prepared by dilution of calcium nitrate (pCa 2–4), contained a constant background concentration of 0.1 *M* sodium(I).

While the potential of an ideally functioning calcium electrode (*vs.* a

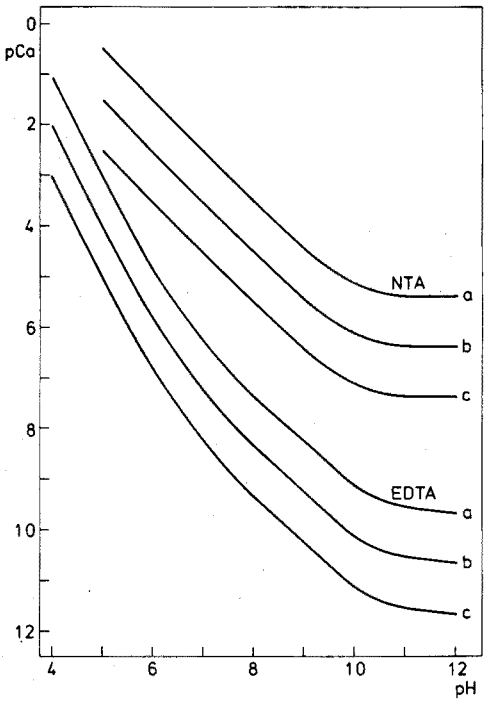

Fig. 3. pCa values as a function of pH for L=NTA and EDTA. The pCa values are given by eqn. (6): $\log [L']/[CaL'] = (a) -1$, (b) 0, (c) +1; $\log K_{CaNTA} = 6.4$, $\log K_{CaEDTA} = 10.7$.

reference electrode) is given by eqn. (3), the potential of a calcium electrode of selectivity for i kinds of interfering ions, carrying the charges z_i (always of the same sign) may in the generalized case be written:

$$E = E^0_{ISE} + \frac{RT}{2F} \ln ([Ca^{2+}] + \sum_i K_{Ca/Mi} \cdot [M^{z_i}]^{2/z_j}) \tag{7}$$

where $K_{Ca/Mi}$ is the selectivity constant and

$$[Ca^{2+}] = [Ca']/\alpha_{Ca} \tag{8}$$

If complexing agents other than hydroxide ions are absent (*i.e.*, dilutions), $\alpha_{Ca} = \alpha_{Ca(OH)} \simeq 1$ (if very alkaline solutions are not prepared).

In the presence of a complexing agent, L, which with calcium can form the complex CaL (*e.g.* calcium buffers), α_{Ca} will be equal to $\alpha_{Ca(L)} = 1 + [L]K_{CaL} \simeq [L]K_{CaL}$, where $[L] = [L']/\alpha_L$. If practically all the calcium in the system can be assumed to be complexed, eqn. (8) may be written:

$$[Ca^{2+}] = \frac{[Ca']}{\alpha_{Ca(L)}} = \frac{[CaL]}{[L]K_{CaL}} = \frac{[CaL']\alpha_L}{[L']\alpha_{CaL}} \cdot \frac{1}{K_{CaL}} \tag{9}$$

i.e., the value derived in eqn. (6).

As long as the first term within the parentheses of eqn. (7) is dominant,

the equation predicts that pCa as a function of E (the electrode calibration curve) will be a straight line of slope $-RT/2F \cdot 0.4343$. When the value of the two terms is equivalent, the curve will flatten out, the limit of sensitivity of the electrode towards calcium ions being a function of K_{Ca/M_i} and the concentration of the interfering ions.

EXPERIMENTAL

Calcium buffers

Two series of calcium buffers were prepared: (*a*) where the pH was adjusted to *ca.* 6.5 by addition of maleate buffer; and (*b*) where the pH was adjusted to *ca.* 9 by addition of borate buffer. These buffers totally covered a pCa range from *ca.* 3.5 to 10.3. In the region of pCa = 2–4, it was found that solutions prepared very carefully by the normal dilution technique were satisfactory. All solutions, buffered as well as unbuffered, were prepared to contain a sodium background of pNa = 1, and to be of an ionic strength of approximately 0.1. These two prerequisites are reciprocal dependent, hence, the maleic acid Ca-buffers were slightly higher in ionic strength (up to 0.13).

The pCa value of each buffer was computed according to eqn. (6). In the (*a*) series, the ligand used was NTA; while the (*b*) series comprised two sub-series, one where L was NTA and one where L was EDTA. The calculated pCa values are summarized in Table I, where the following complex constants have been used[33]:

$$\log K_{CaNTA} = 6.4 \quad \text{and} \quad \log K_{CaEDTA} = 10.7$$

TABLE I

CALCIUM BUFFERS. CALCULATED pCa VALUES

Series		*Ligand*						
		NTA				*EDTA*		
(a)	pH	6.45	6.60	6.65	6.71			
	pCa	3.6	4.1	4.3	4.4			
(b)	pH	9.18	9.10	9.18		8.98	8.98	8.98
	pCa	4.63	5.57	6.63		8.28	9.28	10.28

Electroactive materials

Synthesis of HDOPP (di-n-octylphenylphosphoric acid). Pyridine (1 mole) and phosphorus oxide trichloride (0.2 mole) were dissolved in diethyl ether. Then *p*-octylphenol (0.5 mole), dissolved in diethyl ether, was added dropwise to the reaction mixture, which was subsequently boiled under reflux for 2 h. During this process, water-free diethyl ether was used, and all solutions were protected against air humidity. The next step—aqueous hydrolysis and acidification—was done by adding 25 ml of water (dropwise), followed by 100 ml of concentrated hydrochloric acid. The ether phase was then separated from the mixture, washed, and evaporated in vacuum. The remaining oil was dissolved in methanol and

precipitated as the calcium salt by mixing with an aqueous calcium chloride–sodium hydroxide solution of pH 10. The white powder obtained was finally purified by repeated solvent extraction and scrubbing with hydrochloric acid yielding a colourless oil of HDOPP.

The calcium salt of HDOPP used for charging the electrodes was prepared by equilibrating a methanolic solution of the acid with the stoichiometric amount of a saturated, filtered aqueous solution of calcium hydroxide for several hours, until a constant pH value between 8 and 9 was reached. The white precipitate obtained was filtered, washed and dried.

It should be added that an alternative procedure, suggested for the synthesis of HDDP[34], might be used for the preparation of the HDOPP material.

HDDP. Di-n-decylphosphoric acid (m.p. 46°; Specialty Organics Inc.) was purified and converted into the calcium salt as described for HDOPP.

DOPP-n. Dioctylphenylphosphonate (distillation range 181–183°; Specialty Organics Inc.) was used as received.

Membrane preparation

Polyvinylchloride (0.180 g; Breon 113 or S 110/10; BP Chemicals International, Ltd.) was dissolved in 7 ml of tetrahydrofuran and combined with a mixture of 0.450 g of dioctylphenylphosphonate and the calcium salt of either HDDP or HDOPP in the weight ratio 10:1. (The calcium salts dissolve slowly in the solvent, and any undissolved residue should be removed by centrifugation.) The membrane was cast in a 40-mm diameter glass ring, by the method of Griffiths *et al.*[15]. For use in the selectrode construction, the membrane was reinforced by a nylon net (obtained by washing away the cellulose in a Millipore filter, WHWPO4700, with tetrahydrofuran), which was simply placed in the glass ring, resting on the glass plate, before the addition of the PVC–ion exchanger–tetrahydrofuran solution. The prepared master membranes were dried for at least 24 h. The 6-mm discs actually used in the selectrodes, were then cut with a cork borer and mounted.

Reference paste

Mercury(I) chloride and metallic mercury (weight ratio 1:1) were thoroughly mixed, and 1 g of solid potassium chloride and 0.50 g of solid calcium sulphate dihydrate were added together with a few drops of saturated KCl solution. By further thorough mixing, a paste was obtained which, unless dried, could easily be rubbed into the teflon–graphite surface of the selectrode.

Electrodes

The membrane selectrode (Fig. 4) was made on the basis of the F3012 Universal Selectrode (Radiometer, Copenhagen) body, furnishing it with a 10-mm thread. In addition, the selectrode was provided with a teflon tube and a cup, as depicted in Fig. 4. The hole in the teflon cup (diam. 2.1 mm) has to be cleanly cut out; otherwise the sample solution could leak into the electrode. If this happens, the electrode will, of course, exhibit a constant potential close to zero mV, regardless of the composition of the sample solution.

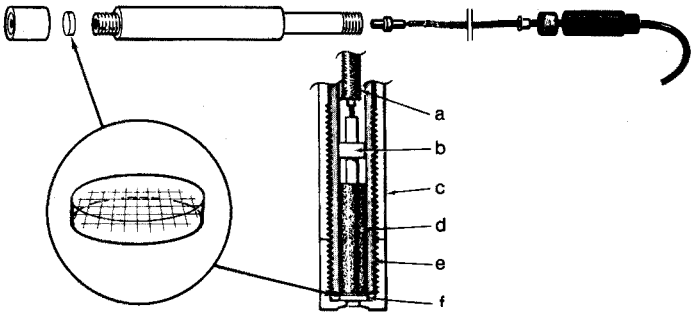

Fig. 4. The construction of the membrane selectrode: (a) screened cable; (b) metallic contact; (c) outer tube made of Teflon; (d) Teflon–graphite cylinder; (e) selectrode (F3012) body; and (f) PVC membrane, reinforced by a nylon net. The reference layer, covering the surface of the Teflon–graphite, is depicted between (d) and (f).

The Thomas PVC electrode (cell A3) and its modification (cell A4) were prepared as described previously[15,34], except that in the modified version a Radiometer calomel reference electrode (K 401) was used.

The Orion calcium electrode (model 92-20) was assembled according to the manufacturer's instructions[4]. Its potential, in agreement with the manufacturer's data, was *ca.* +5 mV in $1 \cdot 10^{-3}$ *M* calcium chloride. Supposing that $1 \cdot 10^{-3}$ *M* calcium chloride is also used as the inner reference solution[8], the asymmetry potential would have been as large as +151 mV, because REF_1 is Ag/AgCl, while REF_2 is SCE. The inner reference solution supplied (Orion, batch No. 9825) was therefore analyzed and, surprisingly, found to consist of 0.14 *M* NaCl + $1 \cdot 10^{-2}$ *M* $CaCl_2$ (plus solid silver chloride). This true composition of the inner solution (cell A2) corresponds then to an asymmetry potential of about −10 mV. Even less precise information is given by the manufacturer regarding the composition of the ion exchanger. In agreement with the observations of Griffiths *et al.*[34], the Orion product was found to contain, besides DDP and DOPP-n, several other components, one of them yellow (turning red-violet on reduction with zinc in acid medium). Therefore the DDP–DOPP-n ion exchanger was prepared from pure compounds (yielding a colourless liquid), and used in both the Orion construction as well as in the PVC membrane. No difference, however, was observed between electrodes charged with this, and the original liquid supplied by Orion. Consequently, only experiments with the Orion ion exchanger are described here and referred to as the DDP or Orion electrodes.

The electrodes for pH measurements were glass electrodes (Radiometer, type G 202B). As reference electrodes, Radiometer calomel electrodes (type K 401) were used.

Apparatus

All potential measurements were made by means of a digital pH meter (Radiometer, model pH52), accurate within ±0.1 mV. For automatic pCa/pH measurements, an automatic scanning potentiometer, an Autoburette ABU 13, two pH meters 51 (Radiometer) and an X–Y recorder (Watanbe WX 431) were used.

Unless otherwise stated, the curves were scanned from low to high pH values, at a rate of 0.5 pH min^{-1}, by automatic addition of sodium hydroxide to calcium chloride solutions acidified by hydrochloric acid. Such an amount of sodium chloride was added initially to the measured solutions, that the total sodium amount (at pH 7) corresponded to the amount indicated on the respective recorded curves. Automatic titrations were done with an Autoburette ABU 13, a pH meter 51 and a Servogor recorder (Goertz, Austria).

Measurement techniques

The measurement techniques have been described previously[3,2]. All measurements were carried out at $25 \pm 1°$, in 100 ml of well stirred solutions.

The selectivity parameters were measured by the mixed solution method[8] for H^+ and Na^+ interference, *i.e.*, from the calibration curves or from the potential–pH diagrams. The formula used by Moody and Thomas (eqn. (16), p. 12, ref. 8) was then used for computation of the $K_{Ca/H}$ values. The selectivity constants for other ions were calculated by the separate solution method[8]. Although the latter method is somewhat objectionable, the results obtained still give a fair comparison of the selectivities of the DDP and DOPP electrodes, because all measurements were executed in exactly the same manner.

Computations. All slopes were calculated by means of regression analysis on the linear part of the calibration curves. All values of slope, E^0_{ISE} and selectivity constants stated are mean values of measurements on at least three electrodes.

RESULTS AND DISCUSSION

The development of the calcium electrode involved three major steps:

(*a*) testing of existing calcium electrodes in pCa buffers and EDTA titrations;

(*b*) synthesis of DOPP ion exchanger, and its comparison with DDP ion exchanger;

(*c*) comparison of the Orion calcium electrode and the calcium selectrode.

At first, the Orion electrode (model 92-20) and the Thomas PVC membrane electrode, both utilizing DDP-based ion exchanger, were tested by scanning the potential–pH curves in calcium chloride solutions ($1 \cdot 10^{-2}$–$1 \cdot 10^{-4}$ *M*) as well as in calcium-buffered solutions (curves CaL/L) at low and high (nearly physiological) sodium levels. The behaviour of the Orion electrode (Fig. 2) in these solutions of widely varying pCa and especially at different pCa/pNa and pCa/pH levels confirms the presence of characteristic "dips". The positions of these minima are indeed pCa/pH dependent and their depth pCa/pNa dependent. The following points are noteworthy.

(*a*) The minima appear to be more shallow if the curves are recorded from higher to lower pH values, than if recorded in the opposite direction. This is not the case at low scanning speeds (1 pH unit/20 min), while at high scanning rates (2 pH units/min) the pCa/pH dependence is obscured.

(*b*) Any of the curves recorded in calcium chloride cannot be satisfactorily reproduced immediately after buffered solutions (curves CaL/L) have been measured, especially if the buffers contain high amounts of sodium.

(*c*) The nonporous PVC membrane behaves similarly, except that the minima

are more pronounced and the electrode shows smaller hysteresis at different scanning directions and rates.

These peculiarities all point to the fact that changes of calcium–proton–sodium ratios occur within the membrane phase. This causes not only the change in the electrode response, but also the shift in the E^0_{ISE} value due to the differences in the composition of various layers within phase α. The behaviour of the non-porous (PVC) membranes reflects the fact that the restricted mobility of the organic phase within the polymer matrix tends to preserve the established gradient of Ca, Na and H sites within the membrane ($\alpha \neq \alpha'$); while in the porous membranes, convection levels out the differences. The hysteresis observed on curves scanned in different directions at high scanning rates is due to the known fact that exchange reactions in two-phase equilibria, *e.g.* $M^{n+} + n(HA)_o \rightleftarrows (MA_n)_o + nH^+$, usually proceed faster from left to right than *vice versa.*

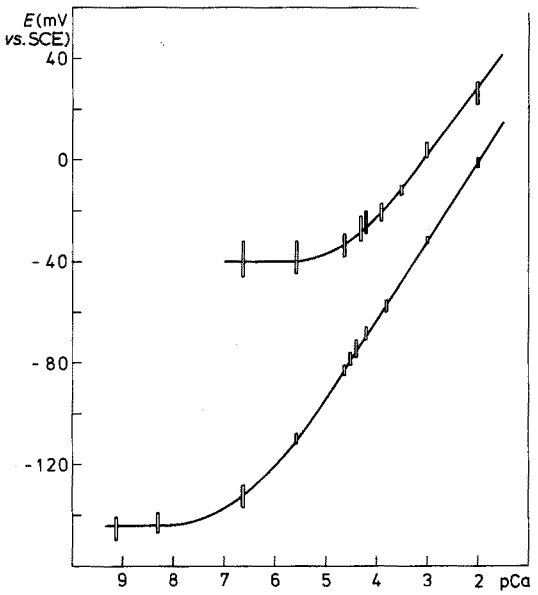

Fig. 5. Calibration curves for calcium electrodes measured in pCa buffers at pNa = 1.0. The points indicate measurements regularly recorded over a six weeks period. Top curve: the Orion electrode; bottom curve: the selectrode with a DOPP membrane.

The calibration of the Orion electrode in buffer solutions (pH > 6, ionic strength 0.1, pNa = 1) confirmed its nearly Nernstian response (27.0 mV/pCa, with a standard deviation of 0.58 mV; Fig. 5, Table II) over the first three weeks of operation, during which the electrode was stored in pCa = 2, pNa = 1 solutions. After the third week, the electrode slowly deteriorated, and at the end of seven weeks, a slope of 23.6 mV/pCa was observed. The stability of the electrode potential, as judged from the calculated E^0_{ISE} value (83.7 mV $\pm$ 2.49 mV), over the first three weeks was quite satisfactory. At the end of the test period, a value of $E^0_{ISE} = 75.8$ mV was reached and thus the asymmetry potential increased from originally -10 mV to -18 mV (compare cell A2).

TABLE II

THE STABILITY OF POTENTIAL AND RESPONSE OF CALCIUM ELECTRODES[a]

Electrode	*Week*	*0*	*1*	*2*	*3*	*4*	*5*	*6*	*7*	*During 3 weeks*[b]		*During 7 weeks*[b]		*Range*[c]
										$\bar{x}$	*s*	$\bar{x}$	*s*	*pCa*
Orion (DDP)	Slope	26.5	27.5	27.5	26.5	25.0	23.6	24.1	23.6	27.0	0.58	25.54	1.66	2–3.9
	E^0_{ISE}	84.5	86.8	82.4	81.1	74.8	69.8	75.3	75.8	83.7	2.49	78.81	5.76	
Selectrode (DOPP)	Slope	30.66	31.27	31.04	30.87	30.39	30.75	30.82	31.37	30.96	0.25	30.89	0.32	2–5.57
	E^0_{ISE}	59.78	65.22	64.45	60.40	58.94	58.77	57.79	59.15	62.05	2.56	60.56	2.75	

[a] All values calculated by regression analysis and stated in mV.
[b] $\bar{x}$ = mean value; s = standard deviation.
[c] Indicates the linear part of the calibration curve, from which values were taken for the computations.

The nonporous PVC membrane electrode, also with the DDP ion exchanger, showed an initial slope of 31.50 mV/pCa, but its long-term stability and durability were not investigated, because its superior behaviour has been described elsewhere[8,14]. The E^0_{ISE} value of this electrode (58.0 mV)—which was made as a modified Thomas construction—corresponds to an asymmetry potential of *ca.* 2 mV (compare cell A4).

Because of changes within the membrane, caused by a low selectivity of the DDP ion exchanger towards calcium, titrations of calcium with EDTA suffered from ill-pronounced potential jumps—especially in 0.1 *M* Na^+ solutions (Fig. 6). This behaviour, predictable from the shape of the potential–pH diagram (Fig. 2; note the distance between the 10^{-3} *M* Ca^{2+} and the CaL/L line for the particular pH and sodium level), has also been described elsewhere[10]. It was observed that repeated calcium–EDTA titrations at 0.1 *M* or higher sodium levels ruined the membrane of the Orion electrode beyond recovery, while PVC nonporous membranes could be restored in calcium chloride solutions.

The polymeric, nonporous PVC membrane was then compared with a porous membrane in the following way. In both the Orion (cell A2) and the modified Thomas construction (cell A4), the inner aqueous solution (β') was replaced by a 2.0 *M* sodium chloride solution. The DDP ion exchanger (in the calcium form) was used in both cases, but in a PVC membrane for the Thomas construction and in a porous disc in the Orion one. Thus in both electrodes, the stability of the

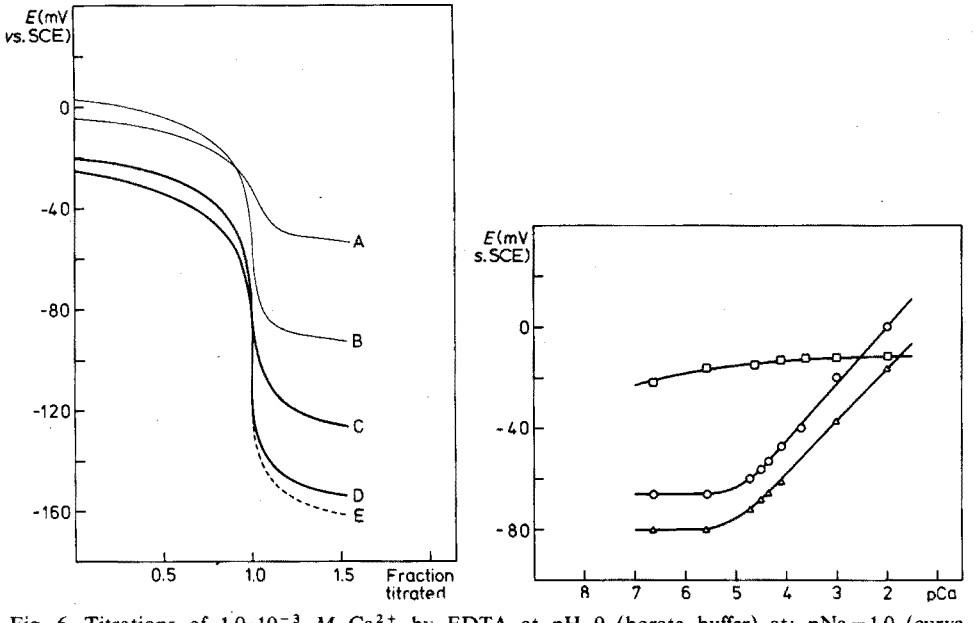

Fig. 6. Titrations of $1.0 \cdot 10^{-3}$ *M* Ca^{2+} by EDTA at pH 9 (borate buffer) at: pNa = 1.0 (curve A and C); at pNa = 2.3 (curve B and D); and at pK = 2.3 (curve E). The thin lines represent the Orion electrode; the thick and broken lines represent the Selectrode with a DOPP membrane.

Fig. 7. Porous (Orion) and nonporous (PVC) membranes containing DDP, mounted in electrodes containing 2.0 *M* NaCl as the inner reference solution. (□) Porous and (○) nonporous membranes immediately after preparation; (△) the nonporous membrane 16 days later.

inner reference system (REF_1) was still preserved; but the calcium in the membrane phase should gradually be replaced by sodium, so that all available sites within the membrane would be in the sodium form, owing to the low selectivity of the DDP-based ion exchanger. Consequently, the electrodes should eventually lose their calcium sensitivity. This indeed was the case with the Orion electrode (Fig. 7), which immediately failed to respond to changes in calcium activity. The nonporous PVC membrane, however, retained a somewhat lower, yet well pronounced calcium sensitivity (22.5 mV/pCa) and selectivity ($K_{Ca/H} = 1 \cdot 10^{-3}$), even after 16 days (when the slope was still 21.0 mV/pCa). During this testing period, E^0_{ISE} decreased from +45 mV to +25 mV, which corresponds to an increase of the asymmetry potential of the calcium, or a decrease of the asymmetry potential of the sodium electrode. This surprising, yet very useful, property of the PVC membrane can be explained by the absence of convection and by vastly reduced diffusion within the polymer membrane, where the ion exchanger is immobilized. Thus, while phase α' in the vicinity of π' is changed to the sodium form, phase α in the vicinity of π still remains in the calcium form as the sample solution β always contains a certain, however low, calcium activity. In the porous membrane electrode, the differences in the composition of α at various sites of the membrane are not preserved and the calcium response is lost.

Di-n-octylphenylphosphate-based ion exchanger

The calcium salt of the DOPP ion exchanger[35], prepared in this laboratory (see Experimental), was dissolved in di-n-octylphenylphosphonate and used in the Orion electrode with a porous membrane (cell A2), in the Thomas electrode construction (cell A3 and cell A4) with a nonporous PVC membrane, and finally in the selectrode construction (cell A1) again with a PVC membrane. It was observed that even the Orion electrode, charged with the DOPP ion exchanger, had an almost Nernstian response (27.5 mV/pCa), and a selectivity towards sodium of $K_{Ca/Na} = 8.7 \cdot 10^{-5}$, which is considerably better than the selectivity of the same electrode with the DDP ion exchanger. Moreover, the selectivity towards hydrogen ion was improved, and the "dips" on the potential–pH curve shifted towards the acid region.

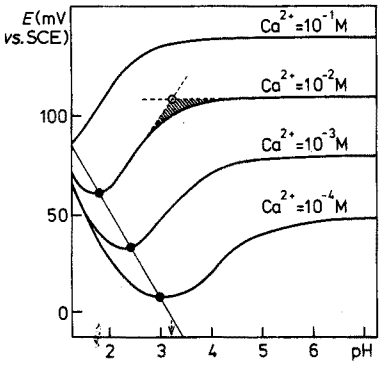

Fig. 8. Potential–pH diagram of DOPP/PVC electrode at various pCa levels, showing the influence of pH on the position of the minimum of the curve.

The nonporous membrane, however, is preferable and therefore DOPP-based PVC membranes were prepared and mounted in the Thomas construction (cell A3). These electrodes exhibited a Nernstian slope and an even better selectivity towards sodium ($K_{Ca/Na} = 5 \cdot 10^{-6}$) than the porous membrane electrode with same ion exchanger, and did not deteriorate in any respect during a seven-week testing period. The selectivity towards hydrogen ions was estimated from the potential–pH diagram (Fig. 8), which was recorded in solutions of calcium chloride and hydrochloric acid. The characteristic minimum peculiar to organophosphate extractants was now shifted 1.5 pH units towards the acid side, compared with the Orion electrode, and its position changed *ca.* 0.5 pH unit per 1 pCa unit. When the curves were obtained, similar hysteresis as with DDP-based electrodes was observed, but as the "dips" are farther away from the ordinarily applied measuring range (*cf.* Fig. 2), the membrane composition remained undisturbed and so did the E^0_{ISE} value.

With regard to the actual value of the selectivity constants for hydrogen ion, the following points should be noted in making a fair comparison of these electrodes. Any of the usual methods for determining the selectivity constants[8] of cation-sensitive electrodes is based on the measurement of positive potential deviations caused by the interfering cation. Hydrogen ions, however, interfere by causing a negative deviation. For the computation of the $K_{Ca/H}$ values, the break-point in the potential–pH curves caused by this deviation was graphically located (Figs. 2 and 8). The obtained pCa and pH values gave (calculated by the "mixed solution method"[8]) a value of $K_{Ca/H} = 10^{8.0}$ for the DDP (Orion) electrode (Fig. 2) and $K_{Ca/H} = 10^{9.0}$ for the DDP/PVC membrane electrode. For the DOPP/PVC membrane electrode a value of $K_{Ca/H} = 10^{4.2}$ was found (Fig. 8). Although these data clearly show that the DDP electrodes are much less selective than the DOPP electrodes (Figs. 2, 8 and 9), there are considerable discrepancies with the values recorded in the literature, where more favorable constants, *e.g.* $K_{Ca/H} = 10^7$ and 10^5, can be found for the Orion electrode, and even a value of $K_{Ca/H} = 40$ is given for the DDP/PVC membrane[8]. A possible explanation of this disagreement may be found in the hysteresis encountered in the potential–pH curves (see above). By recording from high to low pH values, more favorable $K_{Ca/H}$ values can be obtained, depending on the scanning rate, and in the extreme case, the pCa/pH dependence of the "dip" position can be completely obscured[9]. At any rate, whatever the "true value" of the respective $K_{Ca/H}$ constants are, the DOPP-based electrodes have about 10^4 better selectivity of calcium over hydrogen ions than the DDP electrodes—as demonstrated by the measurements, which were all carried out in exactly the same, comparable manner, by scanning from low to high pH.

The interfering effect of other foreign cations was determined by the separate solution method[8], and the results obtained for the DDP (Orion) and DOPP/PVC membrane electrodes are summarized in Table III.

The interfering effect of anions was also briefly investigated. Their effect, manifested by a negative deviation of potential, is most pronounced at high calcium activities and decreases in the order $ClO_3^- \gg I^- \gg NO_3^- > Cl^-$. While chloride interference is negligible and that of nitrate is very small, use of perchlorate (*e.g.* for adjustment of the ionic strength) must be avoided. The nature of this interference indicates that it is caused by ion association of anions with the phos-

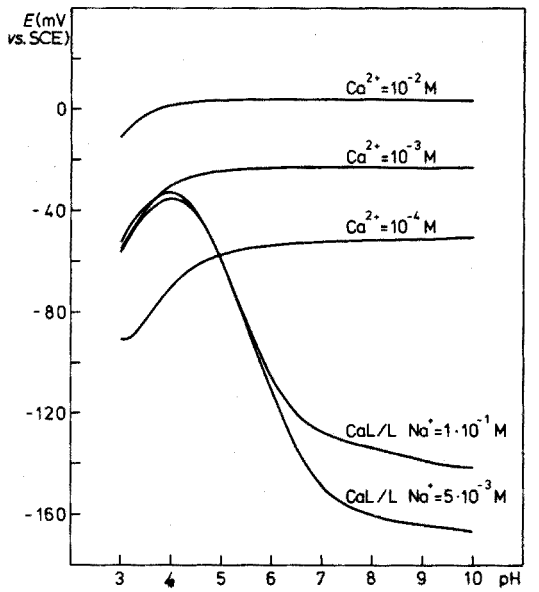

Fig. 9. Potential–pH diagram of the selectrode with a DOPP membrane, at various pCa and pNa levels, in absence and presence (CaL/L) of EDTA.

TABLE III

SELECTIVITY CONSTANTS OF CALCIUM ELECTRODES

(All values expressed as $-\log K_{Ca/M} = pK_{Ca/M}$)

Ion	*Electrode*	
	DDP (Orion electrode)[a]	*DOPP (Selectrode)*[b]
Mg^{2+}	1.85	3.60
Sr^{2+}	1.77	1.77
Ba^{2+}	2.00	3.60
Cu^{2+}	0.57	3.80
Zn^{2+}	−0.51	1.22
Cd^{2+}	1.52	3.52
Li^{+}	—	4.24
K^{+}	4.00	5.70
Na^{+}	3.50[c]	5.20[c]
H^{+}	−8.00[c]	−4.20[c]

[a] Model 92-20.
[b] With nonporous PVC membrane.
[c] As measured by mixed solution method. See text and Figs. 2, 5 and 7.

phonate (DOPP-n) used as a solvent; therefore the effect should be common for both DDP and DOPP electrodes.

Selectrodes with DOPP ion exchanger and a solid-state reference system.

The progress in the development of PVC[8,35,36] and other nonporous polymer

membranes has made unnecessary the reservoir of organic ion exchanger within the electrode body, such as that found in the Ross construction[3] or the liquid-state selectrode[18]. This has made it possible to apply the concept of the reference selectrode[18] (which employs a humidified solid salt instead of a saturated solution of electrolyte) in the development of the present solid-state inner reference system. Thus in the calcium selectrode (Fig. 4), a paste made of mercury–calomel–potassium chloride–calcium sulphate is rubbed into the teflon–graphite surface, forming a reference layer between the teflon–graphite body (d) and the PVC membrane (f) which is placed on the reference layer and held in position by a teflon cap. The teflon tube (c) ensures the water tightness of the electrode cavity and is threaded so that the cup can be screwed onto the electrode body (e).

The calibration curve of the electrode, measured in cell A1, where the sample was provided by calcium buffers, remained practically unchanged during a seven-week testing period (Fig. 5; Table II) with an average slope of 30.89 mV/pCa and with a standard deviation of 0.32 mV; the E^0_{ISE} value was 60.56 with a standard deviation of 2.75 mV, corresponding to an asymmetry potential of *ca.* +2 mV. The linear response range of the DOPP-based selectrode covered pCa 2–5.7, which is a significant improvement on the DDP-based electrodes.

The selectivity parameters towards foreign ions as measured over a seven-week period remained unchanged (being close to the values reproduced in Table III), and so did the potential–pH dependence (Fig. 9), which was recorded in exactly the same manner as for the Orion electrode (Fig. 2). In addition to the curves obtained in calcium chloride solutions ($1.0 \cdot 10^{-2}$–$1.0 \cdot 10^{-4}$ *M*), curves (denoted CaL/L) were recorded in solutions of $1.0 \cdot 10^{-3}$ *M* $CaCl_2 + 2.0 \cdot 10^{-3}$ *M* EDTA at two different sodium levels. As denoted by eqn. (7), these curves depict the maximum electrode sensitivity at the respective sodium background levels. The plateau on the curves, at high pH values (*i.e.*, also at high pCa values), is due to sodium interference, which is much more serious for the Orion (DDP) electrode than for the DOPP-based calcium selectrode. These limits of detection are in very good agreement with those measured in calcium buffers (Fig. 5), and with the end-point potentials recorded in complexiметric titrations of calcium by EDTA at various sodium levels. The shape of these titration curves ought, of course, to be predictable from the potential–pH diagrams for any particular pH, initial pCa level and background pNa value[32]. In order to confirm this automated titrations of $1.0 \cdot 10^{-3}$ *M* calcium solutions were carried out at pH 9 (borate buffer) at pNa = 2.3 and pNa = 1, respectively, in exactly the same manner with the Orion electrode and the selectrode. The recorded curves (Fig. 6) clearly show the difference in magnitude of the potential jumps at the equivalence point for the two electrodes, owing to the different selectivities of the DDP and DOPP membranes. When the potentials at the end of the titration are compared with the CaL/L curves of Figs. 2 and 9, it should be borne in mind that the CaL/L curves correspond to a value of fraction titrated (f) equal to 2, which, however, corresponds to a potential 9 mV less positive than for $f = 1.5$. Finally, the dotted titration curve of Fig. 6, also depicting a calcium–EDTA titration, should be mentioned. Here, all the sodium, even in the EDTA salt, was replaced by potassium, so that the titration was carried out at a potassium level of pK = 2.3. As the calcium selectrode has a better selectivity towards potassium than towards sodium, a slightly higher potential jump is observed.

Influence of solvent on the electrode function

Much speculation is possible on the role of the dioctylphenylphosphonate used as a solvent in the DDP- and DOPP-based electrodes. Unfortunately, the data available on synergetic extractions with phosphate–phosphonate mixtures deal only with equilibria at low loadings of the organic phase which is diluted with a carrier solvent like toluene or kerosene[28,37]. Therefore, for electrode membranes, which operate under quite different conditions, the necessity of using phosphonate-based solvents can be supported only by experimental evidence, like that presented in Fig. 10. Here, calibration curves are depicted for (A) the DOPP–dioctylphenylphosphonate–PVC membrane; (B) the dioctylphenylphosphonate–PVC membrane; (C)

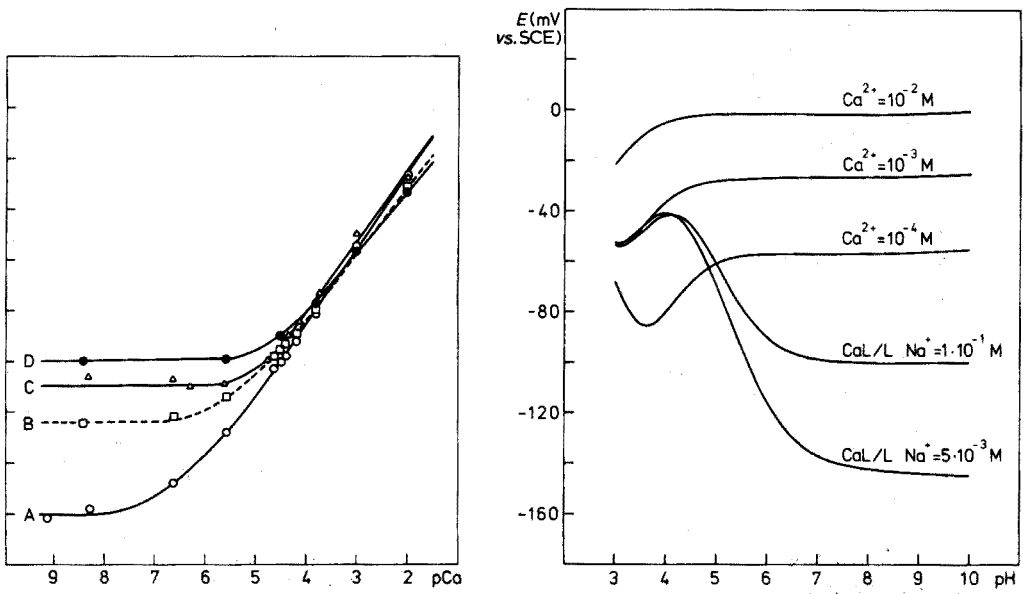

Fig. 10. Calibration curves of selectrodes in pCa buffers at pNa = 1.0, obtained with the following membranes: (A) DOPP/DOPP-n/PVC; (B) DOPP-n/PVC; (C) DDP/DOPP-n/PVC; (D) DOPP/tributylphosphate/PVC.

Fig. 11. Potential–pH diagram of the selectrode, with the membrane containing only the solvent (DOPP-n), at various PCa and pNa levels, in absence and presence (CaL/L) of EDTA.

the DDP–dioctylphenylphosphonate (Orion)–PVC membrane; and (D) the DOPP–tributylphosphate–PVC membrane. Most surprisingly, electrode B, containing solvent only, has better selectivity towards sodium than electrode C, containing the same solvent in combination with DDP. The potential–pH diagram obtained with electrode B (Fig. 11) is even more revealing as it not only confirms the better selectivity of this electrode compared to Orion electrode (C), but also shows a characteristic minimum located approximately half-way between those of the Orion (DDP) and the DOPP electrodes. As the solvent dioctylphenylphosphonate (DOPP-n) was found to contain an unknown acid in an amount of $6 \cdot 10^{-3}$ moles kg^{-1}, the likely reason for this behaviour is the presence of organophosphonic acid, such as HOPP or HOPP-n (p. 161), which forms an extractable calcium

chelate[27]. No attempts were made to purify the solvent, because the organophosphate and organophosphonate compounds are very difficult to purify, and when pure, decompose again readily to form a mixture of mono- and disubstituted compounds.

CONCLUSION

The comparison of extraction data with electrode behaviour has confirmed their intimate connection, and has assisted in selecting a new electroactive material with improved calcium selectivity parameters. It has been shown that the peculiar shape of the potential–pH curves, which long has remained unexplained, can always be expected, with organophosphate extractants at least, when species of different extractabilities are formed at various pH levels[29,30].

The outstanding properties of nonporous PVC membranes have been confirmed. These observations, together with the experience obtained during experiments with a valinomycine-based potassium electrode (with a nonporous polymer PVC membrane)[36], has led to the conclusion that the liquid porous membrane electrodes have become obsolete. For this reason, work on liquid-state selectrodes[18], employing a porous membrane and a porous pellet, has been terminated. The same basic electrode construction, however, has been used in the present study to accommodate the PVC membrane and a solid-state inner reference system. This combination, which also has yielded a successful potassium selectrode, is the basis for the membrane selectrodes, which are at the same time versatile, robust and easy to assemble. The same electrode body can be used many times, and can in turn accommodate various combinations of membranes and reference systems. These features have indeed been found useful in the present study, during which hundreds of various calcium selectrodes were made and tested, with only about half a dozen electrode bodies.

With regard to the calcium selectrode, the possibilities for its application seem to be many. Thus the direct potentiometric titration of calcium in sea water by means of EDTA has already been successfully demonstrated[38], in spite of the presence of considerable amounts of magnesium. Likewise, the calcium selectrode offers great possibilities for the determination of the total calcium content in blood. Initial experiments on measurements of calcium activities in serum have proved highly successful[39].

Finally, it should be emphasized that the use of calcium electrodes should be based on careful calibration of the electrodes in calcium buffers. Without access to such solutions, the present development of the calcium selectrode would not have been possible.

The authors wish to express their gratitude to Mrs. Eva Thale for valuable technical assistance; to the Danish Government Fund for Scientific and Industrial Research for financial support of the preliminary studies[19]; to Dr. H. W. Holy from the Technicon International Division (Switzerland) for donations of various rare chemicals; to Dr. J. R. D. Thomas from UWIST, Cardiff (UK) for samples of PVC; and to Dr. T. F. Christiansen of Radiometer A/S (Copenhagen) for critical cooperation and valuable discussions.

SUMMARY

The correlation between extraction data and electrode behaviour assisted in explaining the vital properties of organophosphate-based calcium electrodes, and in suggesting a new liquid ion exchanger, di-(n-octylphenyl) phosphoric acid. This compound has been synthesized and used in various electrode constructions including a newly developed membrane selectrode with a solid-state inner reference system. The resulting calcium(II) selectrode, calibrated in a series of calcium buffers, has been subjected to potential–pH measurements, and used in EDTA titrations. The selectivity parameters of this electrode towards Na^+, H^+ and other foreign ions were found to be substantially better than those of any other calcium sensors previously described.

RÉSUMÉ

Une nouvelle sélectrode calcium est proposée, avec acide di-(n-octylphényl)phosphorique comme échangeur d'ions liquide. Ce composé a été synthétisé et utilisé dans la fabrication de diverses électrodes. La sélectrode calcium proposée, calibrée à l'aide d'une série de tampons calcium, a été appliquée à des mesures de potentiel–pH et utilisée pour des titrages au moyen d'EDTA. Les paramètres de sélectivité de cette électrode vis-à-vis de Na^+ et autres ions étrangers sont nettement meilleurs que ceux obtenus précédemment.

ZUSAMMENFASSUNG

Auf Grund der Wechselbeziehung zwischen Extraktionseigenschaften und Elektrodenverhalten wurden die wesentlichen Eigenschaften von Calciumelektroden auf Organophosphat-Basis erklärt und ein neuer flüssiger Ionenaustauscher, Di-(n-octylphenyl)-phosphorsäure, vorgeschlagen. Diese Verbindung wurde dargestellt und für verschiedene Elektrodenkonstruktionen verwendet, zu denen eine neu entwickelte Membran-Selektrode mit einem Festkörper-Bezugssystem gehörte. Die hiermit erhaltene Calcium-Selektrode, die mit einer Reihe von Calcium-Pufferlösungen geeicht worden war, wurde Potential–pH-Messungen unterworfen und bei EDTA-Titrationen verwendet. Die Selektivitätsparameter dieser Elektrode gegenüber Na^+, H^+ und anderen Fremdionen erwiesen sich als wesentlich besser als die von allen anderen bisher beschriebenen Calcium-Sensoren.

REFERENCES

1 W. M. Clark, *The Determination of Hydrogen Ions*, William and Wilkins, Baltimore, 1923.
2 R. Z. Luther, *Phys. Chem.*, 27 (1898) 364.
3 J. W. Ross, *Science*, 156 (1967) 1378.
4 Orion Research, *Instruction Manual, Calcium Ion Electrode Model 92-20*, 1968.
5 Beckman, *Select Ion Electrodes, Bulletin 7145-A.*
6 Corning–EEL Scientific Instruments, *pH and Ion-Selective Electrodes.*
7 Philips Analytical Equipment, *Liquid Membrane Calcium Electrode No. IS560-Ca.*
8 G. J. Moody and J. R. D. Thomas, *Selective Ion Sensitive Electrodes*, Merrow, 1971.
9 J. Bagg and R. Vinen, *Anal. Chem.*, 44 (1972) 1773.
10 M. Mascini and A. Liberti, *Anal. Chim. Acta*, 53 (1971) 202.

11 G. A. Rechnitz and M. T. Hseu, *Anal. Chem.*, 41 (1969) 111.
12 *Radiometer Test Report on Hisel Electrode*, Copenhagen, 1971; *Israel Patent 26.233.*
13 A. Shatkay, *Anal. Chem.*, 39 (1967) 1056.
14 G. J. Moody, R. B. Oke and J. R. D. Thomas, *Analyst*, 95 (1970) 910.
15 G. H. Griffiths, G. J. Moody and J. R. D. Thomas, *Analyst*, 97 (1972) 420.
16 J. Růžička and J. Chr. Tjell, *Anal. Chim. Acta*, 47 (1969) 475.
17 J. Růžička and J. Chr. Tjell, *Anal. Chim. Acta*, 49 (1970) 346.
18 J. Růžička, C. G. Lamm and J. Chr. Tjell, *Anal. Chim. Acta*, 62 (1972) 15.
19 E. Gwozdz, *Some Investigations on Calcium-Specific Liquid-State Electrodes*, Report for the Danish Government Fund for Scientific and Industrial Research, Chem. Dept. A, Techn. Univ., Denmark, 1972.
20 J. Koryta, *Anal. Chim. Acta*, 61 (1972) 329.
21 H. James, G. Carmack and H. Freiser, *Anal. Chem.*, 44 (1972) 856.
22 J. Růžička and J. Chr. Tjell, *Anal. Chim. Acta*, 50 (1970) 1.
23 H. J. James, P. G. Carmack and H. Freiser, *Anal. Chem.*, 44 (1972) 853.
24 *Belgian Patent No. 668409; U.S. Patent 3.445365.*
25 J. Stary, *The Solvent Extraction of Metal Chelates*, Publishing House "Peace", Moscow, 1966.
26 K. Kimura, *Bull. Chem. Soc. Jap.*, 33 (1960) 1038.
27 D. F. Peppard, G. W. Mason, S. McCarty and D. F. Johnson, *J. Inorg. Nucl. Chem.*, 24 (1962) 321.
28 Y. Marcus and A. S. Kertes, *Ion Exchange and Solvent Extraction of Metal Complexes*, Wiley–Interscience, London, 1969, Ch. 9.
29 W. J. McDowell and C. F. Coleman, *J. Inorg. Nucl. Chem.*, 28 (1966) 1083.
30 F. D. Shevcenko, V. A. Ageev and A. D. Sazhenjuk, *Zh. Neorg. Khim.*, 17 (1972) 204.
31 R. G. Bates and M. Alfenaar, Activity Standards for Ion Selective Electrodes, in R. Durst, *Ion-selective Electrodes*, NBS Spec. Publ. 314, Washington, 1969, Ch. 6.
32 E. H. Hansen, C. G. Lamm and J. Růžička, *Anal. Chim. Acta*, 59 (1972) 403.
33 A. Ringbom, *Complexation in Analytical Chemistry*, Interscience, New York, 1963.
34 G. H. Griffiths, G. J. Moody and J. R. D. Thomas, *J. Inorg. Nucl. Chem.*, 34 (1972) 3043.
35 J. Chr. Tjell and J. Růžička, *British Patent No. 45291/72.*
36 U. Fiedler and J. Růžička, *Anal. Chim. Acta*, 67 (1973) 179.
37 D. F. Peppard, Liquid–Liquid Extraction of Metal Ions, in *Advances of Inorganic Chemistry and Radiochemistry*, Vol. 9, Academic Press, New York, 1966.
38 D. Jägner, private communication.
39 J. Melchior-Rasmussen, lecture for *The Danish Society for Clinical Chemistry, Copenhagen, 1972.*

Analytica Chimica Acta, 67 (1973) 179–193

SELECTRODE—THE UNIVERSAL ION-SELECTIVE ELECTRODE

PART VII. A VALINOMYCIN-BASED POTASSIUM ELECTRODE WITH NONPOROUS POLYMER MEMBRANE AND SOLID-STATE INNER REFERENCE SYSTEM

U. FIEDLER

Department of Analytical Chemistry, Chemical Center, University of Lund, S-220 07 Lund 7 (Sweden)

J. RŮŽIČKA

Chemistry Department A, The Technical University of Denmark, Building 207, 2800 Lyngby (Denmark)

(Received 2nd April 1973)

The most successful potassium electrode, suggested by Pioda *et al.*[1] utilizes a macrocyclic substance from a group of depsipeptides—valinomycin, containing a 36-membered ring. This antibiotic, produced by the cultures of *Streptomyces fulvissimus*, forms complexes with alkali metal ions[2], the stabilities of which decrease in the order $Rb^+ > K^+ \gg Na^+ > Li^+$. The remarkable difference in the stabilities of the potassium and sodium complexes is not only of importance in biomedical sciences[3], but is also the reason for the high selectivity of the potassium electrode ($K_{KNa} \sim 1 \cdot 10^{-4}$)[1,4] based on this compound.

The structure of the potassium–valinomycin complex resembles a cylinder with a diameter of 15 Å and a height of 12 Å with all polar groups oriented towards the centre of the molecule—where the potassium ion is held, while the apolar, lipophilic groups are turned outwards. Various mechanisms of potassium transfer across the membrane have been suggested and investigated[5,6], the most likely being the "carrier relay" or the "mobile site" mechanism.

The first valinomycin electrode[1] utilized diphenylether as a solvent (0.009 *M*) and so does its commercial version, manufactured by Philips[7]. Although Frant and Ross tried a variety of organic solvents[8,9] (such as nitrobenzene and its higher homologues, chlorobenzene and bromobenzene), the final version of Orion electrode is also said to employ a solution of valinomycin in diphenylether (0.0045 *M*)[6]. The reasons for selecting this particular solvent were never explained, yet this choice is rather peculiar—at least for two reasons. First, diphenylether has a melting point of 28°, but "frozen" membranes do not respond to potassium[6]; secondly, diphenylether alone yields an electrode responding to both potassium and sodium[8,9] ($K_{KNa} = 0.025$). Thus a mixed potential will be measured at high Na^+/K^+ activity ratios, causing a decrease of electrode selectivity.

The purpose of the present work was to investigate the influence of organic solvents on the performance of valinomycin-based potassium electrodes and to incorporate the resulting ion exchanger into a polymer membrane. Various membranes were therefore mounted and tested in the following cells:

Cell I:

$$\overbrace{Ag|AgCl|KCl(1\cdot 10^{-2}M)|membrane}^{ISE}|\ sample\ \ldots\ \ldots\overbrace{\|NaCl(2M)\|KCl(sat.)|Hg_2Cl_2|Hg}^{Ref.}$$

Cell II:

$$\overbrace{Teflon/Graphite,\ Hg|Hg_2Cl_2|KCl(sat.)|membrane}^{ISE}|\ sample\ \ldots\ \ldots\overbrace{\|NaCl(2M)\|KCl(sat.)|Hg_2Cl_2|Hg}^{Ref.}$$

Here "Ref." denotes a double-junction calomel electrode and "ISE" the ion-selective electrode. In cell I, the actual ion-selective electrode was the electrode produced by Philips[1,7] with a porous membrane, while in cell II, the ion-selective electrode was the selectrode with the solid-state inner reference system[10,11] and nonporous polymer membrane.

The behaviour of electrodes was judged in the usual manner, *i.e.* the extent to which the e.m.f. of the cell agreed with the value predicted by the Nernst equation:

$$E = E^0 + \frac{RT}{F} \ln \left([K^+] + \sum_i K_{KM} \cdot [M^{z_i+}]^{1/z_i} \right) \qquad (1)$$

At 25°, E^0 (obtained by extrapolation from the calculated E at pK 2) for cell I should be +213 mV *vs.* S.C.E., and for cell II −26 mV *vs.* S.C.E., if zero junction potentials between sample–2 *M* NaCl–sat. KCl and the absence of interfering ions and of asymmetry potential are assumed. Other symbols in eqn. (1) have the usual meaning[12], except that activities have been replaced by concentrations, because the ionic strengths of all sample solutions were adjusted to a constant level ($\mu = 0.10$) with sodium chloride. This approach, although questionable, is the most relevant from a practical viewpoint, because the sodium chloride level is similar in serum samples, where the potassium electrode is most frequently used.

EXPERIMENTAL

Reagents

Electroactive material. Valinomycin was donated by CIBA. Analysis by means of e.s.c.a. proved that the product was completely unloaded with respect to potassium.

Solvents. Dioctyladipate and dioctylphthalate were of technical grade (Scandinol, Copenhagen), all other solvents being of analytical-grade quality.

Polymers. Polyvinylchloride (PVC; Breon 113; B.P. Chemicals (U.K.), Ltd.), and polyurethane (Estane; B.F. Goodrich Chemical Company) were used.

Inner reference system. Calomel paste was prepared by mixing 3 g of mercury–mercury(I) chloride with 1 g of potassium chloride, and moistening with saturated potassium chloride.

Calibration solutions

All sample solutions were prepared to have a constant ionic strength ($\mu = 0.10$). Thus the ionic activity was directly proportional to the concentration of potassium ions forming the basis for an operational pK scale defined by $pK = -\log[K^+]$. The contribution from the activity coefficient is incorporated into the E^0 term. Hence the true position of the calibration curve may remain virtually unknown, although it is well fixed. Moreover, by keeping the ionic strength constant, any variation in the junction potential of the reference electrode is avoided, the constant term E_j being included in the E^0 value.

Unfortunately, the concept of metal buffers[13] cannot be applied to potassium, for no suitable complexing agent exists. Thus, calibration solutions in the region pK 2–7 were prepared by dilution of potassium chloride. The ionic strength of all solutions was made up to 0.10 by addition of a calculated amount of sodium chloride (Merck, suprapur; containing less than 10^{-3}% K). The water used throughout was deionized and freshly redistilled. All solutions were stored in plastic bottles.

Electrodes

The selectrode construction used in these experiments has already been described[10,11]. The *potassium-selectrode* was prepared by rubbing the calomel paste into the teflon–graphite surface (solid-state inner reference system), and then fixing the polymer membrane in position by screwing the cup. *Membranes* were prepared as described by Griffiths *et al.*[14]. The valinomycin solution (0.180 g) and polymer (0.075 g for 29% polymer-content) were dissolved in about 3 ml of A.R.-grade tetrahydrofuran and poured over a nylon net placed in a 26-mm i.d. glass ring, resting on a glass plate, followed by slow solvent evaporation. The nylon net was incorporated into the membrane in order to increase its mechanical strength. From this prepared membrane (0.3 mm thick) a 6-mm diameter disc was cut with a cork borer and fixed to the selectrode body by means of the cup.

Philips potassium electrode, type IS 560-K was assembled according to manufacturer's instructions.

Electrodes used for pH checks and recording were the *glass electrode* (Radiometer type G 202 B) together with a *reference calomel electrode* provided with a double junction (Radiometer type K701) filled with 2 M sodium chloride.

Apparatus

All potential measurements on potassium electrodes were performed with a digital pH meter 52 (Radiometer A/S, Copenhagen) accurate to within ± 0.1 mV. For automatic pK/pH measurements, an automatic scanning potentiometer, an autoburette ABU 13, two pH meters 51 (Radiometer) together with an X-Y recorder (Watanabe) were used. Automatic titrations were performed with the autoburette ABU 13, the pH meter 51 and a Servogor recorder.

Measurement techniques

All measurements (except temperature dependence) were carried out at $25 \pm 1°$, and potentials are referred to the double-junction saturated calomel electrode (S.C.E.).

pK response. Before use, the commercial electrode was treated according to manufacturer's instructions and the selectrodes were conditioned in 0.01 *M* potassium solution for 6 h. Testing of all electrodes was done by immersing them in 100 ml of well mixed calibration solutions (all 0.10 *M* with respect to sodium), and the potentials were measured after a stable value (±0.2 mV) had been obtained. The static response times, when calibrating from dilute to more concentrated solutions, were up to 5 min for high p*K* values (>5) but usually *ca.* 1 min for low ones (<5). The dynamic response times were all less than 10 s.

Temperature dependence. Electrodes were calibrated in solutions of various temperatures between 5° and 50°. Before measurement, both electrodes and sample solutions were allowed to equilibrate at the given temperature for 1 h.

Selectivities for different cations were measured in mixed solutions of primary and interfering ion by taking a constant background of interfering ion, 0.10 *M*, and varying the potassium-ion activity. The selectivity coefficients were then calculated in two different ways (ref. 4, p. 14) for comparison:

$$(a) \qquad K_{KM} = \frac{a_{K^+}}{(a_{M^{z+}})^{1/z}}$$

where a_{K^+} is defined by the intercept of the horizontal interfering ion response line with the potassium calibration line, and z is the valency of the interfering ion M.

$$(b) \qquad a_{K^+} = K_{KM}((a_{M^{z+}})^{1/z} \cdot 10^{(E_{12}^1 - E_2)/59.16} - [a_{M^{z+}}^1]^{1/z})$$

where E_2 is the potential in solution containing the interfering ion of activity $a_{M^{z+}}$, and E_{12}^1 is the mixed potential obtained in a solution of potassium (a_{K^+}) and interfering ion ($a_{M^{z+}}^1$).

All activities in this study were calculated from the following form of the Debye–Hückel equation at 25°:

$$-\log f = 0.511\, z^2 \left(\frac{\sqrt{\mu}}{1+\sqrt{\mu}} - 0.2\mu\right)$$

The potential–pH curves were recorded automatically at a speed of one pH unit per 2 min. The scanning always started at pH 3 and was done by automated addition of sodium hydroxide. Potential values below pH 3 and above pH 10 were obtained manually, point-wise.

Potentiometric titrations were also carried out automatically. Potassium solution (100 ml) was titrated with 0.10 *M* sodium tetraphenylborate solution, added to the test solution at a constant speed of 0.14–1.08 ml min^{-1} (depending on the concentration of potassium) from the autoburette. Titrations in the presence of 0.10 *M* sodium ion were also performed.

Computations

All slopes were calculated by means of regression analysis on the linear part of the calibration curve. The E^0 value was obtained by extrapolation to p*K* 0, and the intercept between the calibration line and the lower detection limit determined the selectivity coefficient in the solution used. Selectivity coefficients K_{KM} are expressed as $pK_{KM} = -\log K_{KM}$. This value indicates the maximum

sensitivity obtained towards potassium in a 1 M solution of interfering ion, independent of its valency (neglecting the difference in activity coefficients).

All values of slope, E^0 and pK_{KM} stated in this work are mean values of measurements on at least three electrodes.

RESULTS

The properties of two electrodes—the Philips porous membrane type with diphenylether as solvent, and the selectrode with polyvinylchloride–dioctyladipate nonporous membrane—are described in detail. Some of the results obtained with polyurethane membranes are briefly mentioned. The main features of all the other electrodes tested are summarized in Table I. The aim of these additional measurements was to gather sufficient material for a more general discussion on polymer membranes.

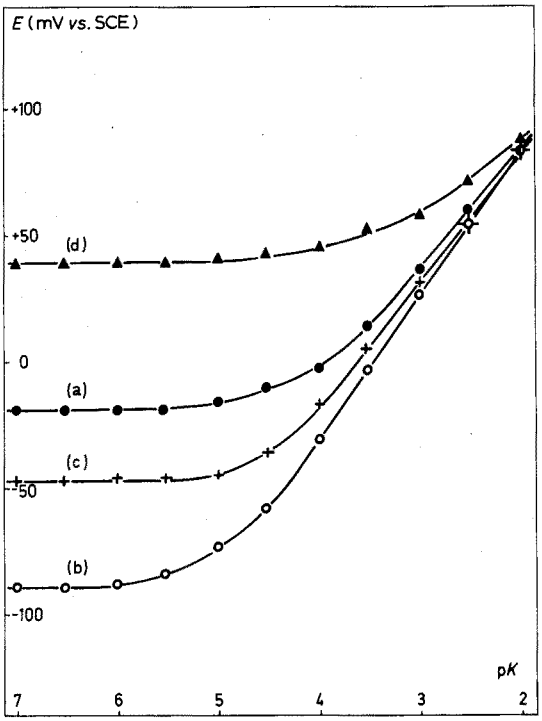

Fig. 1. Calibration curves for Philips potassium electrode with (a) "empty" membrane (pure diphenylether); and with a membrane containing a solution of valinomycin in diphenylether: (b) immediately after conditioning, (c) after "freezing" experiments, and (d) after use in titrations with sodium tetraphenylborate.

Philips potassium electrode

The original, freshly supplied Philips ion exchanger in the Philips electrode construction and membrane (cell I) yielded a very good electrode, which responded as described by Pioda *et al.*[1] as well as by the manufacturer's specifications[7]

TABLE I POTASSIUM SELECTRODES WITH POLYMER MEMBRANES

Parent membrane no.	*Polymer*	*Polymer content (%)*	*Solvent*[a]	*Approx. concn. of valinomycin (M)*	*Slope mV/pK*	pK_{KNa}	E^0_{ISE} *(mV)*	*Physical properties of membrane*[b]
1	PVC	29	DOA	—	9.0	2.33	−89	T
2	PVC	29	DOA	0.010	57.1 ± 0.4[d]	4.22 ± 0.12[d]	−14.8 ± 5.4[d]	T
3	PVC	29	DOA	0.100	57.1	4.29	−34	T
4	PVC	29	DOP	0.010	49.6	3.95	+28	T
5	PVC	29	D	0.010	50.7	4.00	+20	T Membrane exudes solvent, yielding a stiff membrane ($T_g > 25°$). Very slow response
6	Polyurethane	100	—	—	~3	~2	−48	T
7	Polyurethane	100	—	+VAL[c]	29.0	3.30	+89	T
8	Polyurethane	50	DOP	—	19.0	2.63	+16	T
9	Polyurethane	83	DOP	0.010	49.5	2.71	+81	T
10	Polyurethane	70	DOP	0.010	51.0	3.49	+93	T
11	Polyurethane	50	DOP	0.010	53.4	3.98	+72	T
12	Polyurethane	50	DOA	—	30.0	2.50	+35	O
13	Polyurethane	50	DOA	0.010	54.4	4.13	+39[e]	O
14	Polyurethane	75	DOA	0.010	50.8	3.56	+67	T
15	Silicone rubber	67	DOA	—	38.7	3.64	+6	O
16	Silicone rubber	67	DOA	0.050	55.4	3.88	+73	O
17	Polystyrene	70	DOP	0.010	~2	—	−6	T Stiff membrane ($T_g > 25°$)
18	Polystyrene	50	DOP	0.010	42.0	2.67	+8	T
19	Polystyrene	50	DOA	0.010	50.0	3.44	+8	T Membrane exudes solvent
20	Polymethyl-methacrylate	50	DOA	—	44.0	2.91	+7	O Stiff membrane ($T_g > 25°$). Very slow response
21	Polymethyl-methacrylate	50	DOA	0.010	38.0	3.32	−24	O Stiff membrane ($T_g > 25°$)
22	Polymethyl-methacrylate	50	DEP	—	~1	—	−7	T very slow response.
23	Polymethyl-methacrylate	50	DEP	0.010	24.0	2.71	+26	T Low solubility of valinomycin in DEP

[a] DOA = dioctyladipate. DOP = dioctylphthalate. D = diphenylether. DEP = diethylphthalate.
[b] T = transparent. O = opalescent.
[c] Membrane made of solid valinomycin (*ca.* 1%) + polyurethane (~99%).
[d] Calculation of mean value and 95% confidence interval based on results from 16 electrodes. Calculated from $\bar{x} \pm sn^{-\frac{1}{2}} \cdot t_{0.975(n-1)}$ from Student's *t*.

BLE II

LECTIVITY COEFFICIENTS OF VALINOMYCIN-BASED POTASSIUM ELECTRODES

l selectivity coefficients expressed as $-\log K_{KM} = pK_{KM}$)

erfering	VAL–DOA–PVC selectrode		Philips electrode IS 560-K			Orion electrode
	Method a 0.10 M	Method b 0.10 M	Method a 0.10 M	Method b 0.10 M	Pioda et al. (ref. 1) 0.10 M	Frant and Ross (ref. 8) 0.01–0.10 M
+	0.33[a]	0.39	0.33[a]	0.37	0.40	0.00
+	−0.67[a]	−0.60	−0.67[a]	−0.60	−0.28	—
+	4.22	4.11	4.02	3.89	3.60	4.15
	3.62	3.38	3.66	3.41	3.70	—
H_4^+	1.88	1.65	1.80	1.55	2.00	1.70
+	4.36	4.03	3.76	3.42	8.70[b]	—
$^{2+}$	4.35	4.17	4.39	4.23	3.70	3.70
2+	4.31	4.16	4.38	4.22	3.60	3.70
2+	3.94	3.74	3.98	3.77	4.22	—
2+	4.78	4.66	4.85	4.74	3.40	—
2+	4.46	4.38	4.39	4.24	—	—

$^{z+}$ located by: ΔE (interferent line − calibration line) = 18/z mV (ref. 4, p. 15).
eems improbable.

(Fig. 1, curve b; Table II). The same ion exchanger, however, after three months of storage at room temperature, gave electrodes with slightly lower slope (57.0 mV/pK compared to 58.8 mV/pK originally) and also slightly worse selectivity towards sodium ($pK_{KNa} = 4.02$ compared to $pK_{KNa} = 4.21$ originally). In contrast to observations by Eyal and Rechnitz[6], that diphenylether–valinomycin electrodes cease to function upon freezing (measured on Orion electrode), the Philips electrode retained a slope of 54.2 mV/pK (and $pK_{KNa} = 3.83$) even at 5° with an isopotential point[15] at pK 3. Subsequent measurements at 25°, however, showed that the electrode deteriorated somewhat after such a treatment (Fig. 1, curve c). Comparative experiments with the liquid-state selectrode construction[10] with a porous membrane and a graphite–KH_2PO_4/K_2HPO_4 inner reference system, were performed with valinomycin solution in diphenylether (0.010 M) and in a (1+1) diphenylether–mesitylene mixture (0.010 M). These electrodes exhibited an almost Nernstian slope (57.7 mV/pK and 58.1 mV/pK, respectively) and showed an extremely good selectivity towards sodium ($pK_{KNa} = 4.49$ and $pK_{KNa} = 4.55$ respectively). Freezing experiments showed that the diphenylether electrodes indeed ceased to function, while the ion exchanger containing mesitylene, the freezing point of which is lowered below 0°, functioned well even at 5° (slope 53.2 mV/pK and $pK_{KNa} = 4.56$), and the electrodes did not deteriorate upon cooling.

The selectivities of a freshly prepared Philips electrode, measured by the mixed solution method[4] with a constant level of interfering ion, was in good agreement with literature data (Table II). The potential–pH diagram of a Philips electrode showed an almost negligible pH dependence (Fig. 2). The stability of electrode potential was also satisfactory, the starting point after 24 h of conditioning (in 0.10 M KCl, 0.01 M NaCl)[7] being +197 mV (E^0) while after 1 week

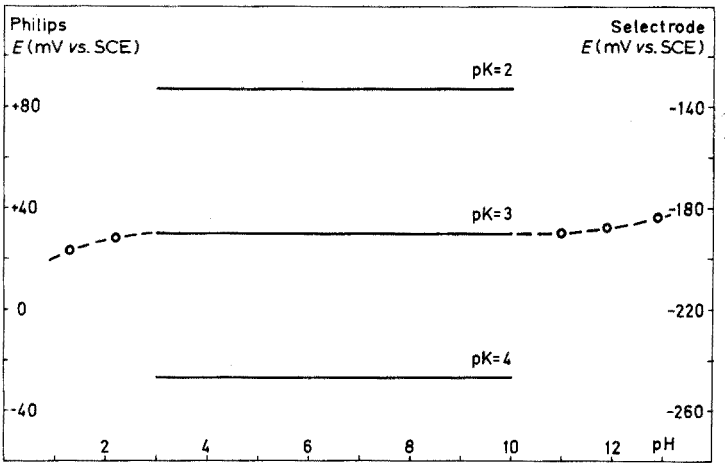

Fig. 2. Potential–pH diagram for Philips potassium electrode and for the potassium selectrode in solutions of $pK = 2$, 3 and 4, respectively, at constant ionic strength and 0.10 M sodium content.

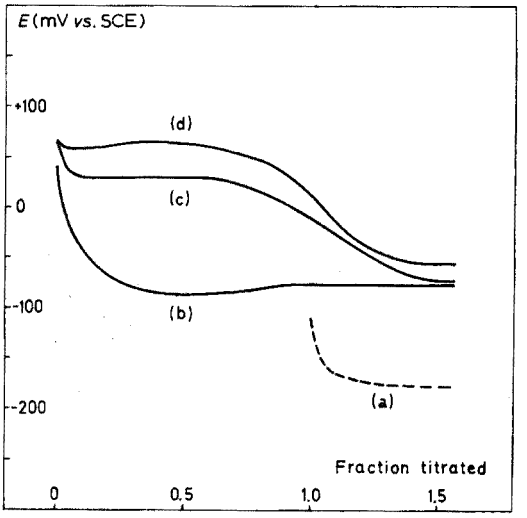

Fig. 3. Successive titrations of potassium ions by sodium tetraphenylborate with the Philips potassium electrode in (a) pure water (addition of 0.5 ml of 0.1 M titrant) and in potassium solutions of (b) $pK = 3.00$, (c) $pK = 2.30$ and (d) $pK = 2.00$.

the E^0 value was +175 mV. The asymmetry potential E_{ISE}^{AS} increased during the same period from −16 mV to −38 mV. Measurements with an electrode containing only pure solvent, confirmed the previous observations[6,8,9] on diphenylether response to potassium and sodium (Fig. 1, curve a).

During titrations of potassium with sodium tetraphenylborate, a peculiar electrode behaviour, already described by Lal and Christian[16] and Anfält[17], was observed (Fig. 3). After addition of an initial amount of titrant, a sudden drop of potential occurred, followed by a slow increase with time and also on addition of

further portions of titrant. The shape of the titration curve was further affected during subsequent titrations, as the initial potential became progressively more negative. The analysis of samples containing less than $5 \cdot 10^{-3}$ *M* potassium(I) was not feasible. It should be noted, however, that the relatively high solubility of potassium tetraphenylborate (0.065 g l^{-1} or $3.3 \cdot 10^{-8}$ M^2)[18] gives an equilibrium concentration of *ca.* $2 \cdot 10^{-4}$ *M*, thereby limiting the usefulness of this reagent for titration of very dilute potassium olutions. However, in the case of valinomycin-based potassium electrodes, it seems that a specific interaction between valinomycin and potassium tetraphenylborate takes place, and this is rather independent of the membrane material and solvent used (Figs. 3, 5). Under the influence of valinomycin, it is very probable that potassium tetraphenylborate is being dissolved in the organic membrane phase, thus causing a drop in potential. This also affects the slope and sodium sensitivity, as can be seen from calibrating the electrode after use in titrations (Fig. 1, curve d). However, upon treatment with pure potassium solution, the electrode is slowly restored owing to dissolution from the membrane. It is also noteworthy that pure sodium tetraphenylborate solution does not affect the membrane at all (probably because of lower complexation by valinomycin).

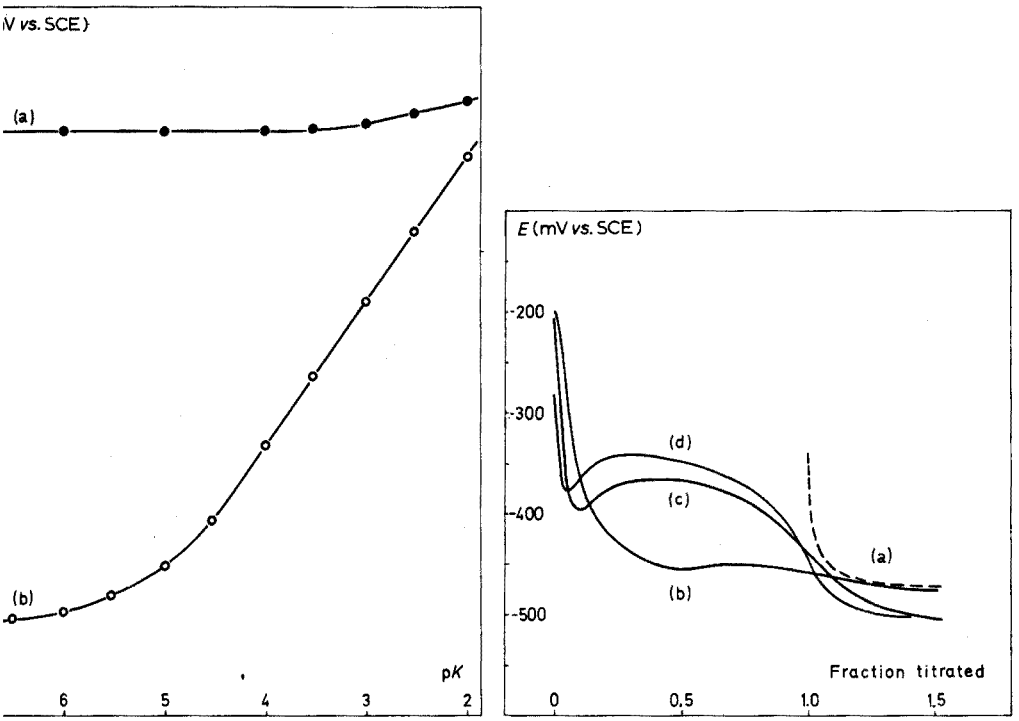

Fig. 4. Calibration curves for the potassium selectrode with (a) "empty" membrane (DOA–PVC) and (b) membrane containing valinomycin (valinomycin–DOA–PVC) after conditioning.

Fig. 5. Successive titrations of potassium ions by sodium tetraphenylborate with the potassium selectrode in (a) pure water (addition of 0.5 ml of 0.1 *M* titrant) and in potassium solutions of (b) $pK = 3.00$, (c) $pK = 2.30$ and (d) $pK = 2.00$.

Selectrodes with polymer membranes

Valinomycin–dioctyladipate–*polyvinylchloride* membranes mounted in the selectrode construction (Fig. 3 of ref. 11), cell II, yielded a slope close to the theoretical one (Fig. 4, curve b) with $E^0 = -15$ mV and the asymmetry potential $E_{ISE}^{AS} = +11$ mV (after 6 h of conditioning in $1 \cdot 10^{-2}$ *M* K^+). The higher values of E^0 and E_{ISE}^{AS} (+26 mV and +52 mV, respectively), as measured on freshly made electrodes, are probably due to the fact that the valinomycin used in this study was not originally loaded with potassium (see Reagents), and this conversion occurred at different rates from both sides of the membrane. During conditioning, the response improved from 55.5 mV/p*K* to 57.1 mV/p*K*. This is in agreement with the observation, that saturation of valinomycin by potassium is a slow process[3]. The loading effect was more pronounced with polymer membranes with "immobilized" ion-exchange sites than with porous membranes having greater intrinsic mobility. Electrodes conditioned in this way remained practically unchanged during at least 3 weeks of operation with a slope of 57.1 mV/p*K*, a sodium selectivity $pK_{KNa} = 4.22$ and an E^0 value of −15 mV. Additional measurements in saturated potassium chloride solution proved that the working range for the electrode indeed extended from 5 *M* to 10^{-6} *M* potassium(I) solutions. In contrast to "empty" diphenylether electrodes, no potassium response was observed with a dioctyladipate–PVC membrane (Fig. 4, curve a).

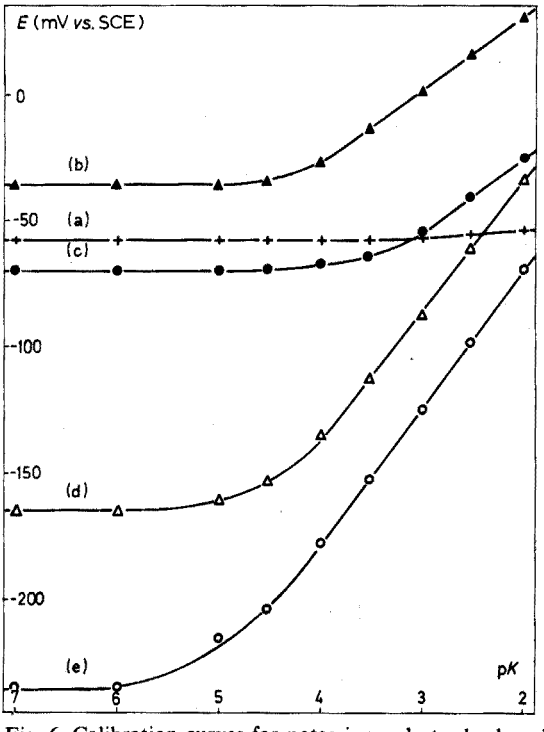

Fig. 6. Calibration curves for potassium selectrodes based on polyurethane (PU): (a) PU membrane, (b) valinomycin–PU membrane, (c) DOA–PU membrane, (d) and (e) valinomycin–DOA–PU membranes containing 75% and 50%, respectively, of polymer.

The pH dependence of the valinomycin–dioctyladipate–PVC selectrode (Fig. 2) is exactly the same as that of Philips electrode, but the selectivity towards sodium is higher for the selectrode (Table II). Its response at different temperatures (5–50°) is close to the Nernstian one, with an isopotential point at pK 2. Furthermore, it does not deteriorate upon cooling, having a slope of 52.7 mV/pK and a pK_{KNa} of 4.18 even at 5°.

Titrations of potassium by tetraphenylborate, although possible, were not reliable at low potassium concentrations (Fig. 5), as the same effects of potential drop were observed with polymer membrane selectrodes as with the Philips electrode.

Polyurethane also yields transparent membranes with good mechanical character, but, in contrast to PVC, even without addition of plasticizing solvent. It was therefore possible to study membranes made of pure polyurethane and of valinomycin–polyurethane in addition to the usual combinations of plasticizer–polyurethane and valinomycin–plasticizer–polyurethane (Fig. 6). The last combination with dioctyladipate as plasticizer resulted in a working electrode with properties very similar to the valinomycin–dioctyladipate–PVC selectrode. Dioctylphthalate plasticizer was also found to be useful. The expected pH sensitivity for pure polyurethane membranes was observed, but was found to be totally suppressed in the presence of electroactive material (valinomycin).

DISCUSSION

The results with valinomycin-based potassium electrodes described here, together with experiments on organophosphate-based calcium electrodes[11] confirm the superiority of polymer membranes. This construction feature is only a logical extension of the concept of the liquid membrane electrode[10] with a porous membrane soaked by a water-immiscible liquid. It has been recognized[4] that the smaller the pore diameter and the more viscous the organic liquid, the more stabilized is the membrane phase. In cast polymer membranes, the "pore size" is drastically diminished to macromolecular dimensions, while at the same time the intrinsic viscosity of the incorporated organic liquid is increased. In this "solidified" organic phase, convection is totally avoided, and diffusion of large molecules is considerably hindered. The resulting membrane appears to have a "dry" interior and swollen outer layers and can tolerate, like a glass electrode, high concentration of electrolytes and an excess of interfering ion, because the interior layer retains its original composition.

It appears that the individual components of the membrane can be selected according to the following rules, which are suggested on the basis of the results summarized in Table I.

1. Both electroactive compound and polymer must be soluble in the organic solvent used and the proportion of the components must be chosen so that a one-phase system is obtained.

2. Both polymer and solvent should be nonpolar and hydrophobic, and should ideally not contain any electroactive functional groups.

3. The solvent should dissolve as much as possible of the electroactive compound, must be insoluble in water, and should have a low vapour pressure

and preferably a high viscosity.

4. The glass transition temperature (T_g) of resulting polymer membrane should be well below room temperature.

The mutual compatibility of *all three* components is an obvious requirement, supported by all experimental evidence. Thus membranes containing valinomycin–dioctyladipate–PVC or valinomycin–dioctylphthalate–PVC, and the analogous polyurethane membranes for potassium (Table I), as well as organophosphate–phosphonate–PVC[4,11], tributylphosphate–PVC[11,19], organophosphate–tributylphosphate–PVC[11] and organophosphate–phosphonate–polyurethane membranes for calcium, were all transparent and functioned well. On the other hand, no, or only poor, potassium sensitivity was observed with membranes made of valinomycin–diphenylether–PVC (no. 5, Table I), owing to incompatibility of solvent and polymer. Although somewhat transparent, the membrane exuded the solvent, eventually yielding a porous membrane; similar behaviour was found with membrane no. 19 (Table I) made of valinomycin–dioctyladipate–polystyrene. An other example of incompatibility occurs when a solid precipitates within the membrane, owing to improperly chosen proportions of solvent and polymer, thus giving rise to an opaque membrane. Although this is also undesirable, as one-phase membranes are preferable, some membranes of this type could be used (no. 13, Table I).

The second rule requires the lack of any electroactive function in the polymer or solvent itself. Thus, for example, polymer membranes, based on cellulose acetate were tested in the HISEL electrodes[20], but were reported to have only about 80% of the theoretical slope and a pK_{KNa} value of 3. This is in agreement with the experience of Griffiths *et al.* that charged or hydrophilic membranes are not useful[14]. Although an "empty" membrane should have no electroactive function, this kind of membrane should always be prepared and tested, so that any contribution to the membrane potential can be evaluated. In the ideal case, the potassium electrode response would be entirely due to the presence of valinomycin. Closest to this behaviour are the valinomycin–dioctyladipate membranes made with PVC (Fig. 4) and polyurethane (Fig. 6), whereas an "empty" silicone rubber membrane is rather sensitive to potassium (no. 15, Table I).

The most interesting example of these electrodes, where both solvent and electroactive material exhibit a very pronounced electrode function, are organophosphate–phosphonate sensors for calcium[11]. The problems of such multicomponent systems, in which two or even several electroactive materials contribute to the potential, require much attention. Until more is known, as much as possible of electroactive material should be incorporated into the membrane—as suggested by the third rule (Fig. 6). This view seems to be supported by the results obtained with dioctyladipate and dioctylphthalate membranes (nos. 2, 4, 11, 13, Table I), for dioctyladipate always yielded better electrodes, owing to the higher solubility of valinomycin in the adipate than in the phthalate. Similarly, calcium–dioctylphenylphosphate–dioctyladipate–PVC membranes, although transparent and mechanically faultless, did not respond to calcium at all, whereas in electrodes containing a more suitable solvent for the calcium salt, *e.g.* dioctylphenylphosphonate or tributylphosphate, satisfactory calcium response and selectivity were obtained[11].

Below the glass transition temperature (T_g) polymers are hard and brittle, while above it they are soft and flexible. The glass transition occurs at the temperature when the liquid-like motion of large molecules becomes more restrained and is accompanied by a decrease of free volume. Polymers with T_g values below room temperature, *e.g.* polyurethane or silicone rubbers, are suitable for making membranes, and so is polyvinylchloride if the T_g (81°) is decreased by addition of plasticizers such as dioctyladipate, tributylphosphate, etc. The literature on polymer plasticizers[21] is very useful for choosing a suitable solvent (and its favourable proportion to polymer), as commercial plasticizers usually also fulfil most of the requirements stated above. However, organic solvents with good plasticizing properties (*e.g. p*-nitrocymene used in the PVC nitrate electrode[22]) can be found outside the range of commercial plasticizers—as they do not fulfil the requirements of low cost or nonflammability.

The significance of the T_g value and the role of bulk properties or molecular motion cannot yet be discussed definitively. The experiments described here show that membranes based on PVC, polyurethane and silicone rubber can be made responsive, while membranes made from polystyrene ($T_g = 100°$) and polymethylmethacrylate ($T_g = 105°$) were less successful, because of high T_g, low valinomycin solubility or simply the incompatibility of the components in the resulting membrane (nos. 17–23, Table I).

With regard to the potassium electrode, valinomycin is undoubtedly the most selective electroactive material. The peculiar behaviour of all valinomycin-based electrodes (regardless of the state of the membrane and the origin of the valinomycin) during titrations with tetraphenylborate limits the usefulness of the electrode in titrimetry. The valinomycin–dioctyladipate–polyvinylchloride membrane electrode described here has slightly better selectivities than the Philips valinomycin–diphenylether–porous membrane electrode, does not deteriorate at lower temperatures, and allows the use of simpler electrode construction with a solid-state inner reference system. Further improvement of electrode parameters seems to be possible only by using a better electroactive compound than valinomycin—possibly its analogue cyclo-[–L–Val–D–Pro–D–Val–L–Pro–]$_3$, which has recently been synthesized and reported to have a higher affinity for potassium[23].

CONCLUSION

By replacing diphenylether with a solvent compatible with a polymer material such as polyvinylchloride, polyurethane or even silicone rubber, nonporous membranes suitable for a potassium selectrode have been prepared. Some rules for the selection of appropriate polymer–solvent combinations are suggested on the basis of both successful and unsuccessful experiments with polymer membranes prepared in this work and experimental results of Moody and Thomas[4], Bloch *et al.*[19] and Kedem *et al.*[24] on PVC membrane electrodes.

It is believed that these rules will lead to the development of new combinations of materials so that all porous liquid membrane electrodes could be replaced by polymer membranes into which various extraction systems could be incorporated.

It is perhaps relevant to mention here that, just as the division between

"homogenous" and "heterogenous" solid-state electrodes has vanished, so will the distinction between solid-state and liquid-state membranes. Thus the only and most relevant classification is to first and higher order electrodes, and to membrane electrodes. The selectrode construction, which can accommodate both membrane[10,11] and non-membrane[13,25,26] electrodes, will remain useful.

The authors wish to express their sincere thanks to Professor N. Hofman-Bang for his interest in this work, to E. H. Hansen for helpful discussions, to G. Tuxen, CIBA, Copenhagen and H. Byckel, CIBA, Basel, for the gift of valinomycin, to Dr. J. D. R. Thomas for the gift of PVC, and to Assistant Professor B. Törnell for the gift of polyurethane. Finally, thanks are due to the Chemistry Department A for providing facilities and instrumentation for one of us (U.F.).

SUMMARY

A potassium electrode utilizing a solution of valinomycin in diphenylether and a porous membrane is compared with selectrodes in which the diphenylether has been replaced by a suitable plasticizer and the porous membrane support by a polymer net-work. The development of the polymer membrane allows the use of simplified selectrode construction with a "solid-state" calomel reference system. Rules for a successful choice of a suitable solvent–polymer combination are suggested and used for development of new polyvinylchloride- and polyurethane-based membranes.

RÉSUMÉ

Une électrode potassium, avec solution de valinomycine dans le diphényléther et membrane poreuse est comparée à des sélectrodes constituées d'un polymère non-poreux et d'un plastifiant approprié. Le développement de ces membranes à base de polymère permet l'utilisation d'une sélectrode simplifiée avec système de référence au calomel, à l'état solide. On indique les possibilités de combinaison solvant–polymère pour le développement de nouvelles membranes au chlorure de polyvinyle et polyuréthane.

ZUSAMMENFASSUNG

Eine Kaliumelektrode, bei der eine Lösung von Valinomycin in Diphenyläther und eine poröse Membran verwendet werden, wird mit Selektroden verglichen, in denen der Diphenyläther durch einen geeigneten Weichmacher und der poröse Membranträger durch netzartige Polymere ersetzt worden sind. Die Entwicklung der Polymermembran ermöglicht die Verwendung einer vereinfachten Selektrodenkonstruktion mit einem "Festkörper"-Kalomel-Bezugssystem. Regeln für eine erfolgreiche Wahl einer geeigneten Lösungsmittel–Polymer-Kombination werden vorgeschlagen und auf die Entwicklung neuer Membranen auf Polyvinylchlorid- und Polyurethan-Basis angewendet.

REFERENCES

1 L. A. R. Pioda, V. Stankova and W. Simon, *Anal. Lett.*, 2 (1969) 665.
2 M. M. Shemyakin, Yu. A. Ovchinnikov, V. T. Ivanov, V. K. Antonov, E. I. Vinogradova, A. M. Shkrob, G. G. Malenkov, A. V. Evstratov, I. A. Laine, E. I. Melnik and I. D. Ryabova, *J. Membrane Biol.*, 1 (1969) 402.
3 P. Läuger, *Science*, 178 (1972) 24.
4 G. J. Moody and J. D. R. Thomas, *Selective Ion-Sensitive Electrodes*, Merrow, 1971.
5 H. K. Wipf, W. Pache, P. Jordan, H. Zähner, W. Keller-Schierlein and W. Simon, *Biochem. Biophys. Res. Commun.*, 36 (1969) 387.
6 E. Eyal and G. A. Rechnitz, *Anal. Chem.*, 43 (1971) 1090.
7 Philips, *Liquid Membrane Potassium Electrode, Type No. IS 560-K.*
8 M. S. Frant and J. W. Ross, *Science*, 167 (1970) 987.
9 Orion Research Inc., *Newslett.*, 2 (1970) 14.
10 J. Růžička, C. G. Lamm and J. Chr. Tjell, *Anal. Chim. Acta*, 62 (1972) 15.
11 J. Růžička, E. H. Hansen and J. Chr. Tjell, *Anal. Chim. Acta*, in press.
12 J. Koryta, *Anal. Chim. Acta*, 61 (1972) 329.
13 E. H. Hansen, C. G. Lamm and J. Růžička, *Anal. Chim. Acta*, 59 (1972) 403.
14 G. H. Griffiths, G. J. Moody and J. D. R. Thomas, *Analyst*, 97 (1972) 420.
15 L. E. Negus and T. S. Light, *Instrum. Technol.*, dec. 1972, p. 23.
16 S. Lal and G. D. Christian, *Anal. Lett.*, 3 (1970) 11.
17 T. Anfält, *Doctoral Thesis*, Gothenburg, 1972.
18 J. Rosin, *Reagent Chemicals and Standards*, D. Van Nostrand, 1967.
19 R. Bloch, A. Shatkay and H. A. Saroff, *Biophys. J.*, 7 (1967) 865.
20 Radiometer A.S., *Test Report on Hisel Electrodes*, 1970.
21 J. Brandrup and E. H. Immergut, *Polymer Handbook*, Interscience–Wiley, New York, 1966.
22 J. E. W. Davies, G. J. Moody and J. D. R. Thomas, *Analyst*, 97 (1972) 87.
23 B. F. Gisin and R. B. Merrifield, *J. Amer. Chem. Soc.*, 94 (1972) 6165.
24 O. Kedem, E. Loebel and M. Furmansky, Hydronautics-Israel Ltd., *Patent appl. No. 2027 128*, West Germany, 1970.
25 J. Růžička and C. G. Lamm, *Anal. Chim. Acta*, 54 (1971) 1.
26 J. Růžička and E. H. Hansen, *Anal. Chim. Acta*, 63 (1973) 115.

Analytica Chimica Acta, 67 (1973) 195–201

AN IMPROVED ELECTRODE FOR THE ASSAY OF UREA IN BLOOD

G. G. GUILBAULT, GEZA NAGY and S. S. KUAN

Department of Chemistry, Louisiana State University in New Orleans, New Orleans, La. 70122 (U.S.A.)

(Received 9th March 1973)

Several analytical methods have been reported for measuring nitrogen-containing organic compounds by using an enzyme-catalyzed ammonium ion-releasing reaction. The ammonium ion produced is generally measured spectrophotometrically[1] or potentiometrically[2]. The development of urea and L-phenylalanine electrodes has been reported[3,4]. These electrodes combined the advantages of an immobilized enzyme catalyst of the ammonia releasing reaction and the convenience of electrochemical ammonium detection. Unfortunately, the selectivity of the electrochemical sensor used (Beckman Glass 39137) did not permit the use of these electrodes in biological fluids, unless an ion exchanger was used to remove the interfering sodium and potassium ions. The use of ion exchangers in blood samples of very small volumes, or the complete removal of sodium and potassium ions from a sample diluted by a buffer (TRIS) free of these ions is not easy.

Recently, the construction of an improved urea electrode has been reported[5]. The electrochemical sensor for this electrode was made from a silicone rubber membrane containing the antibiotic nonactin as the active ingredient. The properties of the antibiotic nonactin as a complexing agent have been studied by Pioda *et al.*[6] and a liquid exchanger ammonium electrode containing nonactin as active ingredient has been reported by Scholer and Simon[7].

The selectivity properties of the solid type of ammonium electrode and the level of cations in human blood indicated the utility of the improved urea electrode in the urea determination of clinical blood samples without an ion-exchange pretreatment. The improved urea electrode was made by covering the active surface of the solid type ammonium electrode by an immobilized urease enzyme layer of the same kind as was used by Guilbault and Montalvo[3]. Unfortunately, this kind of physically immobilized urease was not very stable.

Recently, many new methods for the insolubilization of enzymes have been developed[8,9]. The covalent coupling of urease to an insoluble organic or inorganic carrier may offer a better method of preparing a stable and reactive enzyme layer for the electrode.

In this paper, the further development of the urea electrode is reported. By using a chemically immobilized enzyme–gel reaction layer, the fabrication of the urea electrode has been simplified, and the stability of the electrode has been improved.

If the urea electrode was calibrated in a solution of a constant interfering ion (K^+) level, and a monitored dilution of the blood samples was made to this inter-

ference level, it was possible to measure the urea concentration in clinical and artificial blood serum samples with satisfactory accuracy, and in a fast and convenient manner. The monitored dilution was accomplished by the application of an auxiliary ammonium ion electrode to measure the interfering ion (NH_4^+, Na^+, K^+) activity originating from the salt concentration of the blood samples.

EXPERIMENTAL

Preparation of electrodes

The active membranes of the ammonium ion-selective electrode were prepared by mixing 500 mg of silicone rubber (No. 3140 RTV, Dow Corning Corp., Midland, Mich.) thoroughly with 300 mg of nonactin. The paste obtained was pressed between two glass plates coated with paraffin. After about 48 h, small discs with a diameter of 5 mm and a thickness of about 0.2 mm were cut from the elastic membrane. These small membranes were placed onto the end of a glass tube with an outer diameter of 5 mm. The tube was filled with a 0.1 *M* ammonium chloride solution. The electrodes were soaked for 30 min in buffered ammonium chloride solution before use and were stored in the same solution between measurements and overnight.

The active surface of the ammonium ion-selective electrode was covered by a thin layer of finely ground, chemically immobilized urease gel. A dialysis layer fixed to the electrode body with rubber rings covered and kept the enzyme reaction layer on the electrode surface. The urea electrodes were stored in 0.1 *M* TRIS buffer solution (pH 7).

A standard fiber junction calomel electrode was used as reference electrode connected to the solution through a junction capillary.

Measurement of urea

Readings were obtained in stirred, thermostated solutions at 25°, after allowing sufficient time to reach a steady state value. The potential was measured with a Corning 110 digital pH meter.

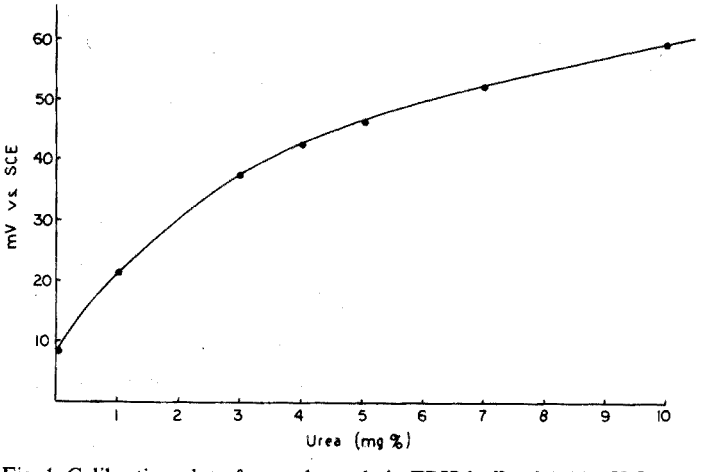

Fig. 1. Calibration plot of urea electrode in TRIS buffer, 0.1 *M*, pH 7, containing KCl (120 mg l^{-1}).

For the determination of the urea concentration of blood serum samples, the urea electrode was first calibrated in a solution of 10^{-1} *M* TRIS buffer, pH 7, containing 120 mg of potassium chloride per l (Fig. 1), with a urea and a calomel electrode.

Procedure for assay. Measure the potential difference between an ammonium ion-selective electrode and a calomel electrode, in 1 ml of TRIS buffer (pH 7, 0.1 *M*) containing 120 mg of potassium chloride per l once each day.

To a 2-ml beaker add 0.2 ml of the serum to be assayed, and immerse the above electrode pair. Add 0.5 ml of TRIS buffer (0.1 *M*, pH 7) from a calibrated pipet, and read the potential. Add more TRIS buffer until the potential recorded is the same as that observed in the first step of the procedure. Record the total volume of buffer added (V_B). About 0.8–1.0 ml should be sufficient.

After this dilution of the sample to the same interference level as that in the standard buffer–KCl solution used for the calibration curve (Fig. 1), place the urea electrode into the solution and record the potential of this electrode *vs.* the calomel electrode. Read the apparent mg % urea from Fig. 1. Calculate the concentration of urea as follows:

$$\text{mg \% urea} = \text{apparent mg \% urea} \left(\frac{V_B + 0.2}{0.2}\right)$$

In the spectrophotometric urea determinations, the standard diacetyl clinical analytical procedure[1] was used. The absorbance of the solutions was measured at 560 nm with a Beckman DB spectrophotometer.

Immobilization of urease

The carrier used for the immobilization of urease was prepared from acrylic acid in this laboratory. The acrylic acid was polymerized and converted to an aryl nitro derivative. The gel was then cross-linked by treating the derivative with ethylenediamine. The nitro derivative was reduced and the amine groups were then diazotized and coupled to the enzyme. The immobilization procedure was as follows: 10–150 mg of urease were dissolved in 15 ml of 0.05 *M* phosphate buffer pH 5, 5 g of azo derivative (wet weight) was added, and the suspension was agitated at room temperature for 3 h. The enzyme–polymer gel was washed three times with distilled water and finally rinsed with 0.05 *M* phosphate buffer pH 6. The immobilized enzyme gel was stored in a test tube at 4° in a refrigerator until use.

Chemicals

All the electrochemical measurements were made in 0.1 *M* TRIS buffer, pH 7. The water used in making all solutions was triply distilled. The urea solutions were prepared freshly every day. The urease enzyme (Sigma Chemicals, Inc., St. Louis, Mo.) had an assayed activity of 1.5 units mg^{-1} (1 unit produces 1 mg of ammonia from urea in 5 min at pH 7.0 and 30°). The nonactin (SW 15859-Batch No. LBH-3599-90-10) was provided by the Squibb Institute for Medical Research. The chemicals used in the preparation of the enzyme gel were of reagent or technical grade and were used as received.

RESULTS AND DISCUSSION

Properties of the urea electrode

The chemically immobilized enzyme reaction layer applied on the urea electrode did not modify the selectivity properties of the electrochemical sensor. The selectivity for NH_4^+ over K^+ and Na^+ was 6.5 and $7.5 \cdot 10^2$, respectively. The response of the urea electrode to lithium ion activity was very poor.

The dependence of the potential of the urea electrode on urea concentration in a TRIS buffer solution containing potassium chloride (120 mg l^{-1}) and in pure TRIS buffer are shown in Figs. 1 and 2. The shapes of the E *vs.* log[urea] curves are in a good agreement with the approximate expression derived earlier for the performance of the enzyme electrode function[5]:

$$E = E_0 + \frac{RT}{ZF} \ln \left[\frac{k_2}{D_p} \cdot \frac{[E] D_s [S]}{D_s [S] + D_s K_m + k_2 E} + \Sigma k_{a_i}^{\frac{1}{Z}} \right]$$

where E, E_0, R, T, F, k_2, K_m, S, have the usual meaning; k is the selectivity ratio, a_i is the activity of the interfering ion, and Z is the charge of the interfering ion. $D_p = D_{op}/\Delta l$; $D_s = D_{os}/\Delta l$, where D_{os} is the diffusion constant of the substrate, D_{op} is the diffusion constant of the product, and Δl is the thickness of the reaction diffusion layer.

The stability of an enzyme electrode depends on three important factors: (*a*) the stability of the electrochemical sensor; (*b*) the physical stability of the enzyme reaction layer in solutions of different ionic strength (according to the swelling property of the gel used, the thickness of the reaction layer can vary with time depending on the ionic strength of the solution); and (*c*) the stability of the catalytic reactivity of the enzyme.

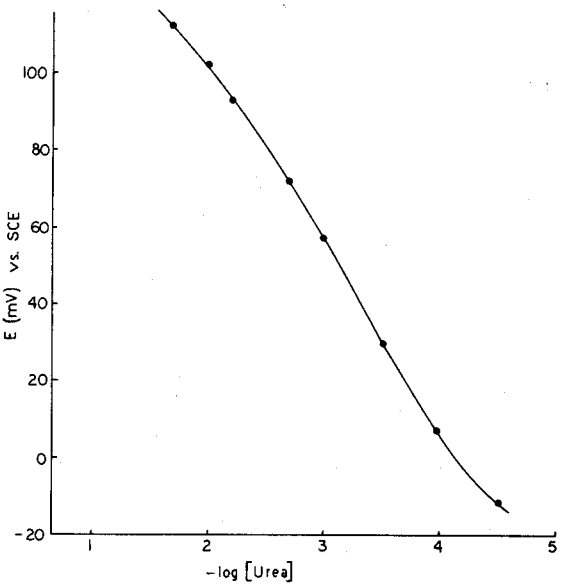

Fig. 2. Calibration plot of urea electrode in TRIS buffer, 0.1 *M*, pH 7.

As reported previously[5], the electrochemical sensor appeared to be stable through the fifth week of the examination. In this study, it was found that the silicone rubber-based antibiotic-type ammonium electrode maintained a constant potentiometric activity and selectivity over a 5-month period.

It is difficult to prepare a gel which has both satisfactory physical stability and enzyme-coupling capacity, because these two factors seem to be antagonistic to each other. Several batches of gels prepared with different degrees of cross-linkage were tested. It was found that 6 cross-linkages to one active coupling site was the best. The degree of cross-linkage was achieved by adding a calculated amount of ethylenediamine during the gel preparation.

The enzyme-gel made by the procedure described was kept at 4° over four months without noticeable loss of activity.

The improved urea electrodes made of chemically immobilized enzyme layers were kept in TRIS buffer at room temperature. During one month, only a slight change in the potentiometric response was observed (0.5–2 mV change in response to a $5 \cdot 10^{-4}$ urea concentration). This slight change did not affect the practical analytical value of the enzyme electrode.

Measurement of urea in blood

Table I shows the measured urea concentration of artificial and clinical blood serum samples obtained both spectrophotometrically and by the urea enzyme electrode.

TABLE I

COMPARISON OF THE RESULTS OF UREA DETERMINATION IN CLINICAL AND ARTIFICIAL BLOOD SERUM SAMPLES

Sample number	*Urea concentration determined*		
	Spectrophotometrically (mg%)	*Urea electrode (mg%)*	*Difference (%)*
16	37.5	36.6	2.4
17	20.0	20.4	2.0
34	21.5	20.9	2.8
42	26.0	26.8	3.08
3T 4	28	28.1	0.36
A_1[a]	33.5	32.9	1.8
A_2[a]	67.5	63.3	6.2

[a] Artificial blood serum samples (A_1 Dade Labtrol; A_2 Dade Pathtrol). Other samples provided by Methodist Hospital, New Orleans, from patients.

The response time of the urea electrode was measured by the time interval necessary to achieve 98% of the steady-state response potential. It was found to vary between 60–180 s, depending on the urea concentration and the thickness of the reaction layer. In very small sample volumes (< 0.5 ml), the electrode potential may not achieve a steady-state value. This is due to the reactor effect of the electrode: the electrode continuously decreases (by reaction) the urea concentration in the

sample and increases the interfering ammonium ion concentration. In small volumes this change continuously affects the reading. Because of this, it is advantageous to accomplish the measurement in a total volume of 0.5 ml or more.

Conclusions

The application of a chemically immobilized urease gel as a reaction layer results in an improved urea electrode with increased stability and simplified fabrication. The applied controlled dilution of the samples to a constant interference level, together with the good selectivity properties of the electrochemical sensor, provides a convenient method for the assay of urea in clinical blood serum samples. The two main error sources in the spectrophotometric assay of urea, the ammonium ion content, and the turbidity of the samples, do not affect the results of this potentiometric urea determination.

The authors gratefully acknowledge the financial support of the National Science Foundation (Grant No. GP-31518).

SUMMARY

An improved urea enzyme electrode is applied for the determination of urea in blood samples. The electrode is based on the enzymatic hydrolysis of urea, and potentiometric detection of the ammonium ion produced. A silicone rubber-based nonactin ammonium ion-selective electrode serves as the sensor. The selectivity coefficients of this electrode were 6.5 for NH_4^+/K^+; 750 for NH_4^+/Na^+, and much higher for other cations. The reaction layer of the electrode was made of urease enzyme chemically immobilized on polyacrylic gel. The prepared gel was stable at 4° for over four months. The electrodes retained their activity for over one month. A three-electrode system, which allowed dilution to a constant interference level, was applied to avoid interfering effects in blood samples. Analyses of blood sera showed good agreement with a standard spectrophotometric method. Routine clinical assays of blood urea are feasible.

RÉSUMÉ

Une électrode spéciale "enzyme-urée" est proposée pour le dosage de l'urée dans le sang. Elle est basée sur l'hydrolyse enzymatique de l'urée et la détection potentiométrique de l'ion ammonium formé. Ses coefficients de sélectivité sont 6.5 pour NH_4^+/K^+; 750 pour NH_4^+/Na^+ et beaucoup plus pour les autres cations. La couche active de cette électrode est constituée d'uréase, chimiquement immobilisée sur gel polyacrylique. Un système à 3 électrodes, permettant une dilution à un niveau d'interférence constant, est appliqué afin d'éviter l'influence d'autres cations dans les échantillons à analyser. Les résultats concordent bien avec ceux obtenues par spectrophotométrie. Des dosages cliniques de routine, dans le sang, sont possibles.

ZUSAMMENFASSUNG

Eine verbesserte Harnstoffenzymelektrode wird auf die Bestimmung von

Harnstoff in Blutproben angewendet. Die Elektrode beruht auf der enzymatischen Hydrolyse von Harnstoff und dem potentiometrischen Nachweis der gebildeten Ammoniumionen. Als Sensor dient eine ammoniumionenselektive Elektrode auf Siliconkautschuk-Basis. Die Selektivitätskoeffizienten dieser Elektrode waren 6.5 für NH_4^+/K^+, 750 für NH_4^+/Na^+ und viel höher für andere Kationen. Die Reaktionsschicht der Elektrode wurde aus Urease-Enzym hergestellt, das chemisch an Polyacryl-Gel fixiert worden war. Das präparierte Gel war bei 4° über vier Monate lang beständig. Die Elektroden behielten ihre Aktivität über einen Monat lang. Ein Drei-Elektroden-System, das die Verdünnung auf einen konstanten Störungspegel erlaubte, wurde angewendet, um die störenden Einflüsse in Blutproben zu vermeiden. Die Analysen von Blutseren zeigten eine gute Übereinstimmung mit einer spektrophotometrischen Standardmethode. Klinische Routinebestimmungen von Blut-Harnstoff sind ausführbar.

REFERENCES

1 N. W. Tietz, *Fundamental of Clinical Chemistry*, W. B. Saunders Co., Philadelphia, Pa., 1970, pp. 718–722.
2 T. A. Neubecker and G. A. Rechnitz, *Anal. Lett.*, 5 (1972) 653.
3 G. G. Guilbault and J. Montalvo, *J. Amer. Chem. Soc.*, 92 (1970) 2533.
4 G. G. Guilbault and E. Hrabankova, *Anal. Chem.*, 42 (1970) 1779.
5 G. G. Guilbault and G. Nagy, *Anal. Chem.*, 45 (1973).
6 L. Pioda, M. Wachter, R. Dohner and W. Simon, *Helv. Chim. Acta*, 50 (1967) 1373.
7 R. P. Scholer and W. Simon, *Chim. (Aarau)*, 24 (1970) 372.
8 L. A. Manson, *Biomembranes*, Vol. 1, Plenum Press, New York, 1971.
9 O. R. Zaborsky, *Immobilized Enzymes*, Chemical Rubber Company, Cleveland, Ohio, 1972.

Analytica Chimica Acta, 67 (1973) 202–203

SHORT COMMUNICATION

Result of an inter-laboratory program for the determination of tin in a standard reference ore: A caveat

G. H. FAYE, W. S. BOWMAN and R. SUTARNO

Mineral Sciences Division, Mines Branch, Department of Energy, Mines and Resources, Ottawa, Ontario K1A 0G1 (Canada)

(Received 20th February 1973)

The Mines Branch has recently issued a zinc–tin–copper–lead ore, MP-1, as a standard reference material with recommended values for nine elements, the value for tin being 2.50%. In the inter-laboratory certification program for MP-1, 227 tin results were obtained from 16 laboratories[1]. An assessment of these results indicated that certain variations of the titrimetric method gave appreciably lower results than did the methods involving an instrumental finish. Because the accurate determination of tin in ores is generally troublesome[2–4], and because titrimetric analysis is a popular method for tin, it was considered worthwhile to publish more widely the correlation between the tin results and the analytical methods.

The tin-bearing minerals in MP-1 are cassiterite and stannite–kesterite. Because of the refractory nature of cassiterite and other minerals in MP-1, all laboratories used a sodium peroxide fusion for sample decomposition except two that used the X-ray fluorescence spectroscopic technique and one that used the ammonium iodide–volatilization process[3]. After sample decomposition in the chemical methods, a variety of commonly accepted procedures was used to make separations and to prepare the sample solution for the determinative step.

Table I gives the mean values for the tin content of ore MP-1 as determined by a number of methods, as well as the confidence limits for some of the means. An analysis of variance showed that there are significant differences between the means of results reported by different laboratories for a given method; these were taken into account when computing the confidence intervals[5]. For example, the interval for the mean of the instrumental methods was based on 10 laboratories reporting 118 results rather than on 118 independent results.

It is assumed that the reader will accept our comments on the significance of the means, and details of the analysis of variance and the calculation of the confidence intervals listed in Table I are not given. In the interests of conciseness the untreated individual results for tin are not given here; they are reported in Mines Branch Report TB 155[1].

Table I shows that the mean tin value of 2.50%, obtained by instrumental methods, is appreciably higher than that given by the titrimetric methods (2.36%). It is also evident that the results of the titrimetric methods are dependent, in part, on the nature of the metal used in the hydrogen-reduction step. Four laboratories used

TABLE I CORRELATION OF TIN RESULTS WITH ANALYTICAL METHODS

Analytical method	*No. of labs.*	*No. of results*	*Mean % tin*	*95% Confidence limits of the mean*
Polarographic	3	30	2.40	
Atomic absorption	5	53[a]	2.58	
X-ray fluorescence	2	35	2.48	
Total, instrumental	10	118	2.50	2.38–2.62
Titrimetric, Fe reduction	4	55[a]	2.48	2.25–2.71
Titrimetric, excluding Fe reduction				
Ni reduction	1	10	2.40	
Al reduction	1	10	2.23	
Pb reduction	4	40	2.22	
Other reduction	1	4	2.28	
Total	7	64	2.25	2.15–2.35

[a] Table I contains additional results that were obtained subsequent to the certification program[1]; nine atomic absorption results, and ten by the Fe-reduction method.

iron powder; a mean result of 2.48% was obtained which agrees closely with that of the instrumental methods, but is significantly higher than the mean results obtained when other reducing metals were used. The reason(s) for the superior performance of iron is not fully understood; therefore, a further study of this matter may be warranted.

It is of interest to note that the laboratory which used the ammonium iodide–volatilization decomposition step[3] in conjunction with an atomic-absorption finish, obtained a mean value of 2.48% tin (12 results), a value that is in good agreement with means for the instrumental and titrimetric iron-reduction methods. This supports the comments of Hefferman *et al.*[3] who stated that the above combination of steps tends to give better results than those provided by the more commonly used classical methods.

The results given in Table I strongly suggest that titrimetric methods are prone to serious negative errors, owing to incomplete reduction of tin(IV), or to atmospheric oxidation of tin(II). Other workers have made similar observations[3]. It is recommended, therefore, that, for low-grade ores at least, instrumental methods (finishes) should be used whenever possible because these are not critically dependent on the valence state of tin. However, the titrimetric method is capable of yielding good results if proper conditions for the reduction of tin are maintained.

REFERENCES

1 G. H. Faye, *Mines Branch Tech. Bull. TB 155*, Department of Energy, Mines and Resources, Ottawa, Canada, 1972.
2 T. R. Sweatman, Y. C. Wong and K. S. Toong, *Trans. Inst. Min. Met.*, 76B (1967) 149.
3 B. J. Hefferman, R. O. Archbold and T. J. Vickers, *Aust. Inst. Min. Met. Proc.*, 223 (1967) 65.
4 B. Lister and M. J. Gallagher, *Trans. (Section B) Inst. Min. Met.*, 79 (1970) B213.
5 K. A. Brownlee, *Statistical Theory and Methodology in Science and Engineering*, John Wiley, New York, 1961.

Analytica Chimica Acta, 67 (1973) 204–206

SHORT COMMUNICATION

The crystal structure of diphenylthiocarbazide

M. HARDING, M. J. ADAMS, P. A. ALSOP and H. M. N. H. IRVING

Department of Inorganic and Structural Chemistry, University of Leeds, LS2 9JT; Chemistry Department, Edinburgh University, West Mains Road, Edinburgh EH9 3JJ; and the Chemical Crystallography Laboratory, South Parks Road, Oxford (England)

(Received 6th March 1973)

Whilst one of us (P.A.A.) was completing a single crystal X-ray determination of the structure of dithizone (3-mercapto-1,5-diphenylformazan; diphenylthiocarbazone; Ph·NH·NH·CS·N:NPh)[1], attention was drawn to an earlier thesis[2] which described the structure of a crystal then believed to be dithizone. Bond-length and planarity considerations had led to the tentative conclusion that the material was in fact diphenylthiocarbazide (Ph·NH·NH·CS·NH·NHPh). However, a spectrophotometric assay as 85% dithizone and the fact that the structure had not been completely solved until some four years after the data had been collected, so that it was impossible to re-examine the starting material, left the issue in doubt and the structure was not published.

Reference by Adams[2] to the transparency and birefringence of the crystals examined, indicated that the sample could not possibly have been pure dithizone which is intensely coloured[1]. Reference to the ease of oxidation and the approximate assay for dithizone again suggested the properties of the carbazide, which is a penultimate stage in Fischer's well-known synthesis of dithizone. In view of its very ready oxidation, diphenylthiocarbazide commonly gives the same products as dithizone on reaction with metals, so that the assay of 85% for the dithizone content is not unambiguous.

The identity of Adams' crystal with diphenylthiocarbazide was established by a comparison (Table I) of the powder pattern of an authentic sample with the unit cell dimensions and F values given by Adams[2]. As the full structure has not been published, an abstract is presented in Table II. The crystals were grown from benzene–petroleum and are monoclinic. The space group is $P2_1/n$ with $a=18.46$, $b=12.56$, $c=5.65$ Å; $\beta=92.4°$; $D_{obs}=1.27$, $D_{calc}=1.30$, $Z=4$ molecules per unit cell. (It is interesting that dithizone crystallizes in the same space group[1] with $a=11.95$, $b=22.24$, $c=4.69$ Å, $Z=4$.) Intensity data for 1300 reflections were recorded photographically and measured visually for layers hk0 to hk3; the structure was solved by Patterson and Fourier methods and refined by five cycles of block-diagonal least-squares with isotropic temperature factors to a final R value of 0.146.

TABLE I

COMPARISON OF POWDER PATTERN FOR DIPHENYLTHIOCARBAZIDE[1] WITH EARLIER DATA[2]

Powder data for diphenylthiocarbazide[1]		*Single crystal data*[2]		
d (Å)	*I*	*h k l*	F_{obs}	d_{calc} *(Å)*
9.00	30	2 0 0	52	9.223
7.43	10	2 1 0	14	7.434
6.30	20	0 2 0	45	6.280
5.18	30	2 2 0	32	5.191
4.42	60	2 1 1	32	4.424
4.06	100	1 2 1	79	4.066
		3 0 1	36	4.074
3.77	20	2 2 1	56	3.777
3.53	20	5 1 0	46	3.540
3.39	30	0 3 1	61	3.363
		3 2 1	94	3.418
3.18	50	5 2 0	41	3.181

TABLE II

COORDINATES FOR DIPHENYLTHIOCARBAZIDE

Atom	*x*	*y*	*z*	u_{iso} *(Å²)*
S	0.89890	0.99496	0.75687	0.0446
N (1)	0.87857	0.13220	0.30617	0.0273
N (2)	0.94031	0.14927	0.45497	0.0281
N (3)	0.01394	0.11809	0.78556	0.0284
N (4)	0.05757	0.20596	0.71397	0.0294
C (1)	0.95295	0.09411	0.65680	0.0245
C (2)	0.83330	0.22225	0.26477	0.0263
C (3)	0.79163	0.22470	0.05176	0.0296
C (4)	0.74364	0.31008	0.00678	0.0379
C (5)	0.73916	0.39182	0.17122	0.0358
C (6)	0.77891	0.38687	0.39007	0.0403
C (7)	0.82755	0.30182	0.43962	0.0346
C (8)	0.06442	0.28683	0.90145	0.0317
C (9)	0.00444	0.31463	0.02771	0.0390
C (10)	0.01353	0.39410	0.19965	0.0495
C (11)	0.08023	0.44095	0.25873	0.0547
C (12)	0.13932	0.41111	0.12286	0.0563
C (13)	0.13270	0.33367	0.93870	0.0402

The structure is shown in Fig. 1. The atom of sulphur is coplanar with the adjoining carbon atom, C_1, and the four nitrogen atoms N_1, N_2, N_3, and N_4 (plane 1). The dihedral angles between planes 1 and 2, and between planes 1 and 3 are 73° and 76° respectively. In contrast the whole molecule of dithizone is effectively coplanar[1] with no atom deviating by more than 0.15 Å from the plane.

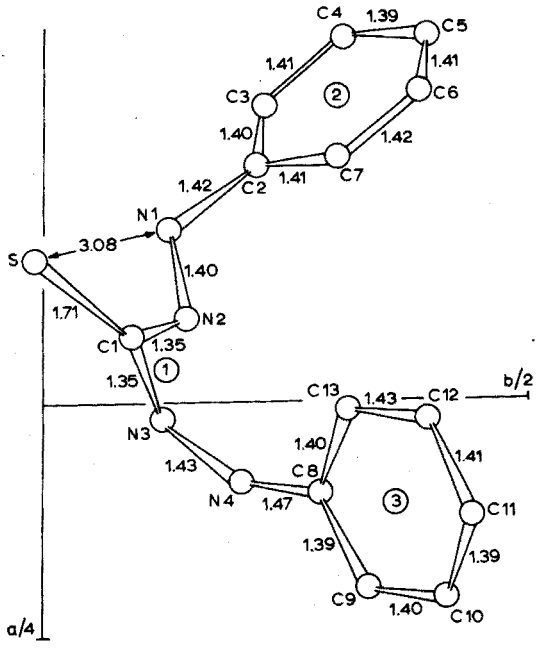

Fig. 1. Structure of diphenylthiocarbazide. S, C1, N1, N2, N3 and N4 are coplanar, plane 1. Dihedral angle between planes 1 and 2 = 73°; 1 and 3 = 76°.

Experimental. Diphenylthiocarbazide was synthesized by Fischer's method[3] and formed white needles from chloroform, ethanol or benzene which readily oxidized in the air on keeping, and then showed the spectral and chelating properties of dithizone itself. X-Ray powder photographs were taken with a Philips 5.73-cm powder camera on samples mounted in Lindemann glass capillaries.

REFERENCES

1 P. A. Alsop, *Ph.D. Thesis*, London, 1971.
2 M. J. Adams, *Part II Thesis*, Oxford, 1962.
3 E. Fischer, *Ann.*, 190 (1878) 67.

Analytica Chimica Acta, 67 (1973) 207–208

SHORT COMMUNICATION

Collection of trace elements on powdered organic reagents in an ultrasonic field

KATSUAKI FUKUDA and ATSUSHI MIZUIKE
Faculty of Engineering, Nagoya University, Chikusa-ku, Nagoya (Japan)
(Received 15th February 1973)

In previous papers[1], it has been reported that the application of ultrasonics accelerates remarkably the adsorption of nanogram and microgram quantities of silver ions on powdered dithizone, and antimony ions on alumina, from aqueous solutions. This technique can be conveniently employed for separating trace elements, and possibly also in radiochemical analysis. The present communication describes a more effective and simpler technique for applying ultrasonics, *i.e.* the immersion of an ultrasonic transducer in a sample solution.

Procedure

Place 25 ml of 0.1 *M* nitric acid containing 0.1–10 μg of iron(III), cobalt(II) or silver(I) labeled with iron-59, cobalt-60 or silver-110m, respectively, in a 50-ml beaker, and add α-nitroso-β-naphthol or dithizone (particle diameter *ca.* 300 μm) as collector. Immerse a cylindrical ultrasonic transducer covered with epoxy resin (15-mm diam.) 2 mm deep in the solution, and apply ultrasonics (29 kHz, 45 W) to effect vigorous stirring. After the prescribed time, transfer the contents of the beaker quantitatively to a 50-ml round-bottomed centrifuge tube, and centrifuge for 3 min at 4000 rev min^{-1}. Discard the supernatant liquid, rinse the collector with 5 ml of 0.1 *M* nitric acid by swirling, and centrifuge again for 2 min. Discard the supernatant liquid, and add 5 ml of hot nitric acid to dissolve the collector. Dilute the solution to 10 ml with water in a volumetric flask, and measure the γ-activity of a 2-ml aliquot with a well-type NaI(T1) scintillation counter.

Results and discussion

Table I shows the marked acceleration effect of ultrasonics on the adsorption of trace elements on the collectors. The trace recoveries reached 97–100% within 10 min. The collectors were pulverized during the collection in a sound field to give a fairly stable dispersion, the particle diameter being 20–70 μm after 10 min. By the proposed technique, 5 μg of silver was separated in greater than 95% yields with 20 mg of dithizone from 0.1 *M* nitric acid solution containing 1 g of zinc or cadmium ions within 10 min. Zinc or cadmium accompanying silver was determined by polarography after wet oxidation of dithizone with sulfuric acid and ammonium persulfate, and found to be 0.1–0.5 mg. Therefore, the concentration factors were $(0.2–1.0)\cdot 10^4$.

TABLE I

COLLECTION OF TRACE ELEMENTS FROM 25 ml OF 0.1 *M* NITRIC ACID IN AN ULTRASONIC FIELD

Collector	*Trace element (μg)*	*Trace recovery (%) after*[a]					
		1 min	*2 min*	*3 min*	*5 min*	*8 min*	*10 min*
α-Nitroso-	Fe 0.1	—	—	—	99	—	—
β-naphthol,	Fe 10	—	—	—	96	—	98
50 mg	Co 0.1	45	70(0)	—	95(0)	98	100(0)
	Co 1.0	—	—	—	95	—	—
	Co 10	—	—	—	98	—	99
Dithizone,	Ag 1.0	65(8)	—	95	99(21)	—	100(29)
20 mg	Ag 10	—	—	—	95	—	97

[a] Without ultrasonics (with mechanical stirring) in parentheses.

REFERENCE

1 K. Fukuda and A. Mizuike, *Anal. Chim. Acta*, 51 (1970) 77, 527.

Analytica Chimica Acta, 67 (1973) 209–212

SHORT COMMUNICATION

Determination of the composition of the U_3O_8 phase from the decomposition of β-UO_3

E. S. RAMAKRISHNAN

Chemistry Division, Bhabha Atomic Research Centre, Bombay 400 085 (India)

(Received 19th March 1973)

It is known[1–4] that the U_3O_8 phase exhibits some oxygen deficiency at high temperatures, but the exact phase-boundary composition and other thermodynamic data are lacking[2,5,6]. A knowledge of the exact composition of this phase in air is essential, because the simple oxidation of urania phases in air to U_3O_8 is used as a method for the determination of oxygen/uranium ratios[7–9]. The nonstoichiometry of the U_3O_8 phase has been demonstrated[4] by oxidizing urania between 400 and 835°. The present work was undertaken to establish whether these observed compositions represented equilibrium compositions or were the kinetically limiting compositions. The U_3O_8 phase was produced by decomposing β-UO_3 in air at 650, 750 and 850° and the resultant product was analysed.

Experimental

β-UO_3 was prepared by decomposing ammonium diuranate at $520 \pm 5°$. Portions of this β-UO_3 were heated in air at $520 \pm 5°$ to constant weight (3–4 h) and then heated at the required temperature. The reaction

$$UO_3 \rightarrow UO_{2.667-x} + \tfrac{1}{2}(0.333 + x)O_2 \qquad (1)$$

was allowed to go to completion (5–6 h). The composition of the U_3O_{8-x} phase formed was first calculated from the weight loss of the sample, the initial sample being assumed to be stoichiometric β-UO_3*.

The composition of the final product (U_3O_{8-x}) was also determined by a modified titrimetric method[10] with cerium(IV) sulphate as the reagent. The method consisted of dissolving a weighed quantity of U_3O_{8-x} in a known excess of acidified 0.1 *M* cerium(IV) ammonium sulphate solution which was 1.5 *M* in sulphuric acid. The amount of cerium(IV) utilized in the conversion of uranium(IV) to uranium(VI) was determined by back-titration of the excess of cerium(IV) with a freshly prepared iron(II) ammonium sulphate solution, with ferroin as indicator. The cerium(IV) solution was standardized simultaneously against the iron(II) solution. From these two titration values the composition of the U_3O_{8-x} phase was calculated*.

Moisture pickup by the U_3O_{8-x} during weighing was avoided by using a

* A sample calculation is presented in the appendix.

platinum crucible with a tight lid and by using anhydrous magnesium perchlorate as desiccant.

In addition, a few oxidation runs were carried out with pure uranium metal (metallic impurities < 200 p.p.m.). A weighed quantity of the metal was first partially oxidized by heating at 150° in a stream of carbn dioxide to eliminate any temperature effect, and then in air at the experimental temperature. The composition of the product was determined from the weight gain and also by the titrimetric method described above.

Discussion

From Table I it is evident that the U_3O_{8-x} phase formed by the decomposi-

TABLE I

OXYGEN/URANIUM RATIO OF U_3O_{8-x} PHASE IN AIR

(Except where specified, each result is the average of 15–20 determinations)

Temp. ±2°	*O/U composition*		*Remarks*
	From wt. change data	*From titrimetry*	
650	2.645±0.005	2.665±0.002	The U_3O_{8-x} was obtained
750	2.635±0.005	2.664±0.002	by decomposing β-UO_3
850	2.620±0.005	2.657±0.002	in air
450	2.695±0.010[a]	2.675±0.003[a]	Obtained by oxidation of uranium metal,
850	2.668±0.010[a]	2.655±0.002[a]	first in CO_2 and then in air
450	—	2.669±0.002	Oxidation of urania (this work)
435[b]	2.667±0.002	2.671±0.002	Oxidation of urania[4]
610[b]	2.649±0.002	2.660±0.002	
835[b]	2.640±0.002	2.652±0.002	

[a] Average of 5–6 independent estimations.

[b] The significantly lower O/U compositions calculated from weight-change data are probably the result of small but significant (1 μg mg^{-1}) amount of residual moisture in the urania sample even after prolonged desiccation confirmed by separate microweighing[11].

TABLE II

COMPOSITION OF THE U_3O_{8-x} PHASE FORMED BY DECOMPOSING β-UO_3 IN AIR AT 850° FOLLOWED BY REHEATING AT 450° FOR 24 h

Wt. of β-UO_3 taken (mg)	*Wt. of U_3O_{8-x} formed (mg)*	*O/U composition*	
		From wt. loss	*From titrimetry*
229.27	224.36	2.616	2.656
167.04	163.50	2.621	2.653
194.57	190.47	2.623	2.657
249.00	243.73	2.623	2.659
286.00	280.00	2.623	2.657
		Av. 2.620±0.003	2.656±0.002

tion of β-UO_3 in air above 700° is significantly oxygen-deficient. This deficiency is not removed during cooling or even on prolonged reheating at 450° (Table II). Compositions evaluated from weight loss differ from those obtained from titrimetry; this is probably due to the presence of some volatile impurities in the starting material, which would greatly affect the final composition calculated from weight loss, but not the titrimetric results. The compositions evaluated titrimetrically represent the equilibrium composition of U_3O_{8-x} in air; this conclusion is supported by the fact that the same final composition was obtained whether the starting material was uranium metal, urania or β-UO_3.

Goto[3] has reported from a thermogravimetric study of the oxidation of urania, that the compositions of the U_3O_{8-x} phase at 650, 800 and 1000° are 2.660, 2.653 and 2.645, respectively, which is in good agreement with the present results.

Though the available data for the dissociation pressure for U_3O_{8-x} below 1000° are meagre, an estimate of the partial pressures of oxygen, p_{O_2}, in equilibrium with the U_3O_{8-x} phase at 850° can be made by assuming $\Delta\bar{S}_{O_2}$, the relative partial molar entropy, and $\Delta\bar{H}_{O_2}$, the relative partial molar enthalpy of oxygen to be temperature-independent. From the relation,

$$\Delta\bar{G}_{O_2} = \Delta\bar{H}_{O_2} - T\Delta\bar{S}_{O_2} = -2.303\,RT\log p_{O_2} \qquad (2)$$

where $\Delta\bar{G}_{O_2}$ is the partial molar free energy of oxygen and R the gas constant (1.987 cal $mole^{-1}$ deg^{-1}), the following values were calculated from the tabulated data of Rand and Kubaschewski[5]:

$\log p_{O_2}$ (atm)	−0.60	−0.80	−2.00	−2.96
O/U	2.667	2.660	2.650	2.640

The extrapolation of the low-temperature data of Cordfunke and Aling[6] on the γ-UO_3–U_3O_8 equilibria yields a value of $p_{O_2} \approx 150$ atm at 850° for the stoichiometric composition. The agreement between these extrapolated data is poor, but both point to the fact that at 850° the U_3O_{8-x} phase cannot have a stoichiometric composition. Hence the prevailing practice of oxidizing urania in air at 850° to determine its oxygen/uranium ratio should be discredited.

The author wishes to thank Dr. J. Shankar for his interest in this work, Dr. M. S. Chandrasekhariah for help in data analysis and in the preparation of the manuscript, and Mr. S. R. Dharwadkar for his useful suggestions and for making available his unpublished data. Thanks are also due to the Department of Atomic Energy for providing a fellowship.

Appendix

(a) Sample calculation of O/U at 650° from weight-change data.

Weight of sample (β-UO_3) = 219.88 mg
Weight loss at 650° = 4.33 mg
The decomposition proceeds as $UO_3 \rightarrow UO_{3-x} + xO$.
For the stoichiometric composition, $x = 0.333$, *i.e.*, O/U = 2.667, 286.03 mg UO_3 loses 5.33 mg oxygen to give $x = 0.333$.
219.9 mg UO_3 loses 4.33 mg oxygen to give

$$x = (4.33/5.33)\cdot(286.03/219.9)(0.333) = 0.353$$

Thus the composition of the product formed

$$UO_{3-x} = UO_{2.647} \quad i.e. \quad O/U = 2.647$$

(b) Calculation of O/U from titrimetric data.

$(1+x)$ moles of U(IV) requires $2(1+x)$ moles of Ce(IV) for oxidation.
A g of sample (U_3O_{8-x}) reacts with a moles of Ce(IV).
Hence M g of sample (U_3O_{8-x}) reacts with $(a\cdot M)/A$ moles of Ce(IV), where M is the mol.wt. of U_3O_{8-x}.

Thus $(a\cdot M)/A = 2(1+x)$ and $x = (M/2)\cdot(a/A) - 1$.

As an example:

Sample weight of $U_3O_{8-x} = 0.22436$ g
Ce(IV) required $5.501\cdot10^{-4}$ moles
Hence $x = (842/2)\cdot[(5.501\cdot10^{-4})/(0.22436)] - 1 = 0.033$
$U_3O_{8-x} = U_3O_{7.967}$ or $O/U = 2.656$.

REFERENCES

1 E. D. Lynch and J. H. Handwerk, *ANL-6893*, 1965.
2 K. Hagemark and M. Broli, *J. Inorg. Nucl. Chem.*, 28 (1966) 2837.
3 K. Goto, *Nippon Kagaku Zasshi*, 89 (1968) 927.
4 S. R. Dharwadkar and M. S. Chandrasekhariah, *BARC-416*, 1969; accepted for publication in *High Temp. Sci.*
5 M. H. Rand and O. Kubaschewski, *The Thermochemical Properties of Uranium Compounds*, Oliver and Boyd, 1963.
6 E. H. P. Cordfunke and P. Aling, *Trans. Faraday Soc.*, 61 (1965) 50.
7 R. J. Ackermann, E. G. Rauh and M. S. Chandrasekhariah, *J. Phys. Chem.*, 73 (1969) 762.
8 F. Gronvold, J. J. Kveseth, A. Sveen and J. Tichy, *J. Chem. Thermodyn.*, 2 (1970) 665.
9 G. T. Reedy and M. G. Chasanov, *J. Nucl. Mater.*, 42 (1972) 841.
10 S. R. Dharwadkar and M. S. Chandrasekhariah, *Anal. Chim. Acta*, 45 (1969) 545.
11 S. R. Dharwadkar, M. D. Karkhanavala and M. S. Chandrasekhariah, private communication.

Analytica Chimica Acta, 67 (1973) 213–215

SHORT COMMUNICATION

Decomposition of antimony concentrates with ammonium iodide

D. P. SCHWEINSBERG
Department of Chemistry, Queensland Institute of Technology, Brisbane (Australia)
B. J. HEFFERNAN
Department of Mining and Metallurgical Engineering, University of Queensland, Brisbane (Australia)
(Received 18th April 1973)

Ammonium salts, because of their acidic properties, may be used to decompose basic mineral sulphides and oxides[1]. Verbeek *et al.*[2] have extensively investigated the use of ammonium hydrogensulphate–ammonium nitrate–ammonium chloride mixtures for the decomposition of sulphide and oxide minerals and ores of iron, zinc, copper, lead and manganese. The volatility of certain metal iodides makes ammonium iodide particularly attractive as a flux, and since the early studies by Caley and Burford[3], various workers[4–6] have used this reagent to decompose tin-bearing ores and concentrates. Its application to the decomposition of soils and ores containing relatively low concentrations of antimony has also been investigated[7,8].

This communication describes the extension of the ammonium iodide fusion technique to the decomposition of materials containing high concentrations of antimony, *viz.*, sulphide and oxide-type mill middlings and concentrates.

Experimental

Samples. A number of mill products with antimony contents ranging from *ca.* 20 to 70% and consisting of oxide, sulphide and mixed oxide–sulphide type ores were selected. Each sample was reduced for analysis by grinding in a "Siebtechnik" rotary disc mill for 40 s.

Reagents. Analytical-grade reagents were used throughout. The 0.1 *N* potassium permanganate solution was standardized against pure dried sodium oxalate.

Preliminary studies. The radiant pot furnace previously described[4] was used to provide controlled heating of the reaction mixture which was contained in a 25 × 250 mm pyrex test tube (wall thickness 1 mm).

Combined differential thermal–thermogravimetric analysis was investigated as a means of establishing the minimal furnace temperature for complete extraction of antimony as the iodide. Pure antimony(III) oxide was mixed with 10 times its weight of ammonium iodide and the analysis was performed in a static air atmosphere at a heating rate of 10° min^{-1}. The DTA and TG curves obtained by means of a Rigaku differential thermal–thermogravimetric analyser with alumina

as the reference material are shown in Fig. 1. Antimony(III) oxide does not show any thermal reactions or weight losses up to 400° [9]. Thermogram A indicates the sublimation of ammonium iodide. The mixture of antimony oxide with excess of ammonium iodide shows complex endotherms (thermogram B) which are probably due to the formation of antimony(III) iodide followed by sublimation of the excess of ammonium iodide. The DTA and TG curves indicate that complete sublimation of antimony(III) iodide probably occurs at 255°. This agrees with other extraction studies[8] on a stibnite ore in which 100% antimony recovery was achieved with the pot furnace operated at 250°; 300° was finally selected as a convenient temperature. Although the reaction between antimony(III) oxide and ammonium iodide may be complex, thermal analysis appears to be a convenient and rapid method of establishing the required extraction temperature.

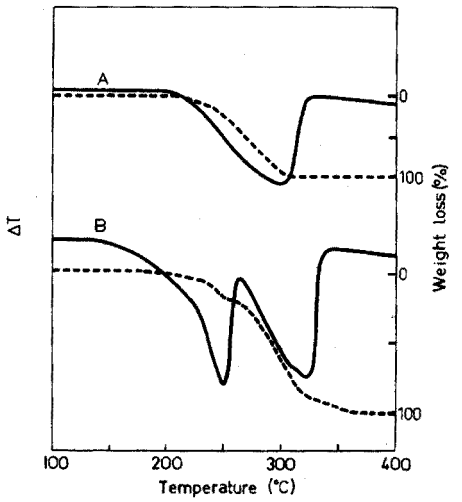

Fig. 1. Combined differential thermal–thermogravimetric analysis. (——) DTA; (------) TGA; (A) ammonium iodide alone; (B) antimony oxide with excess of ammonium iodide.

From previous work[8], a 20-min heating period was adopted to ensure complete volatilization of antimony from 0.200 g of sample mixed with 2 g of ammonium iodide.

Procedure. Weigh a 0.200-g sample into a 25 × 250 mm pyrex test tube fitted with a pouring lip. Add *ca.* 2 g of ammonium iodide and mix intimately with the ore by rotating the tube. Place the tube in the pot furnace at 300° for 20 min. After allowing the contents to cool, dissolve the antimony iodide in 30 cm^3 of sulphuric acid (1+4) by warming gently over a Bunsen burner.

Transfer the solution and residue to a 500-cm^3 Erlenmeyer flask with the minimal amount of sulphuric acid (1+4). Add a few glass beads and bring the mixture to the boil on a medium-temperature hot-plate. Add about 10 drops of concentrated nitric acid and heat until all the evolved iodine and finally water have been driven off. Add $\frac{1}{8}$th of a 9-cm filter paper (to reduce arsenic and antimony to the trivalent state) and heat on a high-temperature hot-plate until strong fumes of sulphur trioxide are evolved. Boil until the solution becomes

colourless. Leave to cool, carefully wash down with 50 cm^3 of water, and add 100 cm^3 of concentrated hydrochloric acid. After testing for arsenic, determine antimony titrimetrically with potassium permanganate after isolation as the sulphide with hydrogen sulphide[10].

Results and discussion

The effectiveness of the ammonium iodide fusion method for the dissolution of antimony middlings and concentrates was tested by analysing the samples in the same way but with a conventional sulphate–sulphuric acid decomposition method[10]. The results obtained by the two methods (Table I) are in good agreement. The ammonium iodide fusion is rapid and effective for the decomposition of high antimony content mill products derived from sulphide and oxide ore types. The use of an all-glass reaction vessel is advantageous.

TABLE I

DETERMINATION OF ANTIMONY IN MILL PRODUCTS

Sample type	*Antimony (%)*	
	Iodide fusion	*Sulphate fusion*
Oxide 1	22.4	21.8
Oxide 2	27.5	27.5
Oxide/sulphide 3	38.0	36.9
Sulphide 4	58.4	58.6
Oxide/sulphide 5	59.4	60.4
Sulphide 6	66.0	65.6
Mean error (%)	0.38	0.30

Appreciation is expressed to Professor R. L. Whitmore and Dr. R. F. Cane for use of facilities.

REFERENCES

1 L. Erdey, *Gravimetric Analysis*, Vol. 1, Pergamon, London, 1963, p. 29.
2 A. A. Verbeek, J. B. B. Heyns and R. A. Edge, *Anal. Chim. Acta*, 49 (1970) 323.
3 E. R. Caley and M. G. Burford, *Ind. Eng. Chem., Anal. Ed.*, 8 (2) (1936) 114.
4 B. J. Heffernan, R. O. Archbold and T. J. Vickers, *Proc. Aust. Inst. Min. Metall.*, No. 223 (1967) 65.
5 J. A. Bowman, *Anal. Chim. Acta*, 42 (1968) 285.
6 D. P. Schweinsberg and B. J. Heffernan, *Talanta*, 17 (1970) 332.
7 D. J. Nicolas, *Anal. Chim. Acta*, 55 (1971) 59.
8 D. P. Schweinsberg and B. J. Heffernan, *Proc. Aust. Inst. Min. Metall.*, No. 241 (1972) 87.
9 B. W. King and A. I. Andrews, *J. Amer. Ceram. Soc.*, 23 (8) (1940) 225.
10 A. H. Low, A. J. Weinig and W. P. Schoder, *Technical Methods of Ore Analysis*, Wiley, New York, 11th Ed., 1948, p. 37.

Analytica Chimica Acta, 67 (1973) 216–219

SHORT COMMUNICATION

Sorbentien als Hilfsmittel bei der Neutronenaktivierungsanalyse von Flüssigkeiten

CHRISTIAN SEGEBADE

Bundesanstalt für Materialprüfung, Laboratorium 6.33 "Anwendung von Radionukliden", Berlin-Dahlem (Deutschland)

(Eingegangen den 9. Dezember 1972)

Die Notwendigkeit, geeignete Sorbentien als Hilfsmittel bei der Neutronenaktivierung zu ermitteln, ergab sich bei der Aktivierungsanalyse von Legierungselementen im Stahl mit 14 MeV-Neutronen. Sorbentien sind ausserordentlich zweckmässig, wenn man Flüssigkeiten auf den Gehalt an bestimmten Elementen untersuchen will.

Für feste Proben benutzt man eine Rohrpost, die einen schnellen Probentransport ermöglicht[1]. Dagegen mussten flüssige Proben bislang in eine Glasampulle eingeschmolzen und in einem gepolsterten Rabbit durch die Rohrpost in die Bestrahlungsposition transportiert werden. Nach der Bestrahlung musste die Probe aus der Ampulle in ein anderes Gefäss gegossen und vor den Detektor gebracht werden, da im Glas zuweilen störende Elemente (Al, Si, etc.) vorhanden sind. Diese zeitraubenden und umständlichen Arbeitsgänge können durch Verwendung von Sorbentien vermieden werden, wobei sich im einzelnen folgende Vorteile ergeben: Wegfall der Glas- oder Quarzampulle (Vermeidung störender Aktivitäten); Wegfall des Einschmelzens, keine Möglichkeit für eine thermische Zersetzung oder Entzündung des Lösungsmittels. Bei Verwendung von Polyäthylenkapseln ist kein Umfüllen erforderlich, und es wird eine Zeitersparnis erreicht, die bei kurzer HWZ des Folgenuklids für die Genauigkeit der Bestimmung entscheidend sein kann.

Man kann eine Flüssigkeit im Sorbens praktisch wie eine feste Probe behandeln. In vielen Fällen kann man auf ein Einengen des Probevolumens verzichten, was besonders bei leicht zersetzlichen organischen Verbindungen von Vorteil ist.

Die Sorbentien werden in Polyäthylenkapseln mit der Rohrpost in die Bestrahlungsposition transportiert. Die Kapseln haben zylindrische Form (Durchmesser 27 mm, Höhe 8.5 mm), sie sind luft- und flüssigkeitsdicht verschliessbar, bei hoher mechanischer Beanspruchung (Transport durch die Rohrpost) bruchsicher und erzeugen nach Bestrahlung mit 14 MeV-Neutronen kein nennenswertes Eigenspektrum. Nach der Bestrahlung werden die Kapseln durch die Rohrpost in die Messposition transportiert. Das Gammaspektrum wird im Energiebereich von 0 bis 2 MeV in einem 400-Kanal-γ-Spektrometer abgebildet.

Das beschriebene Verfahren führt zu reproduzierbaren Ergebnissen, da die geometrischen Daten bei Bestrahlung und Messung konstant bleiben, was bei der Aktivierung in Reagenzgläsern und manuellem Transport nicht immer gewährleistet ist.

Die Sorbentien mussten vier Forderungen erfüllen:

1. Sie sollten kein oder ein nur geringes Eigenspektrum nach der Bestrahlung aufweisen.
2. Die Handhabung mit den Sorbentien sollte einfach und ungefährlich sein.
3. Sie sollten ein grosses Adsorptionsvermögen besitzen.
4. Die Flüssigkeit muss sich im Sorbens homogen verteilen.

Fünf Sorbentien wurden untersucht: Aktivkohle, Al_2O_3, Zellulose, HgJ_2 und $HgBr_2$.

Die homogene Flüssigkeitsverteilung in der Zellulose wurde mit folgender Methode nachgewiesen: Die Zellulose wurde in die Kapsel gelegt, 1 ml 5%ige $Cr_2(SO_4)_3$-Lösung eingetropft, das Sorbens nach 2 min wieder aus der Kapsel genommen und bei 105° getrocknet. Dann wurde die Zellulose in 20 gleichgrosse Quadrate geteilt, aus jedem Quadrat das Cr^{3+} herausgelöst und kolorimetrisch bestimmt. Die Abweichung der tatsächlichen Gehalte vom theoretischen Gehalt bei homogener Verteilung (663 μg Cr^{3+} pro Quadrat) betrug $\pm 2\%$.

Wie aus Abb. 1 ersichtlich, ist bei Al_2O_3, HgJ_2 und $HgBr_2$ die Forderung nach geringem Eigenspektrum nicht erfüllt; sie können nur bedingt als Sorbentien verwendet werden. Aktivkohle zeigt zwar kein nennenswertes Eigenspektrum, wird aber wegen der unangenehmen und zeitraubenden Handhabung nicht empfohlen.

Beispiel 1

Es ist nicht möglich, Chrom im Stahl mit 14 MeV-Neutronen zerstörungsfrei zu bestimmen, wenn auch Mangan anwesend ist, da aus beiden Elementen als Folgenuklid ^{52}V entsteht. Die zu bestimmenden Elemente waren in unserem Fall: Chrom, Mangan, Vanadin und Aluminium. Das Chrom wurde zunächst durch Extraktion und Säulenchromatographie abgetrennt[2]. Ist der Chromgehalt im Stahl $\geqslant 1\%$ (Einwaage: 1 g), so kann die chromhaltige Fraktion des Eluates, nachdem sie in einem Messkolben auf 25 ml aufgefüllt worden ist, in aliquoten Teilen von 2 ml direkt im Sorbens bestrahlt und gemessen werden. Die anderen Elutionsfraktionen können in gleicher Weise behandelt werden, sofern ihre Konzentrationen ebenfalls $\geqslant 1\%$ sind. Da der Gehalt an Chrom kleiner als 1% war, wurde das Eluat auf 5 ml eingeengt, 2 ml mit einer Pipette entnommen, in das Sorbens getropft und bestrahlt. Bei der Aktivierung von Chrom entsteht als Folgenuklid[3] u.a. ^{52}V, das zur Auswertung der Analyse herangezogen wurde: $^{52}Cr(n,p)^{52}V$ ($\sigma = 105$ mb, $T_{\frac{1}{2}} = 3.77$ min, $E_\gamma = 1.44$ MeV). Als Sorbens wurde hier Zellulose benutzt. Die Bestrahlzeit betrug 6 min. Nach einer Wartezeit von 30 s war das ^{16}N, das aus dem in der Zellulose und in der Lösung reichlich vorhandenen Sauerstoff nach der Reaktion $^{16}O(n,p)^{16}N$ ($T_{\frac{1}{2}} = 7.352$ s) entstanden war, praktisch vollständig zerfallen. Die Zählzeit betrug 5 min.

Beispiel 2

Besonders zu empfehlen ist der Gebrauch von Sorbentien bei der Aktivierung von organischen Substanzen, die in reiner Form instabil und leicht flüchtig sind. Bei der Aktivierungsanalyse von Chlor und Brom in einem Pflanzenschutzmittel wurden Sorbentien als Hilfsmittel erfolgreich verwendet[4], da das untersuchte Pestizid nur in Aceton oder Xylol löslich und ausserdem thermisch instabil ist. Zellulose ist als Sorbens nicht geeignet, wenn das Folgenuklid des zu bestimmenden Elements

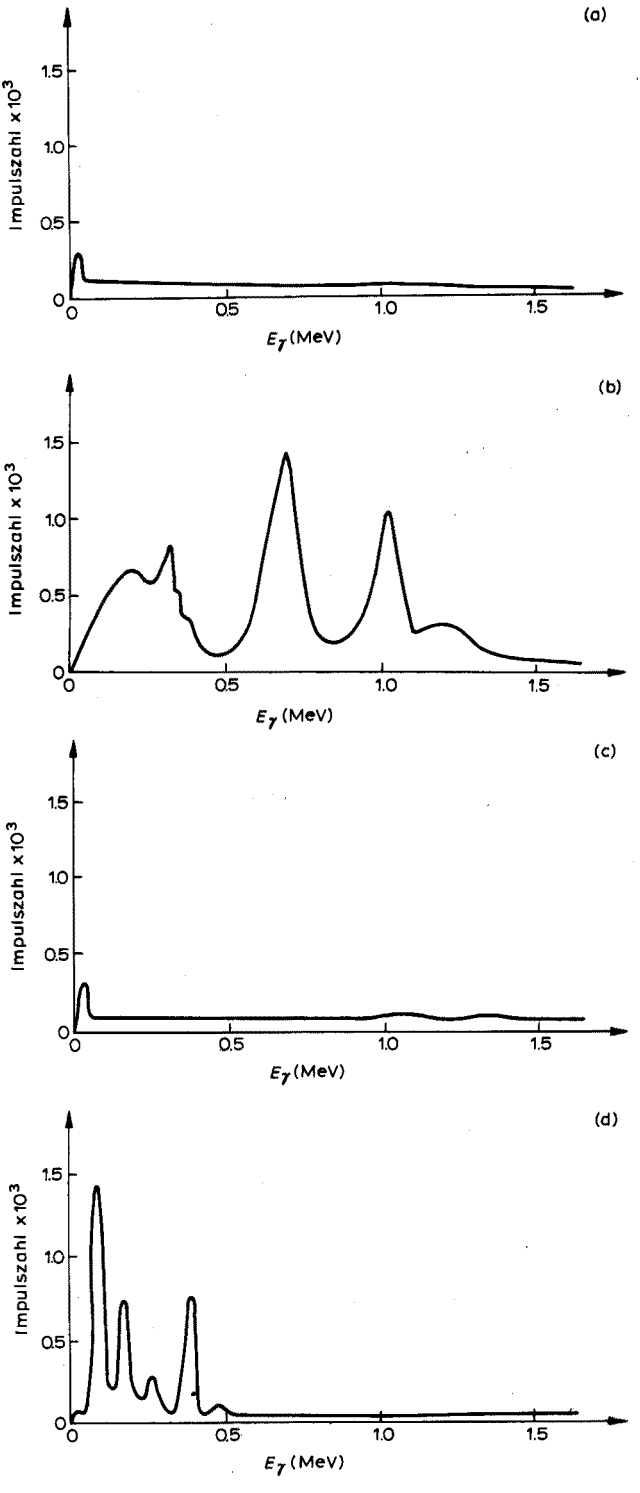
(a)
Impulszahl x10³
1.5
1.0
0.5
0
0
0.5
1.0
1.5
Eγ (MeV)
(b)
Impulszahl x10³
1.5
1.0
0.5
0
0
0.5
1.0
1.5
Eγ (MeV)
(c)
Impulszahl x10³
1.5
1.0
0.5
0
0
0.5
1.0
1.5
Eγ (MeV)
(d)
Impulszahl x10³
1.5
1.0
0.5
0
0
0.5
1.0
1.5
Eγ (MeV)

eine sehr kurze Lebensdauer aufweist, etwa im Sekundenbereich. Der Sauerstoffuntergrund von Zellulose oder auch Al_2O_3 würde die Analyse erheblich stören. Bei der Chlorbestimmung in einem Pflanzenschutzmittel nach der Reaktion $^{37}Cl(n,\alpha)^{34}P$ ($\sigma = 50$ mb, $T_{\frac{1}{2}} = 12.40$ s, $E_\gamma = 2.13$ MeV (25% abs.)) muss ein sauerstoffarmes

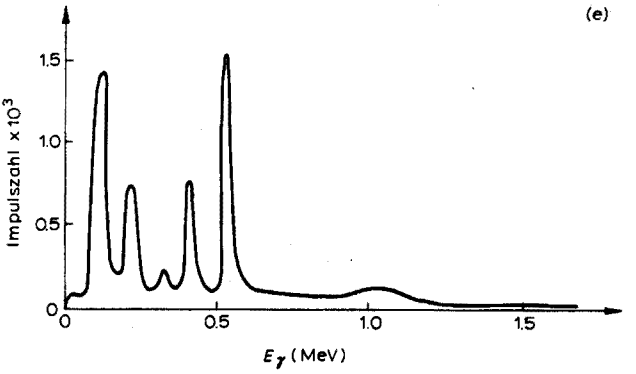

Abb. 1. γ-Spektrum nach Bestrahlung mit 14 MeV-Neutronen. m = Masse des Sorbens, t_b = Bestrahlzeit, t_w = Wartezeit, t_z = Zählzeit. (a) Aktivkohle: $m = 200$ mg, $t_b = 6$ min, $t_w = 20$ s und $t_z = 5$ min. (b) Aluminiumoxid: $m = 300$ mg, $t_b = 2$ min, $t_w = 20$ s und $t_z = 3$ min. (c) Zellulose: $m = 200$ mg, $t_b = 6$ min, $t_w = 20$ s und $t_z = 5$ min. (d) Quecksilber(II)-jodid: $m = 700$ mg, $t_b = 1$ min, $t_w = 2$ s und $t_z = 1$ min. (e) Quecksilber-(II)-bromid: $m = 700$ mg, $t_b = 1$ min, $t_w = 2$ s und $t_z = 1$ min.

Sorptionsmittel verwendet werden. Die zu bestimmende chlorhaltige xylolische Lösung wurde in HgJ_2 getropft. Die Wartezeit nach der Bestrahlung betrug 2.5 s, was der Laufzeit durch die Rohrpost entspricht. Hier kann auch $HgBr_2$ verwendet werden, da es, ebenso wie HgJ_2, im Energiebereich von 2–3 MeV keinen Untergrund erzeugt.

Ich danke Prof. Dr. Neider, Dipl.-Ing. B. F. Schmitt und Dr. P. Reimers für ihre Mithilfe und wertvollen Anregungen.

LITERATUR

1 R. Neider, B. F. Schmitt, P. Reimers und P. Mlitz, *Materialprüfung*, 11 (1969) 28.
2 B. F. Schmitt und C. Segebade, in Vorbereitung.
3 C. M. Lederer, J. M. Hollander und I. Perlman, *Table of Isotopes*, J. Wiley, New York, 6th Ed., p. 18.
4 C. Segebade, in Vorbereitung.

Analytica Chimica Acta, 67 (1973) 220–224

SHORT COMMUNICATION

Phosphorimetric determination of traces of boron

M. MARCANTONATOS, G. GAMBA and D. MONNIER

Department of Inorganic and Analytical Chemistry, University of Geneva, Geneva (Switzerland)

(Received 20th March, 1973)

It has been shown[1] that boric acid forms a highly luminescent complex with dibenzoylmethane, the phosphorescence emission of which in a 8% sulfuric acid (96%)–diethylether (v/v) glassy medium (77°K) permits a quantitative determination of nanogram amounts of boron.

Benzoylacetone is also capable of forming phosphorescent complexes with boric acid, under similar conditions. Compositions (1:1, 2:1), stability constants ($\beta_1 = 1.4 \cdot 10^5$, $\beta_2 = 2.4 \cdot 10^8$) and probable structures of these chelates have been given from phosphorescence excitation–emission, spectral and mean life-time determinations[2,3].

In a recent extensive study of the "boric acid–dibenzoylmethane" system, it has been shown[4] that the phosphorescence calibration curves previously obtained[1] are based on the $T \rightarrow S_0$ emission of a 2:1 dibenzoylmethane–boric acid chelate which most probably has the structure II, formed as follows:

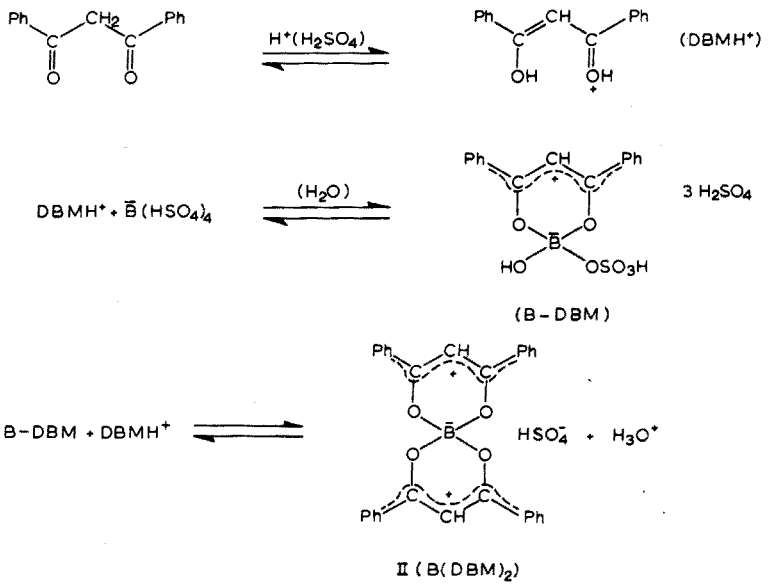

This chelate has the following spectroscopic properties (S = singlets; T_1 = lowest triplet; τ = mean life-time):

$S_3(\pi\pi^*)$: 39210 cm^{-1}; $S_2(\pi\pi^*)$: 31350 cm^{-1}; $S_1(\pi\pi^*)$: 24390 cm^{-1};

$T_1(\pi\pi^*)$: 19610 cm^{-1}; S_1–T_1: 4780 cm^{-1}; $\tau = 0.65$ s.

Until now, neither of these two highly sensitive luminescence reactions of boric acid has found analytical application and no other phosphorimetric method has been proposed for the determination of traces of boron.

In the present study, the technique described previously[1] is applied to the direct determination of micro-amounts of boron in sea water and in solutions containing an interfering metal.

Experimental

Apparatus. An Aminco-Keirs phosphorimeter was used for excitation and emission determinations. Spectra and phosphorescence decay curves were obtained with a Houston Omnigraph recorder, Model HR-96, and a Tektronix oscilloscope, Type 564.

Calibrations can be made either with a boric acid–dibenzoylmethane solution of definite composition ($[DBM] \geqslant 200[BO_3H_3]$), prepared as described below, or with a fresh standard solution of solid 1:1 boric acid–benzoylacetone complex (for its preparation, see ref. 2) in 8% sulfuric acid (96%) – diethylether (v/v).

Reagents. Boric acid, sulfuric acid ($d = 1.84$), ether and ethanol were of analytical-grade quality (Merck). Dibenzoylmethane (Fluka) was purified by double recrystallization with water–ethanol (85 + 15).

Preparation of solutions for phosphorescence determinations. In a silica test tube, graduated to 5 ml, heat 0.4 ml of 96% sulfuric acid containing nanogram-amounts of boron as boric acid, in an oven at 70° for 60 min. After cooling, add small portions of ether, mix cautiously and complete the volume to 5 ml. Introduce a portion of this solution into a 2-mm diameter phosphorimetric cell, and measure the emission (77°K) at 508 nm, with an excitation wavelength of 402 nm.

Results and discussion

Calibration curves and limits of determination. Phosphorescence calibration curves with benzoylacetone were constructed in the ng B ml^{-1} range and compared with those obtained with dibenzoylmethane[1]. Relative errors with the benzoylacetone reagent were approximately the same as with dibenzoylmethane, but the apparent phosphorescence efficiency was about three times lower.

The limits of determination were found to be 0.4 ng B ml^{-1} with benzoylacetone and 0.1 ng B ml^{-1} with dibenzoylmethane.

Effects of diverse ions. The boron–dibenzoylmethane reaction was chosen for analytical purposes and the effects of the following ions were investigated for solutions containing 22 ng B ml^{-1} of sulfuric acid–diethylether ([ion]/[boron] = 100): Cr^{6+}, Ce^{4+}, Ni^{2+}, Cu^{2+}, Mg^{2+}, Mn^{2+}, Pb^{2+}, Cd^{2+}, Zn^{2+}, Sn^{2+}, Mo^{6+}, Li^+, Na^+, K^+, Al^{3+}, V^{5+}, Fe^{3+}, Co^{2+}, Zn^{2+}, Ag^+, Te^{6+}, Hg^{2+}, In^{3+}, Tl^+, NH_4^+, W^{6+}, F^-, Br^-, Cl^-, I^-, NO_3^-, SCN^-, PO_4^{3-}, $S_2O_3^{2-}$, CH_3COO^-.

All the ions mentioned gave errors of less than 10%, except for molybdenum

and tungsten which caused positive interferences as follows:

	B	*B+Mo*	*B+W*
Phosphorescence intensity	75	270	85

Effects of tungsten and molybdenum. An investigation of molybdenum–dibenzoylmethane and tungsten–dibenzoylmethane solutions in diethylether–sulfuric acid (the metal ions were added as $(NH_4)_6Mo_7O_{24}$ and Na_2WO_4) prepared as described above for the boric acid–dibenzoylmethane solution, showed the formation of phosphorescent complexes. This was not unexpected, for complexation of molybdenum and tungsten by dibenzoylmethane in acidic media is well known[5].

As the excitation and emission bands of these two complexes were found to be situated very close to those of the boron–dibenzoylmethane (principal bands: excitation, 403 nm (W), 405 nm (Mo); emission, 506 nm (W), 509 nm (Mo), positive interferences result from emission contributions.

This, however, was only part of the observed effects. External heavy-atom perturbations were also found to be responsible for the increase in phosphorescence intensity of the boron–dibenzoylmethane complex.

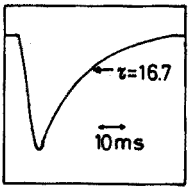

Fig. 1. Mo–DBM decay curve. [DBM]/[Mo]=3; [Mo]=$2 \cdot 10^{-4}$.

Molybdenum heavy-atom perturbation. The mean life-time τ_{Mo} of the phosphorescent molybdenum–dibenzoylmethane species was found to be 16.7 ms (Fig. 1). This is sufficiently different from the τ_B value for the boron–dibenzoylmethane chelate (0.65 s), for it to be possible to determine boron in the presence of molybdenum (Fig. 2), with reference to a calibration curve, from curves of log P_t against time, where P_t, the total phosphorescence, is $(P^0_{Mo}\,e^{-t/\tau_{Mo}} + P^0_B\,e^{-t/\tau_B})$.

For $t \gg \tau_{Mo}$, the function log P_t reduces to

$$\log P_B = \log P^0_B - (t/2.303\ \tau_B) \qquad (1)$$

It can be seen from the results in Table I and from Fig. 3 that the presence of molybdenum causes an increase of *ca.* 30% in the phosphorescence emission of the boron–dibenzoylmethane complex.

Possible boron impurities in ammonium heptamolybdate, high enough to make a significant contribution to the boron–dibenzoylmethane phosphorescence, are improbable, as can be seen from the time and purely exponential form of the molybdenum–dibenzoylmethane emission decay (Fig. 1).

However, for solutions containing molybdenum, the mean life-time τ_B of the boron–dibenzoylmethane complex, obtained from the slopes of eqn. (1) is 0.61 s, which corresponds to a 40 ms decrease in the τ value of the boron–dibenzoylmethane complex in pure solution.

These two variations—increase in phosphorescence intensity and decrease in the τ value—are well known to be due to a heavy-atom perturbation.

TABLE I

DETERMINATION OF BORON IN THE PRESENCE OF MOLYBDENUM

(P_B^0 and P_B^{0*} are the phosphorescence intensities of boron–dibenzoylmethane in the absence and in the presence of molybdenum, respectively. P_B^{0*} is obtained from $\log P_B = f(t)$ (see eqn. 1). Excitation, 402 nm; emission, 508 nm.)

B taken (*ng ml*$^{-1}$)	P_B^0	P_B^{0*a}	*B found* (*ng ml*$^{-1}$)	$(P_B^{0*} - P_B^0)\ 100/P_B^0$ (%)
10.8	35.8	47.3±0.4	13.3	+32.1
10.8	35.8	44.8±0.1	12.5	+25.1
21.6	73.5	91.4±2.4	25.9	+24.4
21.6	73.5	99.7±2.6	27.6	+35.7

[a] Values from four decay curves. $[Mo]/[BO_3H_3] = 100$.

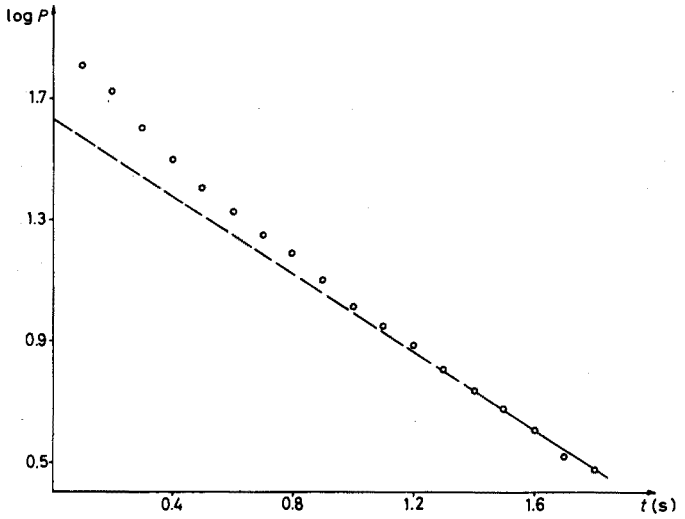

Fig. 2. Log of total phosphorescence (P_t) *versus* time; 10^{-6} *M* $H_3BO_3 + 1 \cdot 10^{-4}$ *M* Mo $+ 6 \cdot 10^{-4}$ *M* dibenzoylmethane in sulfuric acid–diethylether.

Determination of boron in sea water.

This determination was carried out by taking 0.05–0.3 ml of a stock solution (0.5 ml of sea water sample n 10 ml of 96% surfuric acid), and adding it to 0.1 ml of $4 \cdot 10^{-2}$ *M* dibenzoylmethane in 96% sulfuric acid. The solution was diluted to 0.4 ml with 96% sulfuric acid and heated at 70° for 1 h. After cooling, small portions of ether were added to a total volume of 5 ml and the emission intensity (77°K) was measured at 508 nm with an excitation wavelength of 402 nm.

The only precaution one must take is that the final solution should not contain more than 3% of water, a limit above which transparent glasses could not be obtained at 77°K.

The results obtained by means of a reference solution containing 10 ng of boron are given in Table II.

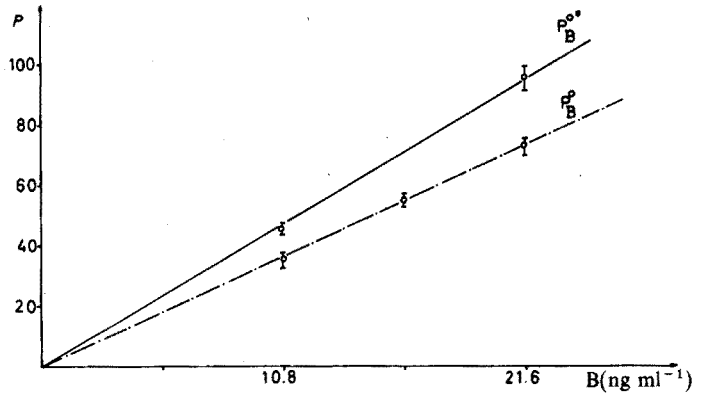

Fig. 3. Phosphorescence intensity *versus* boron concentration. P_B^0 and P_B^{0*}: in the absence and in the presence of molybdenum, respectively. In the two cases, the phosphorescence intensity is due to the boron–dibenzoylmethane complex alone.

TABLE II

PHOSPHORIMETRIC DETERMINATION OF BORON IN SEA WATER (BORDEAUX)

V^a	P^b	*ng B* ml^{-1}	*p.p.m. B*	*V*	*P*	*ng B* ml^{-1}	*p.p.m. B*
0.10	19.1	4.68	4.68	0.20	34.5	8.76	4.38
0.10	16.9	4.10	4.10	0.20	34.0	8.64	4.32
0.10	17.0	4.13	4.13	0.20	34.0	8.64	4.32
0.10	18.0	4.39	4.39	0.20	35.0	8.90	4.45

Average value: 4.35 ± 0.15 p.p.m. B.

[a] V = ml of stock solution.
[b] P = phosphorescence intensity referred to a blank.

REFERENCES

1 M. Marcantonatos, G. Gamba and D. Monnier, *Helv. Chim. Acta*, 52 (1969) 538.
2 M. Marcantonatos, G. Gamba and D. Monnier, *Helv. Chim. Acta*, 52 (1969) 2183.
3 G. Gamba and M. Marcantonatos, *Helv. Chim. Acta*, 54 (1971) 1509.
4 M. Marcantonatos and G. Gamba, unpublished work.
5 J. Stary and E. Hladky, *Anal. Chim. Acta*, 28 (1963) 227.

Analytica Chimica Acta, 67 (1973) 225–228

SHORT COMMUNICATION

On the chemiluminescent reaction of ozone with rhodamine B

F. CELARDIN and M. MARCANTONATOS

Department of Inorganic and Analytical Chemistry, University of Geneva, Geneva (Switzerland)

(Received 26th March 1973)

The chemiluminescent reaction between ozone and rhodamine B was first applied to the determination of ozone by Bersis and Vassiliou[1]. More recently, this reaction has been applied with improved results by Hodgeson *et al.*[2] and by Guicherit[3]. As pointed out by Hodgeson *et al.*, the mechanisms related to the chemiluminescent emission are not well understood. The data they obtained with rhodamine B and eosin Y suggested that a resonance energy transfer, from excited intermediate to unreacted dye, occurs as an integral part of the mechanism.

Our observations of the reaction between rhodamine B and ozone in glacial acetic acid, indicate that it is a product of this reaction which yields, on further reaction with ozone, an electronically excited species. Energy transfer from this excited moiety to the excess of rhodamine B in solution, is found to be responsible of the chemiluminescent emission of the dye at 590 nm.

Experimental

Ozone was generated by passing dry oxygen over a high-voltage discharge lamp. Solutions of rhodamine B were prepared by dissolving the analytical grade dye (Merck), in 100% acetic acid (Merck G.R.).

Chemiluminescent and spectral measurements were made with a modified Aminco-Bowman spectrofluorimeter equipped with an RCA IP 28 photomultiplier tube. The reaction cell with a fritted glass bottom for ozone entry was designed to fit the cell holder of the instrument.

Absorption, excitation and fluorescence spectra were recorded with Beckman DB-G and Hitachi Perkin Elmer MPF-2 spectrophotometers.

Results and discussion

Investigations were made under ozone steady-state conditions at room temperature.

Chemiluminescent emission *versus* time showed an induction period (Fig. 1) followed by a rapid increase in intensity to a maximum value which remained constant over a period proportional to the initial concentration of rhodamine B and to the rate of ozone flow. When the variation of rhodamine B concentration was followed during the reaction by absorption spectrophotometry, it was found that a continuous decrease of the rhodamine B absorption at 556 nm occurred

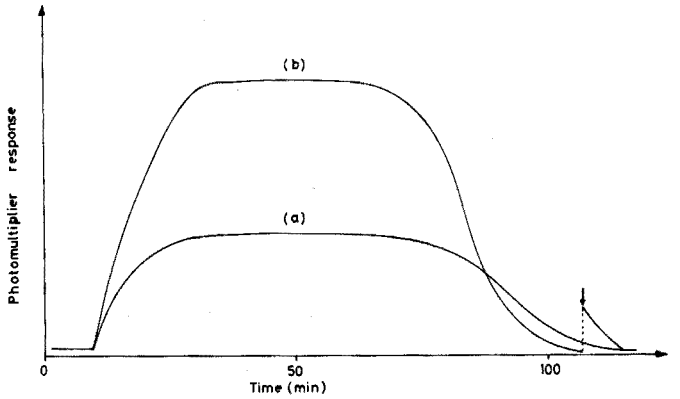

Fig. 1. (a) Total chemiluminescence emission *versus* time. (b) Chemiluminescence emission at 600 nm followed by emission at 540 nm (↓).

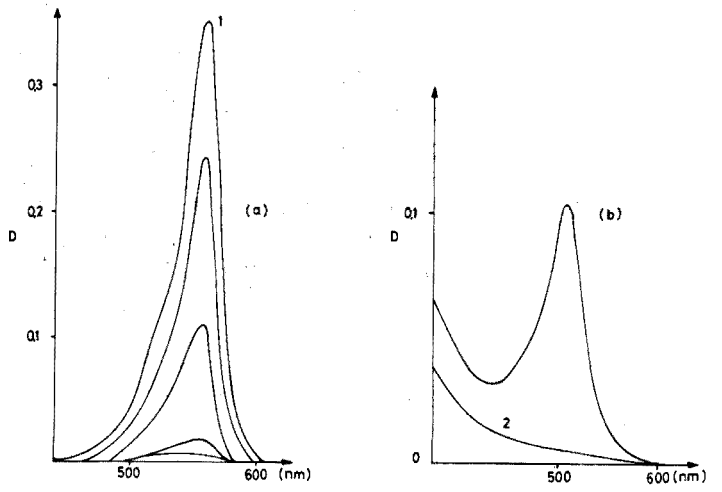

Fig. 2. (a) Absorption spectra of reaction mixture (8-μl aliquots diluted to 1 ml with glacial acetic acid) at different times (1, start). (b) Absorption spectra of reaction mixture at the end of reaction (2, end).

even during the time interval corresponding to the chemiluminescence induction period (Fig. 2a). Towards the end of the reaction, the solution exhibited a weak absorption at 510 nm which disappeared on further introduction of ozone (Fig. 2b). Monitoring of the reaction by fluorescence spectroscopy at an excitation wavelength of 490 nm, showed a decrease of rhodamine B emission at 586 nm and an increase of the resultant compound emission at 535–540 nm (Fig. 3).

Both the presence of an induction period and the initial consumption of rhodamine B without chemiluminescent emission suggest that the excited species (X*) is not formed directly by the reaction of ozone with the dye, but is rather a product of the consecutive reaction of the intermediate compound (A) with ozone (see reaction scheme below). The immediate intensity drop to zero after the ozone supply has been cut off, supported this reaction sequence (Fig. 4). There was

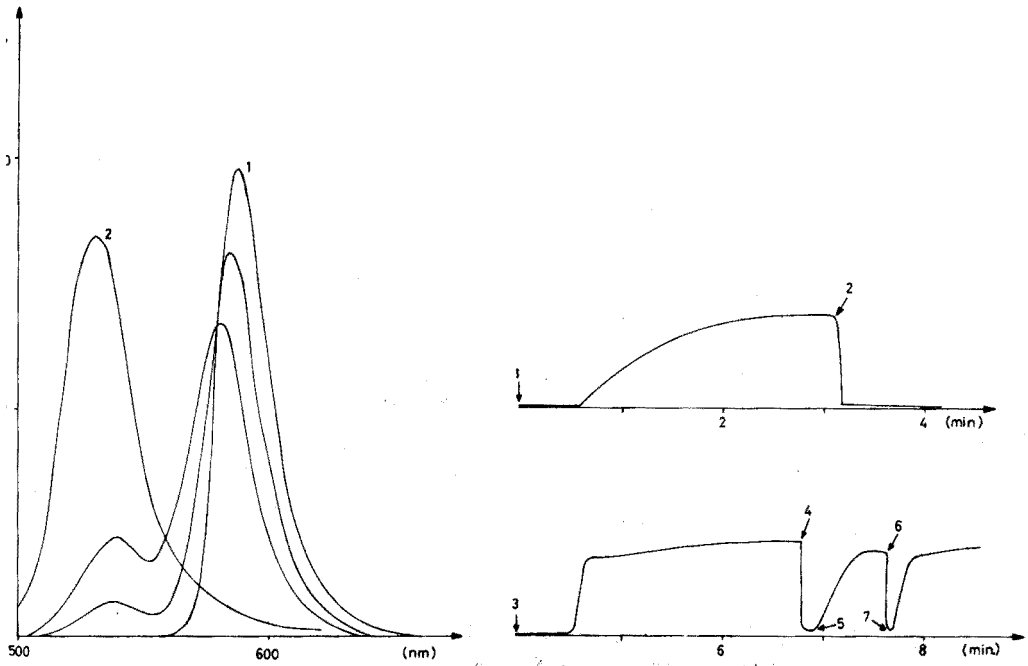

Fig. 3. Fluorescence spectra of reaction mixture at different times (excitation wavelength, 490 nm) (1, start; 2, end).

Fig. 4. Chemiluminescence emission *versus* time with ozone flow on (1, 3, 5, 7) and off (2, 4, 6).

virtually no induction period when the ozone supply was restarted immediately after its cut-off. The longer the time elapsed after ozone cut-off, the longer the induction period preceding the chemiluminescent emission. This supports the view that the accumulated intermediate compound (A) is of limited stability at room temperature.

Chemiluminescent spectra corroborate the intermediate compound–ozone reaction giving the excited state (reaction 2) and suggest that there is in fact energy transfer from the excited molecule (X*) to rhodamine B (reaction 3). Throughout the reaction, chemiluminescent emission occurs at 590 nm, which corresponds to the fluorescence emission of the dye. But as soon as the rhodamine B concentration falls to zero, the chemiluminescence emission occurs at 540 nm and decreases exponentially towards zero intensity (Fig. 1b). It is very likely that this emission is due to the excited state of the final compound (X*). The strong overlap of the emission band of the excited moiety at 540 nm with the absorption band of rhodamine B at 556 nm favours the idea of an energy-transfer step (Fig. 5).

On the basis of these preliminary observations, the following reaction sequence is proposed:

$$\text{Rh–B} + \text{O}_3 \xrightarrow{k_1} \text{A} \qquad (1)$$

$$\text{A} + \text{O}_3 \xrightarrow{k_2} \text{X}^* \qquad (2)$$

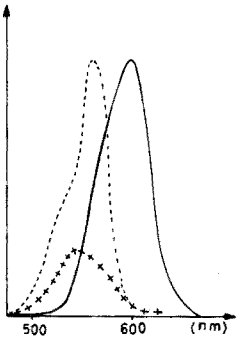

Fig. 5. Chemiluminescence spectrum of reaction mixture (——). Chemiluminescence spectrum when no rhodamine B remains (+ + +). Absorption spectrum of rhodamine B (– – – –).

$$X^* + Rh\text{-}B \xrightarrow{k_3} X + (Rh\text{-}B)^* \quad (3)$$

$$(Rh\text{-}B)^* \xrightarrow{k_4} Rh\text{-}B + h\nu_1 \quad (4)$$

$$X^* \xrightarrow{k_5} X \quad (5)$$

Thus, rhodamine B reacts with ozone to give an intermediate A which reacts with ozone to form an excited molecule X*. There is emission from rhodamine B after energy transfer from X*. After total consumption of rhodamine B, there is emission according to

$$X^* \xrightarrow{k_6} X + h\nu_2 \quad (6)$$

In this scheme, radiationless deactivation processes of rhodamine B have been neglected since the dye has a high fluorescence efficiency; moreover, all radiationless deactivations of X* besides reaction (3) are summed up by reaction (5). Further investigations on these topics are in progress.

REFERENCES

1 D. Bersis and E. Vassiliou, *Analyst*, 91 (1966) 499.
2 J. A. Hodgeson, K. J. Krost, A. E. O'Keefe and R. K. Stevens, *Anal. Chem.*, 42 (1970) 1795.
3 R. Guicherit, *Z. Anal. Chem.*, 256 (1971) 177.

Analytica Chimica Acta, 67 (1973) 229–233

SHORT COMMUNICATION

Enhancement of sensitivity for the determination of mercury in waters

E. HARSÁNYI, L. PÓLOS and E. PUNGOR
Institute for General and Analytical Chemistry, Technical University, Budapest (Hungary)
(Received 2nd April 1973)

The application of pesticides and plant protective agents means that the amount of mercury in the biosphere is continually increasing[1,2]. The increasing mercury content of waters is particularly important, for methyl mercury is extremely poisonous[3,4]. Although other techniques have been used, the flameless atomic absorption method is probably the most appropriate for the trace amounts of mercury involved, and this method has been widely studied[5–25]. In the flameless atomic absorption methods, the mercury compounds in the solution are reduced with tin(II) chloride, and the mercury vapours are driven by an air stream into the measuring cuvette[5]. Any methyl mercury in the water can be decomposed, as described by Omang[19], on standing for 24 h with sulfuric acid and potassium permanganate. Kopp *et al.*[12] also used potassium persulfate for the decomposition of mercury compounds. The sensitivity of the flameless mercury determination is usually 0.04 ng ml^{-1}, if the tin(II) chloride reduction is used.

In the case of low mercury concentrations, a large volume of solution is necessary. The removal of mercury then needs a large volume of gas, so that the amount of mercury reaching the atomic absorption cuvette during a unit of time is small, *i.e.* the process appears to be slow. This means that noise problems can become severe, and accuracy is affected.

Topping and Pirie[25] have suggested a preconcentration method in which mercury from a 4-l sample of sea water is aerated into 20 ml of a permanganate–sulfuric acid solution, after treatment of the water sample with tin(II). This solution is then treated with tin(II), and mercury is further aerated into the measuring cell. This procedure appears to have several advantages, and so a further study of the parameters was undertaken, in order to establish if the sensitivity and speed of the method could be improved.

Experimental

Apparatus. A Beckman DU 2 spectrophotometer, with a Varian mercury lamp (lamp current, 4 mA) was used. The absorption cuvette was a glass tube of 22 cm length and 16 mm in diameter covered at both ends by plane-parallel silica plates. The absorption was measured at 253.7 nm. The slit-width of the monochromator was 0.1 mm.

The design of the apparatus for enrichment of mercury is shown in Fig. 1.

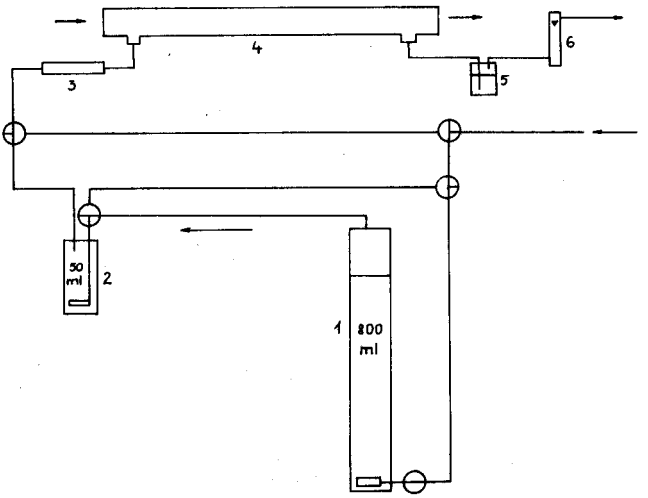

Fig. 1. Equipment for mercury enrichment and determination by atomic absorption. (1) Sample vessel: a 1-l cylindrical tube of 5 cm diameter with a glass-sinter inlet tube. (2) Mercury enriching vessel: a gas-washing bottle of 150 ml capacity. (3) Drying tube. (4) Absorption cuvette (see text). (5) Mercury absorber. (6) Rotameter.

Enrichment of the sample. Any organic mercury compounds present in the water were first decomposed as described by Omang[19]. The mercury contained in 800 ml of solution was then reduced by tin(II) chloride (10 ml of 20% solution) and driven by an air stream into 50 ml of an absorption solution obtained by mixing 0.2 ml of 6% (w/v) potassium permanganate and 10 ml of 20% (v/v) sulfuric acid, and diluting with water.

In order to check if absorption of mercury was complete, a known amount of mercury vapour was absorbed in the 50 ml of solution; this was then reduced with 2 ml of 20% tin(II) chloride solution. The mercury was driven by an air stream into the cuvette of the atomic absorption apparatus, connected directly after the absorption vessel, and the signal at 253.7 nm was observed on the recorder.

The enrichment technique can, of course, be applied to any other kind of mercury determination.

Dependence of sensitivity on the volume of sample solution

When the direct flameless atomic absorption method was used, and when identical amounts of mercury were aerated from various volumes, the height of the absorption signal decreased with increase of the sample volume (Fig. 2, Curve A). Since the peak height, or more exactly the peak area, is proportional to the amount of mercury, a mercury loss seems probable. However, it will be seen that it was only the signal-form which changed.

For determinations of mercury in natural waters, the amount of sample is usually not limited. By analysing larger volumes of solution of a given mercury concentration, an increase in the absorption peak should be obtained (Fig. 2, Curve B). However, there are limits to this possibility of increasing the sensitivity. First, the width of the absorption signal, *i.e.* the time necessary to drive out all

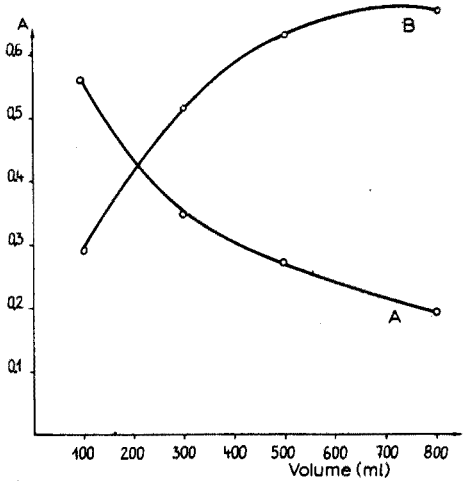

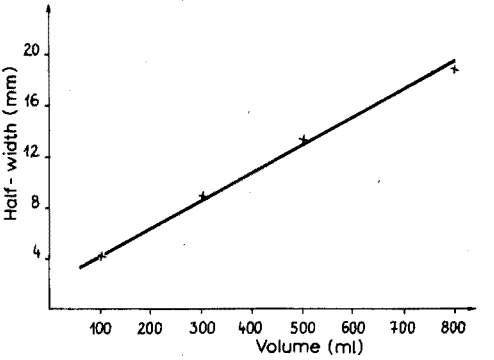

Fig. 2. Curve A: Changes in the absorbance of 1 μg of mercury reduced from different volumes of solution. Curve B: Changes in the absorbance as a function of increasing solution volume and mercury amount; the solution contained 5 ng Hg ml^{-1}.

Fig. 3. The change of the half-width of the absorption peak as a function of solution volume at the same mercury content (1 μg).

the mercury, will increase; peaks become blurred, reproducibility deteriorates, and transference of mercury is incomplete. The linear increase in the half-width of the absorption signals with increase in the volume of sample solution is shown in Fig. 3. Unfortunately, the absorption peaks are not symmetrical, the descending branch being very protracted; it is therefore difficult to evaluate the curve quantitatively, and the signal can hardly be separated from the noise. For comparison, the absorption peak for 500 ng of mercury was recorded directly after reduction with tin(II) in 800 ml of solution, and after concentration into 50 ml of solution and further reduction and aeration; Fig. 4 shows that the peak height increased significantly, the time of removal of mercury was reduced, and the correlation between signal and noise was improved.

Examination of the enrichment parameters

The influence exerted on the sensitivity by the rate of the air stream driving out the mercury from a large volume was examined. For flow rates in the range 20–100 l h^{-1}, no essential changes in sensitivity were observed, but a flow rate of 40 l h^{-1} was found optimal. This is in reasonable agreement with the results of Topping and Pirie[25], who used much larger sample volumes. At this flow rate, the absorption values of the measured peak heights were studied as a function of time. The absorption signal increased rapidly as the aeration time increased up to 8 min, and then remained constant for aeration times up to 40 min; a time of 10 min was therefore selected. It was also established that the optimal flow rate for aeration of mercury from a 50-ml volume is 20 ml h^{-1} (Fig. 5).

Under the established optimal conditions, an analytical curve was prepared for the range 25–500 ng of mercury; the mercury was driven from 800 ml of

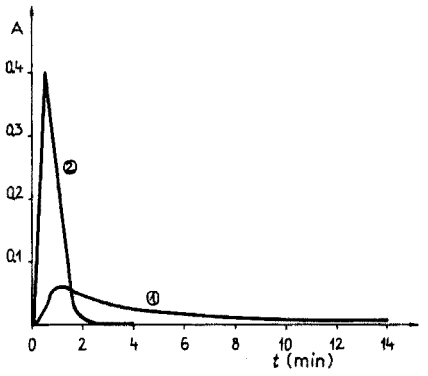

Fig. 4. Shape of the absorption peaks. (1) Reduction of 500 ng of mercury directly from 800 ml of solution; (2) aeration of 500 ng of mercury from 800 ml of solution into 50 ml of solution and further aeration into the absorption cuvette.

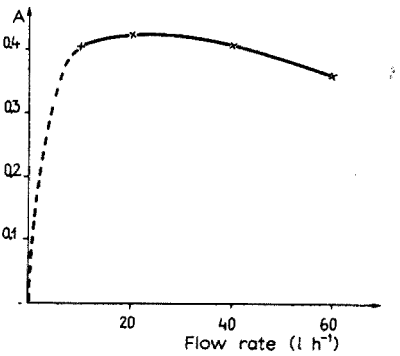

Fig. 5. Change of the absorption signal as a function of the flow rate of air. Mercury: 500 ng. Solution volume: 50 ml.

solution into a 50-ml volume, a 16-fold enrichment being achieved. Blank tests of the reagents were similarly obtained after enrichment, and corrections were always made for these blanks. The working curve was found to be almost rectilinear over the range 25–500 ng of mercury. Analytical curves were prepared for both peak heights and peak areas. The deviation of the absorption measurements was 3.5% for peak heights and 3.0% for peak areas.

Evaluation of the method

The value of the detection limit was determined from the deviation of the reagent blank results; with the proposed enrichment technique, it was found to be 0.008 ng Hg ml^{-1}, which could be further reduced by decreasing the blank value.

In a study of the efficiency of the enrichment, a 7% average decrease in the signal compared to direct aeration from a 50-ml volume was observed, *i.e.* the efficiency of the transference of mercury into the smaller volume was 93%. The relative standard deviation of the enriching operation was 4% for 7 parallel determinations.

The proposed enriching method was compared in the examination of waters with an enriching method based on extraction with dithizone; the efficiency of the latter method was 85% after a single extraction, but greater amounts of reagents were required, so that the blank values were larger. The reproducibility was the same in both cases.

The enrichment method, owing to its simplicity and rapidity, is very suitable for the determination of mercury in waters. Independently from the atomic absorption measurements, the enriching operation can be done on several samples simultaneously.

REFERENCES

1 L. J. Goldwater, *The Harben Lectures 1964*, Royal Institute of Health and Public Hygiene.

2 Report of an International Committee, Maximum Allowable Concentrations of Mercury Compounds, *Arch. Environ. Health*, 19 (1969) 891.
3 P. H. Abelson, *Science*, 169 (1970) 237.
4 S. Jensen and A. Jernelöv, *Nature*, 223 (1969) 753.
5 N. S. Poluektov, R. A. Vitkun and Y. V. Zelyukova, *Zh. Anal. Khim.*, 18 (1963) 33; 19 (1964) 937.
6 D. C. Manning, *At. Absorption Newslett.*, 9 (1970) 97.
7 J. K. Duffer, *J. Paint Technol.*, 43 (1971) 67.
8 W. R. Hatch and W. L. Ott, *Anal. Chem.*, 40 (1968) 2085.
9 G. Cumont, *Chim. Anal.*, 53 (1971) 634.
10 V. I. Muscat and T. J. Vickers, *Anal. Chim. Acta*, 57 (1971) 23.
11 M. Olivier, *Z. Anal. Chem.*, 257 (1971) 187.
12 J. F. Kopp, M. C. Longbottom and L. B. Lobring, *J. Amer. Water Works Ass.*, 64 (1972) 20.
13 L. P. Morgenthaler, *App. Notes*, 51 (1970) 25.
14 J. Y. Hwang, P. A. Ulluci and A. L. Malenfant Morane, *3. C.I.S.A.F.A., Paris, 1971.*
15 F. Yamauchi and Y. Katsumo, *Soda To Enso*, 22 (1971) 303.
16 E. G. Pappas and L. A. Rosenberg, *J. Ass. Offic. Anal. Chem.*, 49 (1966) 782.
17 H. Brandenberger and H. Bader, *Helv. Chim. Acta*, 50 (1967) 1409.
18 I. J. Oiva, *Appl. Spectrosc.*, 25 (1971) 526.
19 S. H. Omang, *Anal. Chim. Acta*, 53 (1971) 415.
20 A. Cavallaro and G. Elli, *Boll. Lab. Chim. Prov.*, 22 (1971) 1968.
21 D. C. Burrell, *3. C.I.S.A.F.A., Paris, 1971.*
22 H. L. Kahn, *At. Absorption Newslett.*, 10 (1971) 58.
23 D. Smith and R. A. Nicholson, *Nature*, 232 (1971) 393.
24 G. W. Kalb, *At. Absorption Newslett.*, 9 (1970) 84.
25 G. Topping and J. M. Pirie, *Anal. Chim. Acta*, 62 (1972) 200.

Analytica Chimica Acta, 67 (1973) 234–235

SHORT COMMUNICATION

Complexiметric determination of phosphate

ARTHUR DE SOUSA

Research Laboratories, Alfa Materials Technology, Inc., P.O. Box 816, Pottstown, Pa. 19464 (U.S.A.)

(Received 19th December 1972)

Several indirect complexiметric methods for the determination of the phosphate ion are known[1], but they are generally tedious owing to the time required for complete precipitation. The method described here is based on the rapid quantitative precipitation of silver orthophosphate ($K_s = 1.3 \cdot 10^{-20}$) from a neutral or slightly alkaline phosphate solution. The freshly precipitated silver phosphate was then dissolved in an ammoniacal solution of potassium tetracyanonickelate as suggested by Flaschka for silver halides[2]. Three g-ions of nickel(II) are released for two g-ions of phosphate, and the freed nickel is titrated with EDTA to a visual end-point with murexide as indicator[2]. The time required for a phosphate determination is about 30 min.

Experimental

Potassium tetracyanonickelate solution. Titrate a measured portion of 0.2 *M* nickel sulfate solution, after addition of ammonia, with 1 *M* potassium cyanide solution until murexide changes from yellow to purple. Repeat the titration and average the results. Mix equivalent amounts of the two solutions, add some ammonia, and dilute with water to a tetracyanonickelate concentration of about 0.1 *M*. The resulting solution, if sufficiently alkaline, is stable for some months.

Procedure. Add dropwise, preferably in a dark corner of the laboratory, a slight excess of an aqueous saturated silver nitrate solution to an aliquot of the phosphate solution made neutral or slightly alkaline. Check if the addition of further drops of silver nitrate causes any cloudiness in the clear supernate, and add more if necessary. Filter the precipitate on a G4 crucible and wash 3–4 times with water. Transfer the filter with the precipitate to a beaker containing sufficient potassium tetracyanonickelate solution to cover the filter. Heat gently while stirring until all the precipitate has dissolved. Remove the filter carefully from the beaker and rinse well with water, collecting the washings in the beaker. Titrate the displaced nickel with 0.1 *M* EDTA solution, using murexide as indicator. The end-point is indicated by the sudden change in colour from yellow-orange to purple. (1 ml of 0.1 *M* EDTA corresponds to 6.33 mg of phosphate.)

Results

The method described gave satisfactory results for the determination of phos-

phate in the range 10.0–150.0 mg; the accuracy varied from 1.0% to 0.5% over this range. There was no interference from moderate amounts of Al, Ni, Co, Mn, Zn, Cd, Cu, Pb, Ca, Sr, Ba, and Mg, but vanadate, chromate, molybdate, tungstate and halide ions interfered.

REFERENCES

1 G. Schwarzenbach and H. Flaschka, *Complexímetric Titrations*, Methuen, London, 1969.
2 H. Flaschka and F. Huditz, *Z. Anal. Chem.*, 137 (1952) 104; H. Flaschka, *Mikrochem.*, 40 (1952) 21.

Analytica Chimica Acta, 67 (1973) 236–239

SHORT COMMUNICATION

The determination of water in copper(II) compounds by Karl Fischer titration

P. VAN ACKER, F. DE CORTE* and J. JOSTE
Institute for Nuclear Sciences, Rijksuniversiteit, Ghent (Belgium)
(Received 25th April 1973)

In the determination of water by titration with Karl Fischer reagent, the presence of interfering oxidizing or reducing agents in the titrated solution is a well-known problem[1]. This communication describes a back-titration method for the determination of water in copper(II) compounds.

When the water content of a copper(II) compound is titrated directly in an automatic Karl Fischer aquameter with amperometric end-point detection, the titration stops after the addition of a few drops of reagent, because the microammeter indicates a cell current above the preset value. This phenomenon is caused by the fact that the iodide, formed by the reaction of the Karl Fischer reagent with water, is oxidized by copper(II), with the formation of copper(I) and iodine. In this way, iodine and iodide are present in the solution, so that current can pass. Consequently, the driving motor of the buret piston remains blocked and the aquameter indicates the end-point.

Back-titration followed by successive approximations

If a known amount of Karl Fischer reagent is added in excess to a solution of a copper(II) salt in methanol, the quantity of water needed for the back-titration (performed with methanol with known water content), will be a function of two opposite effects:

(*a*) the water in the copper(II) compound, leading to the reaction

$$H_2O + I_2 + SO_2 \rightarrow 2\,HI + SO_3 \qquad (1)$$

which causes a decrease in iodine concentration and an increase in iodide concentration; and (*b*) the copper(II) compound, leading to the reaction:

$$2\,Cu^{2+} + 2\,I^- \rightarrow 2\,Cu^+ + I_2 \qquad (2)$$

which causes a decrease in iodide concentration and an increase in iodine concentration.

The net results of the back-titration will be influenced by both reactions, *i.e.* by the ratio of Cu^{2+}/H_2O in the copper(II) compound.

* Research associate of the N.F.W.O.

If Δ is the difference (expressed in mg of water) between the experimentally determined amount of water needed for the back-titration, and the theoretical amount of water in the absence of the copper(II) compound (calculated from the volumes and titers of the methanol and Karl Fischer solutions), it can be expressed as:

$$\Delta = |\Delta_{Cu} - \Delta_{H_2O}| \quad (3)$$

where Δ_{Cu} is the shift (expressed in mg of water) caused by copper(II) (reaction 2); and Δ_{H_2O} is the shift (expressed in mg of water) caused by water in the copper(II) compound (reaction 1).

It should be taken into account that, according to the reactions (1) and (2), one molecule of water is equivalent to two copper(II) ions. Obviously, it is an essential requirement that the copper(II) ions are quantitatively reduced to the monovalent state.

As eqn. (3) contains two unknowns, the desired Δ_{H_2O} value can only be calculated by successive approximations. If the titrated copper(II) salt is of the general composition $Cu_aA_b \cdot c\ H_2O$, where the indices a and b are known, and if an arbitrary c value is assumed, it becomes possible to calculate the corresponding molecular weight M_1, and for a given weight of the compound, $\Delta^1_{H_2O}$ and Δ^1_{Cu} can be computed. When this Δ^1_{Cu} value is introduced into eqn. (3), a second approximation of the water content, $\Delta^2_{H_2O}$, can be calculated. With the aid of this $\Delta^2_{H_2O}$ value, second approximations of M_2 and Δ^2_{Cu} can be found, which allows calculation of the next $\Delta^3_{H_2O}$ value. This procedure can be continued, resulting in converging values of $\Delta^i_{H_2O}$.

Experimental

Apparatus and reagents. Automatic Beckman KF_4 aquameter titrator.

Karl Fischer stabilized single solution (Beckman aquameter reagent) standardized with sodium tartrate dihydrate.

Methanol for Karl Fischer titrations (water content $\leqslant 0.05\%$).

Copper(II) salts: analytical-grade copper(II) sulphate pentahydrate.

Procedure. Methanol (40 ml) in the reaction cell was automatically titrated to the end-point with standardized Karl Fischer reagent (blank value). A known excess of the reagent was added to this titrated solution. The copper(II) salt was dissolved in methanol and made up to the mark in a measuring flask; 10 ml of this solution was pipetted into the titration vessel. Back-titration of this mixture was performed with methanol so as to reach a lower cell current than the preset value of 40 μA. Finally, this solution was automatically titrated to the end-point with the reagent. The volumes of methanol for the back-titration mentioned in Table I, are corrected for this final titration.

Water determination in $CuSO_4 \cdot 5H_2O$

To check the accuracy of the method, and especially in order to check the quantitative reduction of the copper(II) to the monovalent state, the above back-titration technique was applied to the determination of water in copper sulphate pentahydrate (theoretically 36.06% water). The water content of this salt was determined gravimetrically[2] by dehydration at 420°. The analysis was carried out in

TABLE I

KARL FISCHER TITRATION OF WATER IN $CuSO_4 \cdot 5H_2O$ ($M_1 = 250$)

No.	*$CuSO_4 \cdot 5H_2O$ (mg)*	*Karl Fischer excess (ml)*	*Back-titration methanol (ml)*	*Δ (mg H_2O)*	*Δ^1_{Cu} (mg H_2O)*	*$\Delta^1_{H_2O}$ (%)*	*$\Delta^2_{H_2O}$ (%)*	*$\Delta^3_{H_2O}$ (%)*	*$\Delta^4_{H_2O}$ (%)*
1	26.0	5.00	15.48	8.43	0.936	36.02	36.02	36.02	36.02
2	37.0	5.00	2.99	12.18	1.332	36.52	36.50	36.50	36.50
3	28.2[5]	4.00	1.86	9.30	1.017	36.53	36.51	36.51	36.51
4	33.9	5.00	5.94	11.29	1.222	36.87	36.85	36.84	36.84
5	36.3	5.00	3.76	11.95	1.308	36.52	36.50	36.50	36.50
						Average value 36.5 ± 0.1% H_2O[a]			

[a] Standard deviation on the mean.

five-fold. An average value of $36.4 \pm 0.1\%$ was found (standard deviation on the mean). The copper(II) compound was then titrated as described above. The titer of the Karl Fischer solution was 3.22 mg of water per ml of reagent. The blank value was found to be 40 ml of methanol per 3.75 ml of Karl Fischer reagent. The results of the successive approximations when Δ^1_{Cu} was calculated from the formula $CuSO_4 \cdot 5H_2O$ ($M_1 = 250$; 25.4% Cu), are summarized in Table I. As a control, the water contents were computed from the same experimental data, starting from an arbitrary value of $M_1 = 200$ (31.77% Cu). The results of these calculations are shown in Table II.

TABLE II

KARL FISCHER TITRATION OF WATER IN $CuSO_4 \cdot 5H_2O$ ($M_1 = 200$)

No.	Δ^1_{Cu} *(mg H_2O)*	$\Delta^1_{H_2O}$ *(%)*	$\Delta^2_{H_2O}$ *(%)*	$\Delta^3_{H_2O}$ *(%)*	$\Delta^4_{H_2O}$ *(%)*	$\Delta^5_{H_2O}$ *(%)*	$\Delta^6_{H_2O}$ *(%)*
1	1.170	36.91	36.26	36.09	36.04	36.02	36.02
2	1.665	37.41	36.75	36.52	36.50	36.50	36.50
3	1.271	37.41	36.85	36.58	36.53	36.51	36.51
4	1.526	37.49	37.09	36.91	36.85	36.84	36.84
5	1.634	37.41	36.74	36.56	36.51	36.50	36.50

From the data in Tables I and II, it can be concluded that the results of the Karl Fischer back-titration are in good agreement with the gravimetrically determined value of $36.4 \pm 0.1\%$ water. This is an indication that copper(II) is quantitatively reduced by the Karl Fischer solution. Furthermore, a comparison of the Tables shows that the results are not dependent on the first approximation of M_1.

The method was also successfully applied to the determination of water in copper acetate.

The financial support of the "Nationaal Fonds voor Wetenschappelijk Onderzoek" is gratefully acknowledged.

REFERENCES

1 J. Mitchell, Jr. and D. M. Smith, *Aquametry*, Interscience, New York, 1948.
2 C. Duval, *Inorganic Thermogravimetric Analysis*, Elsevier, Amsterdam, 1953.

Analytica Chimica Acta, 67 (1973) 240–242

SHORT COMMUNICATION

A universal ion-selective electrode based on graphite paste

JOSEPH P. SAPIO, J. F. COLARUOTOLO and J. M. BOBBITT
Department of Chemistry, University of Connecticut, Storrs, Conn. 06268 (U.S.A.)
(Received 9th February 1973)

Ruzicka and his co-workers have recently described[1–4] a design for a universal electrode which can be used as an ion-selective electrode for a number of anions electrode[5] and represents a continuation of our work on these electrodes[6].
Teflon-treated graphite powder compressed into a semi-solid rod. One end of this graphite rod holds the material responsible for the ion selectivity. This material

The electrode consists of a graphite paste prepared from a liquid ion containing the ion of interest. In this communication, a design is proposed for a universal ion-selective electrode with many of the advantages of the Selectrode and a much simplified construction (Fig. 1). It is based on the Adams graphite paste electrode[5] and represents a continuation of our work on these electrodes[6].

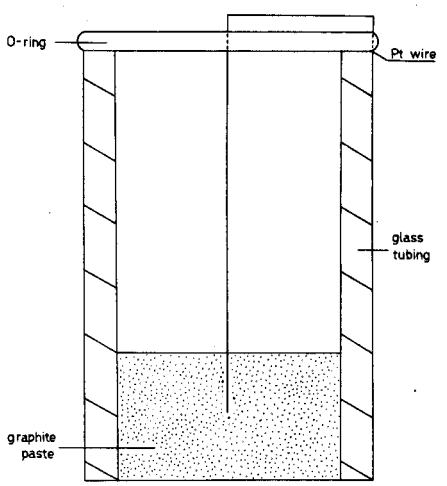

Fig. 1. An ion-selective graphite paste electrode.

Construction of electroaes

The electrode consists of a graphite paste prepared from a liquid ion exchanger containing the ion of interest (a cation or an anion) and commercial graphite powder (technical grade, cat. no. G-64, Fisher Scientific Co., Fairlawn, N.J.; washed with 6 *M* hydrochloric acid, water, and methanol; and dried at 110° for 3 h).

A chloride ion-selective paste was prepared from 5 g of graphite and 3 ml of Aliquat 336, a liquid quaternary ammonium chloride (General Mills Chemicals Inc., Minneapolis)*. A nitrate ion-selective paste was prepared similarly, with Aliquat 336 in the nitrate form. The exchanger was converted to the nitrate form by shaking 25 ml of the exchanger (in the chloride form) in 100 ml of hexane with six 100-ml portions of 1.5 *M* sodium nitrate. A calcium ion-selective paste was prepared by mixing the same proportions of graphite powder and the liquid ion-exchanger solution, 0.1 *M* calcium didecylphosphate in di-n-octylphenylphosphonate (Orion Research. Inc., Cambridge, Mass.). A 10-mm thick layer of the graphite paste was packed into one end of a length of 6 mm to 11 mm o.d. glass tubing around a platinum wire which was secured at the other end of the tubing with a rubber O-ring. No other conditioning of these electrodes was necessary.

Potential measurements were made at 25° with a Leeds-Northrup pH meter (model 7401) with a saturated calomel reference electrode. With the chloride electrode, a double-junction reference electrode was used, with saturated potassium nitrate solution separating the SCE from the chloride solutions.

Results and discussion

The chloride and nitrate ion-selective electrodes were found to give linear plots of *E vs.* $-\log a$ over the activity range of 0.003–0.85 *M*, with a slope of 54 mV/decade activity change (curve A, Fig. 2). Although this slope is not Nernstian (59.5 mV/decade at 25°), the potential measurements were reproducible (within a few hours) over the activity range of 0.0001–0.85 *M*. With regard to selectivity, it was found that, at an activity level of 0.001 *M* chloride, interference-free measurements were obtained with the chloride electrode in the presence of 0.0001 *M* Br^-, I^-, NO_3^-, and ClO_4^-. Similarly, at an activity level of 0.001 *M* nitrate, interference-free measurements were obtained with the nitrate electrode in the presence of 0.0001 *M* Cl^-, Br^-, I^-, and ClO_4^-. For both electrodes, measurements at pH greater than 9 should be avoided because of interference from the hydroxide ion.

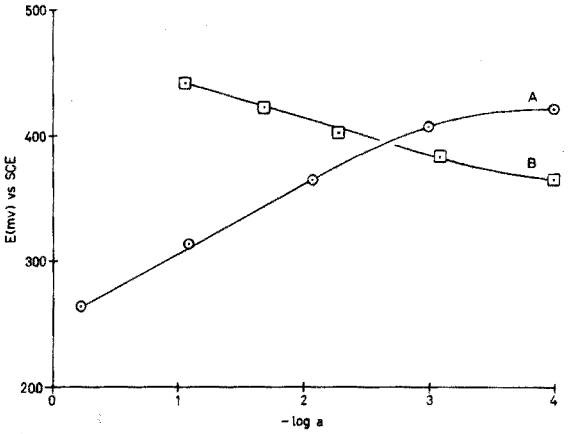

Fig. 2. Response of the paste electrode to the activity of chloride or nitrate ion (A) and calcium ion (B).

* For applications of Aliquat 336 involving other ions, see ref. 7.

The calcium ion-selective electrode was found to give a linear plot of E *vs.* $-\log a$ over the activity range of 0.001–0.1 M with a slope of 30 mV/decade activity change (curve B, Fig. 2). However, the potential measurements were reproducible (within a few hours) over the activity range of 0.0001–0.1 M. The calcium electrode displayed a somewhat better selectivity over interferences than the chloride and nitrate electrodes. At an activity level of 0.0001 M calcium(II), interference-free measurements were obtained in the presence of 0.001 M Mg^{2+} and Ba^{2+}, and 0.01 M Na^{+}.

Measurements at pH less than 6 should be avoided because of interference by the hydrogen ion.

The drawbacks to these electrodes are their sensitivity to stirring and their need for periodic restandardization. The measurements were carried out in unstirred can easily be converted to selective pastes[7].
fluctuations in potential measurements of ± 3 mV. The value of E^0, which was obtained for each of these electrodes by extrapolating the plot of E *vs.* $-\log a$ to $-\log a = 0$, changed with daily use.

A number of new electrodes could result from further investigation of paste systems. Many ions, both anions and cations, can be exchanged into such liquids as Aliquat 336 (for anions) and the liquid phosphonates (for cations), and these can easily be converted to selective pastes[7].

We wish to thank Professor J. T. Stock of this Department for his many helpful suggestions.

REFERENCES

1 J. Ruzicka and K. Rald, *Anal. Chim. Acta*, 53 (1971) 1.
2 J. Ruzicka and C. G. Lamm, *Anal. Chim. Acta*, 53 (1971) 206.
3 J. Ruzicka and C. G. Lamm, *Anal. Chim. Acta*, 54 (1971) 1.
4 J. Ruzicka, C. G. Lamm and J. C. Tjell, *Anal. Chim. Acta*, 62 (1972) 15.
5 R. N. Adams, *Electrochemistry at Solid Electrodes*, Marcel Dekker, New York, 1969, pp. 280–283.
6 J. M. Bobbitt, J. F. Colaruotolo and S. J. Huang, *J. Electrochem. Soc.*, 120 (1973) 773.
7 C. J. Coetzee and H. Freiser, *Anal. Chem.*, 40 (1968) 2071.

Analytica Chimica Acta, 67 (1973) 243–245

SHORT COMMUNICATION

A liquid ion-exchange nitrate-selective electrode based on carbon paste

G. ALI QURESHI and J. LINDQUIST
Department of Analytical Chemistry, University of Uppsala, S-751 21 Uppsala 1 (Sweden)
(Received 13th April 1973)

The commercially available liquid ion-exchange membrane electrodes require supports of some porous inert material to hold the organic liquid within their framework; this membrane is continuously supplied with the organic liquid from an internal reservoir. The interface formed is, however, rather ill-defined and the membrane offers poor mechanical resistance to pressure. It is troublesome to change the support after the surface has been poisoned, and re-charging of the organic ion exchanger is frequently required. The central part of the electrode is usually filled with the internal aqueous electrolyte and a reference electrode.

To overcome the disadvantages of inner reference electrodes and membranes it would be useful to mix the ion exchanger with carbon powder to obtain a paste with low resistance. This paste could then be tamped into a holder to form an electrode in the same way as the so-called "carbon paste electrodes" for voltammetry introduced by Adams[1]. It is easy to renew the surface of such electrodes and there is no need for an inner reference electrode. A metal contact is enough.

Růžička[2] has used carbon in the "Selectrodes"; a carbon–teflon mixture is compressed to form a solid rod into which is rubbed a thin layer of active material (*e.g.* copper and silver sulphides). Růžička's "liquid-state" electrode[3] was made from a hydrophobized carbon rod impregnated by immersing it in a solution of active liquid (metal dithizonate) under slight vacuum. The surface could be renewed either by dipping the electrode in the organic phase, by scratching off the electrode surface or by a combination of both. No inner reference electrodes were needed. The "Selectrodes" seem to be very practical and useful, especially for solid active materials like silver halides and metal sulphides, etc. For liquid ion exchangers, it would be much simpler to form a homogeneous paste to improve the reproducibility of resurfacing.

This communication describes the construction and general performance of a nitrate-selective electrode based on the Orion Liquid 92-07-02 mixed with wax-treated carbon powder (the surface of the carbon has to be isolated with a thin layer of wax in order to prevent a pH-response because of the surface oxides).

Experimental

Ceresin wax (1.5 g) was dissolved in 10 ml of n-hexane, and 9 g of

graphite powder (Merck 4206) was added. The mixture was heated on a water bath and stirred with a glass rod until most of the hexane had evaporated. The dried powder was carefully mixed with Orion liquid 92-07-02 in the ratio 4:1 (w/w). The paste holder was a teflon rod 10 mm in diameter, with a hole, 10 mm deep, at one end, and a movable metal piston at the bottom. The paste was tamped into the holder and the surface was cut with a stretched length of 0.2-mm piano wire, the holder being mechanically rotated during cutting[4]. The surface of the electrode was easily renewed by pressing out the paste a few tenths of a millimeter and repeating the cutting procedure.

The reference electrode was a saturated calomel electrode with a fiber junction. The metal piston (stainless steel) served as electric contact with the paste.

Measurements were made with a digital pH-meter (Metrohm E 500) readable to ± 0.2 mV. A recorder (Philips 8100) was used for obtaining the time response. All solutions were stirred in 50-ml beakers and the temperature was $23 \pm 1°$. The water used for the preparation of the solutions was obtained by distilling de-ionized water.

Results and discussion

Calibration of the electrode in pure nitrate solutions. Potentials were recorded for standard solutions of analytical-reagent grade sodium nitrate in the concentration range 10^{-1}–10^{-6} *M*. The electrode surface was renewed before each measurement. The potentials were taken after 8 min. The reproducibility was within ± 0.2 mV (standard deviation).

The potential response was linear over the range 10^{-1}–$10^{-4.5}$ *M* nitrate with a slope of 58 mV/decade activity; this compares favourably with commercial nitrate electrodes.

During one day's use the potential varied by ± 2–4 mV. The drift over a period of 1 week was about 11 mV. The slope of the calibration graph did not change with time up to a period of 8 weeks.

Interferences. Separate solutions were used to measure the selectivity coefficients. The values at a concentration of 0.1 *M* were compared with the data for some commercial electrodes (Table I). The coefficients for the carbon paste

TABLE I

SELECTIVITY COEFFICIENTS OF NITRATE LIQUID ION-EXCHANGE MEMBRANE ELECTRODES

Interfering ion	*Beckman No. 39618*	*Corning No. 476134*	*Orion No. 92-07-02*	*Carbon paste electrode*
$H_2PO_4^-$	—	—	$3 \cdot 10^{-4}$	$3 \cdot 10^{-4}$
SO_4^{2-}	10^{-5}	10^{-3}	$6 \cdot 10^{-4}$	$7 \cdot 10^{-5}$
Cl^-	10^{-2}	$4 \cdot 10^{-3}$	$6 \cdot 10^{-3}$	$3 \cdot 10^{-3}$
HPO_4^{2-}	—	—	$8 \cdot 10^{-5}$	$6 \cdot 10^{-5}$
Br^-	$2.8 \cdot 10^{-1}$	10^{-1}	$9 \cdot 10^{-1}$	$4 \cdot 10^{-2}$
ClO_4^-	10^2	$>10^3$	10^3	14
I^-	5.6	25	20	4

electrode are as good as, or even better than, those for the commercial electrodes; the case of perchlorate is particularly remarkable.

Effect of pH. The pH range for commercial nitrate electrodes is about 2–12 (Orion), but depends on the nitrate concentration. The operating pH range for the Corning nitrate electrode is given as 2.5–10 in 10^{-2} *M* potassium nitrate. In the present study, both the potential and pH values were measured in nitric acid (10^{-2} and 10^{-3} *M*) after successive small additions of sodium hydroxide (Fig. 1). Change in pH had little effect in the range 3–8.

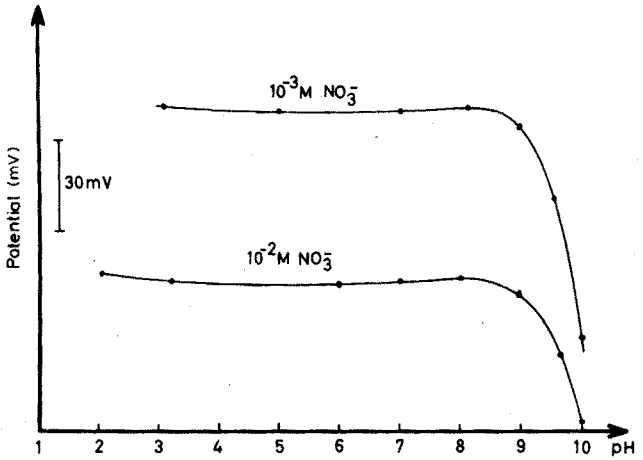

Fig. 1. The effect of pH on the response of the carbon paste electrode at constant nitrate concentration.

Time response. The responses were determined by rapidly changing the nitrate solutions with short rinsing time between the measurements. The time required to obtain 90% response to a stepwise change from 10^{-4} to 10^{-3} *M* nitrate in a stirred solution was 30 s, and 10 s in the opposite direction; 2 min were required to reach a value less than 1 mV from the equilibrium value. The time required to obtain the equilibrium value with a new surface was 8–10 min.

Conditioning and storage of the electrode. The electrode had a life time of 4–6 months, when stored in a glass tube. The first reading after cutting a new surface required 8–10 min but the response time then became 2–3 min.

REFERENCES

1 R. N. Adams, *Anal. Chem.*, 30 (1958) 1576.
2 J. Růžička and C. G. Lamm, *Anal. Chim. Acta*, 54 (1971) 1.
3 J. Růžička and J. Chr. Tjell, *Anal. Chim. Acta*, 51 (1970) 1.
4 J. Lindquist, *J. Electroanal. Chem.*, 18 (1968) 204.

Analytica Chimica Acta, 67 (1973) 246–250

SHORT COMMUNICATION

Peak integration in polarography

H. L. KIES and M. DEN OS
Laboratory of Analytical Chemistry, The University of Technology, Delft (The Netherlands)
(Received 23rd March 1973)

Graphical evaluation of polarograms is rather time-consuming. This applies not only to the normal sigmoid-shaped curves but also, to a lesser degree, to the measurement of peak heights if other procedures are followed. It was therefore thought worthwhile to investigate peak integration, which technique has been widely accepted in gas chromatography[1], and is now occasionally used in quantitative infrared spectrophotometry[2,3] and even in flame emission spectrometry[4]. A possible digital print-out could substantially lighten the work.

Automation of the integration process requires a triggering unit that starts and stops integration, and facilities for baseline compensation. Commonly, integration is started as soon as the slope of the diagram passes a prefixed value, and the end of the process is established similarly. Accordingly, it is easily understood that difficulties may arise because of the oscillations in the signal, which are inherent in the use of a dropping electrode. These oscillations cannot be fully suppressed by increasing the degree of damping, because this entails undesired secondary effects. It appeared far better to reduce the drop-time by means of a drop-life timer, such as is usual in rapid polarography[5,6].

The signal is rather small and, what is worse, it contains a relatively large amount of noise. The latter aspect makes amplification unattractive, because false triggering would be promoted and the reliability of the apparatus decreased. However, this difficulty could be overcome by using a retransmitting (slave) potentiometer coupled to the same shaft as the rotor of the motor that is responsible for driving the recorder pen. This smoothing procedure was satisfactory in practice. It is clear that the result, expressed in counts, is proportional not only to the concentration but also to the recorder sensitivity. The method proposed is based on a principle that is quite different from that of another attempt to evaluate automatically polarographic data, published a few years ago[7].

Apparatus

As a complete commercial integration system was not available, a simpler assembly, with some provision for baseline correction, was devised. The block diagram is presented in Fig. 1. As mentioned above, the device was connected to the usual polarographic recorder by means of a retransmitting potentiometer. The signal path consisted of a track and hold circuit, T-H, and a subtractor, S. The sensing path

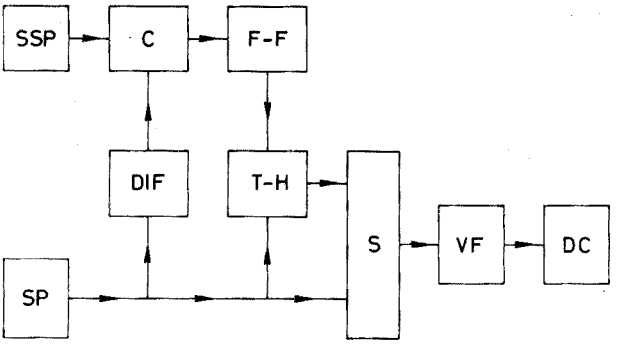

Fig. 1. Block diagram. (C) Comparator; (DC) digital counter; (DIF) differentiator; (F-F) bistable element (flip-flop); (S) subtractor; (SP) slave potentiometer; (SSP) slope setpoint; (T-H) track and hold circuit; (V-F) voltage to frequency converter.

was made up of the differentiator, DIF, with comparator, C. The resulting output signal triggered the bistable element F-F, which operated actually as a flip-flop device. No output signal was obtained from S as long as T-H was in its tracking state. As soon as the differentiated signal exceeded a preset value, F-F was triggered, turning T-H into its holding state. The output voltage of T-H at the moment of triggering was subtracted from the changing input voltage by means of the subtractor S. The output voltage of S was integrated and subsequently digitally displayed.

If an up- or down-slope prevailed in the baseline, a provision present in the track-hold unit afforded the appropriate correction, but situations may occur in which the introduction of a subtractive measuring method would mean a better approach.

Derivative peaks

At first sight, linking up a derivative with an integration step seems rather odd. Indeed, the result of the integration of the derived signal is equivalent to the difference of the limiting current at the top of the normal wave and the residual current at its foot. Hence, it could be argued that two measurements would suffice, though ideally both measurements should refer to the situation at the half-wave potential. Each of these measurements is afflicted with some inaccuracy, which is normally compensated by the well-known graphical construction. A similar compensation is achieved when a peak is integrated; because the result contains the information from all over the whole curve, the effect of any irregularities, particularly at the peak maximum, is smoothed out. Thus, peak integration should show a higher reproducibility than is obtained from measurement of the peak height. An additional advantage is the suitability of the technique for automation.

Derivative polarography was introduced at about the same time by Vogel and Říha[8] and by Lévêque and Roth[9], and many commercial polarographs now have derivative mode facilities. The subject has been thoroughly studied by Lingane and Williams[10], Jäckel[11] and Berbalk[12]. A draw-back of the procedure is that proportionality between peak current and concentration fails. Accidentally, it was observed[13] that the rectilinear part of the calibration curve was considerably

extended by applying higher scan rates; moreover, the sensitivity increased correspondingly (Fig. 2). The same phenomena occurred when peak areas were measured. A Radiometer Polariter PO4 was used in this work.

Fairly good results were obtained for concentrations higher than 10^{-4} *M* (Fig. 3). The standard deviation for $2 \cdot 10^{-4}$ *M* cadmium(II) was 0.3% (17 experiments). At lower concentrations, this value was higher, of course, amounting to 10% for $5 \cdot 10^{-6}$ *M* zinc(II) (14 experiments).

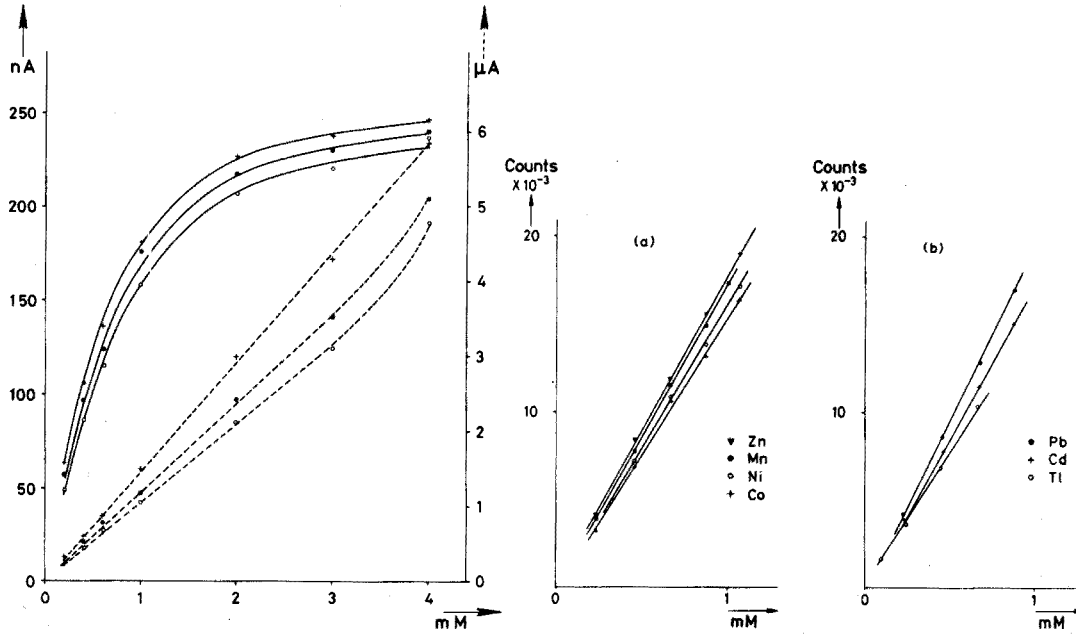

Fig 2. Calibration curves for peak height of derivative polarograms, with different drop times. Scanning rate: (------) 800 mV min^{-1}; (——) 200 mV min^{-1}. $ZnCl_2$ in 0.1 *M* KCl. Drop times: (+) 1 s; (●) 0.5 s; (○) 0.25 s.

Fig. 3. Calibration curves for integrated rapid derivative polarograms. Supporting electrolyte: (a) 0.1 *M* KCl; (b) 0.1 *M* KNO_3.

The influence of preceding waves is obvious from the considerably increased oscillations of the baseline beyond the first wave. Practically, the total content of the nobler components should not exceed ten times the amount of the last component to be recorded.

A.c. polarography

In a.c. polarography, the peak height is independent of the scan rate, except at very high rates[14], when the response time of the recorder becomes inadequate[15]. The peak area appeared to be even less sensitive to fast recording. However, although reasonable a.c. polarograms can be obtained with rapid scanning[14,16–18] the recordings are smoother at normal scan rates which were therefore preferred in this work.

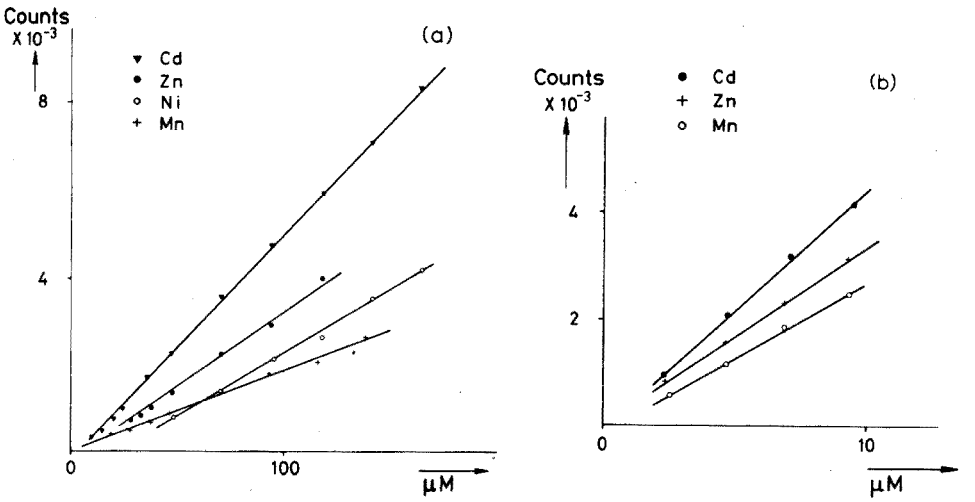

Fig. 4. Calibration curves for integrated a.c. polarograms. Supporting electrolyte, 0.1 *M* KCl. Alternating voltage, 5 mV (a) and 20 mV (b). In Fig. 4b, the integrated waves were preceded by waves of a main component, *viz.* (●) $5 \cdot 10^{-4}$ *M* Fe(II); (+) $2.3 \cdot 10^{-4}$ *M* Cd; and (○) $2.3 \cdot 10^{-4}$ *M* Zn.

The introduction of phase-sensitive detection[19] has provided a significant improvement in a.c. polarography. In the present investigations, a Tacussel polarograph PRG 3, equipped with a potentiostat, was used.

Two series of experiments were completed, one with an applied alternating voltage of 5 mV for the higher concentration range (Fig. 4a), and the other with 20 mV for the lower concentration range (Fig. 4b). The standard deviation found for $7 \cdot 10^{-5}$ *M* zinc(II) was 1% (13 determinations) and for $2.3 \cdot 10^{-6}$ *M* cadmium(II) 2% (13 determinations). Further improvement may be expected from better integrators. The influence of preceding waves was rather small, provided that the half-wave potentials between adjacent waves differed sufficiently; a two-hundred-fold excess of the nobler component was allowable.

We are much indebted to Mr. H. C. van Dam for designing the integration unit.

REFERENCES

1 R. S. Evans and J. Krugers, in J. Krugers, *Instrumentation in Gaschromatography*, Centrex, Eindhoven, 1968, p. 221.
2 V. Z. Williams, V. J. Coates and F. Gaarde, *Anal. Chem.*, 27 (1955) 2017.
3 A. E. Martin, *Infra-Red Instrumentation and Techniques*, Elsevier, Amsterdam, 1966, p. 144.
4 R. Herrmann and C. T. J. Alkemade, *Chemical Analysis by Flame Photometry*, Interscience, New York, 1963, p. 189.
5 D. Wolf, *J. Electroanal. Chem.*, 5 (1963) 186.
6 H. Schmidt and R. von Schorlemer, *J. Electroanal. Chem.*, 5 (1963) 345.
7 T. Kugo, Y. Umezawa and S. Fujiwara, *Chem. Instrum.*, 2 (1969) 189.
8 J. Vogel and J. Říha, *J. Chim. Phys.*, 47 (1950) 5.
9 P. Lévêque and F. Roth, *J. Chim. Phys.*, 46 (1949) 480.

10 J. J. Lingane and R. Williams, *J. Amer. Chem. Soc.*, 74 (1952) 790.
11 Th. Jäckel, *Fresenius' Z. Anal. Chem.*, 173 (1960) 59.
12 H. Berbalk, *Monatsh. Chem.*, 86 (1955) 576.
13 L. Lippens, unpublished results.
14 A. M. Bond, *J. Electrochem. Soc.*, 118 (1971) 1588.
15 I. G. McWilliam and H. C. Bolton, *Anal. Chem.*, 41 (1969) 1762.
16 A. M. Bond and D. R. Canterford, *Anal. Chem.*, 44 (1972) 721.
17 A. M. Bond and T. A. O'Donnel, *Anal. Chem.*, 41 (1969) 1801.
18 A. Ledieu and J. Byé, *Bull. Soc. Chim. Fr.*, (1970) 801.
19 J. W. Hayes and H. H. Bauer, *J. Electroanal. Chem.*, 3 (1962) 336.

Analytica Chimica Acta, 67 (1973) 251–252

BOOK REVIEWS

N. S. Nikolaev, S. N. Suvorova, E. I. Gurovich, I. Peka and E. K. Korchemnaya, *The Analytical Chemistry of Fluorine*, Translated by J. Schmorak, Israel Program for Scientific Translations, Jerusalem, Halsted Press–John Wiley, New York, 1973, ix+222 pp., price £9.35.

The Analytical Chemistry of the Elements, of which the present volume forms part, is a series originally written under the aegis of the Vernadskii Institute of the Russian Academy of Sciences, and so must command respect. The text on fluorine is a translation of the Russian book which appeared in 1970, and so would appear to be less out of date than many other volumes in this translated series. Unfortunately, the progress which has been made in analysis for fluorides over the past few years has been so rapid that this text seems now to appear almost from another world. It is indeed strange to read a book on fluorine analysis published in 1973 which makes absolutely no mention of ion-selective electrodes. The lanthanum fluoride electrode has revolutionized the determination of the fluoride ion and has been used in multitudinous applications; one wonders almost how one managed for so long without it. However, this is not the only shortcoming: from qualitative analysis, through gravimetric, to spectrophotometric analysis, very few of the methods which have gained widespread approval by non-Russian analysts are mentioned. Megregian's procedure has been justifiably included, but there is only a bare mention of alizarin fluorine blue, and even some of the more interesting Russian procedures have been omitted.

The text has some interest in the methods of decomposition suggested for different types of material, but the general impression is one of analysis as it was done some 15 years ago. This is a book which can be recommended only to those with an historical interest in the subject.

A. M. G. Macdonald (Birmingham)

E. Bujdoso, I. Feher and G. Kardos, *Activation and Decay Tables of Radioisotopes*, Elsevier Publishing Company, Amsterdam, 1973, 575 pp., price Dfl 100.00 (*ca.* $35.00).

Apart from a short introductory chapter, this book is composed entirely of tables of data concerning the activation with thermal neutrons of eighty elements by the (n, γ) reaction. For every radioisotope formed by this reaction, there are listed the half-life, and the energies and intensities of predominant γ-rays. The activities of each which can be produced after a wide variety of practicable irradiation and cooling times are tabulated. Where applicable, information about daugther activities is also provided. The reader will certainly have to study carefully the Introduction before attempting to use the Tables; but once the system of presenting activation, decay and counting parameters is understood, the Tables are simple to apply.

To those experimentalists, who for one reason or another routinely predict neutron-induced sample activities with charts, tabulations of decay schemes and so on, these Activation and Decay Tables can be recommended. Pencil and paper are still necessary to work out the final answer; however, unless basic information is transcribed erroneously (as is the case in the worked example on page 15, in which the sign of the exponent of the neutron flux is wrong!), the use of these tables can eliminate much of the drudgery of carrying out and checking calculations which might otherwise be required before activation analysis, or radioisotope production and use.

C. L. Graham (Birmingham)

(Continued from page 4 of cover)

CONTENTS

(continued on inside page of cover)